U.S. DEPARTMENT OF COMMERCE
National Technical Information Service

PB-279 625

Second US/USSR Symposium on Particulate Control Held at Research Triangle Park, North Carolina on May 25-28, 1977

Research Triangle Inst, Research Triangle Park, N C

Prepared for

Industrial Environmental Research Lab, Research Triangle Park, N C

Mar 78

TECHNICAL REPORT DATA
(Please read Instructions on the reverse before completing)

1. REPORT NO. EPA-600/7-78-037	2.	3. RECIPIENT'S ACCESSION NO. PB279625
4. TITLE AND SUBTITLE Second US/USSR Symposium on Particulate Control		5. REPORT DATE March 1978
		6. PERFORMING ORGANIZATION CODE
7. AUTHOR(S) Franklin A. Ayer, Compiler		8. PERFORMING ORGANIZATION REPORT
9. PERFORMING ORGANIZATION NAME AND ADDRESS Research Triangle Institute P.O. Box 12194 Research Triangle Park, North Carolina 27709		10. PROGRAM ELEMENT NO. EHE 624 11. CONTRACT/GRANT NO. 68-02-2612, Task 5
12. SPONSORING AGENCY NAME AND ADDRESS EPA, Office of Research and Development Industrial Environmental Research Laboratory Research Triangle Park, NC 27711		13. TYPE OF REPORT AND PERIOD COVER Proceedings; 6-12/77 14. SPONSORING AGENCY CODE EPA/600/13

15. SUPPLEMENTARY NOTES IERL-RTP project officer is Dennis C. Drehmel, Mail Drop 61, 919/541-2925.

16. ABSTRACT

The proceedings include papers presented during the symposium, sponsored by the Particulate Technology Subgroup of the US/USSR Stationary Source Air Pollution Technology Working Group under the US/USSR Environmental Agreement. The symposium was held at Research Triangle Park, North Carolina, September 25 October 2, 1977. Papers were presented by Soviet specialists from research desig institutes and industry, and by representatives of US government agencies and the private sector. Topics included: electrostatic precipitator (ESP) research and appl cation, ESP gas flow modeling, ESP rapping and reentrainment, ESP reliability, ESP modeling, flue gas conditioning, high-temperature ESP application, use of fabric filters in the US cement industry, emission standards, state-of-the-art of mist eliminators, mist eliminator testing, particle size distribution measurement in the micron and submicron ranges, dust resistivity and back-corona formation in ESPs, and fly ash composition and its effect on resistivity.

17. KEY WORDS AND DOCUMENT ANALYSIS

a. DESCRIPTORS	b. IDENTIFIERS/OPEN ENDED TERMS	c. COSATI Field/Group
Air Pollution, Dust Control, Gas Flow	Air Pollution Control	13B, --, 20D
Electrostatic Precipitators, Reliability	Stationary Sources	--, 14D
Mathematical Models, Entrainment	Particulate, USSR	12A, 07D
Flue Gases, Treatment, Fabrics	Rapping	21B, 14B, 11E
Filters, Cements, Mist, Measurement		13K, 11B, 04B, --
Size Determination, Concentration		
Electrical Resistivity, Coronas, Fly Ash		20C, --, --

18. DISTRIBUTION STATEMENT Unlimited	19. SECURITY CLASS *(This Report)* Unclassified	21. NO. OF PAGES 271
	20. SECURITY CLASS *(This page)* Unclassified	22. PRICE PC A12/MF A01

EPA Form 2220-1 (9-73)

PB 279 625

EPA U.S. Environmental Protection Agency
Office of Research and Development
Industrial Environmental Research Laboratory
Research Triangle Park, North Carolina 27711
EPA-600/7-78-037
March 1978

SECOND US/USSR SYMPOSIUM ON PARTICULATE CONTROL

Interagency
Energy-Environment
Research and Development
Program Report

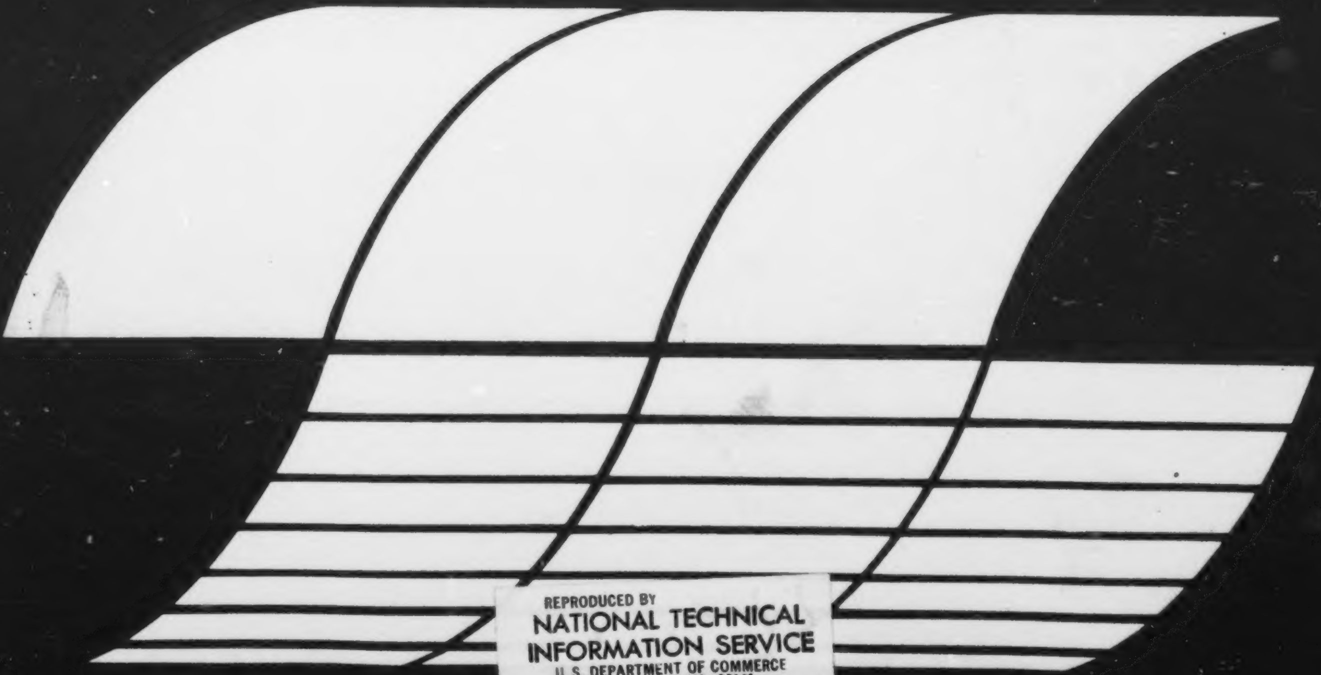

REPRODUCED BY
NATIONAL TECHNICAL
INFORMATION SERVICE
U. S. DEPARTMENT OF COMMERCE
SPRINGFIELD, VA. 22161

RESEARCH REPORTING SERIES

Research reports of the Office of Research and Development, U.S. Environmental Protection Agency, have been grouped into nine series. These nine broad categories were established to facilitate further development and application of environmental technology. Elimination of traditional grouping was consciously planned to foster technology transfer and a maximum interface in related fields. The nine series are:

1. Environmental Health Effects Research
2. Environmental Protection Technology
3. Ecological Research
4. Environmental Monitoring
5. Socioeconomic Environmental Studies
6. Scientific and Technical Assessment Reports (STAR)
7. Interagency Energy-Environment Research and Development
8. "Special" Reports
9. Miscellaneous Reports

This report has been assigned to the INTERAGENCY ENERGY-ENVIRONMENT RESEARCH AND DEVELOPMENT series. Reports in this series result from the effort funded under the 17-agency Federal Energy/Environment Research and Development Program. These studies relate to EPA's mission to protect the public health and welfare from adverse effects of pollutants associated with energy systems. The goal of the Program is to assure the rapid development of domestic energy supplies in an environmentally-compatible manner by providing the necessary environmental data and control technology. Investigations include analyses of the transport of energy-related pollutants and their health and ecological effects; assessments of, and development of, control technologies for energy systems; and integrated assessments of a wide range of energy-related environmental issues.

EPA REVIEW NOTICE

This report has been reviewed by the participating Federal Agencies, and approved for publication. Approval does not signify that the contents necessarily reflect the views and policies of the Government, nor does mention of trade names or commercial products constitute endorsement or recommendation for use.

This document is available to the public through the National Technical Information Service, Springfield, Virginia 22161.

EPA-600/7-78-037
March 1978

SECOND US/USSR SYMPOSIUM ON PARTICULATE CONTROL

Franklin A. Ayer, Compiler

Research Triangle Institute
P. O. Box 12194
Research Triangle Park, N.C. 27709

Contract No. 68-02-2612
Task 5
Program Element No. EHE624

EPA Project Officer: Dennis C. Drehmel

Industrial Environmental Research Laboratory
Office of Energy, Minerals and Industry
Research Triangle Park, N.C. 27711

Prepared for

U.S. ENVIRONMENTAL PROTECTION AGENCY
Office of Research and Development
Washington, D.C. 20460

1a

FOREWORD

The proceedings for the U.S./U.S.S.R. Symposium on Measurement and Control of Particulate Emissions is the final report submitted to the Industrial Environmental Research Laboratory for the U.S. Environmental Protection Agency Contract No. 68-02-2612, Task 5. The symposium was held at the Research Triangle Park, North Carolina, on May 25-28, 1977.

The primary objective of the symposium was to dicuss work done by American and Soviet specialists on particulate abatement technology.

Mr. James A. Abbott, Chief, Particulate Technology Branch, Utilities and Industrial Power Division, Industrial Environmental Research Laboratory, U.S. Environmental Protection Agency, Research Triangle Park, North Carolina, was the symposium General Chairman.

Dr. Dennis C. Drehmel, Particulate Technology Branch, Utilities and Industrial Power Division, Industrial Environmental Research Laboratory, U.S. Environmental Protection Agency, Research Triangle Park, North Carolina, was the symposium Vice-Chairman.

Mr. Franklin A. Ayer, Manager, Technology and Resource Management Department, Center for Technology Applications, Research Triangle Institute, Research Triangle Park, North Carolina, was the symposium Coordinator and Compiler of the proceedings.

Preceding page blank

ABSTRACT

The Second U.S./U.S.S.R. Symposium on Particle Control was sponsored by the Particulate Technology Subgroup of the U.S./U.S.S.R. Stationary Source Air Pollution Technology Working Group under the U.S./U.S.S.R. Environmental Agreement. Papers were presented by Soviet specialists from research design institutes and industry, by representatives of U.S. government agencies, and representatives of the private sector. Topics included: electrostatic precipitator research and application, electrostatic precipitator gas flow modeling, electrostatic precipitator rapping and reentrainment studies, electrostatic precipitator reliability studies, electrostatic precipitator modeling, flue gas conditioning, high temperature electrostatic precipitator modeling, flue gas conditioning, high temperature electrostatic precipitator application, use of fabric filters in the U.S. cement industry, emission standards, state-of-the-art of mist eliminators, mist eliminator testing, particle size distribution measurement in the micron and submicron ranges, dust resistivity and back corona formation in electrostatic precipitators, and fly ash composition and its effect on resistivity.

This report was submitted by the Research Triangle Institute, Research Triangle Park, North Carolina, in fulfillment of Contract No. 68-02-2612, Task No. 5, which was under the sponsorship of the U.S. Environmental Protection Agency.

Table of Contents

PAGE

September 26, 1977

Welcoming Remarks 1
N. A. Jaworski

Overview of Electrostatic Precipitator Applications and Research in the United States 2
L. E. Sparks

The Present Status and Prospects of Development of Studies of Electrical Gas Cleaning in the U.S.S.R. 6
I. K. Reshidov (speaker),
I. A. Kizim,
I. V. Yermilov, and
V. M. Tkachenko

Techniques of Modeling Gas Flow in Electrostatic Precipitators in the U.S. 11
Samuel Bernstein

Investigation of Gas Distribution Systems in Electrostatic Precipitators Collecting Dust and Fly Ash 21
I. E. Idechik,
JA. L. Ginzburg,
M.O. Shteinberg,
V. P. Alecsandrov, and
V.S. Korjagin
N. G. Bulgakova (speaker)

Studies of Particle Reentrainment Resulting From Electrode Rapping 30
Leslie E. Sparks,
Owen J. Tassicker (speaker), and
John P. Gooch

Investigation of Dust Carryover and Optimization of Regimes of Electrode Rapping in Electrostatic Precipitators 47
Yu. I. Sanayev,
I. K. Reshidov (speaker), and
I. A. Kizim

September 27, 1977

Investigations Aimed at the Increasing of Reliability and Time of Service of Electrostatic Precipitator Units and Gas Cleaning Installations as a Whole 53
V. A. Guzayev,
I. V. Yermilov,
L. S. Ryhzov, and
V. N. Saksin
V. M. Tkachenko (speaker)

Table of Contents (con.)

PAGE

Study of Operating and Maintenance Requirements of Electrostatic Precipitators in the U.S.A. 59
Dennis C. Drehmel and
Michael Szabo (speaker)

Mathematical Modeling of Electrostatic Precipitator Filters and Its Application to Industrial Units in the U.S.S.R. 66
I. V. Yermilov and
T. I. Dimitrieva
V. M. Tkachenko (speaker)

Mathematical Modeling of Electrostatic Precipitators in the United States 79
Jack R. McDonald
Grady Nichols (speaker)

The Study of the Components of the Electric Field in Electrostatic Precipitators 100
V. I. Levitov,
G. F. Mustafin, and
V. M. Tkachenko (speaker)

Flue Gas Conditioning in Coal-Fired Power Plants in the United States 113
Edward B. Dismukes

The Problem of Collecting Dusts That Cause Reverse Corona Formation in ESPs 124
S. N. Panev,
V. M. Tkachernko (speaker), and
T. Y. Chelombitko

September 28, 1977

Dynamical Behavior of Collecting Plates of Electrostatic Precipitators and Prediction of Rapping Efficiency 129
V. B. Mescheryakov and
A. I. Zavyalov
I. K. Reshidov (speaker)

Electrical Gas Cleaning at Higher Pressures 140
A. Yu. Valdberg,
V. V. Danilin,
A. G. Ljapin, and
V. M. Tkachenko (speaker)

Air Pollution Control of Emissions From Kilns and Coolers Utilizing Fabric Filters in the Cement Industry 150
Frank R. Culhane
Eric Brandt (speaker)

Table of Contents (con.)

PAGE

Removal of Harmful Particles From the Exhaust of the Cement Plants 168
G. I. Vodolazskiy
Y. Izmodyendov (speaker)

Emission Standards and Background Document on Control Technology in the Cement Industry in the U.S.A. 174
Gary McCutchen,
George E. Weant, III, and
George Walsh (speaker)

State-of-Art Survey of Mist Elimination in the U.S.A. 180
Seymour Calvert

Mist Eliminator Testing at the Shawnee Prototype Lime/Limestone Test Facility 194
John E. Williams

September 29, 1977

Field Measurements of Particle Size Distribution With Inertial Sizing Devices 215
N. G. Bulgakova (speaker),
L. Ya. Gradus, and
S. S. Yankovskiy

Sizing Techniques for Submicron Particles 223
Wallace B. Smith and
D. Bruce Harris (speaker)

Dust Resistivity and Reverse Corona Formation in Electrostatic Precipitators 237
I. K. Reshidov (speaker),
Yu. I. Sanayev, and
I. A. Kizim

A Review of the Influence of Fly Ash Composition on Resistivity 248
R. E. Bickelhaupt

WELCOMING REMARKS

N. A. Jaworski*

On behalf of the United States Environmental Protection Agency, we would like to welcome both our U.S. participants and our Soviet participants to the 2nd U.S./Soviet Symposium on Particulate Control. Many of you who are attending this symposium were at the first joint symposium in San Francisco, and while I personally was not at that symposium, I have heard that it was indeed a success. Since that symposium, considerable research effort has been accomplished both in the U.S.S.R. and in the U.S.

In addition to the research, there has been joint testing by the Soviets and Americans both here in the U.S. and in the U.S.S.R. The information that we have gathered through our research programs and our joint testing programs is valuable to both countries. I am very pleased, being a member of the Working Group involved in this particular area of research, that we can have the opportunity to host this symposium.

The papers to be presented in this program reflect the excellent work being conducted both in the U.S.S.R. and in the U.S. The program also reflects some of the cooperative effort that has been conducted through the U.S./U.S.S.R. Joint Committee on Cooperation in the Field of Environmental Protection. The program has been in existence for the past 5 years and has recently been extended for an additional 5 years. Many of the American participants and Soviet participants in this symposium have been involved in the particulate abatement project of the Working Group on Stationary Source Air Pollution Control Technology since its inception.

After this symposium, research efforts for future joint U.S./Soviet cooperation will be discussed and developed. It is tentatively planned to hold the third Symposium on Particulate Control in the Soviet Union in 1979.

Again, I would like to welcome both the American and Soviet participants of the joint symposium to the Research Triangle Park, North Carolina, and especially to our laboratory, the Industrial Environmental Research Laboratory.

The general chairman of the program is Mr. Jim Abbott and he has done an excellent job working with our Soviet colleagues in organizing this symposium. I am sure we will have a successful exchange of information during the symposium and afterwards in planning our efforts for the next symposium and future cooperative endeavors.

---

*Deputy Director, Industrial Environmental Research Laboratory, Research Triangle Park, N.C.

OVERVIEW OF ELECTROSTATIC PRECIPITATOR APPLICATIONS AND RESEARCH IN THE UNITED STATES

L. E. Sparks*

Abstract

A broad overview of major electrostatic precipitator applications and research program in the United States is presented in this paper. Major emphasis is on coal-fired utility voiler applications and research sponsored by the Environmental Protection Agency's Industrial Environmental Research Laboratory, Research Triangle Park, N. C. Other applications and research sponsored by Electric Power Research Institute are discussed, but in less detail.

INTRODUCTION

The purpose of this paper is to provide a broad overview of the major electrostatic precipitator (ESP) applications and research programs in the United States. The major emphasis of the paper will be on coal-fired utility boiler applications and on the research sponsored by the Environmental Protection Agency's (EPA) Industrial Environmental Research Laboratory at Research Triangle Park, N. C. (IERL-RTP). The reason for this emphasis is: coal-fired utility boilers are the largest single application of ESP and IERL-RTP is the major sponsor of ESP research.

Many of the topics touched on in this paper will be discussed in detail in other papers presented at this symposium.

APPLICATIONS

Coal-Fired Utility Boilers

More than 95 percent of all particulate control devices now in operation on large utility boilers are electrostatic precipitators. The reason for this dominance is that electrostatic precipitators generally have lower operating and maintenance costs than scrubbers and filters. Also, in cases where the electrical resistivity of the fly ash is not excessive (say 5 x 10^{10} ohm/cm or less at 150° C), the capital costs of electrostatic precipitators may be less than those of competing devices.

The increased use of low-sulfur coal in utility boilers has resulted in increased interest in hot-side electrostatic precipitators and fly ash conditioning as techniques for overcoming the adverse effects of the high electrical resistivity of fly ash from low-sulfur coal. Several firms are selling conditioning systems and conditioning agents. Sulfur trioxide is still the major conditioning agent, but several proprietary agents such as those developed by Appollo chemical are being used. Available data, e.g., Sparks

---

*Particulate Technology Branch, Environmental Protection Agency, Industrial Environmental Research Laboratory, Research Triangle Park, N.C.

1976 (ref. 1), indicate that conditioning agents can improve collection of high-resistivity fly ash. It appears that conditioning is a reasonable solution for retrofit situations.

Hot-side electrostatic precipitators (the electrostatic precipitator is located ahead of teh air heater) have been successfully used on several boilers firing low-sulfur coal. In general, the success of hot-side electrostatic precipitators located in the Eastern U.S. has been greater than the success of those located in the Western U.S. However, hot-side precipitators capable of meeting EPA standards have been successfully operated in both parts of the U.S. At present, there is no clear cut preference among all utilities and vendors for either hot-side or large cold-side electrostatic precipitators for low-sulfur coal applications. Both types of electrostatic precipitators have been able to achieve very high particulate removal efficiencies and both have their proponents (ref. 1).

Other Applications

Although large utility boilers are the major application of electrostatic precipitators, they are also widely used in other industries.

Hot electrostatic precipitators are used to control the emissions from cement plants. Nichols and McCain, 1975 (ref. 2), report performance data for such an application which show that very high particulate removal efficiencies are possible. High-efficiency electrostatic precipitators are used in the pulp and paper industry with good success, (see Gooch et al., 1976 [ref. 3] and Paul, 1975 [ref. 4]). Electrostatic precipitators are widely used in both the ferrous and nonferrous metal industries. Their use in these industries was the topic of an EPA sponsored symposium in 1977. Wet electrostatic precipitators have been successfully applied to several industries, (see Gooch and Dean, 1976 [ref. 5]). Other applications of electrostatic precipitators are reviewed by White 1975 (ref. 6).

Two-stage electrostatic precipitators have successfully applied to many sources where hydrocarbon mists must be collected. These two-stage electrostatic precipitators have been able to eliminate the blue haze from many operations.

ELECTROSTATIC PRECIPITATOR DESIGN

The design and selection of electrostatic precipitators for specific applications is difficult and it is generally based on emperical relationships. Each vendor, consultant, and user has his own formulas. Often, each of these formula predicts a different specific collector area for the same application. Several investigators have attempted to develop mathematical models to bring some order to the existing chaos. The most successful of these models (success being defined as an ability to predict both overall mass and fractional efficiencies) is the EPA model developed by Southern Research Institute and described by Gooch et al (ref. 7).

RESEARCH AND DEVELOPMENT

Because dusts with high electrical resistivity are difficult to collect in electrostatic precipitators, most of the research sponsored by EPA and others is aimed at one or more aspects of the resistivity problem. Research on high resistivity generally falls into three areas--prediction of resistivity, reduction of resistivity by conditioning, and elimination of resistivity problems by redesign of electrostatic precipitators.

Bickelhaupt (refs. 8,9) has had some success in predicting electrical resistivity of fly ash from coal and ash chemical composition data. However, the role of sulfur trioxide in resistivity has not yet been successfully incorporated in his work. The Electric Power Research Institite (EPRI) is sponsoring resistivity prediction work based on minicombustors.

EPA has developed a fly ash conditioning system based on sodium carbonated injection. Several companies, as mentioned earlier, have developed proprietary conditioning agents. The overall environmental impact of fly ash conditioning is a major concern. EPA is sponsoring research to determine what the environmental impact may be. This program is just underway and only one test reported by Sparks (ref. 10) has been completed.

Perhaps the most exciting research is that aimed at defeating resistivity caused problems by redesign of electrostatic precipitators. EPA, EPRI, and others are sponsoring work in this area. EPRI has announced plans for large pilot scale tests of their system this year. The EPRI system is based on a high intensity ionizer developed by Air Pollution Systems in Seattle, Washington.

The system being developed by EPA is based on particle charging work conducted at Southern Research Institute. The EPA system is being evaluated at small pilot plant scale which will be followed by large pilot scale demonstration. Successful completion of these two projects will significantly reduce the cost of controlling particulate emissions from sources that produce high resistivity dusts.

EPA and EPRI have both sponsored research on rapping-reentrainment in electrostatic precipitators. This work is discussed in a paper to be given later during this symposium.

EPA is sponsoring research to allow prediction of the electrical operating point of full-scale precipitators. EPA is also sponsoring research to determine the applicability of electrostatic precipitators for controlling particulate in advanced energy processes. Most of these processes require particulate cleanup at high temperatures and pressures. This work is not yet complete, but preliminary results indicate that the basic physics are favorable.

CONCLUSIONS

Electrostatic precipitators are an important tool in keeping the environment clean. The overall outlook is that they will continue to be chosen for high-efficiency particulate control of large gas volumes.

The successful completion of ongoing research is likely to improve the performance and reduce the cost of electrostatic precipitators--especially for high-resistivity dusts.

REFERENCES

1. L. E. Sparks, "Electrostatic Precipitator Options for Collection of High Resistivity Fly Ash," Proceedings Conference on Particulate Collection Problems in Converting to Low Sulfur Coals, G. B. Nichols, Compiler, EPA-600/7-76-016, NTIS PB 260-498/AS, 1976.

2. G. B. Nichols, and J. D. McCain, "Particulate Collection Efficiency Measurements on Three Electrostatic Precipitators," EPA 600/2-75-056, NTIS PB 248-220/AS, 1975.

3. J. P. Gooch, G. H. Marchant, and L. G. Felix, "Particulate Collection Efficiency Measurements on Electrostatic Precipitator Installed on a Paper Mill Recovery Boiler," EPA-600/2-76-141, NTIS PB 255-297/AS, 1976.

4. J. E. Paul, "Application of Electrostatic Precipitators for the Control of Fumes from Low Odor Pulp Mill Recovery Boilers," Symposium on Electrostatic Precipitators for the Control of Fine Particles, C. E. Feezel, Editor, EPA-650/2-75-016, NTIS PB 240-440/AS, 1975.

5. J. P. Gooch and A. H. Dean, "Wet Electrostatic Precipitator System Study," EPA-600/2-76-142, NTIS PB 257-128/AS, 1976.

6. H. J. White, "Role of Electrostatic Precipitators in Particulate Control--A Retrospective and Prospective View," Symposium on Electrostatic Precipitators for the Control of Fine Particles, C. E. Feazel, Editor, EPA-600/2-75-016, NTIS PB 240-440/AS, 1975.

7. J. P. Gooch, J. R. McDonald, and S. Oglesby, "A Mathematical Model of Electrostatic Precipitation," EPA 650/2-75-037, NTIS PB 246-188/AS, 1975.

8. R. E. Bickelhaupt, "Influence of Fly Ash Compositional Factors on Electrical Volume Resistivity," EPA 650/2-74-092, NTIS PB 237-698/AS, 1974.

9. "Effect of Chemical Composition on Surface Resistivity of Fly Ash," EPA-600/2-75-017, NTIS PB 244-885/AS, 1975.

10. L. E. Sparks, "Effect of a Fly Ash Conditioning Agent on Power Plant Emissions," EPA-600/7-76-027, NTIS PB 262-602/AS.

THE PRESENT STATUS AND PROSPECTS OF DEVELOPMENT OF STUDIES OF ELECTRICAL GAS CLEANING IN THE U.S.S.R.*

I. K. Reshidov, I. A. Kizim, I. V. Yermilov, V. M. Tkachenko (U.S.S.R.)

Abstract

Research trends in the U.S.S.R. are presented in the area of electric gas cleaning. The solution of problems on preventing nonpermissible pollution of the atmosphere is being realized through the study and development of new types of electrostatic precipitators, the development of units for electric gas cleaning for various branches of industry, the development of methods for intensifying the operation of these units, and increasing the efficiency of operating electrostatic precipitators by redesigning them. NIIOGAZ conducted a number of studies of electrostatic precipitator electrode systems, established rational geometric dimensions for needle-type coronal electrodes, and showed their essential advantage in comparison to wire-type electrodes. The coronal discharge characteristics were determined for various systems of electrodes with respect to a variation in air temperature from 20° to 400° C and pressure from 0.1 to 0.6 MPa. It was shown that it is possible to achieve high efficiency cleaning of blast furnace gas at higher pressure and temperature in a dry plate type electrostatic precipitator. Procedures have been worked out for calculating the dynamic characteristics of electrode systems and conditions for their rapping. Studies are being conducted on intensifying the operation of high resistivity dust. Studies are also being conducted on predicting back corona manifestations, mathematical modeling of electrostatic precipitators, and electric power supply, etc.

INTRODUCTION

Growth of industrial production is accompanied by increased gas volumes to be cleaned before they are discharged to the atmosphere.

A principal control device used in the U.S.S.R. for particulate collection is the electrostatic precipitator. This device treats about 50-60 percent of the total gas volume to be cleaned. ESPs have found wide usage in utilities, ferrous and nonferrous metallurgy, rock product applicaton, chemical and other industries.

A wide range of measures are carried out to solve air pollution problems. The following are of considerable importance:

1. Study and development of new ESP types.
2. Extend application of ESPs to new sources and improve collection efficiency.
3. Reconstruction of existing ESPs to improve collection efficiency.

---

*For further information regarding the material in this paper, please contact I. K. Reshidov, U.S.S.R. 113105, Moscow, M-105, 1st Nagatinsky Pass., 6, NIIOGAZ.

Study and Development of New Types of ESPs

To meet the goal of environmental protection under the conditions of growth of industrial production, it is necessary that the newly installed ESPs provide persistent cleaning efficiency at the level of 99-99.5 percent. In perspective, there is a need for ESPs with collection efficiency up to 99.9 percent, mainly for industries with high inlet dust concentration and for high-capacity units. The requirement for installation of more efficient ESPs makes necessary constant development of more effective and reliable systems. This development is conducted on the basis of the investigation of electrical and dynamic characteristics of electrode systems and the study of reliability and operating life of the system.

Investigation of the characteristics of ESP electrical fields by method of probe characteristics with and without reverse corona, study of breakdown voltages and particle drift velocities, and examination of efficiency of new electrode systems in the industrial conditions makes it possible to find scientific grounds that account for expediency of using needle electrodes with rational geometric dimensions. It was shown that electrodes of this type surpass by far other types of electrodes. They provide low voltages of corona ignition, higher values of corona currents, and particle drift velocity. Needle electrodes permit even distribution of corona currents on the surface of precipitating electrodes, and this decreases the probability of reverse corona formation.

Based on the results of this investigation, uniform horizontal plate ESPs UG-type with needle corona electrodes and C-shape precipitating electrodes were developed and are being manufactured. They have found their application in various industries. In order to find other ways to improve ESP collection efficiency, studies of combined electrode systems that form interchanging fields of corona discharge and electrostatic field are being undertaken. To investigate such complex fields, a new experimental method to determine vector component of field intensity was developed. It is based on photographing the trajectory of a preliminary charged metal ball in the investigated field.

NIIOGAZ has studied characteristics of corona discharge for various electrode systems when the temperature changed from 20 to 100° C and pressure from 0.1 to 0.6 MPa. The possibility of high-efficiency cleaning of blast furnace gases in a dry plate ESP at a gas pressure of about 0.3 MPa and temperature 230° C was proven at a commercial pilot plant. This is of extreme importance for utilization of energy from blast furnace gas in utility gas-expansion turbines.

To achieve reliable and effective performance of ESPs, it is really important to determine correctly the mass of the rapping hammers in relation to physical and chemical properties of the dust and geometry of electrodes.

For several years, theoretical and experimental studies of acceleration and frequency of vibration of electrodes when rapped were conducted in NIIOGAZ. On the basis of these investigations, a method of calculating dynamical characteristics of electrode systems was developed. This method is now used when new electrode systems are designed.

Practical application shows that the most important characteristics of ESP performance is reliability of its instrument operation. Highly reliable equipment provides stable collection efficiency within the whole period of ESP operation between overhauls. Studies of the reliability of ESPs in actual field operating conditions allows development of recommendations for improving the existing apparatus.

On the basis of these investigations, new types of electrostatic precipitators are being developed, i.e., horizontal ESP for industrial application at temperature up to 330° C. Uniform vertical UV-type ESPs providing an efficiency of about 99.0-99.4 percent are going to be put on serial production. Hot-side ESPs (T up to 450° C) are planned for use in power generation. An ESP has been installed before the air preheaters on a power plant burning high-sulfur, heavy oil. Application of such precipitators, besides reducing the emission level, increases the efficiency of power unit utilization by reducing contamination of the air preheater surface. In the near future, a hot-side ESP will be installed to work out problems connected with collection of high-resistivity fly ash of ekibastuzsk coak, in which the U.S.S.R. is rich.

Development of ESPs for Various Applications and Methods to Increase Particulate Collection Efficiency

Experience in ESP application shows that the auxiliary equipment associated with the ESP for most industrial gases is comparatively uniform and varies mostly in geometrical dimensions. However, the auxiliary equipment for a specific application must almost always be individually designed.

The installation of an ESP besides actually installing the ESP itself comprises:

1. gas-distributing system,
2. dust collecting system,
3. gas conditioning system, and
4. power supply system.

These systems can vary even for the same industrial applications due to the peculiarities of gas feeding and dust removal systems.

While designing the ESP, it is necessary to determine overall dimensions and capacity of the precipitator for the required collection efficiency. Due to the fact that installations with the same design requirements are quite rare, design based on parameters of analogous ESP installations can cause serious mistakes. Design can be done more precisely with the help of methodologies where all the factors influencing the efficiency of cleaning are reflected. The U.S.S.R. ESP mathematical model recently developed begins to find application in design practice. To have a wide use of this method it is necessary to develop procedures forecasting electrical parameters of ESP performance, physical and chemical properties of dust-laden gas flow, and their interconnection.

For effective operation of the ESP installation, questions of gas distribution are of vital importance. In the U.S.S.R., the choice of a gas distributing system is done on the basis of modeling of systems in the scale 1:10 and 1:20. However, now the atlas on utilized gas distributing diagrams has been developed. It permits selection of the optimum variant of diagram for typical ESP arrangement.

It is known that when specific resistivity of collected dust is high, reverse corona appears in the ESP, and that reduces the efficiency of gas cleaning. As it follows from numerous studies conducted in the U.S.S.R. and abroad, specific resistivity of dust is considerably dependent on temperature, humidity, and chemical composition. Therefore, to eliminate reverse corona in the ESP, conditioning systems are employed, i.e.:

1. systems controlling gas humidity and gas temperature, and
2. systems controlling chemical conditioning of gases.

Systems for chemical conditioning of gases are not widely spread in the U.S.S.R. due to the complexity of their performance. More widely used are systems for controlling humidity and temperature of gases, particularly in cement application. Systems for reducing temperature and humidity of gases are now planned for application in heat- and power-engineering to remove fly ash of ekibastuzsk and kuznetzk coal.

So, the question of forecasting reverse corona formation turns out to be the most important one when choosing optimum working temperature and humidity of gases. One cannot always answer this question correctly by measuring specific resistivity of dust. That is why methods directly forecasting reverse corona are being developed.

Obvious increase in efficiency of the ESP can be achieved by optimization of the rapping schedule. Studies undertaken in the U.S.S.R. make it possible to predict the relationship of collection efficiency to mass of dust precipitated on electrodes (dust volume). It turned out that when dust volume increased to a certain limit, collection efficiency increased too. But further growing of the dust layer results in its self-collapsing and reducing of efficiency. The relationship of optimum mass on electrodes to specific resistivity of dust has been found. On the basis of these investigations, methodology for determining optimum intervals of electrode rapping was developed. Presently, this methodology has been applied in the cement industry, heat- and power-engineering, and other industry branches. Optimization of rapping intervals alongside of raising cleaning efficiency makes it possible to increase reliability of performance of ESPs.

Practice shows that optimization of working regimes of power supply units is a reserve to increase ESP efficiency. Optimization of regimes means setting up an optimum spark rate that is supported by a control diagram. Here, a method developed in NIIOGAZ of adjusting units by a subsequent field is used. Transducers for determination dust concentration in gas are supposed to be also used for this purpose.

To take the best advantage of reserves of ESP power supply, NIIOGAZ is conducting studies concerning optimization of voltage control, impulse power supply of ESP, etc.

Development and Realization of Out-Of-Date ESP Models Reconstruction

The above mentioned methods for increasing collection efficiency have found wide application while modernizing out-of-date ESPs. In the cement industry, power-engineering, and other branches of industry, out-of-date precipitators are being systematically replaced. The following technical innovations account for increasing cleaning efficiency of modernized ESP installations:

1. substitution of out-of-date, low-efficiency equipment for more modernized equipment,
2. increase of ESP plate area,
3. improvement of gas distribution,
4. optimization of electrode rapping intervals and supply unit working regimes,
5. increase of reliability of power supply unit performance, and
6. technological preparation of gases to be cleaned.

The reconstruction of gas cleaning installations at the Cherepetskaya, Pribaltijskaya, and Troitzkaya hydroelectric power stations, and Bryansk and Novorossijsk cement plants have shown that gas cleaning efficiency can be raised up to 98-98.5 percent. Further increase of efficiency can be achieved due to the application of 12-meters-high precipitating electrodes instead of those 8-meters-high that were installed on the out-of-date precipitators. Application of high-efficiency ESPs at the industrial sites under construction and modernization of out-of-date apparatus of electrical gas cleaning makes it possible to prevent atmospheric pollution above the standards.

TECHNQUES OF MODELING GAS FLOW IN ELECTROSTATIC PRECIPITATORS IN THE U.S.

Samuel Bernstein*

Abstract

The construction of very large precipitators that satisfy high efficiency requirements for the collection of fine particles poses a challenging design problem. Flow modeling studies, when combined with appropriate analysis, provide a cost-effective design tool. In this paper the modern approach to flow modeling is reviewed by a discussion of the objectives and requirements of flow modeling, modern experimental methods, and advanced techniques. Proper flow simulation requires the appropriate selection of model scales and instrumentation. Experimental techniques have been refined through the use of laser light for smoke flow visualization, through the measurement of velocities with Laser Doppler Anemometry, through automated data acquisition systems, and through computational techniques.

INTRODUCTION

The construction of very large precipitators (typically designed to treat several million cubic feet of gas per minute) and the requirements for fine particle collection have stimulated interest in careful gas flow modeling. Although gas flow modeling studies were introduced into the precipitator field approximately 30 years ago (ref. 1), relatively little research on this subject has been published in the open literature, and there are conflicting reports on the usefulness of flow modeling studies (refs. 2,3,4). The purpose of this paper is to review modern approaches and techniques in flow modeling for precipitator studies. The objectives and requirements of flow modeling studies and modern experimental methods are reviewed and advanced techniques are discussed.

OBJECTIVES AND REQUIREMENTS OF FLOW MODELING FOR INDUSTRIAL ELECTROSTATIC PRECIPITATORS

Flow modeling studies provide flow simulation in a scaled-down model of the precipitator installation. Simulation may be used for precipitator development work or for modeling an industrial installation. In precipitator development work the simulation requires modeling the fundamental physical parameters of the precipitator: the electric forces, the fluid dynamic forces, and the particle dynamics. In the modeling of an industrial installation, the emphasis is on the effect of the particular ducting arrangement on the gas flow distribution, and, consequently, the parameters of interest are the fluid dynamic forces and the particle dynamics. This type of simulation is unique in every installation because each installation requires a different system for ducting around the precipitator box.

The objectives of flow modeling studies for an industrial installation are to simulate the flow distribution and the total pressure drops in a given installation. Flow nonuniformities reduce the efficiency of the precipitator since regions of high or low velocities do not have the optimum flow conditions. In

---

*Flow Research Company, Kent, Washington.

addition, the regions of relatively high velocity provide locally high shear and therefore enhance reentrainment of collected particles and increase the pressure drop through the precipitator. If the flow is also separated, the resulting structural vibration may reduce the life cycle of the precipitator.

Recognition of the importance of flow uniformity and flow models is often stated in the contract for the precipitator work, as has been suggested by the Industrial Gas Cleaning Institute (IGCI) (refs. 5,6). However, the IGCI suggests specific values for gas uniformity, and, based on the above discussion, the requirement in each installation should be reviewed on a case-by-case basis.

The requirement for relatively uniform flow is relevant for precipitators with either laminar flow or turbulent flow; however, in practical installations, the flow is always turbulent. Unfortunately, the effect of the turbulence on the precipitator is not completely understood, and only some general observations are possible.

The turbulent shear force near the collector plate, τ_t, may be expressed by (see, for example, Launder, et al. [ref. 7]):

$$\tau_t = \mu_{eff} \, \partial u/\partial y \ ,$$

where $\partial u/\partial y$ is the mean velocity gradient near the collector plate and μ_{eff} is the effective turbulent viscosity. The effective viscosity of the turbulent flow is much larger than the molecular viscosity in laminar flow, and it is proportional to the turbulent kinetic energy of the fluid and to the turbulence length scale. Consequently, low reentrainment losses will be associated with flows of relatively low turbulence intensity and small-scale turbulence.

Usually, in flow modeling studies, internal-flow correction devices are introduced to improve the flow distribution and total pressure losses. However, flow modeling studies, if performed early enough in the design, could also suggest a more cost-effective ducting arrangement.

MODERN EXPERIMENTAL METHODS OF FLOW MODELING

Effective flow modeling is usually combined with a theoretical analysis of the flow. A preliminary analysis identifies the appropriate scale for the model, the appropriate instrumentation, and the approximate errors that would result from imperfect simulation and measurements.

Model Scales

As suggested in the previous section, the common flow modeling for industrial installations requires the simulation of the fluid dynamics and particle dynamics. The relevant similarity requirements for the fluid dynamic simulation are geometric similarity and similarity of Reynolds number. (The similarity parameters may be derived by a dimensional analysis; see, for example, Johnstone, 1957 [ref. 8].)

Typical plant conditions for a cold-side precipitator include a temperature of 150° C (300° F) and flow rates of several million cubic feet per minute. The resulting range of Reynolds numbers is typically between 10^4 and 10^5, based on the inlet duct diameter. In model studies it is not possible to substantially increase the gas flow velocity above that of the full-scale case because of compressibility effects, and, consequently, it is not practical to match the Reynolds number of the model with that of the full-scale plant.

The consequence of having a lower Reynolds number in the model study may be estimated as long as the flow in the scale model is turbulent. The boundary layer along the model walls and along the collector plates will be thicker than in the full-scale installation, and it might be necessary to reduce the number of collector plates to avoid relaminarization of the flow between the plates. The measured pressure drop coefficients, which are also functions of the Reynolds number, will be higher in the laboratory and should be corrected accordingly. The accepted practice is to use 1/16 scale models; however, the particular choice of scale depends on the complexity of the installation, and to some extent, on the required accuracy.

Simulation of particulate matter in the gas flow model requires particles with sizes proportional to the model scale. The behavior of these very fine particles may be simulated in the model by the use of particles with larger diameters but lower densities. The use of cork of a given particle size to simulate fly ash of smaller size provides the desired simulation of a lower settling time in the ducts and a shorter relaxation time to fluid forces.

Flow Visualization

Flow visualization provides only a qualitative picture of the flow; however, the early identification of separated regions and flow angularities may significantly reduce the necessary testing time. One of the most common techniques for flow visualization is the use of tufts (ref. 9). In this technique, lightweight yarn tufts are mounted on a rake inside the model to identify local flow patterns.

Another common method of flow visualization is the introduction of smoke flow into the channel. Several chemical agents are used to generate the smoke, including titanium tetrachloride, tin tetrachloride, heated kerosene, and smoke bombs, most of which either have objectionable odors or are poisonous (ref. 9). We have obtained high-quality smoke flows without the above limitations in flow tests with the use of a smoke generator designed at the University of Washington (ref. 10).

Velocity Distribution

The velocities of interest for electrostatic precipitator studies range from those in the high-speed region in the ducts, with a typical velocity of 17 m/s (approximately 50 ft/s) to the velocity in the low-speed region in the box, which is between 1.5 and 5 m/s (approximately 5 to 15 ft/s). Pitot tubes and yaw heads (ref. 9) are often used in the high-speed range. There are several designs of yaw heads with several arrangements of pressure taps on a small sphere. The flow direction may be computed by comparing the pressure difference from several locations on the sphere. In practice, the yaw heads and pitot tube are limited to velocities above 3 m/s (10 ft/s), and their response time does not allow the measurement of fluctuations of the turbulent flow at a given location.

Hot-wire anemometers are used for measurements of flows at low velocities. The major advantages of the hot wire are its sensitivity at low speeds and its fast response (typically, the hot wire provides frequency responses of 100 kHz or better [ref. 11]). Hot wires require careful handling and frequent calibration. The more common single wire is sensitive to the flow magnitude only; however, a crosswire arrangement, which allows limited determination of the flow direction in a plane, is also available.

Pressure Measurements

Total pressure losses are measured by traversing a section of the model with a total pressure probe and micromanometer. As discussed above, the measured pressure loss coefficient should be corrected to account for the variation in Reynolds number. (Idelchick [ref. 12] gives some empirical data that contain the effect of the Reynolds number.)

ADVANCED EXPERIMENTAL TECHNIQUES

Recent developments in laser technology and minicomputer systems offer significant improvements in flow visualization techniques, remote velocity measurements, and automatic data acquisition methods. Modern computational techniques for turbulent flows have also recently attained a high degree of refinement to support flow modeling work as a flexible and cost effective design tool.

We recently obtained significantly improved smoke flow visualization pictures when the smoke flow was illuminated by a laser light. In this technique, a laser beam is directed to a cylindrical glass rod, which scatters the beam. This scattered beam forms a thin sheet of light, which selectively illuminates a thin sheet of smoke. By moving the beam, we can move the illuminated plane to view selected planes of the model with fine detail. This arrangement is illustrated in figure 1.

A second implementation of the laser beam is the remote measurement of the gas velocity with Laser Doppler Anemometry (LDA). The basic principle of operation for LDA is to direct two laser beams to a point in the model where the velocity will be measured. The two beams form a dark and light fringe pattern, as shown in figure 2. As the particles in the gas pass through the fringe pattern, they scatter light pulses at the Doppler frequency, a frequency proportional to their travel speed. The scattered light is then collected by a photodetector, and the data is analyzed to compute the flow velocity at the desired point.

There are several arrangements of LDA systems for measuring either single or multiple components of the flow velocity. These arrangements are available as off-the-shelf items from several manufacturers (i.e., DISA Electronics, Spectron, Thermosystems). LDA is a remote sensor of the gas flow (it measures the gas flow by measuring fine-particle trajectories), and it offers fast response; however, the system is quite costly compared to hot-wire anemometers.

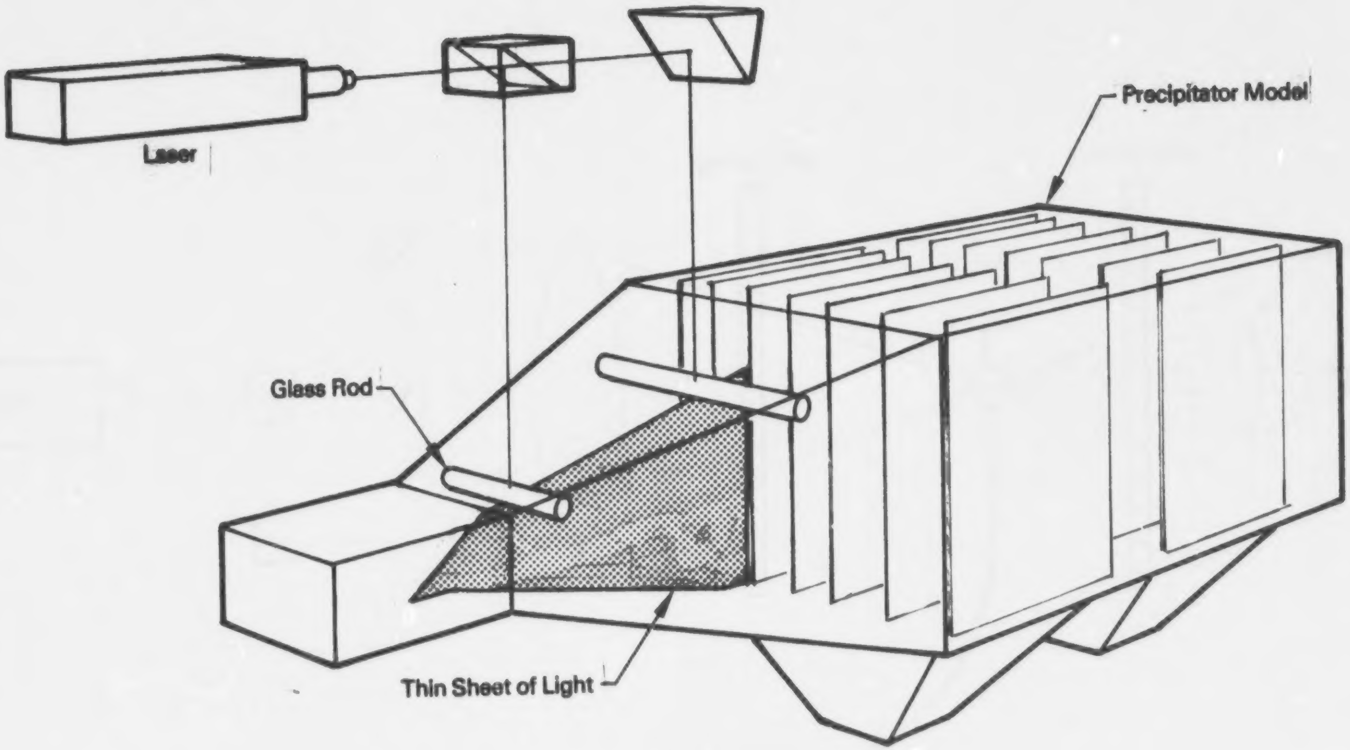
Laser
Precipitator Model
Glass Rod
Thin Sheet of Light

Figure 1. Smoke flow visualization using laser beam illumination.

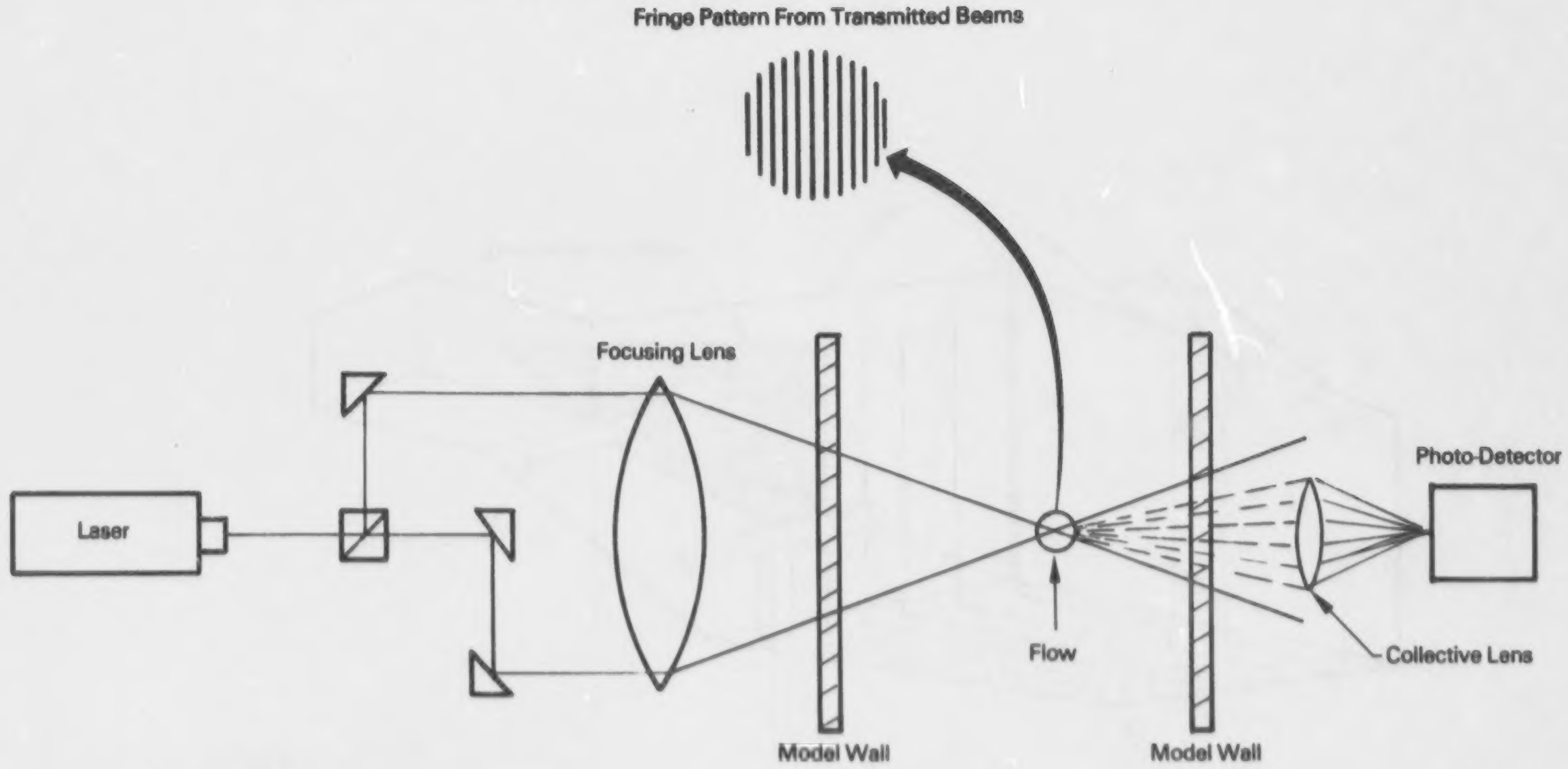
Fringe Pattern From Transmitted Beams
Focusing Lens
Photo-Detector
Laser
Flow
Collective Lens
Model Wall
Model Wall

Figure 2. Schematic illustration of a laser doppler anemometry setup.

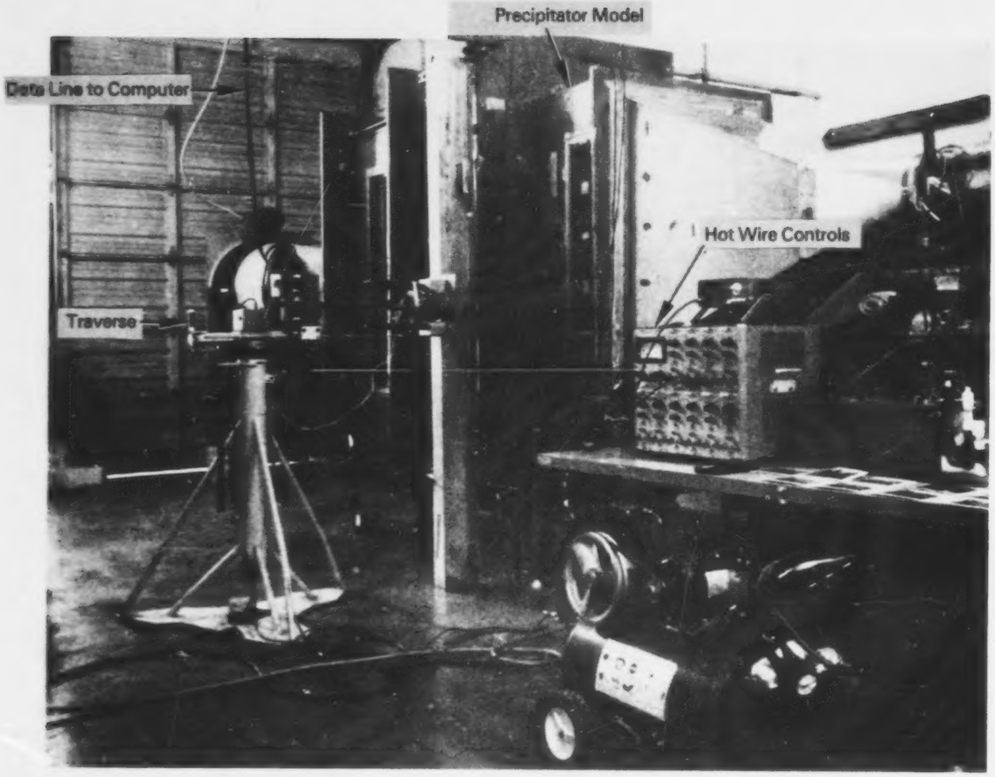
Precipitator Model
Data Line to Computer
Hot Wire Controls
Traverse

Figure 3. Automated traverse system for measuring velocity in an electrostatic precipitator model.

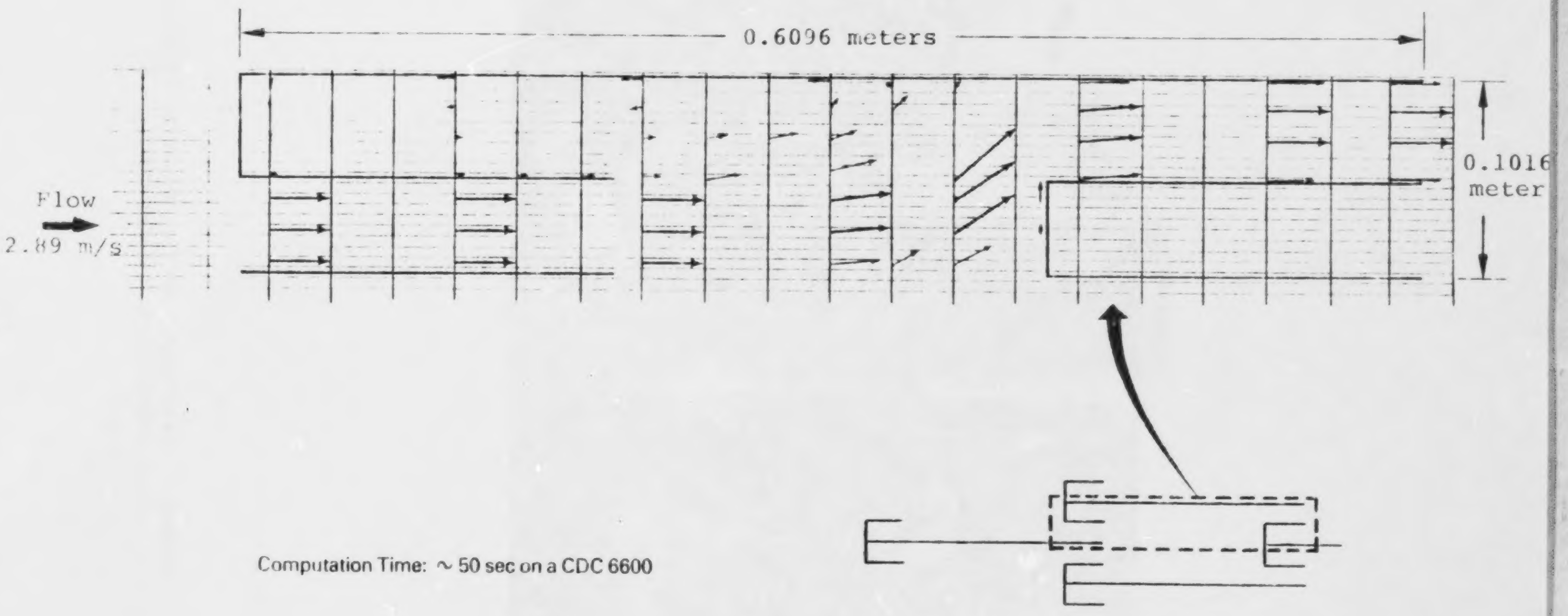
0.6096 meters
0.1016 meter
Flow
2.89 m/s

Computation Time: ~ 50 sec on a CDC 6600

Figure 4. Computed velocity field of turbulent flow around a precipitator structure.

The effectiveness of laboratory modeling has been further improved by automating velocity data acquisition. In one such system, two hot-wire anemometers are mounted on the rod of an automated traverse system, as shown in figure 3 (ref. 13). The two wires reduce the distance the traverse system must travel to measure the flow across the model. The traverse rod position is set by a stepping motor, which is controlled by a Nova 800 minicomputer. The traversing rod is stopped at each stepping interval for several tenths of a second while a few thousand data points are recorded. The minicomputer stores the calibration curves for the hot-wire anemometers, and the data from the hot-wire anemometers are collected, reduced, plotted, and printed out by the computer in several minutes. Data analyses and velocity histograms may also be generated by the minicomputer at a substantial savings of manpower.

Recent developments in computational techniques for turbulent flows have increased their utility in supporting flow modeling work. In this approach, the turbulent flow around a complex precipitator component is computed using a finite difference scheme for the complete flow equations including an experimentally verified turbulence model. Such a computer code may be easily modified to predict the effect of changing the local geometry of the duct, and the addition of flow correcting devices near a bend. Additional computation may be performed to compute particle trajectories using the detailed flow solution to calculate the forcing functions on the particles. An example of flow field calculation around a complex geometry is illustrated in figure 4. The arrows in the figure represent the magnitude and direction of the averaged velocity around the structure, and the grid represents the number of computed points in the finite difference scheme. The versatility and economy of the computational method may save considerable effort in evaluating a precipitator during flow modeling studies.

CONCLUSIONS AND RECOMMENDATIONS

The assessment of the status of experimental techniques for modeling flow in electrostatic precipitators may be summarized as follows: Modeling is a cost-effective design tool when the model is properly designed and analyzed. The data generated in flow modeling require a careful assessment of their experimental limitations.

The accuracy of the experimental predictions will continue to improve with the introduction of remote sensors (i.e., LDA) and modern automated data acquisition systems. These systems reduce the sensors' interference in the flow and also increase the reliability of the data.

Numerical techniques will play a greater role in supporting flow modeling work as a cost effective tool.

More research is needed to identify the role of fluid dynamic turbulence in electrostatic precipitators although it may be argued, on basic physical principles, that the effect of turbulence is significant and the turbulence quantities should therefore be measured and documented during model studies.

REFERENCES

1. H. J. White, Industrial Electrostatic Precipitation, Addison-Wesley Publishing Co., Reading Massachusetts, 1963.

2. C. L. Burton and D. A. Smith, "Precipitator Gas Flow Distribution," presented at EPA and Southern Research Institute Symposium on Electrostatic Precipitators, Pensacola, Florida, September 20 - October 2, 1974.

3. J. B. Opfell and W. T. Sproull, "Limitations of Model Studies in Predicting Gas Velocity Distribution in Cottrell Precipitators," Ind. Eng. Chemical Proc. Design Develop., Vol. 4, No. 2 (1965), pp. 173-177.

4. D. J. Gibson, "Scale Model Flow Testing Upgrades Cost-Effectiveness," Research/Development, Vol. 27, No. 11 (1976).

5. Industrial Gas Cleaning Institute, "Criteria for Performance Guarantees," Publication No. EP-3, Stamford, Connecticut, 1973.

6. Industrial Gas Cleaning Institute, "Gas Flow Model Studies," Publication No. EP-7, Stamford, Connecticut, 1973.

7. B. E. Launder and D. B. Spalding, Mathematical Models of Turbulence, Academic Press, New York, 1972.

8. R. E. Johnstone and M. W. Thring, Pilot Plants, Models, and Scale-up Methods in Chemical Engineering, McGraw-Hill, New York, 1957.

9. A. Pope and J. J. Harper, Low Speed Wind Tunnel Testing, John Wiley and Sons, Inc., New York, 1966.

10. O. Shindo and O. Brask, "A Smoke Generator for Low Speed Wind Tunnels," Univ. of Wash., Dept. of Aero. and Astro., Technical Note No. 69-1, 1969.

11. G. Comte-Bellot, "Hot-Wire Anemometry," in Annual Review of Fluid Mechanics, M. Van Dyke, W. G. Vincetti, and J. V. Wehausen, Eds., Vol. 8, Annual Reviews Inc., Palo Alto, California, 1976.

12. I. E. Idelchick, "Handbook of Hydraulic Resistance, Coefficients of Local Resistance and of Friction," AEC-TR-6630, 1966, (Russian Translation available through NTIS).

13. S. Bernstein, L. Piper, and E. Murman, "Flow Modeling Studies for the EPRI Advanced Particulte Control Facility," Flow Research Note No. 105, 1976.

INVESTIGATION OF GAS DISTRIBUTION SYSTEMS IN ELECTROSTATIC PRECIPITATORS COLLECTING DUST AND FLY ASH*

I. E. Idelchik, JA. L. Ginzburg, M. O. Shteinberg,
V. P. Alecsandrov, V. S. Korjagin (U.S.S.R.)

Abstract

The objective of studying gas distribution systems is the development of simple and reliable units that ensure the uniform distribution of gas in the active zone of an electrostatic precipitator and in the parallel operating units. This also includes the development of methods for calculating and designing such systems. In accordance with this objective, the authors describe original designs of gas distribution systems along with their characteristics (degree of gas distribution, nonuniformity, and a coefficient of hydraulic drag). Results are given of a study on the distribution of dust along the collector branches and a collector design is proposed that makes it possible to achieve a more uniform distribution of dust. It is noted that the basic results of the studies are generalized in "The Atlas of Gas Air Distribution Units of Various Industrial Equipment" under the authorship of I. E. Idelchik.

Theoretical and experimental works have shown that the efficiency of dust and fly ash collection by electrostatic precipitators depends on the uniformity of gas flow distribution over the apparatus cross section, and if there is a series of electrostatic precipitators connected in parallel, it depends on the uniformity of gas flow distribution over all precipitators.

If the velocities of a gas flow are nonuniform across the precipitator section, the degree of nonuniformity can be described by the coefficient of momentum in the German's equation:

$$M_K = \frac{1}{F}\int_F \left(\frac{V}{V_m}\right)^2 dF$$

In this case, the German's equation has the following form:

$$c = e^{-\frac{1}{K M_K V_m}} \qquad \eta = 1 - e^{-\frac{1}{K M_K V_m}}$$

where Vm = velocity of gas flow in the section, and

K = a coefficient taking into account the electrical and other characteristics of a precipitator.

The dependences in equation (1) were experimentally tested on the pilot-plant electrostatic precipitator, the electrodes of which had the height 1.8 m, and the total length of two electric fields was 5 m. Perforated lattices with various perforation disposition along their height and rotatable plates in the gas conduit were used at the entry to the field *1* to provide various values. The obtained results are given in figure 1. One can see that they confirm the justice of the formula in equation (1) with precision sufficient for practical purposes.

---

* For further information regarding the material in this paper, please contact I. K. Reshidov, U.S.S.R. 113105, Moscow, M-105, 1-st Nagatinsky Pass., 6, NIIOGAZ.

The main volume of work was done with geometrically similar models produced to a scale 1:10-1:20 relative to a full size. The region of the gas conduit feeding the gas to an electrostatic precipitator, the gas distribution system, and the first 1-2 fields of the apparatus were modeled.

We investigated the gas distribution systems in separate electrostatic precipitators with the active height being from 7.2 to 12 m and the active area from 30 to 265 m^2, which were used in dust collectors for large power blocks (from 300 to 800 Mw), in nonferrous metallurgy, and sulfuric acid production.

One of the typical variants of the gas conduits and the gas distribution systems for large electrostatic precipitators used in thermal power production is a vertical pit with baffles and a system of plate perforated lattices (figure 2). The aerodynamics of such a system, which was preliminarily studied by means of model experiments, has been investigated using a pilot-plant electrostatic precipitator of 12 m height. By means of model experiments we obtained Mk = 1.02; by means of plant experiments, Mk = 1.09.

Thus, plant measurements gave results similar to model measurements. This confirmed the competence of gas distribution modeling in electrostatic precipitators.

Besides, the measurements of concentration and particle-size distribution across the active section were made in this electrostatic precipitator. The measurements were made in the mixing chamber between first and second lattices in points 1-6 along three vertical lines (see figure 2). The velocity field is shown in figure 2a, and the dust loading field in figure 2b. These fields are shown in respect to average fields over the active section of the velocity Vm and the dust load μm. One can see that the considered construction of a gas distribution system provides not only a practically uniform velocity field, but also a dust loading field.

In addition to dust loading fields, an appropriate particle-size distribution was determined in each point from 1 to 6. The comparison of particle-size distributions in points 1 to 6 allowed a conclusion to be made about a practically constant fractional composition of particulate matter up to 100 μk over the height of the apparatus at its inlet.

For large degrees of a flow expansion η (ratios of the areas of cross section of active precipitator region and gas feeding conduit), in the range $20 \leq n \leq 50$, the simple and reliable gas distribution system with one perforated lattice and a perforated screen has been developed (figure 3). For a small resistance coefficient related to the velocity at inlet, $\zeta = 1$, such construction provides a satisfactory degree of gas distribution nonuniformity in practice (M = 1.08-1.15).

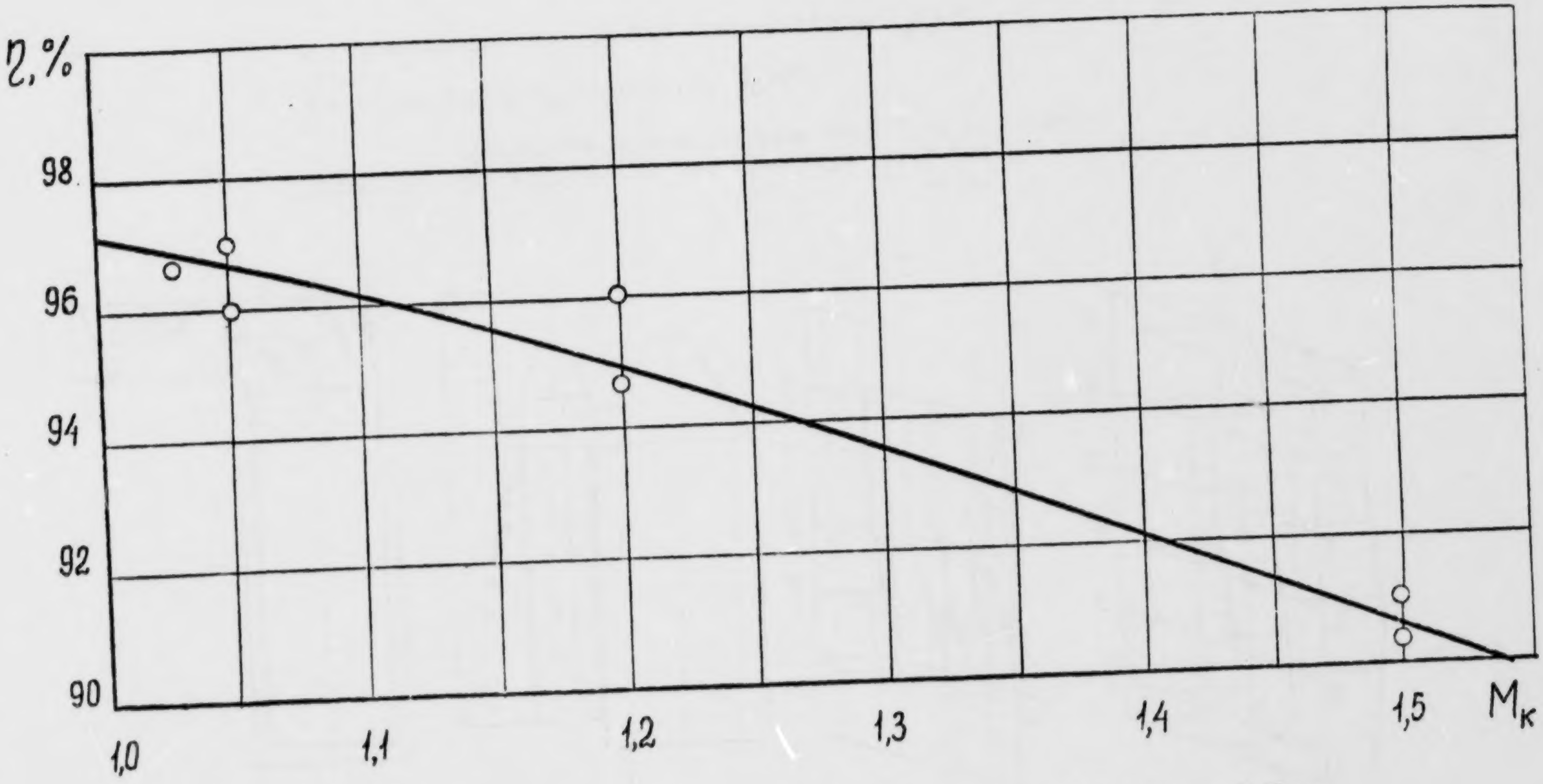

Figure 1. Dependence of precipitator efficiency η on the degree of flow nonunifirmity M_K .

—o— experiment, —— calculation

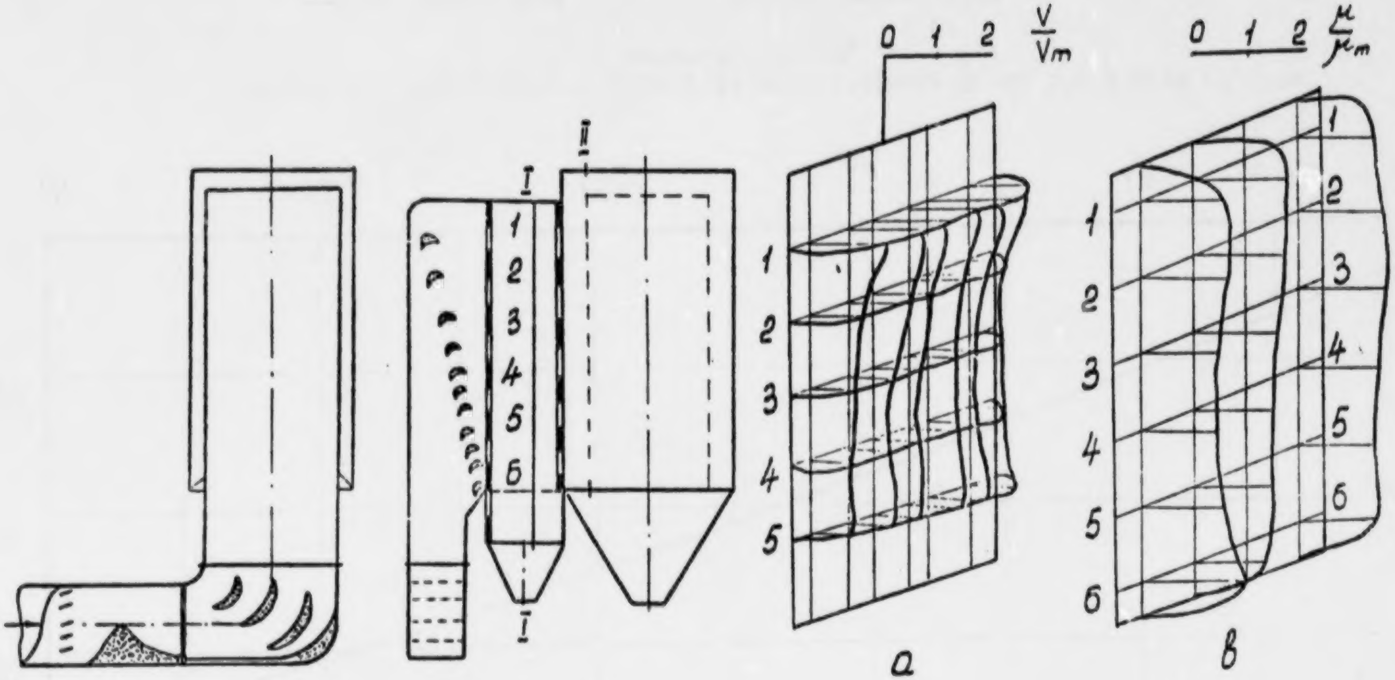

0 1 2 V/Vm
0 1 2 μ/μm
I
II
I
1
2
3
4
5
6
1
2
3
4
5
1
2
3
4
5
6
a
в

Figure 2. Distribtuion of gas flow velocities and fly ash size in the electrostatic precipitator with 12-m electrodes.

a - distribution of velocities V/V_m

b - distribution of fly ash concentrations μ/μ_m

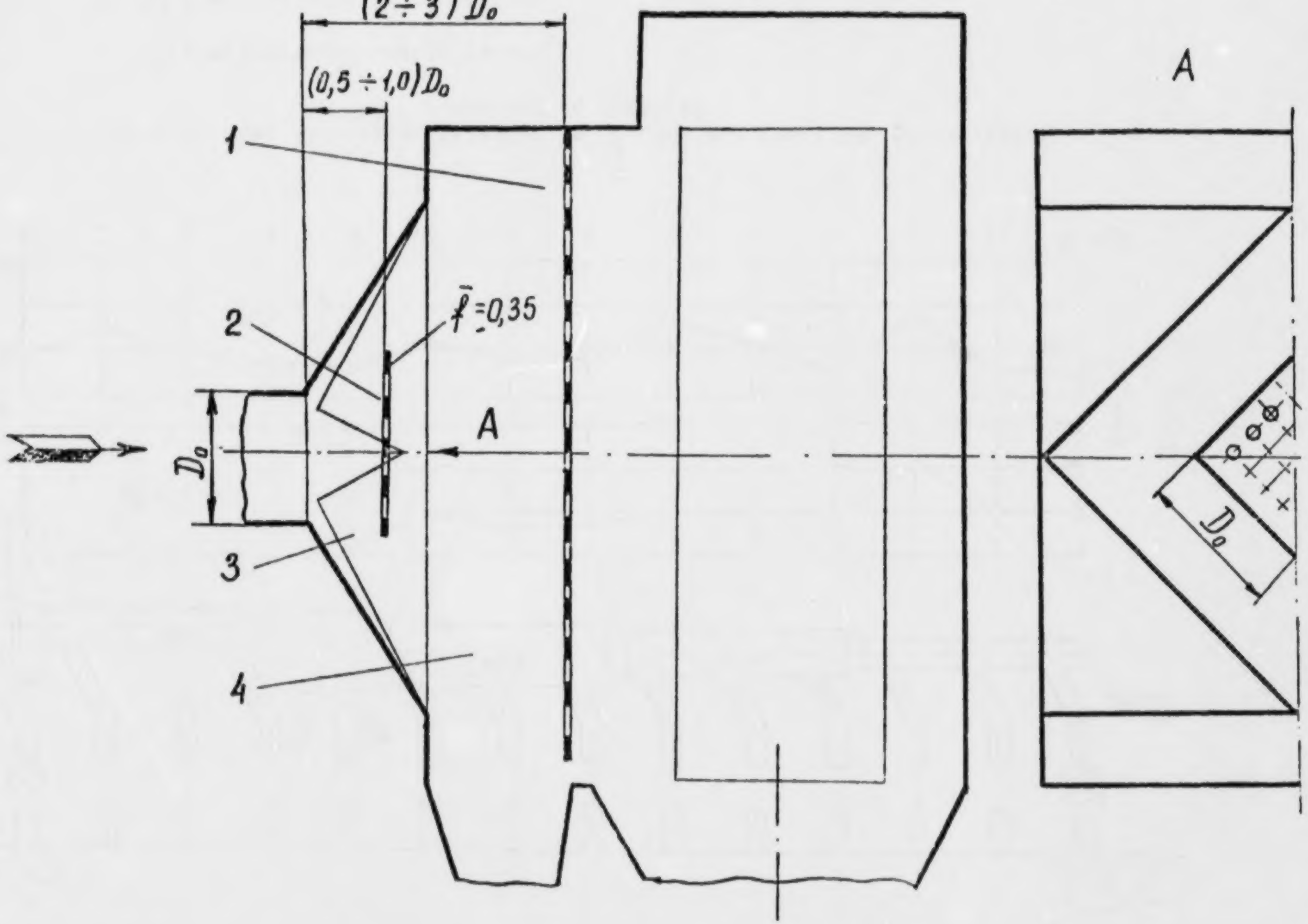
(2÷3) D_o
(0,5÷1,0) D_o
1
2
$\bar{f}$=0,35
3
4
A
D_o
A
D_o

Figure 3. Gas distribution system for electrostatic precipitators with central flow inlet.

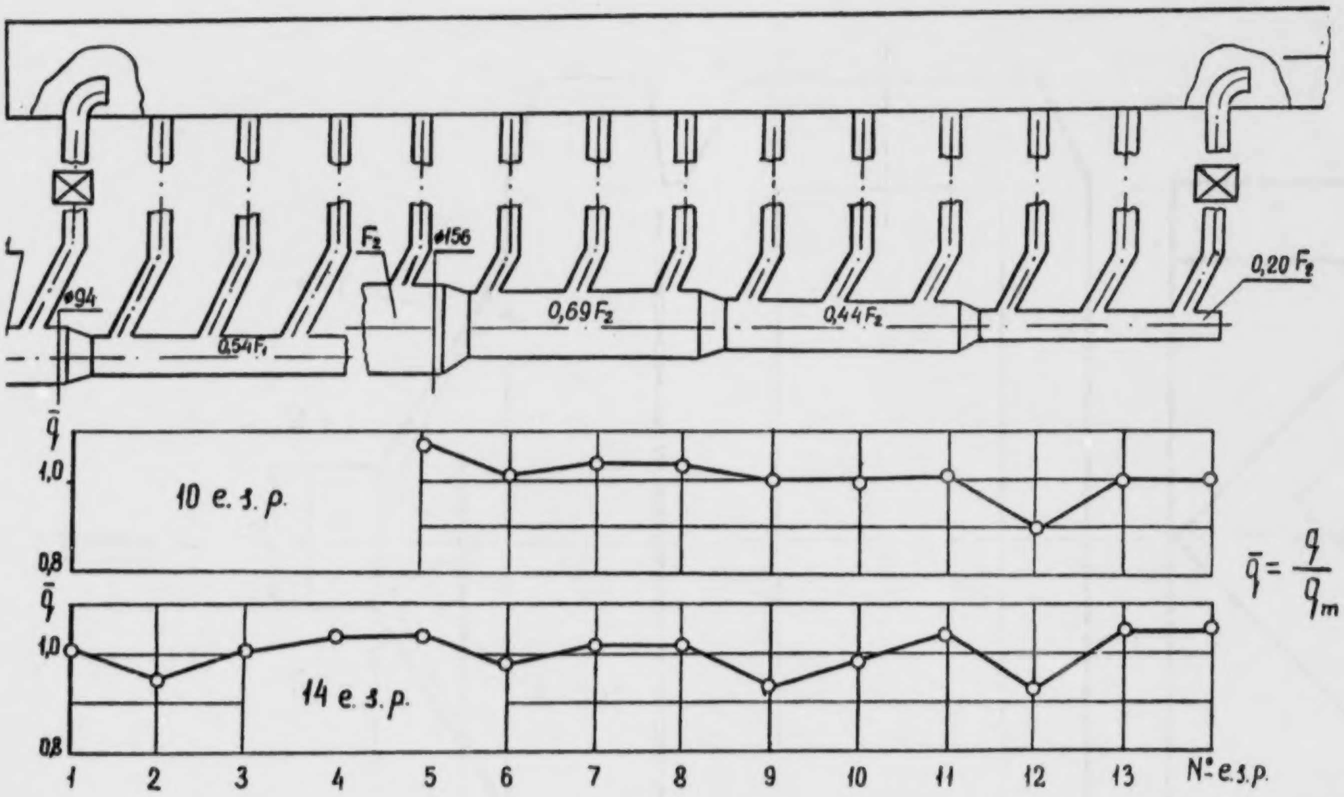
ø94
0,54 F_1
F_2
ø156
0,69 F_2
0,44 F_2
0,20 F_2
$\bar{q}$
1,0
0,8
10 e. s. p.
14 e. s. p.
1
2
3
4
5
6
7
8
9
10
11
12
13
N° e.s.p.
$\bar{q} = \frac{q}{q_m}$

Figure 4. Gas flow rate distribution $\bar{q}$ over electrostatic precipitators connected in parallel.

a - 10 electrostatic precipitators

b - 14 electrostatic precipitators

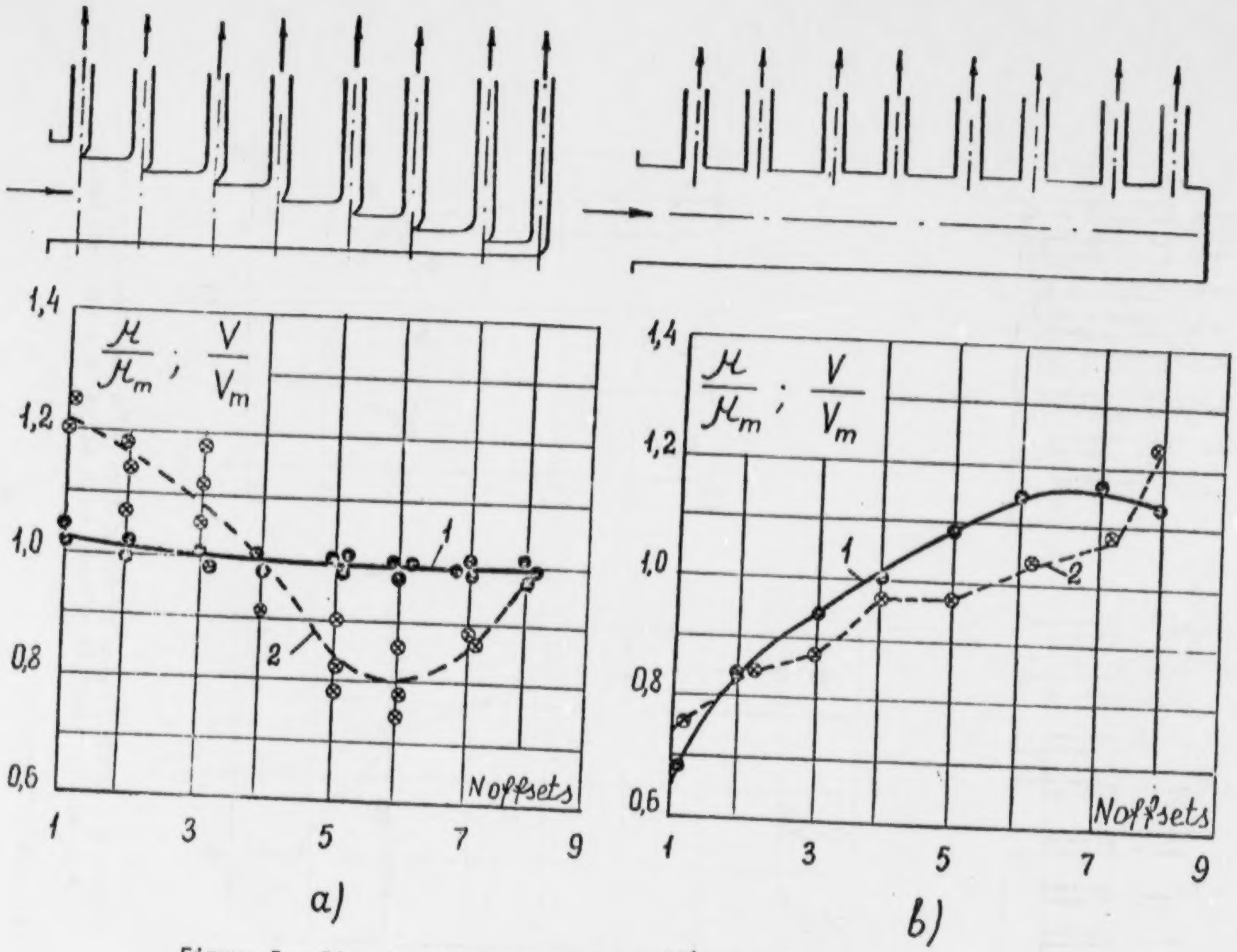

Figure 5. Distribution of velocities V/V_m and flow dust load μ/μ_m across manifold offsets.

a - of uniform variable cross section with smooth offsets

b - of constant cross section. 1 - V/V_m ; 2 - μ/μ_m

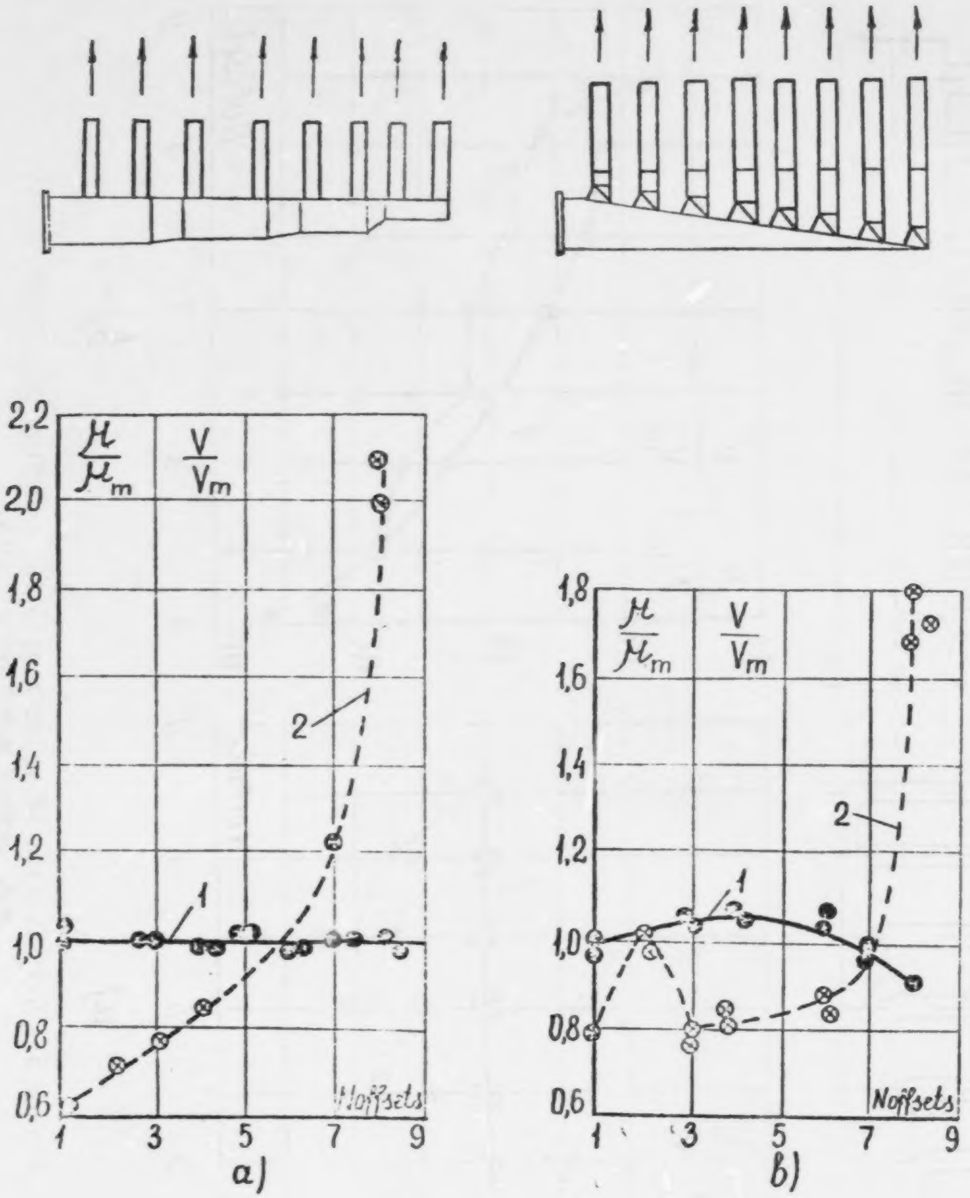

Figure 6. Distribtuion of velocities V/V_m and flow dust load μ/μ_m across manifold offsets with variable cross section.

a - scalariform

b - wedge-form. 1 - V/V_m ; 2 - μ/μ_m

In addition, to study the gas distribution over the electrostatic precipitator cross section, gas and dust distributions over the apparatus installed in parallel in one installation have been investigated. Some of such installations involved complex manifold systems containing up to 14 precipitators installed in parallel (with an active area of one apparatus from 30 to 60 m^2). The diagram of installation and gas flow distribution over the apparatus that is the result of investigations is given in figure 4 as an example. Experimental investigation of dust distribution by means of manifold models shows the significant dependence of distribution on a manifold construction.

Tests were carried out on the coal ash loading air flow: The density of the coal ash was 2.4 g/cm^3, the velocity of the air flow was in the range 15 to 25 m/s. The medium particle size distribution of coal ash was 25 μk. Dust concentration increased in manifold offsets of constant cross section (figure 5b) from the 1st to 8th offset. In the last offset, the concentration is about twice as high as in the first one.

The dust distribution in manifolds of arbitrary cross section is given in figures 5, 6a, and 6b. In the last offset of a scalariform manifold (figure 6a), the dust concentration is 3.5 times as high as in the first one. One can see the tendency towards a decrease in the nonuniformity of dust distribution over the offsets in a wedge manifold with an inclined wall at the side of offsets (figure 6b). A more uniform dust distribution was obtained in a manifold of uniform-variable cross section with smooth offsets (figure 5a).

An increase of dust concentration in the last lateral offsets in a downstream direction can be explained by the inertial separation of large particles from the manifold flow. As the comparison of considered manifold variations has shown, the indicated effect of inertial separation can be reduced and the uniform dust distribution can be obtained creating more favorable conditions for entry of the dust loading gas flow to manifold offsets.

The results of aerodynamics modeling of various inlet (outlet) flows and distributors conforming to the definite types of electrostatic precipitators and apparatus of wide technological type have been symmarized by Professor I. E. Idelchik in the "Atlas of Gas-Air Distributors at Various Plant Apparatus." Diagrams of inlet and outlet manifolds designated for a flow inlet to apparatus installed in parallel and a flow outlet from the apparatus and recommendations to the most beneficial arrangement of apparatus from the angle of maximum uniformity of the flow distribution are also given in the "Atlas." At the same time, the necessary data for calculation of basic manifold dimensions are given to provide an allowable degree of flow nonuniformity over individual apparatus of this series.

There are not only optimal variants of inlet, outlet, and flow distribution over the apparatus cross section and the apparatus installed in parallel, but also a successive improvement of aerodynamic characteristics, as better variants of inlet and outlet regions and steadying devices are used. A great variety of such variants and their aerodynamic characteristics allows the most suitable schemes of apparatus and construction to be selected in each specific case.

STUDIES OF PARTICLE REENTRAINMENT
RESULTING FROM ELECTRODE RAPPING

Leslie E. Sparks,* Owen J. Tassicker,† and John P. Gooch‡

Abstract

Measurements of rapping reentrainment on a pilot-scale precipitator indicated that rapping emissions decreased with increasing time between raps. The percentage of the collected electrode also increased with increased time between raps. Particle size distribution data for the rapping puffs suggested that thicker dust layers produce larger reentrained particles upon rapping. A pronounced vertical stratification of the rapping emissions was found for the pilot-scale studies.

Measurements of fractional efficiency with and without rapping at full-scale precipitator installations show that rapping efficiency losses occur primarily for particle diameters greater than 2.0 μm diameter. The largest rapping losses were measured on hot-side installations. Mass emission data suggest a correlation between the dust removal rate in the last field of the precipitator and the emissions due to rapping.

INTRODUCTION

Collection of particulate matter by the electrostatic precipitation process consists of three separate operations: (1) particle charging, (2) particle collection, and (3) removal and disposal of the collected material. In ideal circumstances, all material collected on the grounded electrodes would be transported to a collection hopper without reentrainment into the gas stream. While this ideal situation is approached in the collection of liquid particles, the process of removing dry particulate from collecting electrodes is usually accompanied by a significant reintroduction of the collected material into the flue gas. This paper discusses particle reentrainment caused by rapping of the collection electrodes in conventional wire-plate electrostatic precipitators.

The purpose of an electrode rapping system is to provide an acceleration to the electrode that is sufficient to generate inertial forces in the collected dust layer that will overcome those forces holding the dust to the electrode. A successfully designed rapping system must provide a proper balance between electrode cleaning and minimizing emissions resulting from rapping reentrainment. As part of an overall program to gain a better understanding of the electrostatic precipitation process, measurements with the objective of quantifying and size-characterizing losses due to electrode rapping have been conducted on one pilot-scale and several full-scale electrostatic precipitators. The pilot-scale study was funded by the U.S. Environmental Protection Agency, and the full-scale tests were sponsored by the Electric Power Research Institute.

---

*Environmental Protection Agency, Research Triangle Park, N.C. 27511
†Electric Power Research Institute, Palo Alto, California 94304
‡Southern Research Institute, Birmingham, Alabama 35205

EXPERIMENTAL STUDIES

Most of the previous work on rapping reentrainment has not included direct measurements of the effects of rapping on overall efficiency and efficiency as a function of particle size. Accordingly, measurement programs have been conducted with the objective of quantifying rapping reentrainment in terms of the percentage and particle size distribution of the reentrainment material.

Methods of Measurement

The quantification of rapping reentrainment requires methods of measuring the mass and particle size distribution of particulate exiting the precipitator with and without rapping. During both the pilot- and full-scale precipitator test programs, optical real-time systems and integrating mass systems were used. For the full-scale tests, particle size measurements were obtained using a method based on electrical mobility analysis for particle diameter less than about 0.20 μm.

Mass Concentration Measurements. Mass measurements were obtained with in-stack filters. The sampling probes used at the inlet and outlet were heated and contained pitot tubes to monitor the velocity at each sampling location for the full-scale tests. Glass fiber thimbles were used at the inlet to collect the particulate and Gelman 47-mm filters were used at the outlet. Different procedures were employed at the pilot-scale unit compared to the full-scale units.

At the pilot plant facility, two outlet sampling trains were used (ref. 1): (1) the upper sampling train for the upper 68 percent of the precipitator outlet and (2) the lower sampling train for the lower 32 percent of the precipitator. The outlet sampling locations were about 1 meter from the plane of the outlet baffles, and only one lane of the precipitator was sampled. Both outlet mass trains were modified to consist of two systems: one of which was used to measure emissions between raps and the other to measure emission during raps. One of the two filters on each of the two outlet probes was designated the between rap sampler and the other the rapping puff sampler. After stable conditions were obtained, the between rap sampling systems were started. Before rapping the plates, sampling was discontinued and the probes were rotated so that both nozzles on each probe pointed downstream. The dust feed was turned off, and after a clear flue was obtained, the second filter was rotated into the gas stream. Sampling was resumed and the plates were rapped. When dust had settled, sampling with this second set of filters was discontinued and the nozzles to the filters were again pointed downstream. The dust feed was then turned on and the sampling was resumed again with the between rap system.

For the full-scale precipitator installation, one would expect to be able to measure rapping reentrainment simply by obtaining data with either a mass train or an impactor sampling system, with a rapping system energized and subsequently deenergized, and then comparing these measurements. However, it was found that during the test program at the first installation (Plant 1) the sensitivity of the electrostatic precipitator to changes in resistivity and other process variables could overshadow the differences in total emissions caused by energizing and deenergizing the rappers. The variation in precipitator performance caused by the resistivity and other process variable changes made it impossible to determine rapping reentrainment losses from a direct comparison of data obtained one day with rappers in the normal mode and rappers deenergized on subsequent days.

In order to minimize this difficulty, a revised sampling strategy was adopted for the remaining installations. This strategy consisted of sampling with mass trains and impactors dedicated to designated "rap" and "no rap" periods. Data with a rapping system energized and deenergized were obtained by traversing selected ports with dedicated sampling systems in subsequent periods on the same day. This procedure, while necessarily distorting the frequency of the rapping program being examined, minimized the effects of resistivity and other process variable changes.

The use of this sampling strategy leads to two possible procedures for calculating the fraction of losses attributable to rapping reentrainment. The first procedure calculates the ratio of emissions obtained with rappers off to rappers on and subtracting from unity. The emissions data utilized in this procedure were obtained during the time in which alternating sampling periods for rap and no rap sampling trains were employed. The second procedure consisted of subtracting the mass emissions obtained with the rappers deenergized from those of the previous day with normal rapping, and dividing by the emissions obtained with the rappers operating normally. It could be argued that if the alternating on-and-off procedure for sampling did not distort the results obtained, and if there were no other variations in parameters affecting the precipitator performance, that data obtained from the "rap" period should be approximately equal to that obtained during periods in which the rappers were operating in a normal fashion. In this paper, we have calculated percentage of rapping emissions using both of these procedures.

Particle Sizing. Three sizes of selected sampling systems were used in the measurement programs, two of which were real time extractive systems (a large particle system and a fine particle system) while the third (cascade impactors) provided time integrated in situ data. The large particle (diameter range 0.6 to 20.2 μm) extractive system was employed only for outlet measurements to provide qualitative information on the relative fractions of the emissions that could be attributed to rapping losses in the precipitator. In addition, this system also provided data on particulate concentration changes with time.

The fine particle system (0.01 to 0.3 μm) was employed at both the inlet and outlet of the full-scale precipitators for purposes of providing fractional efficiency data and to give quantitative information on the contribution of rapping, if any, to emissions in this particle size range.

Description of Installations and Results

Pilot-Scale Precipitator. The pilot-scale rapping tests were conducted on a nearly full-scale pilot precipitator owned and operated by Fluidyne Engineering. Figures 1 and 2 illustrate the features of the test facility. This pilot unit effectively represents one electrical section in a full-scale precipitator. The plate height is 6 m and the plate length is 2.7 m. The total collecting area is 167 m^2, and wire to plate spacing is 11 cm. In the original design, the plates were constructed from expanded metal. For this

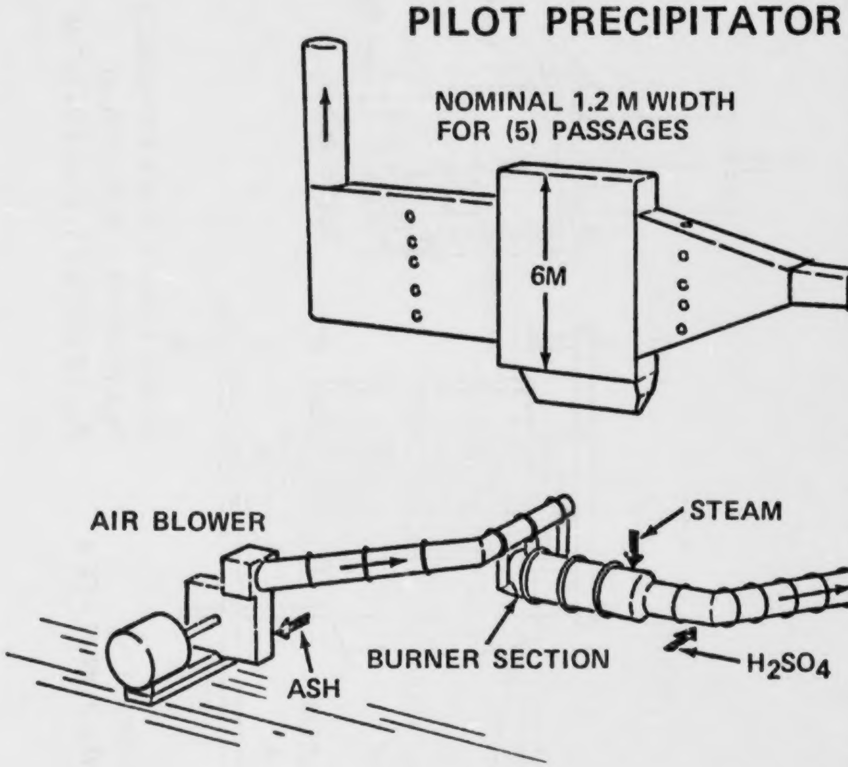

PILOT PRECIPITATOR
NOMINAL 1.2 M WIDTH FOR (5) PASSAGES
6M
AIR BLOWER
STEAM
ASH
BURNER SECTION
H_2SO_4

Figure 1. Pilot precipitator fluidyne.

VARIOUS VIEWS OF FLUIDYNE PILOT PRECIPITATOR

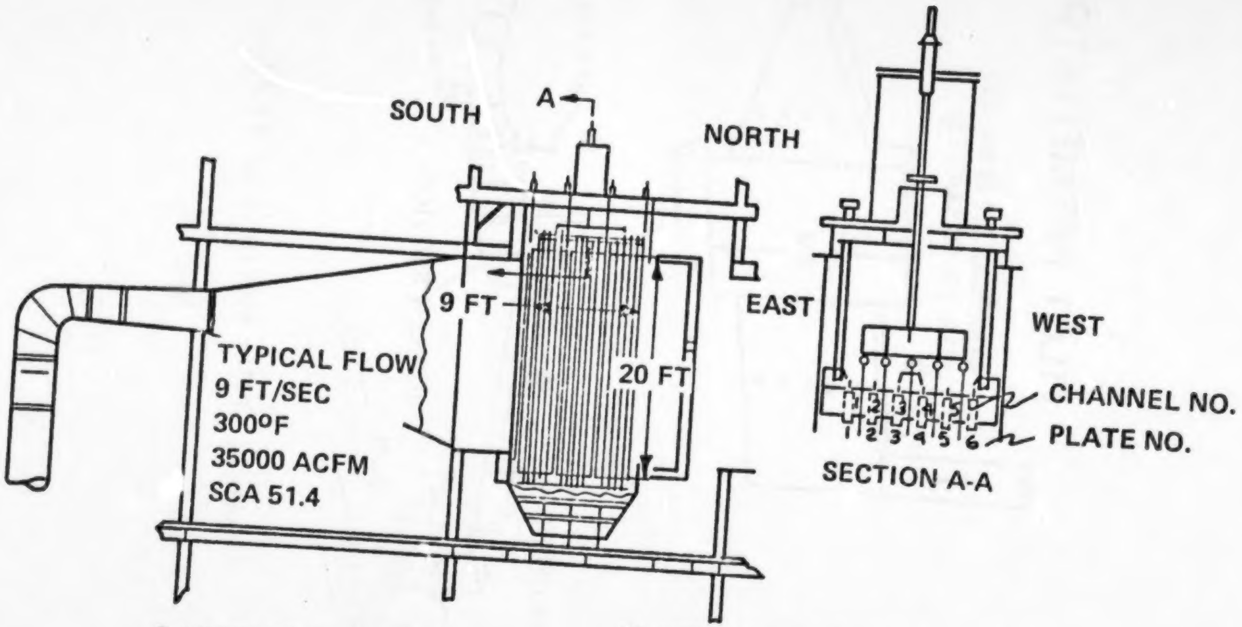
SOUTH
A
NORTH
EAST
WEST
9 FT
20 FT
TYPICAL FLOW
9 FT/SEC
300°F
35000 ACFM
SCA 51.4
CHANNEL NO.
PLATE NO.
1 2 3 4 5 6
SECTION A-A

9 ACCELEROMETERS
ARE MOUNTED ON PLATE 4

PLATE ROWS 1, 2, & 6 EXPANDED METAL
PLATE ROWS 3, 4, & 5 SOLID
PLATE ROWS 2-1, 2-3 WERE 0.5 M

Figure 2. Various views of fluidyne pilot precipitator.

rapping reentrainment study, three of these plates were replaced to provide two lanes with solid plates on each side of the lane. Outlet sampling was confined to the lanes with solid plates.

Table 1 presents a summary of results obtained from the experiments on the Fluidyne Pilot Unit. These results indicate that rapping emissions decreased with increasing time between raps. Figure 3 shows the effect of the rapping interval on efficiency. The percentage of the collected dust removed from the collecting electrode also increased with increased time between raps, as figure 4 illustrates. These results are consistent with a theory of dust removal which indicates that the product of the normal plate acceleration and the dust surface density must be greater than the tensile strength of the layer (ref. 2).

Figure 5 presents particle size distribution of rapping puffs for the indicated rapping interval. These data suggest that thicker dust layers produce larger reentrained particles upon rapping. An inspection of the impactor substrates at the outlet sampling locations 2 and 3 revealed that the majority of the large particles in the rapping puffs were agglomerates. Producing relatively large agglomerates instead of individual particles is desirable because the larger agglomerates are recollected faster than discrete particles or smaller agglomerates.

The measurement of the vertical distribution of the rapping loss at the Fluidyne pilot unit indicated that 82 percent of the rapping emission occurred in the lower 32 percent of the precipitator (ref. 1). This effect was apparently due to both hopper boil-up and gravitational settling of the reentrained material. Figure 6 illustrates the vertical stratification as a function of particle size. All of the particle size bands show a decrease in concentration with increasing distance from the bottom baffle.

Full-Scale Precipitators. Six full-scale electrostatic precipitator installations were tested under the EPRI-sponsored research program (ref. 3). In terms of location in the power plant system and type of fuel burned in the boiler, the units may be classified as follows:

Plants 1 and 2	- Cold-side ESPs collecting ash from low-sulfur Western coals
Plant 3	- Hot-side ESPs collecting ash from low-sulfur Eastern coal
Plants 4 and 5	- Cold-side ESPs collecting ash from high-sulfur Eastern coals.
Plant 6	- Hot-side ESPs collecting ash from low-sulfur Western coal

Table 2 summarizes the important design parameters and the results obtained for the six installations. The installations were characterized by relatively high overall mass efficiency. Rapping losses as a percentage of total mass emissions ranged from over 80 percent for one of the hot-side units to 30 percent for the cold-side units. The high rapping losses at Plant 3 are probably due both to reduced dust adhesivity at high temperatures and the relatively short rapping intervals.

Table 1. Pilot-scale Rapping Experiments

Type of Test	Plate Acceleration G's x,y,z axis	Rap Intervals Min	Gas Velocity m/sec	Avg. Plate Current Density nA/cm^2	Total Penetration %	Penetration Due to Rapping Reentrainment %
Rap	11 16 15	12	0.87	23.3	11.4	53
Rap		32			7.6	32
Rap		52			6.1	18
Rap		150			6.9	25
No Rap		--			5.2	--

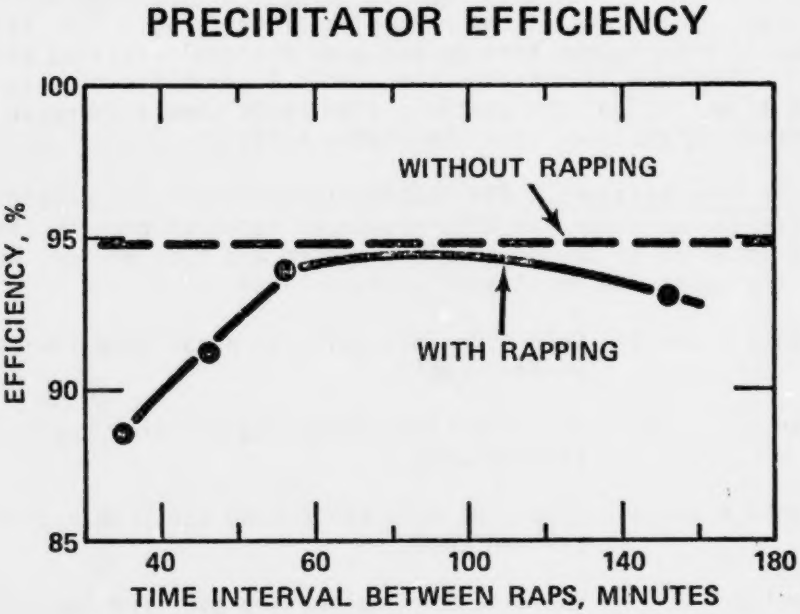

Figure 3. Average efficiency for fluidyne pilot ESP for various rapping intervals.

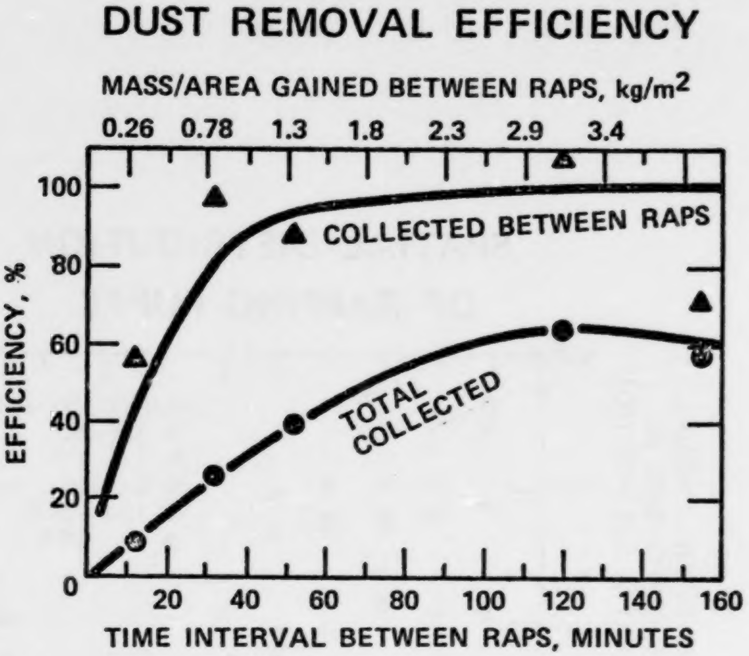

Figure 4. Dust removal efficiency vs. the time interval between raps.

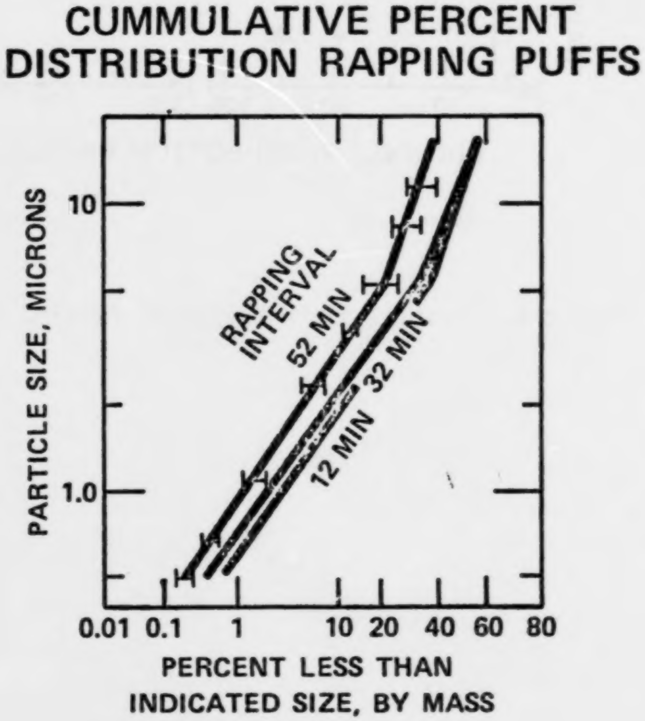

Figure 5. Cumulative percent distribution for rapping puffs.

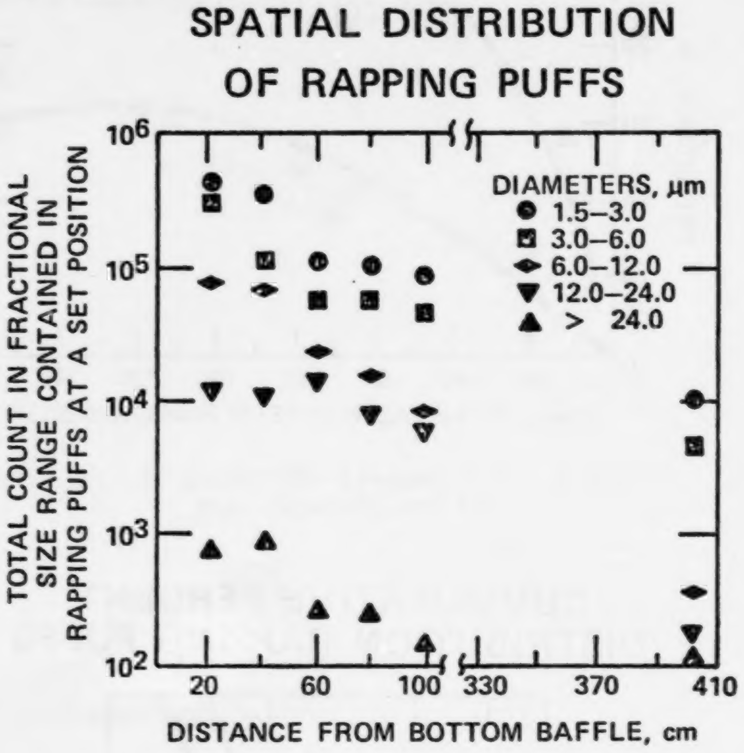

Figure 6. Spatial distribution of rapping puffs.

Table 2. Summary of Results From EPRI Test

Plant	1	4	5	3	2	6
Boiler Load, MW	150	160	122	275	500	800
ESP Vendor	Lodge Cottrell	Lodge Cottrell	ELEX/AAF	Research Cottrell	SF-Carborundum	Joy-Western
Design Gas Flow, ACFM	800,000	906,000	575,000	1,250,000	2,330,890	3,940,000
Design Temperature, °F	270	340	325	650	250	662
Total Plate Area, ft^2	403,200	158,750	127,032	336,960	1,136,256	1,209,600
Design SCA, ft^2/1000 ACFM	534.19	175.22	220.93	270.00	487.5	307.00
Design Efficiency, %	97.0	99.0	98.7	99.2	99.33	99.5
Number of Electrical Fields in Direction of Gas Flow	6	3	4	4	5	6
Plate-to-plate Spacing, in.	12	11	10	9	9 3/4	9
Emitting Electrode Design	Mast with Square Twisted Wires	Mast with Square Twisted Wires	Rigid Barbed Wires	Hanging Round Wires	Electrode Frame With Spiral Wires	Hanging Round Wires
Rapper Design	Drop Hammer	Drop Hammer	Tumbling Hammers	Magnetic Drop Hammer	Tumbling Hammers	Magnetic Impulse Hammers
Portion of ESP Tested	Total	1/2	1/2	1/2	1/6	1/16
Boiler Load During Test, MW	128	160	122	271	508	800
Gas Flow During Test, ACFM	699,622	328,762	248,291	432,071	316,566	268,696
Temperature During Test, °F	306	311	315	610	223	678
SCA During Test, ft^2/1000 ACFM	576.31	241.44	255.81	389.94	598.28	281.36
Measured Efficiency, %	99.92	99.55	99.80	99.64	99.85	98.98
Dust Resistivity at operating Temperature, Ω-cm	1.4×10^{11}	1.7×10^{10}	2×10^{10}	3.2×10^{10}	4.6×10^{11}	
Rapping Frequency						
Field	Raps/hr	Raps/hr	Raps/hr	Raps/hr	Raps/hr	Raps/73min
1	6	10	10	30-60	10	8
2	6	6	10	30-60	5	8
3	3	1	5	30	5	3
4	3	-	5	30	2	3
5	1	-	-	-	1	1
6	1	-	-	-	-	1
% of Mass Emissions Attributed to Rapping[a]	31	65-33	30	85	36-29	63-44

---

[a] Indicating range of values from two methods of calculation.

Figure 7 contains the collection efficiency as a function of particle size at Plant 1 for sampling periods in which the rapping system was energized and deenergized. Due to the previously discussed difficulty with process variations at this location, data from the large particle real-time system were used to estimate the collection efficiency for particles greater than 1.0 μm. Figure 8 presents analogous data from Plant 2, with the exception that the rap and no rap data were obtained with the alternating sampling plan using the ultrafine sizing system and inertial impactors. Fractional efficiency data with the rapping system operating normally are given in figure 9. For particles larger than about 1.0 μm diameter, the fractional efficiency data for the "normal" and rap sequence data sets indicate reasonable agreement.

The fractional efficiency data sets for one of the hot-side units are presented in figure 10. The normal (not shown) and rap sequence data sets again show reasonable agreement for sizes greater than about 1.0 μm. For these locations, it is apparent that rapping losses occur for the most part in the larger particle sizes, primarily as particles larger than 2.0 μm diameter. Thus, it appears that rapping reentrainment does not cause a significant change in fine particle emission for these three installations. However, the rapping losses for both the hot- and cold-side precipitators provide a major contribution to the overall penetration, and illustrate that significant improvement in overall mass collection efficiency may be possible by optimization of the rapping system design and operation.

Figure 11 contains rapping emission for the six installations as a function of the dust calculated to have been removed in the last field of the precipitator. The data suggest a good correlation exists between rapping losses and the dust removal rate in the last field. Data for the two hot-side installations tested show higher rapping losses, which would be expected due to reduced dust adhesivity at higher temperatures. The simple exponential relationships shown are suggested for interpolation purposes. Note that reduction of input power at Plant 4 caused a pronounced increase in rapping emissions.

CONCLUSIONS

Measurements of rapping reentrainment on a pilot-scale precipitator indicated that rapping emissions decreased with increasing time between raps. Particle-size distribution data for the rapping puffs suggested that thicker dust layers produce larger reentrained particles upon rapping.

Measurements of fractional efficiency with and without rapping at full-scale precipitator installations show that rapping efficiency losses occur primarily for particle diameters greater than 2.0 μm diameter. The largest rapping losses were measured on hot-side installations. Mass emission data suggest a correlation between the dust removal rate in the last field of the precipitator and the emissions due to rapping. The electrostatic precipitator with the highest overall mass collection efficiency exhibited a minimum collection efficiency of 99.2 percent at 0.20 μm diameter.

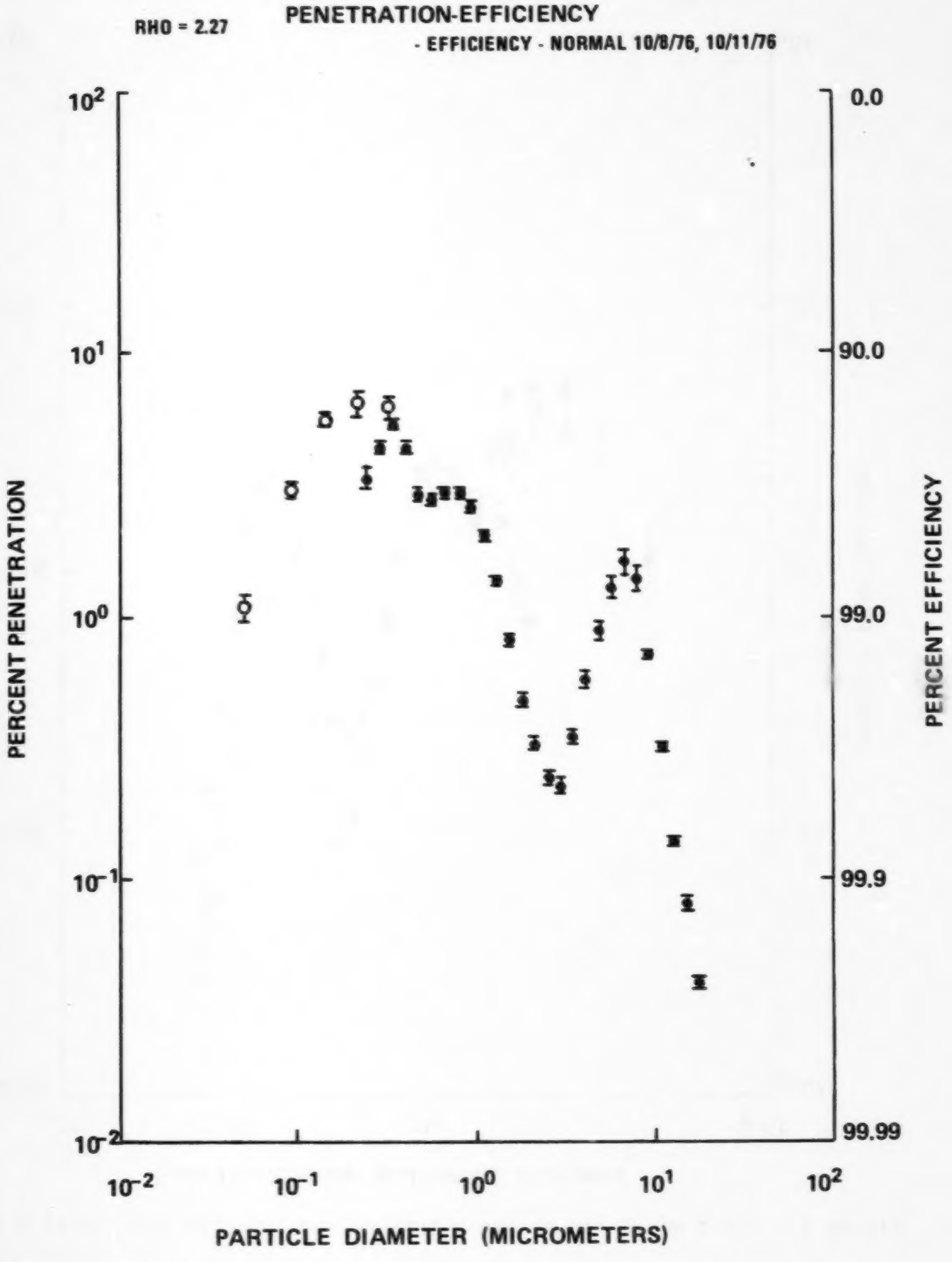

Figure 7. Plant no. 1 rap-no rap fractional efficiency, including ultrafine and impactor measurements.

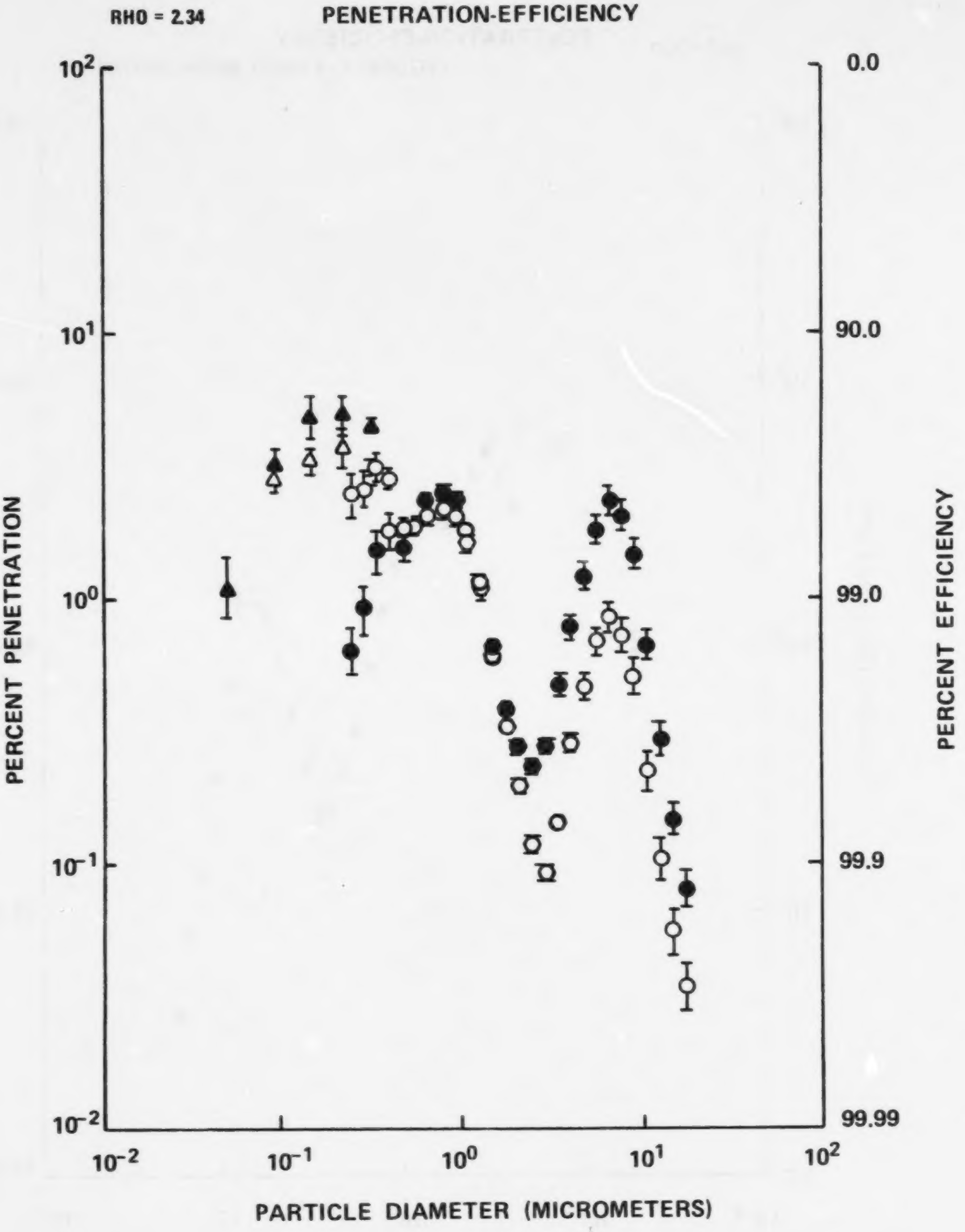

Figure 8. Plant no. 2 rap-no rap ultrafine and impactor fractional efficiencies.

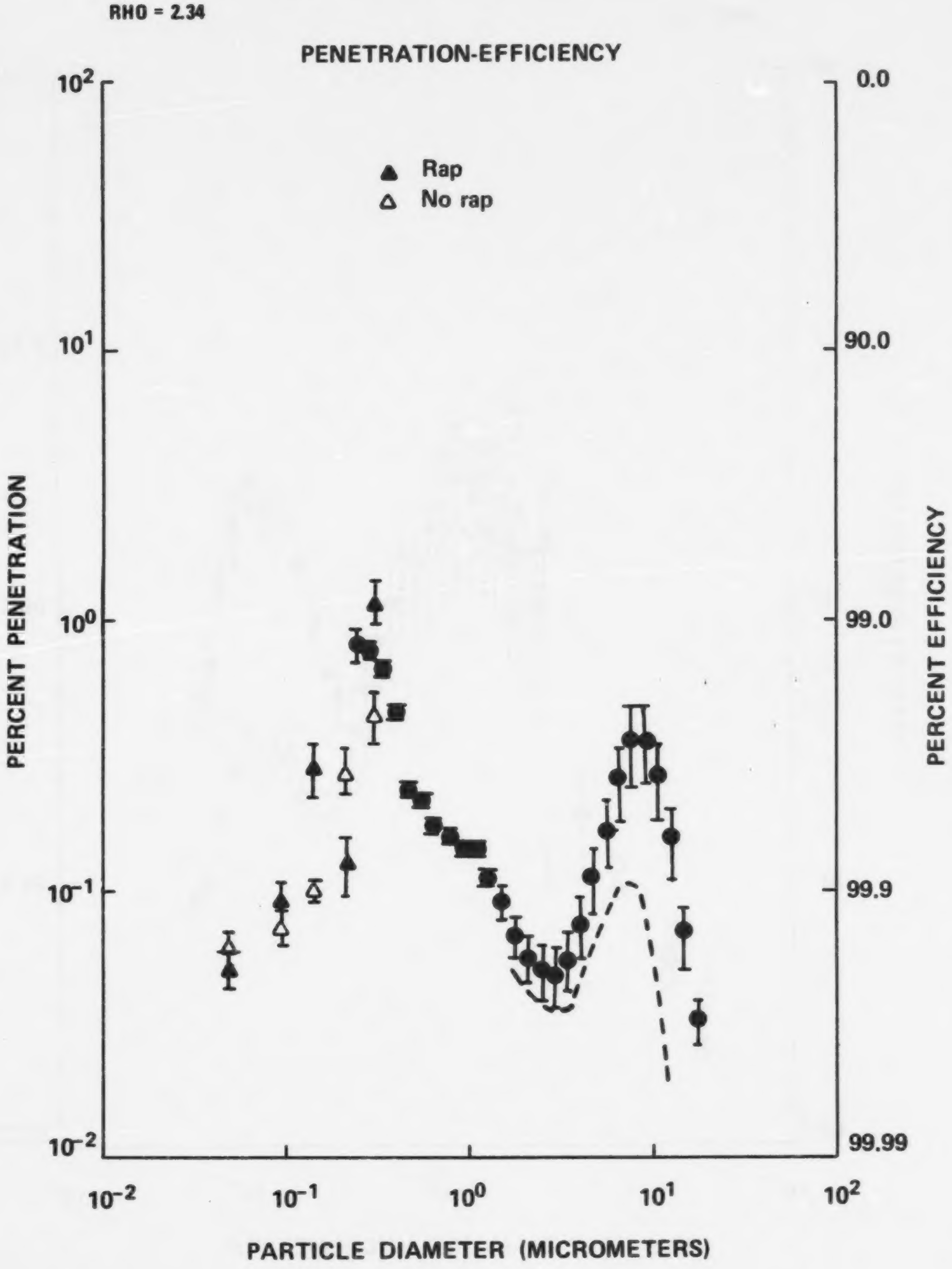

Figure 9. Plant no. 2 normal condition ultrafine and impactor fractional efficiencies.

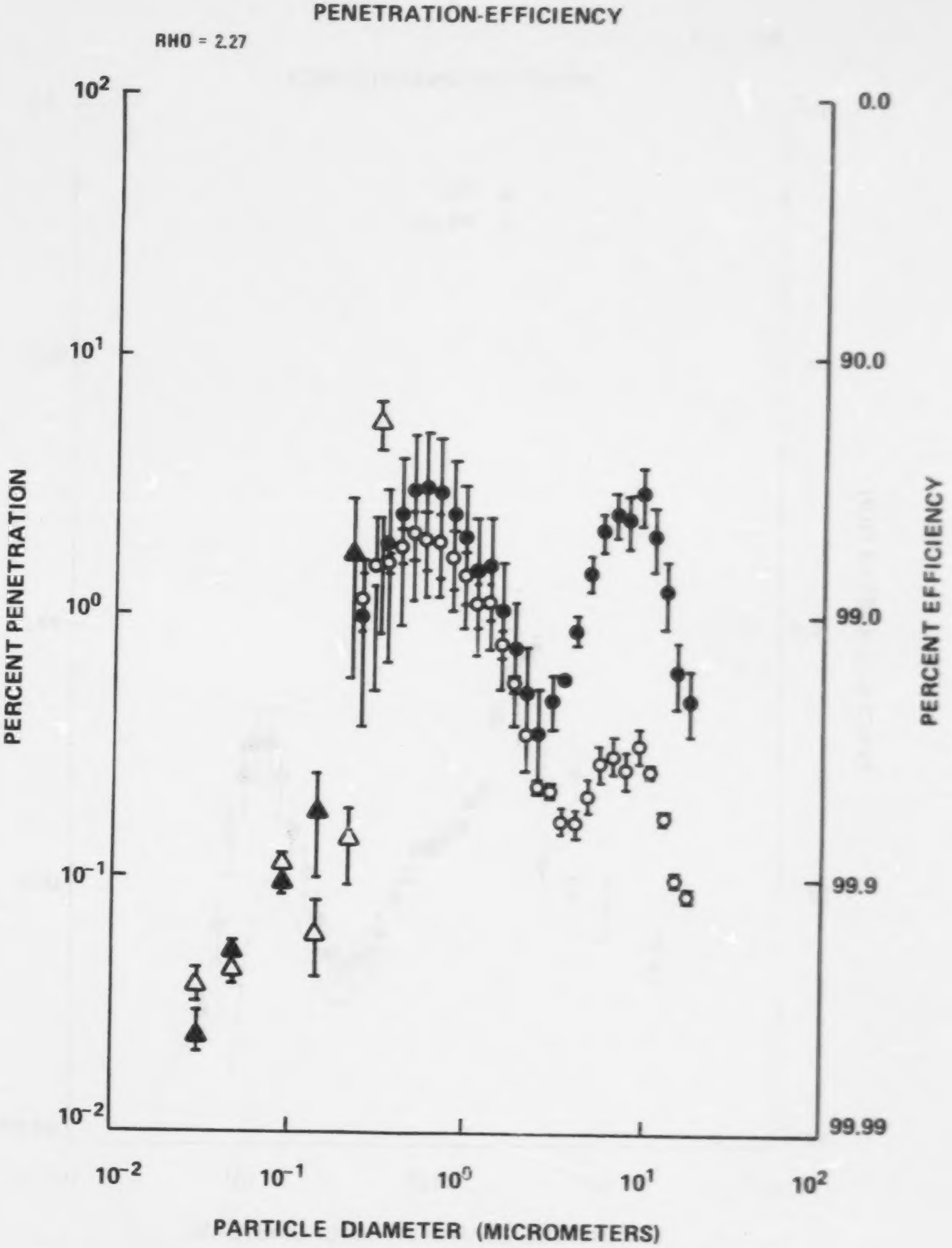

Figure 10. Plant no. 3 ultrafine and impactor rap-no rap fractional efficiencies, duct B1.

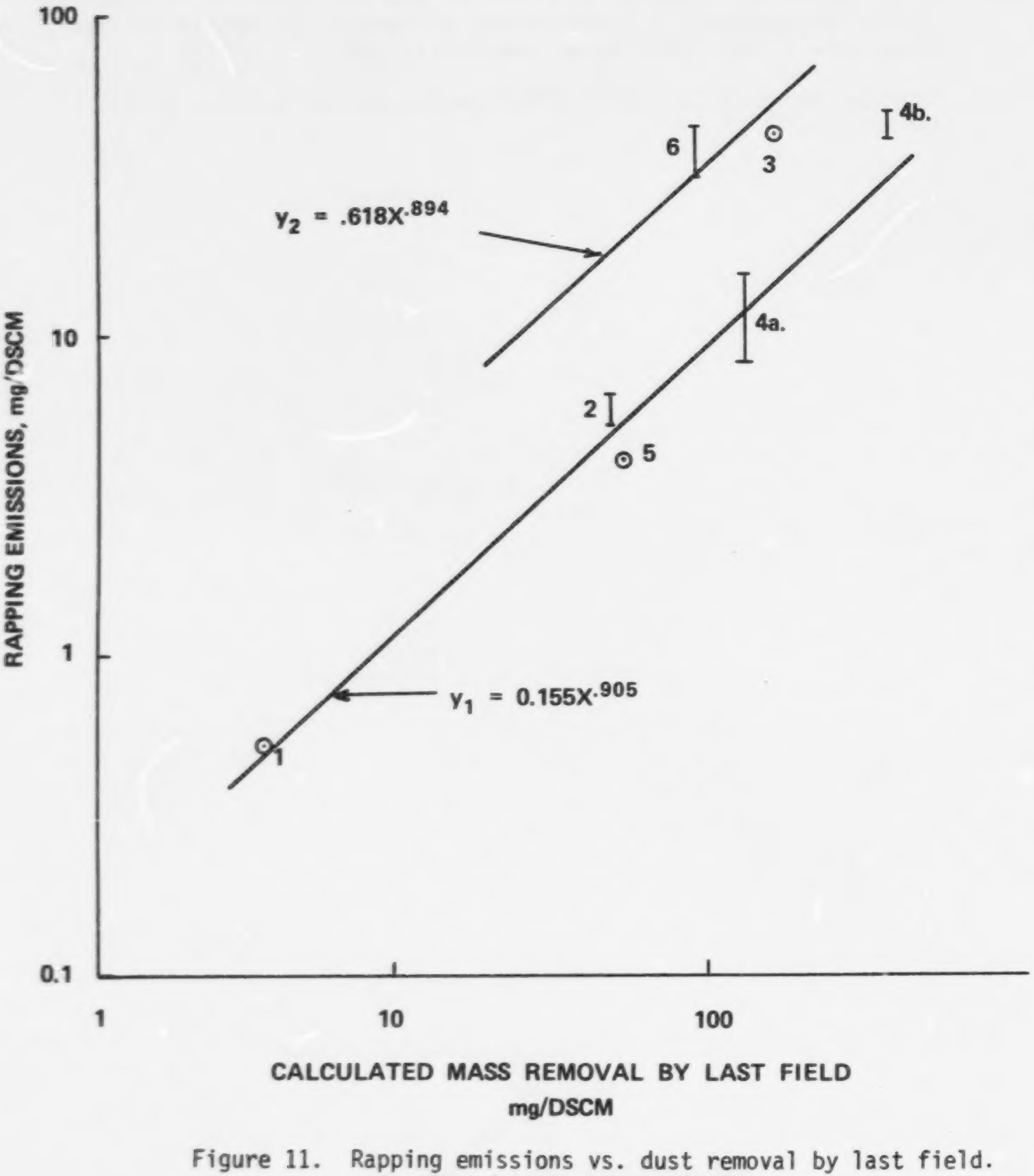

Figure 11. Rapping emissions vs. dust removal by last field.
4a. - Plant 4, Normal Current Density
4b. - Plant 4, 1/2 Normal Current Density

REFERENCES

1. Herbert W. Spencer, III, "Rapping Reentrainment in a Nearly Full Scale Pilot Precipitator," Environmental Protection Agency Publication No. EPA-600/2-76-140, May 1976.

2. O. J. Tassicker, "Aspects of Forces on Charged Particles in Electrostatic Precipitators," Dissertation, Wollongong University College, University of New South Wales, Australia, 1972.

3. Southern Research Institute, Final Report on EPRI Project RP413, in preparation.

INVESTIGATION OF DUST CARRYOVER AND OPTIMIZATION OF REGIMES OF ELECTRODE RAPPING IN ELECTROSTATIC PRECIPITATORS*

Yu. I. Sanayev, I. K. Reshidov, I. A. Kizim

Abstract

The authors present the results of studies on dust entrainment in an electrostatic precipitator. The process of entrainment during precipitation and rapping of precipitator electrodes is studied and possibilities indicated of reducing entrainment during rapping by optimizing rapping conditions. Calculations have been worked out for determining optimal rapping conditions. A programmable unit has been developed for controlling the rapping of precipitator electrodes in order to realize the calculated operating conditions. The introduction of this procedure and the programmable unit makes it possible to save from 1.5 to 23,000 rubles per year in the case of one electrostatic precipitator.

Modern industries, especially power plants, develop by intensifying performance of individual process units. This leads to the growth of production and at the same time to the increase of industrial wastes. Fly ash emissions at large thermal power stations amount to hundreds of tons per day. This deteriorates performance of I.D. fans and heat exchangers, but the main problem is that of environment pollution.

A common device to clean large volumes of waste gases is an electrostatic precipitator. The theory of electrostatic precipitation predicts the possibility of building electrostatic precipitators with high dust removal efficiency. However, design practice encounters many problems. At the present time, dust reentrainment is the main problem that decreases efficiency of electrostatic precipitators.

In this country and abroad, many authors state that dust reentrainment in electrostatic precipitators has been inadequately studied although its influence on precipitator efficiency is significant.

To date, the dust reentrainment factor has not been accounted for in precipitator design. This leads to inadequate design. Continuous rapping of collecting plates is commonly used in practice. This decreases gas cleaning efficiency and precipitator lifetime.

Increasing of dust removal efficiency by way of increasing precipitator size leads to higher cost of equipment. One must look for less expensive means.

The main goal of the present work is to study the physical nature of dust reentrainment and to find parameters that influence it. Obtained information will lead to the development of ways and means to increase precipitator efficiency at considerably lower costs.

---

*For further information regarding the material in this paper, please contact I. K. Reshidov, U.S.S.R. 113105, Moscow, M-105, 1st Nagatinsky Pass., 6, NIIOGAZ.

Theoretical evaluation of dust reentrainment at the present time is impossible. So the best way to study reentrainment is by experiment. The number of factors that influence the reentrainment of dust is quite high and to make them constant in the field tests is impossible. So it was decided first to study the physical nature of the phenomena in the laboratory. Studies distinguished two main kinds of reentrainment: reentrainment that occurs during particle deposition and reentrainment due to rapping of collecting plates. It is assumed in defining reentrainment that particles impacting an adhesive conducting surface are not reentrained. The amount of reentrained dust during deposition was defined as the difference between the quantity of dust collected on the plate coated with adhesive compound and that collected on the clean plate. The amount of dust reentrained during rapping of collection plates was defined as the difference between the quantity of fly ash collected by the precipitator with a rapping device operated and not operated.

The interval of work without rapping of the plates was short enough so that there was no dust removal efficiency decrease as a result of excessive fly ash deposition on collecting plates. To account for the reentrainment, the coefficients K_1 and K_2 were added to the German equation. This permitted evaluation of the influence of reentrainment on the precipitator efficiency.

The laboratory apparatus for studying reentrainment consist of precipitators equipped with the dust feeder especially designed for their purpose and capable of highly uniform dust feeding and continuous weighing of dust. The dusts used in the experiments are various kinds of fly ash and cement.

Analysis and allowance for measurement errors combined with adjustment of the experimental apparatus held the relative error of weighing of collected dust to less than 5 percent. This made it possible to study the quantitative correlation of dust reentrainment.

As the processes taking place during rapping of the collecting plates are short-lived, rapid film shooting was used to study them.

For dust reentrainment studies in the field, a probe was developed for deposition of dust on clean and adhesive discs directly from the active zone of a precipitator.

The studies showed that dust reentrainment during deposition is due to a jarring loose of dust from the dust layer by large particles, forming craters in the dust layer. The process was confirmed by photographs showing particle motion in strobe light. Calculations revealed that layer erosion takes place when particle motion energy is not less than 10^8-10^{10} joules.

For studies of flow and gravitational forces effect on the knocking out of particles, the dust layer on the collecting plates was blown with clean air. The tests showed that these forces do not cause dust reentrainment.

The results of the experiments on deposition of dust on clean and adhesive discs are presented as curves for dust reentrainment by deposition in relation to the gas velocity. It can be seen that for the laboratory electrostatic precipitator, the dust reentrainment by deposition at a gas velocity of 2 m/s amounts to 15 percent; decrease of unevenness of gas stream from 0.28 to 0.17 m/s lowers reentrainment by 5 times. If the field length is 1.5 m, then dust reentrainment by deposition in the laboratory precipitator can lower the effective drift velocity by nearly 2 times.

The dust reentrainment by deposition in an industrial precipitator in the first field can amount to 70 percent.

Studies on an industrial precipitator showed that the reentrainment value by deposition decreases along the length of the precipitator because the particle size diminishes.

In addition to the type of reentrainment discussed above, there exists one due to rapping of electrodes.

The analysis of films taken at the speed of 1,200 shots/s distinguished three main stages of the rapping process.

1. The motion of the main dust mass that takes place at the vicinity of electrodes.
2. Disaggregating of dust taking place during separation of the dust from the surface and contact of moving aggregates with electrodes and with other aggregates.
3. The formation and upward motion of a dust cloud.

The disaggregating of dust takes place over the whole surface of the collecting plate so this process makes the main contribution to the quantity of reentrained gas.

Taking into account the gained impression relative to the nature of reentrainment, the studies were carried out concerning the basic factors effecting dust reentrainment. Dust reentrainment at the velocity of 1 m/s is minor; at the velocity of 3 m/s it increases up to 30 percent. The quantity of shaken dust considerably affects the dust reentrainment. To characterize the mode of shaking, the authors introduce in this study a special term "dust capacity" (m) i.e., the quantity of dust on 1 m^2 of the surface of the collecting plate just prior to rapping.

The studies showed that the collected dust distributes unevenly along the length of the electrode. That is why the term "dust capacity" characterizes the mean value of amount of dust that is equal to the relation of total amount of dust to the area of the electrode.

The relationship of collection efficiency of rapped-off dust is derived and shows that the increase of dust capacity leads to the increase of collection efficiency as a whole.

In precipitators, the spontaneous falling of dust sometimes takes place. It starts at the place of maximum collection of dust when the dust capacity is close to 2 mg/m^2 and gradually propagates over the whole length of the electrode. The total reentrainment due to the spontaneous falling of dust and to the rapping has some minimum value corresponding to the optimal interval of rapping.

The relation of rapping intervals to dust capacity was analyzed during investigations on the pilot plant of the Cherepet thermal power station. During the tests, the relationships were obtained for the dust reentrainment coefficient K_2, the collection efficiency during the period of no rapping, and the collection efficiency during various modes of rapping characterized by dust capacity m.

In the range of $m = 0.75 - 1.3$ kg/m^2, the collection efficiency reaches its maximum. During continuous rapping, the collection efficiency decreases by 5 percent.

The experimental studies were carried out to determine the relationship of collection efficiency versus dust capacity and K_2. Obtained relationships confirm the existence of a functional relation between collection efficiency and dust capacity m.

When investigating precipitators collecting various kinds of fly ash and dust, the dependence of optimal dust capacity on dust resistivity was established. The high resistivity of the dust layer requires the decrease of its thickness in order to avoid considerable voltage drop in the gap.

Investigations on individual precipitators developed a technique of evaluation of rapping intervals. On the basis of the testing of a number of precipitators, the applicability of this technique is shown.

Taking into account the experimental relationship m=f (pv), a formula is derived for evaluation of the absolute duration of the rapping interval. The latter is the function of precipitator geometry and technological parameter of precipitator performance such as gas velocity, dust load, dust resistivity, collection efficiency, field length, and interelectrode gap. Correlation of rapping intervals, as to the fields, is determined by collection efficiency and the number of fields in the precipitator.

To evaluate the mode of rapping by precipitators with often changing modes of operation, a nomogram has been derived.

For realizing optimal intervals, a special regulating instrument has been developed. This instrument has been passed through the Interdepartmental Commission and recommended for mass production. The application of the said technique and the regulating instrument increased collecting efficiency of industrial precipitators and reliability of rapping system.

At the Ladyzhin thermal power station (precipitator EGZ-3-177), the designed collection efficiency has been reached and the emissions decreased as much as three times. At the Refta thermal power station where fly ash with high resistivity (from Ekibastuzk coals) is collected, the emissions are now decreased by 30 percent. The Lurgi precipitator is used here for gas cleaning. At the Voskresensk cement plant (precipitator GP-75-3), a three times decrease has been reached (see table 1).

Optimization of rapping intervals increased the reliability of rapping system units as much as three to ten times. This is accompanied by electric power savngs. Cost savings due to this new way of operation per each precipitator are from 1.5 to 23 thousand rubles per year.

Table 1. Modes of Rapping Before and After Optimization

Parameters		Ladyzhin power station, e.s.p. EGZ-3-177 mode of rapping		Refta power plant, Lurgi e.s.p. mode of rapping		Slantsy cement plant, e.s.p. PGDS-24-3 mode of rapping		Voskresensk cement plant e.s.p. GP-75-3 mode of rapping		Yaroslavl refinery e.s.p. SG-15 mode of rapping	
		before optimiz.	after optim.	before optimiz.	after optim.	before optimiz.	after optim.	before optimiz.	after optim.	before optimiz.	after optimiz.
Gas velocity, m/sec		1.4	1.4	1.2	1.1	1.0	1.0	1.3	1.3	1.4	1.4
Inlet dust load, g/m³ (norm. cond.)		18	16	56	55	34.7	34.7	18 25	25	15	15
Outlet dust load, g/m³ (norm. cond.)		0.43	0.17	2.7	1.9	1.6	1.2	0.62	0.23	0.3	0.15
Collection efficiency percent		97.5	99.0	95.1	96.5	95.0	96.5	96.3	98.6	98.0	99.0
Parameter m,kg/m²	I	0.07	0.86	0.1	0.1	0.1	0.14	0.03	1.1	0.9	1.5
	II	0.02	0.86	0.03	0.1	0.04	0.14	0.012	1.1	0.2	1.5
	III	0.006	0.86	0.008	0.1	0.01	0.14	0.004	1.1	0.04	1.5
Time of pause, min.	I	3.3	40	3.3	3.3	3.3	47	0.75	25	30	48
	II	3.3	138	3.3	9	3.3	14	0.75	70	30	122
	III	3.3	478	3.3	38	3.3	33	0.75	200	30	1020
Dust rentr. coeff., K_2		0.75	0.92	0.80	0.88	0.77	0.8	0.68	0.93	0.86	0.96
Electric conditions:											
volt. field kV	I	32	31	32	32	50	50	49	49	51	51
	II	31	32	31	31	47	47	54	54	50	50
	III	33	32	30	30	44	44	60	60	49	49
corona current, mA	I	800	940	1310	1320	75	75	41	41	50	50
	II	644	800	1280	1290	110	110	57	57	60	60
	III	760	900	1290	1310	119	119	50	50	120	120

CONCLUSIONS AND RECOMMENDATIONS

The main results of investigations are as follows:

1. It is shown that reentrainment of dust deposited on electrodes is one of the main factors considerably decreasing dust collection efficiency.
2. The physical mechanism of dust reentrainment in precipitators has been studied.
3. The technique of evaluation of optimal intervals for rapping of collecting plates has been developed.
4. The realization of optimal rapping intervals made it possible at the Ladyzhin thermal power station (precipitator EGZ-3-177) to reach the designed collection efficiency of 99 percent. The emissions have dropped from 0.47 to 0.7 g/Am^3. At the Refta power station where the Lurgi precipitator collecting fly ash from Ekibastuzk coals is used, the emissions have dropped by 30 percent. At the Slantsy cement plant (precipitator PGDS 24-3), the emissions from a rotary kiln (dry method of production) decreased by 5 tons per day.
5. Cost savings from the application of the new technique and the regulating instrument for optimization of rapping intervals are from 1.5 to 23 thousand rubles per precipitator per year.

Our experience in the Semibratovo branch of NIIOGAZ concerning application of new methods shows that the said cost savings are reached at comparatively low expenses (of the order of 300 rubles, which consists of the price of the instrument and the cost of its mounting).

The developed technique of rapping intervals evaluation has been tested at the cement plants, thermal power stations, regional power plants, oil refineries, and can be applied to the majority of precipitators in other industries.

INVESTIGATIONS AIMED AT THE INCREASING OF RELIABILITY AND TIME OF SERVICE OF ELECTROSTATIC PRECIPITATOR UNITS AND GAS CLEANING INSTALLATIONS AS A WHOLE*

V. A. Guzayev, I. V. Yermilov, L. S. Ryhzov, V. N. Saksin

Abstract

Basic trends of studies on the reliability and durability of gas cleaning equipment in the U.S.S.R. are presented in this paper. Problems in the development of various procedures for determining the reliability of the mechanical components of electrostatic precipitators in light of a number of problems that come up in reliability studies are discussed. Basic reliability criteria are given that find widespread adoption and on the basis of these reliability studies under industrial conditions and bench models, the authors present basic reasons for the failure of mechanical components and relate them to the results of studies concerned with the production of reliable electrostatic components.

INTRODUCTION

At the present time, the problem of reliability and time of service of mechanical equipment units of ESPs is of greatest importance in the field of electrical gas cleaning.

Reliability of ESP operation is directly related to the efficiency of dust precipitation of the installation. Indeed, the rupture of discharge electrode elements, the breakdown of shaft-insulators, and some other kinds of damage can put out of operation whole fields of an ESP. This causes an essential drop of gas cleaning efficiency. Failures of mechanical equipment units located inside the installation, as a rule, can be eliminated only during periods of current and heavy repairs, because technological plants usually are not stopped for elimination of minor defects in an ESP.

Increasing reliability of mechanical equipment units of an ESP is not an easy task. ESP units operate in very hard conditions that strongly interfere with their reliability.

The main factors decreasing reliability are as follows:

1. High temperature (up to 500° C);
2. Abrasive medium;
3. Corrosion;
4. Vibrations caused by rapping of emitting and collecting electrodes.

There are no precedents of operation of equipment in similar conditions. Exact simulation of mechanical equipment unit operation on a laboratory stand is very difficult. Hence, the necessity arises to carry out special tests directly in the field or on special stands.

---

*For further information regarding the material in this paper, please contact I. K. Reshidov, U.S.S.R. 113105, Moscow, M-105, 1-st Nagatinsky Pass., 6, NIIOGAZ.

Investigations of reliability and time of service of ESPs in this country are carried out in the following directions:

1. Development of means of estimation of reliability of individual units and precipitators as a whole, as well as finding out relations between ESP efficiency and its reliability. Investigation of these problems is necessary for compilation of scientifically founded methods of testing mechanical equipment units on the stand, for determination of required levels of individual unit reliability, as well as for estimation of reliability when making decisions as to the overall dimensions of an ESP.

2. Investigation of reliability and service time of units in field conditions with the aim of finding out unreliable units and probable causes of their failure.

3. Investigation of mechanisms of damage of equipment operating in conditions of high temperature, abrasive medium, corrosion, and vibrations; development of methods of increasing reliability and service time of equipment.

4. Development of highly reliable mechanical equipment units.

Development of Methods of Determination of Reliability of ESP Mechanical Equipment Units

Reliability of mechanical equipment units of electrostatic precipitators in this country is commonly characterized by such criteria as the parameter of failure frequency and the probability of faultless operation.

The parameter of failure frequency is estimated by the following equation:

$$f = \frac{\Delta n}{n_o \Delta t}, \quad (1)$$

where Δn = number of units put out of operation in the time interval; and
n = number of units tested.

The parameter of failure frequency gives sufficiently full characteristics of repairable units, including those in ESPs.

The intensity of failures is another frequently used criterion of reliability. It is estimated by the equation:

$$\lambda = \frac{\Delta n}{(n - \Delta n/2)\Delta t}, \quad (2)$$

where n = number of running units by the beginning of tests.

If the intensity of failures is constant in time and the number of units put out of operation is small in comparison to the total number of units, then the parameter of failure frequency and the probability of faultless operation can be estimated by the equation:

$$P = exp\left(-ft\right), \qquad (3)$$

where t = time elapsed from the beginning of tests.

Clarity and simplicity of estimation are the advantages of these criteria of reliability. But, unfortunately, they cannot be used for solution of some important problems encountered in the course of investigations of reliability. Such problems include:

1. Determination of "responsibility" of each unit for the decrease of ESP efficiency;
2. Evaluation of the required level of unit operation reliability;
3. Correlation of reliability of operation of ESPs of various design; and
4. Determination of required overall dimensions of ESPs with accounts of possible efficiency drops due to unreliable operation of units.

The above mentioned problems can be solved using reliability criteria directly related to the degree of gas cleaning efficiency.

An ESP consists of a series of parallel operating channels formed by collecting plates. Gas cleaning takes place in the electrical field of these channels. Generally, a failure of responsible units with time leads to the decrease of the number of running channels or, in other words, to the decrease of the precipitation area of the ESP (but not the area of collecting plates).

The relative decrease of the number of running channels due to the failure of some units can be classified as the coefficient of responsibility K_{resp}.

$$k_{resp} = \frac{\Delta N_i}{N_o \cdot \Delta n_i} = \frac{\Delta N_i}{N_o \cdot f_i \cdot n_{oi} \cdot \Delta t}, \qquad (4)$$

where ΔN_i = number of channels out of running order due to Δn_i failures of units of one and the same type during the time Δt;

N_o = total number of channels.

Similar to equation (1), one can describe an expression for the parameter of failure frequency of working channels due to the failure of units of one and the same type

$$f_{N_i} = \frac{\Delta N_i}{N_o \Delta t} = k_{resp.i} \cdot f_o \cdot n_{oi} \qquad (5)$$

where $\frac{\Delta N_i}{N_o}$ can be found by equation (4).

The parameter of failure frequency of channels due to the faults of units of various types can be estimated by the equation:

$$f_N = \sum_{i=1}^{\alpha} f_{N_i} \qquad (6)$$

where α = total number of unit types.

For estimation of the parameter of failure frequency of working channels, the mutual influence of failures was not taken into consideration as it is negligibly small because the number of units put out of operation in periods between repairs is relatively small.

The probability of faultless operation of an ESP P can be, similar to equation (3), found by the equation:

$$P(t) = \frac{N}{N_o} \cdot exp\,(-f_N \cdot t), \qquad (7)$$

where N = number of working channels in running order by time t.

Relative reentrainment of dust through a field of precipitators with the probability of faultless operation by time t equal to P can be easily found by the equation:

$$1 - \eta_i = (1 - \eta_{oi})P + (1 - \eta'_{oi})(1 - P) \qquad (8)$$

where η_i = gas cleaning efficiency of i field with account for reliability;
η_{oi} = gas cleaning efficiency of the same field by the beginning of the test;
η'_{oi} = gas cleaning efficiency during the period of failure ("mechanical" cleaning).

The first member of the equation (8) shows relative reentrainment through operating gaps of an ESP, the second, through those out of running order. By simple transformation of the equation (8) and taking into consideration that total reentrainment through an ESP is equal to the product of relative reentrainment through individual fields, one can derive the general equation of dust precipitation efficiency, which accounts for reliability of mechanical equipment units:

$$\eta = 1 - \prod_{i=1}^{m} [(1 - P\eta_{oi}) - \eta'_{oi}\ (1 - P)], \qquad (9)$$

where m = number of fields

The equation (9) can be expediently used for precise calculations. Gas cleaning efficiency of individual fields of ESP can be, for example, estimated by the methods described in (1). Taking into consideration that the efficiency of mechanical gas cleaning is about 0.2-0.3, one can use for approximate estimations the simpler equation:

$$\eta = 1 - [(1 - P) + P(1 - \eta_o)^{1/m}]^m, \qquad (10)$$

where η_o = the general gas cleaning efficiency of an ESP in running order.

It should be noted that the probabilities of faultless operation of a field and of an ESP generally coincide.

When deriving equation (10), it was supposed that gas cleaning efficiencies of individual fields are equal, and that the second number of equation

(2) is negligible compared to the first one. Analytical data have shown that the estimation of reentrainment by the equation (10) differs from that by the precise equation (9) by not more than 30 percent with variation of gas cleaning efficiency from 97 to 99 percent, and with broad variations of particle size distribution (mean-root-square error was in the range from 2.2 to 5.6). The error grows with the range of particle size distribution and gas cleaning efficiency.

The results of calculations by the above equations have shown that the main responsibility for operation of an ESP lies with discharge electrodes. Their contribution into the reliability of an ESP is from 65 to 75 percent.

The developed technique allows a sufficiently simple estimation of required unit reliability level on the basis of tolerable decrease of gas cleaning efficiency during the period between repairs. It also allows during designing to provide for necessary reserves of overall dimensions of the ESP to compensate any possible efficiency decrease due to unit failures. Besides, the technique correlates reliability of various design ESPs to their faultless operation.

Field Tests of Reliability and Service Time of Mechanical Equipment Units

Initial information as to reliability of ESPs was obtained mainly through questionnaires sent to industrial plants where precipitators were installed. The relevance of this information was verified by the direct control tests of ESPs when they were stopped for repair. Agreement of the failure frequency parameters obtained by different ways was satisfactory. Analysis of mechanical equipment unit defects has shown that they are due mainly to the following causes:

1. Inadequate assembling of the equipment;
2. Design defects of the units;
3. Low quality of completing sets;
4. Inadequate maintenance of the equipment.

Study of Physical Mechanism of Mechanical Equipment Units

Our practice has shown that field tests of ESP unit reliability cannot give complete answers to some questions related to a kind of fault, a cause of failure, etc. The answers to these questions require special investigations in the laboratory or on the stand to understand the physics of the processes taking place in the ESPs.

Operation of ESP units is investigated on special stands installed in NIIOGAZ. The stands completely simulate operating conditions of an industrial installation, such as high temperature, dust-laden gas flow, etc. For instance, a special stand was installed to find out the causes of fissures in thrust-partition quartz insulators of the type XY-105Y, which appeared in precipitators of the third dimension. This stand can change temperature in the range from 20° C to 250° C, weight loading on the insulator from 0 to 5.5 tons, voltage from 0 to 80 kV. It was found that fissures in the thrust-partition quartz insulators are caused by the great difference of temperature expansion coefficients of quartz and steel.

The investigations have shown that increasing of thickness of the asbestos gasket between the insulator and the bearing flange sharply lowers the probability of insulator mechanical destruction during warming up of the ESP casing. Recommendations were elaborated for prevention of fissure formation.

Development of New Highly Reliable Mechanical Equipment Units

On the basis of the investigations carried out by NIIOGAZ, modified units of EG-type ESP were developed (shafts-insulators, rapping mechanism hammers, bearings, etc.). They are applied in serial production of precipitators.

Further increase of reliability and service time of ESPs can be reached on the basis of new principles:

1. Development of nonmechanical means of electrode cleaning without rotating parts that cannot operate reliably in conditions of abrasive medium, corrosion, and high CaO content in dust;
2. Development of new highly reliable and effective systems of discharge electrodes; and
3. Application of special coatings to prolong service time of discharge and collecting electrodes as well as of other equipment of precipitators.

At the present time, the equipment developed on the basis of new solutions has been tested on the stand and in industrial ESPs in this country.

REFERENCES

1. I. V. Yermilov, "Study in Calculation of Gas Cleaning Processes in Plate Type Electrostatic Precipitators," (authors's abstract of candidate dissertation), Moscow, MEI, 1974, 24 p.

STUDY OF OPERATING AND MAINTENANCE REQUIREMENTS OF ELECTROSTATIC PRECIPITATORS IN THE U.S.A

Dennis C. Drehmel,[*] Michael Szabo,[†]

Abstract

The purpose of studying operating and maintenance requirements of electrostatic precipitators (ESPs) is to establish procedures that will give the highest collection efficiency over a period of time. That is, the ESP will be maintained at its best performance level with a minimum of lost time because of malfunctions. Since it is presumed that the reader is familiar with ESP technology, no description of theory or basic design will be reviewed. This paper describes operating considerations, maintenance requirements, and malfunction problems of modern precipitators. Much of the discussion is based on fly ash application of the wire weight type precipitators. However, much of the information can be applied to the use of precipitators on other processes.

OPERATING CONSIDERATIONS

Power Supply

The optimization of applied power to the precipitator is accomplished by automatic power controls that basically vary the input voltage in response to a signal generated by the sparkover rate. Provisions are also included to make the circuit current sensitive to protect against overload and to allow control in the event that spark level cannot be reached.

The automatic control circuit is divided into three functions: spark control, current limit control, and voltage limit control. In general, spark control is based on storing electrical pulses in a capacitor for each spark occurring in the precipitator. If the voltage of the capacitor exceeds the preset reference, an error signal will phase the mainline silicon controlled rectifier (SCR) back to a point where the sparking will stop. Usually this type of snap action control will tend to over correct, especially at low spark rates.

Proportional control, another type of spark control, is also based on storing of electrical pulses for each spark occurring in the precipitator. The phase back of the mainline SCR, however, is proportional to the number of sparks in the precipitator. The main advantages of proportional control over spark control is that the precipitator determines its own optimum spark rate based on four factors: temperature of the gas, ash resistivity, dust concentration, and internal condition of the precipitator.

---

[*] Industrial Environmental Research Laboratory, Environmental Protection Agency, Research Triangle Park, N. C.

[†] PEDCO-Environmental Specialists, Atkinson Square, Suite 13, Cincinnati, Ohio.

The voltage limit control feature of the automatic control module limits the primary voltage of the high-voltage transformer to its rating. For current limit control, if the primary current exceeds the unit's rating, a signal is generated, as with the spark control, which retards the firing pulse of the firing circuit and brings the current back to the current limit setting.

With all three control functions properly adjusted, the control unit will energize the precipitator at its optimum or maximum level at all times, determined by conditions within the precipitator. This will result in any one of the three automatic control functions operating at its maximum, i.e., maximum voltage, maximum primary current, or maximum spark rate. Once one of the three maximum conditions is reached, the automatic control will prevent any increase in power to reach a second maximum. If conditions require, due to changes within the precipitator, the automatic control will switch from one maximum limit to another.

RAPPERS

The magnetic impulse gravity impact rapper is a solenoid electromagnet consisting of a steel plunger surrounded by a concentric coil, both in a watertight steel case.

The electrical controls provide a number of separate adjustments so that all rappers can be divided into a number of different groups. Each group may be independently adjusted according to transmissometer readings. They are adjusted manually to provide adequate release of dust from collecting plates while preventing undesirable stack puffing.

In some applications, the magnetic-impulse, gravity-impact rapper is also used to clean the precipitator discharge wires. In this case, the blow is imparted to the electrode supporting frame in the same manner, except that an insulator insolates the rapper from the high voltage of the electrode supporting frame.

VIBRATORS

The vibrator is an electromagnetic device, the coil of which is energized by alternating current. The vibration set up by the coil is transmitted to the high tension wire frame through a rod.

For each installation there will be a certain intensity and time period of vibration that will produce the best collecting efficiency. Insufficient intensity of vibrating will result in heavy buildups of dust on the discharge wires. This condition causes the following adverse operating conditions:

- It reduces the sparkover distance bewteen the electrodes, thereby limiting the power input to the precipitator.
- It tends to suppress both the formation of negative corona and the production of unipolar ions necessary in the precipitation process.

- It alters the normal distribution of electrostatic forces in the treatment zone. Unbalanced electrostatic fields can cause the discharge wires and the high-tension frame to oscillate.

Maintenance Requirements

A preventive maintenance schedule should be established for each installation, detailing the precipitator parts to be checked and maintained daily, weekly, monthly, quarterly, semiannually, annually, and on a situational basis. Ideally, one individual with engineering training, or equivalent training with precipitators, should have overall responsibility for the maintenance program. This person should participate in study programs, seminars, and symposiums to broaden his knowledge. Operators and maintenance personnel should also be carefully selected and trained.

Daily. It is obvious that gross departures from normal readings on the transformer-rectifier meter and transmissometer indicate trouble. It is not so widely recognized that small variations, often too slight to be noticed without checking of daily readings, can indicate impending trouble.

Problems that usually have a gradual, rather than sudden, influence on precipitator performance include: (1) air inleakage at air heaters or in ducts leading to the precipitator, (2) dust buildup on precipitator internals, and (3) deterioration of electronic-control components. Such problems can be indicated by a small, but definite, drift of daily meter readings away from baseline values.

For example, sudden tripout of an apparently normal electrical set probably indicates a short or ground in the secondary circuitry. A low but steady voltage reading indicates a high resistance ground--such as that from discharge wires to ground through ash accumulating above a plugged hopper, or from clinker formation on a wire.

Fluctuating voltage, dipping to low values, suggests a broken and swinging discharge electrode. Fluctuation of spark-rate meter readings does not necessarily indicate a problem unless there is confirmation by fluctuating voltage and/or current readings.

Probably 50 percent of all electrical set tripouts are caused by ash buildup. Short of set tripout, buildup above the top of hoppers can cause excessive sparking that erodes discharge electrodes. Further, the forces created by growing ash piles can push internal components out of position, causing misalignment that may drastically affect performance.

Although various indicators and alarms can be installed to warn of hopper-ash buildup and of ash-conveyor stoppage, the operator can doublecheck by testing skin temperature at the throat of the hopper with the back of the hand. If the temperature of one or more hoppers seems comparatively low, the hopper heaters may not be functioning properly. Generally, however, low temperature indicates that hot ash is not flowing through the hopper and that bridging, plugging, or failure of an automatic dump valve has held ash in the hopper long enough for it to cool. The ash collected subsequently will pile up at the top.

If the temperature of all hoppers appears low to the touch, the operator should check the ash-conveyor system to see if it has stopped or if dust agglomeration is so great that the conveyor can no longer handle all of the fly ash.

Daily check of the control-room ventilation system minimizes the possibility of overheated control components, which can cause drift of control set points and accelerated deterioration of sensitive solid-state devices.

Weekly. Solenoid-coil failures, fairly common when high voltage was used, are rare with modern low-voltage equipment. Still, a weekly check of all units is advisable. Rapper action should be observed visually, and vibrator operation confirmed by feel. In addition, since rapping accelerations of 30 g are often required for proper collection, an accelerometer mounted on the plates should be checked to verify that rapping acceleration is adequate. This is best done on a pretest check.

Control sets must be checked internally for deposits of dirt that may have penetrated the filter. Accumulation of dirt can cause false control signals and can damage such large components as contractors and printed circuits.

Finally, filters in the air supply lines to control cabinets and the precipitator top housing should be checked and cleaned, if necessary, to prevent plugging.

Monthly. Most new precipitators incorporate pressurized top housings that enclose the bushings through which high-voltage connections are made to the discharge electrodes within the precipitator box. This prevents leakage from the precipitator into the housing, which could cause ash deposits and/or moisture condensation on the bushings, with a risk of electrical breakdown at the typical operating potential of 45 kV d.c.

Inspect bushings visually and by touch for component vibration. Check differential pressure to be sure that the fan that pressurizes the housing is in good operating condition. Also, operate manually the automatic standby fan to make sure it is service-ready.

Quarterly. Quarterly maintenance includes inspection of electrical-distribution contact surfaces, which should be cleaned and dressed and the pivots lubricated, if this is not done even more frequently. These could cause false signals. Further, since transmissometer calibration is subject to drift, calibration should be verified to avoid the possibility of false indications of precipitator performance.

Semiannually. Routine inspections, cleaning, and lubrication of hinges and test connections should be done semiannually. If this task is neglected, extensive effort eventually will be required to free-up test connections and access doors, involving expensive downtime.

Exterior inspection for corrosion, loose insulation, exterior damage, and loose joints can identify problems while repair is still possible. Special attention should be given to points at which gas can leak out as fugitive emissions.

Annually. Scheduled outages must be of sufficient duration to allow thorough internal inspection of the precipitator. Checks should be made for: (1) possible leakage of oil, gas, or air at gasketed connections, (2) corrosion where heat loss is great or gas temperatures are low, and (3) possible misalignment of internal components. Also, high-voltage switchgear should be inspected for possible binding, misalignment, or defeated interlocks--defects that create a safety hazard in addition to reducing performance.

All insulator support bushings, rapper insulators, and antisway insulators should be cleaned and inspected for hairline cracks and evidence of tracking. Faulty insulators can cause excessive sparking and voltage loss, and can fail abruptly, possibly even explode, if allowed to deteriorate.

Situational. Certain preventive-maintenance and safety checks are so important that they should be performed during any outage of sufficient length, without waiting for scheduled downtime. Air flow readings should be compared with baseline values to detect possible performance deterioration. Further, meter readings taken immediately upon restoring the precipitator to service can serve as a check on any changes that may have resulted from maintenance done during the outage.

Critical internal alignments should be checked whenever an outage allows and immediate corrective action taken if misalignment is discovered. Control-cabinet and top-housing interiors should be checked during any outage of 24 hours or more and cleaned if necessary. Any outage of more than 72 hours provides an opportunity to check grounding devices, alarms, interlocks, and other safety equipment, and to clean and inspect insulators and bushings.

Malfunctions

Discharge Wire Breakage. Probably the most common problem associated with suspended wire electrode-type ESPs is wire breakage, which typically causes an electrical short circuit between the high-tension discharge wire system and the grounded collection plate. This electrical short trips the circuit breaker, disabling a section of the ESP, which will remain disabled until the broken wire is removed from the unit.

Electrical erosion, the predominant cause of failures, occurs when repeated electrical sparkovers or arcs occur in a localized region. A sparkover causes localized heating and vaporization of a minute quantity of metal with each spark. If the sparkover occurs at random locations, no serious degradation of the discharge electrode occurs. If the sparkover occurs repeatedly at the same location, however, significant quantities of material can be removed, with subsequent reduction of cross-sectional area and ultimate failure at this point.

Localized sparking can be caused by misalignment of the discharge electrodes during construction or by electric field variations caused by "edge" effects where the discharge and collection electrodes are adjacent to each other at the top and the bottom of the plates. Corrective measures for eliminating failure at these points are adding shrouds and providing a rounded surface at the end of the collection electrode to reduce the tendency for sparking.

Electrical erosion can also be caused by "swinging" electrodes, which can occur when the mechanical resonance frequency of the discharge wire and weight system is harmonically related to the electrical frequency of the power supply.

Poor workmanship during construction can also cause electrical failures of the discharge electrode. If pieces of the welding electrode remain attached to the collection plate, localized electric field deformation can lead to sparking and ultimate failure of the discharge electrode.

Mechanical fatigue occurs at points where wires are twisted together and a continued mechanical motion occurs at one location. This situation is found at the top of a discharge electrode where the wire is twisted around the support collar. Methods of reducing mechanical fatigue include selection of discharge electrode material that is less susceptible to cold-work annealing after attachment or modification of the design of the corona wire attachment.

COLLECTION HOPPERS AND ASH REMOVAL

Hoppers and ash systems often constitute problems in precipitator operation. If the hoppers become full, the collected dust may short-circuit the precipitator. The power through the dust may fuse the dust, forming a large clinker-type structure called a "hornet's nest." This structure further interferes with ash removal and must be removed. Most problems associated with hoppers are related to providing for proper flow of the dust. Improper adjustment of the hopper vibrators or failure of the conveyor system are the usual causes of failure to empty the hoppers. It may be necessary to provide heat and/or thermal insulation for the hoppers to prevent moisture condensation and resultant cementing of the collected dust.

Malfunctions of the evacuation and removal system include ash water pump failure, water jet nozzle failure, disengagement of vacuum connections, and failure of sequencing controls.

INSULATOR/BUSHING FAILURE

Suspension insulators are used to support and isolate the high-voltage parts of an ESP. Inadequate pressurization of the top, housing the insulators, can cause ash deposits and/or moisture condensation on the bushing, which may result in electrical breakdown at the typical operating potential of 45 kV d.c.

Corrective or preventive measures include inspection of ventilation fans for the top housing and availability of a spare fan for emergencies. Frequent cleaning and checking for damage of the fans by vibration is also necessary to ensure trouble-free operation.

CONCLUSION

Performance of the electrostatic precipitator can be ensured by maintenance practices on daily, weekly, monthly, quarterly, semiannual, and annual schedules. Particular attention should be given to hopper and discharge electrode problems which lead to the most common malfunctions. Proper operation of automatic power supplies, rappers, and vibrators is essential for high collection efficiency.

REFERENCES

1. M. F. Szabo and R. G. Gerstle, "Operation and Maintenance of Particulate Control Devices on Coal Fired Utility Boilers," Pedco Environmental Inc., EPA-600/2-77-129, July 1977.

2. P. P. Bibbo and M. M. Peacos, "Defining Preventative Maintenance Tasks for Electrostatic Precipitators," Research Cottrell, Inc., Power, August 1975, pp. 56-58.

3. H. L. Engelbrecht, "Plant Engineer's Guide to Electrostatic Precipitator Inspection and Maintenance," Air Pollution Division of Wheelabrator Frye Inc., Plant Engineering, April 1976, pp. 193-196.

4. M. F. Szabo and R. G. Gerstle, "Electrostatic Precipitator Malfunctions in the Electric Utility Industry," Pedco Environmental Inc., EPA-600/2-77-006, January 1977.

5. Handbook for the Operation and Maintenance of Air Pollution Control Equipment, Frank Cross Jr., P.E., and Howard E. Hesketh, Ph.D, P.E., Eds., 1975.

6. Sabert Oglesby, Jr., "A Manual of Electrostatic Precipitator Technology," Southern Research Institute, August 1970.

7. "Electrostatic Precipitator Manual," The McIlvaine Co., Chapter VI, Section E, copyright 1976.

MATHEMATICAL MODELING OF ELECTROSTATIC PRECIPITATOR FILTERS AND ITS APPLICATION TO INDUSTRIAL UNITS IN THE U.S.S.R.*

I. V. Yermilov and T. I. Dimitrieva

Abstract

A Soviet mathematical model for designing industrial electrostatic precipitators (ESPs) is described in this paper. The Soviet model is compared with the corresponding American model. Engineering and experimental values of gas cleaning efficiency are given for a number of industrial ESPs in the U.S.S.R. along with engineering and experimental values for the fractional efficiency of dust removal for the case of an industrial pilot ESP at the Cherepetsk State Regional Power Station. An expression is given for the generalized coefficient that takes into consideration the correction for reentrainment, back corona, etc.

INTRODUCTION

The current stage in the growth of industry in developed countries is characterized by greater attention to problems dealing with environmental protection, particularly air pollution from industrial enterprises. The laws of many countries contain rigid standards for permissible levels of dust emission and effective measures have been taken to control these emissions and comply with the given standards. In conjunction with this, requirements have increased for more precise predictions of the design for the gas cleaning efficiency of units, since errors in design result either in noncompliance with standards for dust removal or excessive expenditures for gas cleaning equipment.

Calculating electrostatic precipitator (ESP) efficiency is associated with many difficulties. This is related to the complexity of processes associated with the electrodeposition of dust in the corona discharge field of the ESP and also to a great extent by the probable nature of the gas stream parameters of the gas entering the gas cleaning unit. For this reason, during design, semiempirical procedures for calculation are used that are based on the utilization of experimental data obtained for the efficiency of operating units (analogs). One of the best examples of this type of procedure is given in reference 1.

Semiempirical procedures give good results in designing ESPs that do not differ significantly from the analogs. The calculation of ESPs intended for new production having a higher cleaning efficiency than the analog and using different technology for their basic production is associated with serious errors.

More accurate predictions of cleaning efficiency can be achieved by setting up a scientifically substantiated procedure for calculating ESPs; this procedure is based on knowledge accumulated from the electrodeposition processes for dust in the coronal discharge field. After the fundamental works of Deutsch and Pauthenier (refs. 2, 3), the major contribution in setting up a scientifically substantiated method for calculating ESPs was made by Soviet and American scientists (refs. 4, 5, 6). Nevertheless, the design procedures described in the above literature have not received broad application in design practice. This is because these procedures only very approximately reflect such important physical processes as reentrainment, particle charging, drift velocity, etc. As a consequence, this results in an imprecise calculation of efficiency.

---

*For further information regarding the material in this paper, please contact I. K. Reshidov, U.S.S.R. 113105, Moscow, M-105, 1-st Nagatinsky Pass., 6, NIIOGAZ.

MATHEMATICAL MODELS FOR CALCULATING ESPs

In recent years, both in the U.S.S.R. and in the United States, mathematical models have been developed for calculating the efficiency of industrial ESPs (refs. 7, 8, 9) which take into consideration the latest information associated with calculating dust electro-deposition processes.

The models have a number of common characteristics. First of all, in the case of both models the overall gas cleaning efficiency is calculated on the basis of fractional efficiency. Secondly, both the Soviet and American models take into consideration the reentrainment of dust, gas distribution nonuniformity, and the particle charge component that is conditioned by ion diffusion more precisely than the earlier models.

However, the method of considering these processes is not identical. Reentrainment in the American model is taken into consideration during calculation of fractional efficiency. The correction factor for reentrainment is determined by comparing the calculated and experimental values for fractional efficiency. In the Soviet model, the correction for reentrainment is derived after calculating the overall efficiency. This method of determining reentrainment from our point of view is advantageous because the entrainment factor can be easily determined from experimental data on the efficiency of the unit without having to resort to some specific kind of calculation.

The gas distribution in the American model is taken into consideration with the aid of the correlation factor:

$$\mathcal{F} = 1 + 0.766\,\eta_p\,\sigma^{1.786} + 0.0755\,\sigma \ln\left(\frac{1}{1-\eta_p}\right), \tag{1}$$

where: η_p = is rated gas cleaning efficiency;
σ = is the root-mean-square deviation for gas velocity.

Gas distribution in the Soviet model is accounted for by an analogous factor:

$$k_u = \sigma^2 + 1. \tag{2}$$

Calculations using formulas (1) and (2) for values σ and η meet in practice, yield close values for the factors, and practically coincide at not very high gas cleaning efficiencies.

Particle charging in the Soviet model is calculated as the sum of charges obtained by the impact and diffusion charging mechanism (ref. 10). In the

American model, charge is calculated by a more complex model, which ultimately yields results close to those obtained by the Soviet model.

The Soviet and American models calculate ESP field intensity differently. In order to calculate the field in the Soviet model, the operating voltage and corona onset voltage must be known. While in the case of the American model, the voltage current and ion mobility must be known.

In the case of the Soviet model, a number of additional processes are taken into consideration:

1. Increased particle entrainment through the inactive (or more accurately, semiactive) zones of the ESP;
2. Particle charging in a higher intensity field of the corona electrodes;
3. Dust concentration profile nonuniformity in the ESPs.

The above factors were introduced into the model as the result of studying the electrodeposition processes with the studies carried out both on laboratory and industrial ESPs in the U.S.S.R. (refs. 11, 12).

Both the Soviet and the American models utilize a single experimental factor called the reentrainment factor. In the case of the Soviet model, this factor equals 0.7 for thermal electric power stations with continuous electrode rapping (one blow on the electrodes in 3 minutes for each field) and 0.8 in the case of optimal rapping intervals for each field. In the case of ESPs used in cement plants, this factor equals 0.80 and 0.95 respectively.

The Soviet mathematical model was verified using experimental data associated with the efficiency of industrial ESPs in the U.S.S.R. (refs. 7, 8). Nevertheless, the quantity of experimental data used for comparison and the range of parameter variation for the gas stream did not make it possible to evaluate the accuracy and universality of the computational model. An additional circumstance was that the comparison was carried out only on domestic (Soviet) ESPs that were similar in their design. For this reason it would be interesting to verify the computational model on ESPs with designs other than the Soviet one, and also under conditions of a wider range of gas stream parameter variation, in particular, dust resistivity. Results are presented below from such a comparison.

SOVIET INDUSTRIAL ESPs

Table 1 gives the calculated $\eta_{p/}$ along with the experimental η_{3} for the overall gas cleaning efficiency in ESPs established in the U.S.S.R., along with the initial data necessary for calculation. The procedure described in references 7 and 8 was used for carrying out the calculations.

As can be seen from table 1, the calculated efficiency values are in satisfactory agreement with experimental values in the absence of back corona ($\rho < 5 \cdot 10^9$ ohm/m). At large resistance values, experimental values for efficiency are lower than the calculated values. This is related to the fact that back corona shows up large resistance values for the trapped fly ash. This back corona is not taken into consideration in a computational model.

Table 1. Experimental and calculated gas cleaning efficiencies of industrial ESPs in the USSR.

Plant		Type of ESP	U кV	U_0 кV	h_0 м	L м	d_0 м	r_0 10^{-3} м	T °K	P мм	u $\frac{м}{с}$	j $10^{-3}\frac{A}{м}$	ν $10^{-4}\frac{м^2}{с}$	d_{50} 10^{-6} м	σ	ε	l_m	s_0	$k_{уп}$	ρ ом м	$\eta_э$ %	η_p %	γ_0	η_{ps} %
Ladyzhinsk	GRES	EGZ-3-177	35,7	I9,2	0,I375	I2,0	0,I8	0,294	388	745	I,09	0,098	0,248	23,0	3,I5	6000	I,I	0,9I5	0,7	$2{,}I5\cdot I0^9$	98,6	99,I	0,65	98,9
Tripol'sk	GRES	YG2-4-53	4I,I	2I,7	0,I375	I0,0	0,I8	0,294	4I0	748	I,93	0,093	0,272	29,0	4,83	5000	I,4	0,89	0,8	$I{,}5\cdot I0^9$	96,7	97,4	0,70	95,9
Berezovsk	GRES	PGD-3-50	45,8	22,4	0,I625	7,5	0,I9	0,75	427	750	I,I2	0,I04	0,290	20,7	2,88	5000	I,4	0,88	0,7	$I0^9$–$I0^{I0}$	95,6	96,4	0.67	95,9
Novosibirsk	TETs	UG2-4-53	52,0	28,6	0,I375	I0,0	0,I8	0,294	4I8	750	I,7I	0,I5I	0,265	I8,0	3,I6	5000	I,4	0,89	0,7	$I{,}8\cdot I0^9$	97,8	98,I	0,68	97,8
Reftinsk	GRES	"Lurgi"	3I,8	25,5	0,I50	I3,65	0,I6	0,75	406	748	I,04	0,056	0,272	I4,0	3,I2	5000	I,I	0,956	0,8	$I{,}35\cdot I0^{II}$	96,2	97,0	0,70	95,4
Troitsk	GRES	UGZ-4-265	36,3	25,0	0,I375	I6,0	0,I8	0,294	400	748	1,38	0,060	0,246	30,0	3,62	5000	1,1	0,9I5	0,7	$I{,}1\cdot I0^{II}$	97,2	98,8	0.55	96,9
Troitsk	GRES	Pilot	33,2	23,5	0,I375	I0,0	0,I8	0,294	399	744	2,09	0,069	0,260	30,0	3,62	5000	1,1	0,9I5	0,7	$I{,}05\cdot I0^{II}$	9I,2	94,8	0,60	92,0
Troitsk	GRES	Pilot	32,8	23,0	0,I375	I0,0	0,I8	0,294	394	746	I,87	0,080	0,254	30,0	3,62	5000	I,I	0,9I5	0,7	$7{,}7\cdot I0^{I0}$	93,4	95,4	0,57	9I,9
Cherepetsk	GRES	DGPN-2-55	38,2	20,0	0,I625	6,6	0,I8	0,294	422	732	I,24	0,045	0,276	30,0	3,3	5,2	I,55	0,86	I,0	$8{,}3\cdot I0^9$	95,7	95,5		
Cherepetsk	GRES	Pilot	40,0	22,0	0,I375	5,0	0,I8	0,294	403	740	I,50	0,I80	0,259	I9,0	3,66	8,0	I,05	0,9	I,0	$2{,}9\cdot I0^9$	98,5	98,0		
Cherepetsk	GRES	Pilot	35,0	22,0	0,I375	5,0	0,I8	0,294	403	740	I,60	0,090	0,259	I9,0	3,66	8,0	I,05	0,9	I,0	$2{,}9\cdot I0^9$	96,4	96,5		
Cherepetsk	GRES	Pilot	30,0	22,0	0,I375	5,0	0,I6	0,294	40I	742	I,50	0,042	0,259	I9,0	3,66	8,0	I,05	0,9	I,0	$2{,}9\cdot I0^9$	95,5	93,I		
Ul'yanovsk Cement Plant		PGD-4-38	59,3	28,2	0,I625	10,0	0,I9	0,75	460	750	I,28	0,07I	0,3I5	I4	3,38	5000	I,I5	0,88	0,8	$3\cdot I0^8$	99,0	98,9	0,79	98,8
Balakleysk Cement Plant		PGD-4-50	58,6	27,9	0,I625	I0,0	0,I9	0,75	483	748	I,I2	0,065	0,3I2	I2	2,75	5000	I,I5	0,88	0,8	$2\cdot I0^8$	99,8	99,2	0,82	99,3
Vol'sk Cement Plant		DGPN-3-35	57,0	27,I	0,I625	9,96	0,I85	0,75	463	749	I,42	0,085	0,3I8	8,0	2,96	5000	I,I5	0,88	0,8	$3\cdot I0^8$	97,9	97,6	0,79	97,5
Slantsev Cement Plant		PGD-2-20	55,3	26,3	0,I625	5,0	0,I8	0,75	323	758	1,07	0,I40	0,I83	3,8	I,9	5000	I,I5	0,9I	0,8	$I0^8$	98,0	95,7	0,88	96,8

Note: 1/ Experimental data were obtained by workers of SFNIIOGAZ under the guidance of I.A. Kizim, V.N. Nesin, V.D. Pustovoyt, V. G. Razumnyi, A.I. Pol'shchikov, I.V. Ermilov.

2/ The degree of gas cleaning of the ESPs at the Cherepetsk State Regional Electric Power Plant was attained with no electrode rapping.

3/ The specific dust resistivity was measured in the laboratory under a working gas temperature and current density of $(04.0\text{-}0.4)\ 10^{-3}\ \frac{A}{M}2$.

In order to calculate the cleaning efficiency over a broader range of dust resistance values, gas velocity, electrode height, etc., it is advisable to take into consideration reentrainment, back corona, and the correction for the dielectric permeability of particles by means of the generalized correction coefficient K_0.

$$K_0 = k_{ym} k_\rho k_\varepsilon = 1 - a_1 \left(\frac{\rho}{\rho_0}\right)^{a_2} \left(\frac{u}{u_0}\right)^{a_3} \left(\frac{h}{h_0}\right)^{a_4} \left(\frac{B}{B_0}\right)^{a_5} \left(\frac{d}{d_0}\right)^{a_6} e^{a_7 \frac{m}{m_0}}, \quad (3)$$

where: ρ = the specific volumetric resistance of dust,
u = gas velocity,
h = precipitator electrode height,
B = gas moisture content,
d = average median particle size,
m = dust mass on the precipitator electrode,
$\rho_0, u_0, h_0, B_0, d_0, m_0$ = base parameter values,
k_{ym} = reentrainment factor,
k_ρ = factor taking into consideration the back corona, and
k_e = factor taking into consideration the relative charge reduction of dielectric particles in comparison with the conducting particles.

Table 1 shows the calculated values for the correction factor K_0 and overall cleaning efficiency η_{pz}, calculated with consideration given to this correction factor. The agreement of the calculated and experimental results in this case is significantly better than in the first instance.

Figure 1 shows the experimental and calculated fractional gas cleaning efficiency for the industrial pilot-type ESP at the Cherepetsk State Regional Electric Power Station. The experimental values for efficiency were obtained in the absence of electrode rapping. The satisfactory agreement of the calculated and experimental values obviously attests to the fact that the basic factors are reflected quite adequately in the model where these factors affect gas cleaning in the absence of electrode rapping.

AMERICAN INDUSTRIAL ESPs

Table 2 presents the calculated η_p and the averaged experimental values for the test period of the total cleaning efficiency η_3 of some American industrial ESPs. The experimental values necessary for the calculations and the cleaning efficiency values were obtained during the course of a joint study of the operation of the ESPs at the Allen Electric Power Station, which was conducted by a group of Soviet and American specialists (ref. 14).

The calculations, the same as in the first case, were carried out using the procedure presented in references 7 and 8. The initial parameters that were necessary for the calculation were averaged for the test period (table 2).

Some difficulties were encountered in averaging the dispersion composition of the trapped fly ash. The dispersion composition of the fly ash at the inlet to the unit, as presented in reference 13, is not given in relative units but in absolute units ($\frac{g}{m}$3). In order to calculate the dispersion composition in relative units, it is necessary to know the total fly ash concen-

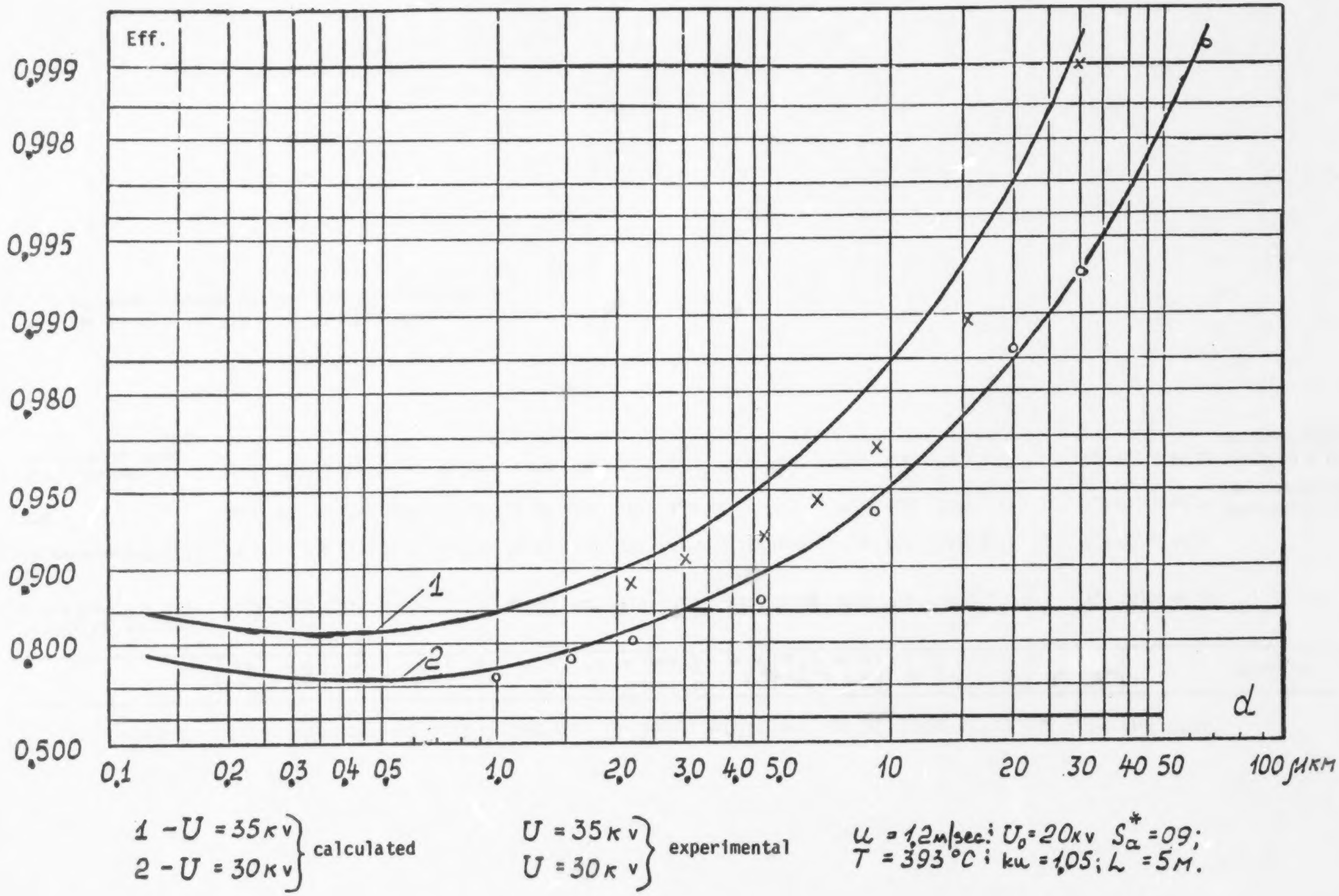

Figure 1. Experimental and calculated fractional efficiencies of dust particle collection of the industrial-pilot ESP at the Cherepetsk State Regional Power Station.

Table 2. Experimental and calculated gas cleaning efficiencies of industrial ESPs in the USSR.

	U кВ	U_0 кВ	h_0 м	L м	a_0 м	r_0 10^{-3} м	T °K	P ммрт	u $\frac{м}{с}$	i 10^{-3} $\frac{A}{м}$	ν 10^{-1} $\frac{м^2}{с}$	δ_{50} 10^{-6} м	б	ε		S'_A	k_r			Comments
"GORGAS" Electric Power Plant ESP (13)	32,5	I2,0	0,II43	I0,97	0,I75	I,384	427	745	1,8	0,07I	0,288	25,0	5,0	5000	I,15	I	0,7	99,69	99,82	
High-temperature ESP (13)	23,4	I2,0	0,II43	I2,2	0,I75	I,384	575	750	1,23	0,160	0,465	9,0	4,2	5000	I,I5	I	0,7	99,30	99,43	
ESP	29,6	I6,0	0,II43	I0,97	0,229	I,384	602	750	1,26*	0,165	0,5	29,6	3,95	5000	I,I5	I	0,7	99,66	99,7I	According to U.S. measurement data
ESP at the Allen Electric Power Plant (14)	29,6	I6,0	0,II43	I0,97	0,229	I,384	603	750	1,26*	0,165	0,5	27,6	3,I	5000	I,I5	I	0,7	99,42	99,82	According to USSR measurement data

* - gas velocity in the ESP at the Allen Electric Power Plant was taken to be average according to Soviet and U.S. measurements.

Table 2. Experimental and calculated gas cleaning efficiencies of industrial ESPs in the USSR.

	U кВ	U_0 кВ	h_0 м	L м	a_0 м	r_0 10^{-3} м	T °K	P мм рт	W м/с	l 10^{-6} м	ν 10^{-5} м²/с	a_{50} 10^{-6} м	σ	ε		S'_a	k_T	\		Comments
"GORGAS" Electric Power Plant ESP (13)	32,5	12,0	0,1143	10,97	0,175	1,384	427	745	1,8	0,071	0,288	25,0	5,0	5000	1,15	I	0,7	99,69	99,82	
High-temperature ESP (13)	23,4	12,0	0,1143	12,2	0,175	1,304	575	750	1,23	0,160	0,465	9,0	4,2	5000	1,15	I	0,7	99,30	99,43	
ESP	29,6	16,0	0,1143	10,97	0,229	1,384	602	750	1,26*	0,165	0,5	29,6	3,95	5000	1,15	I	0,7	99,66	99,71	According to U.S. measurement data
ESP at the Allen Electric Power Plant (14)	29,6	16,0	0,1143	10,97	0,229	1,389	603	750	1,26*	0,165	0,5	27,6	3,1	5000	1,15	I	0,7	59,42	99,82	According to USSR measurement data

---

* - gas velocity in the ESP at the Allen Electric Power Plant was taken to be average according to Soviet and U.S. measurements.

tration in the gas. Nevertheless, the fly ash concentration that was measured in work by a dust probe was higher than that measured by the impactor (ref. 13). From our point of view, this was related to the precipitation of large dust fractions on the nozzle and partially on the walls of the impactor, which decreased the overall concentration. In conjunction with this, the dispersion composition of dust in relative units was calculated on the basis of the concentration that was measured by the dust probe. Under these conditions, the obtained distribution contains an error in the large fraction range (d > 10 mkm). However, this does not have to reflect on the accuracy of the calculations for the overall efficiency, since the fly ash entrainment is determined primarily by the fine fractions.

The dispersion composition of fly ash at the inlet and outlet to the ESP at the Allen Station was also averaged for the test time. The data that were averaged separately were obtained with the aid of Soviet equipment (impactor 2 and the 2-cyclone separator) and by American equipment (table 2). In all cases, the dispersion composition of dust at the inlet was satisfactorily described by a log-normal distribution. At the outlet in the fine fraction range (d < 1 mkm) and in the large fraction range, deviation was observed from the lognormal law.

In conjunction with the fact that the coronal electrodes in the above described industrial ESPs are longer than the precipitator electrodes, the on-active zone was taken to be equal to 0 in conjunction with $\delta_a^{\cdot} = I$. A gas distribution grid with guide vanes was mounted at the ESP inlet at the Allen Electric Power Station in order to level the gas stream velocity field. Since accurate information concerning the guide vanes and the connecting duct work was not known, it was not possible to measure the field velocity nonuniformity coefficient on the model. An analysis of analogous gas distribution systems with a single grid (with an active cross section of 0.45-0.5) and guide vanes with gas coming up from below showed that the nonuniformity coefficient varies within the following limits $k_м$ = 1.06-1.25 (ref. 15). For this reason $k_м$ was taken in the calculations as equal to the average value--1.15.

Taking into account the above-mentioned observations, calculations were made that showed good agreement between calculated and experimental gas cleaning efficiency values. The discrepancy between the calculated and experimental values may be explained, on the one hand, by errors in the initial data used in the calculations (dispersion composition, $k_м$) and, on the other hand by errors in measuring the degree of cleaning.

Attempts were also made to compare the calculated and experimental values of fractional efficiency of entrainment with rapping. It should be noted that the Soviet model does not provide for calculating the fractional efficiency of entrainment with rapping, since secondary entrainment is taken into account after calculating the total efficiency. However, this represented a special interest from the point of view of broadening the understanding of the electrodeposition process.

Calculation of the fractional efficiency taking into account entrainment with rapping was made on the assumption that the coefficient of entrainment for the various fractions is constant. Comparison of calculated and experimental values for the fractional efficiency should have reflected the acceptability of such an assumption.

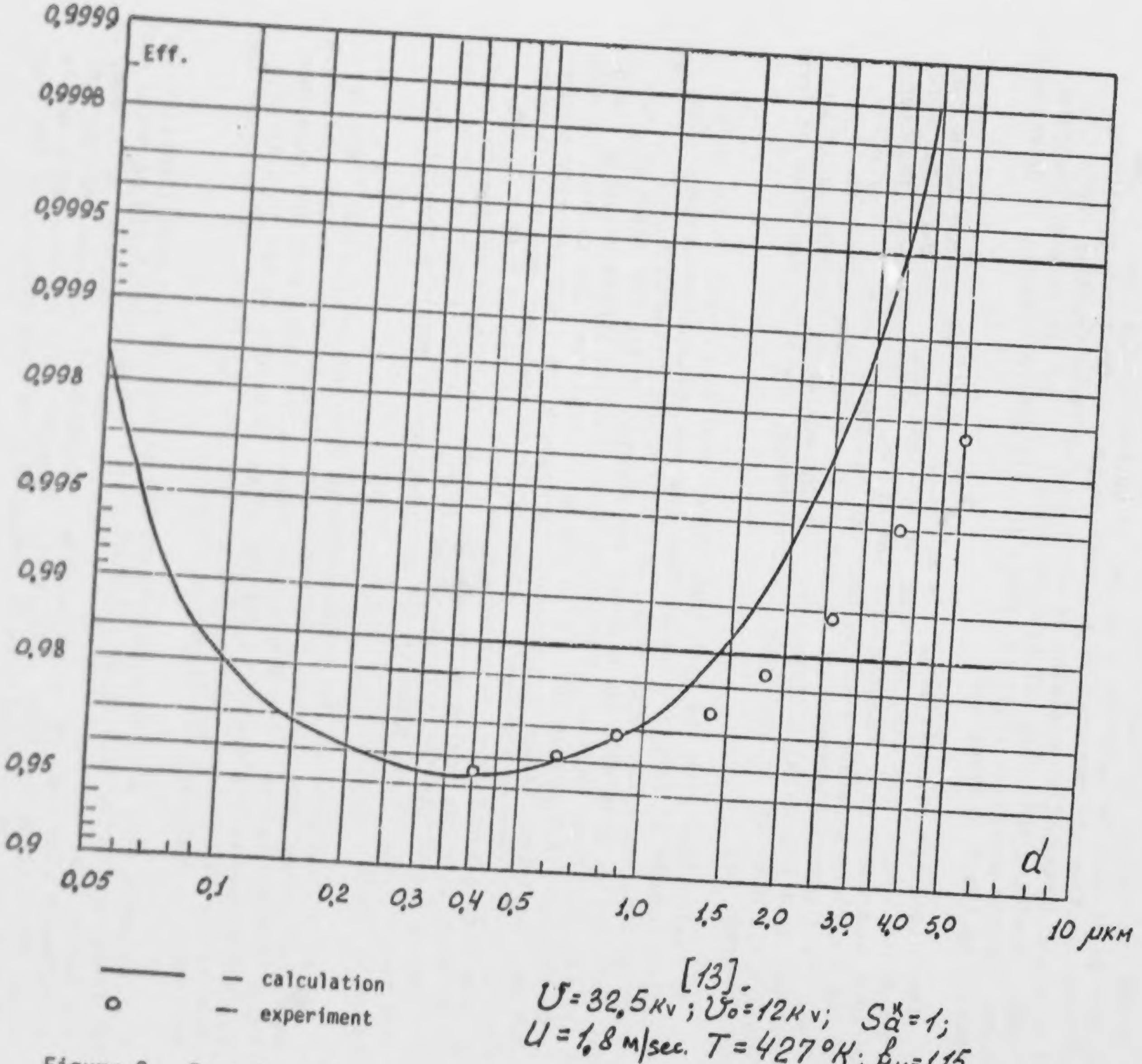

Figure 2. Experimental and calculated fractional gas cleaning efficiencies at the "GORGAS" Electric Power Plant, USA (13).

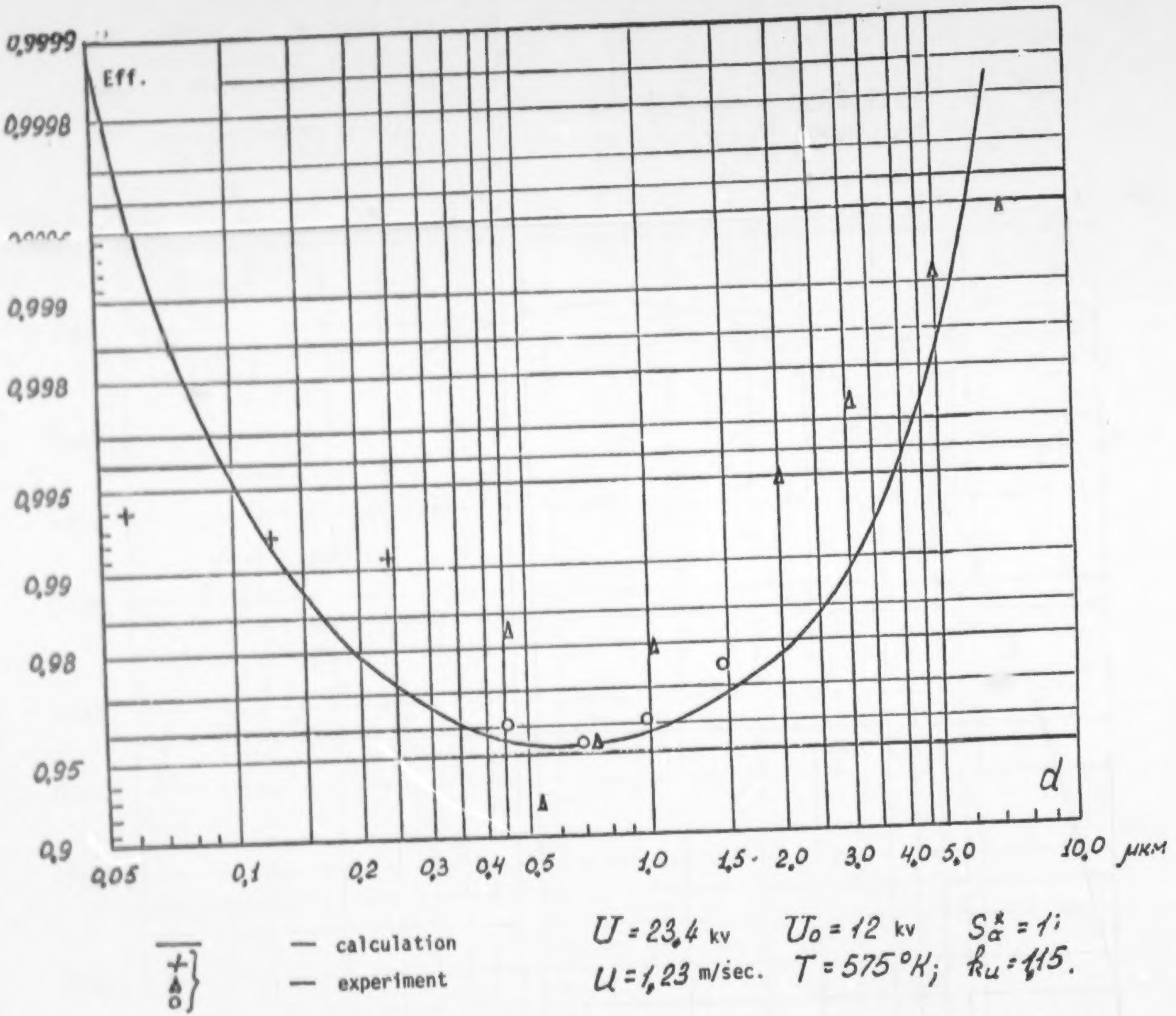

Figure 3. Experimental and calculated fractional gas cleaning efficiencies in a high-temperature ESP in the USA (13).

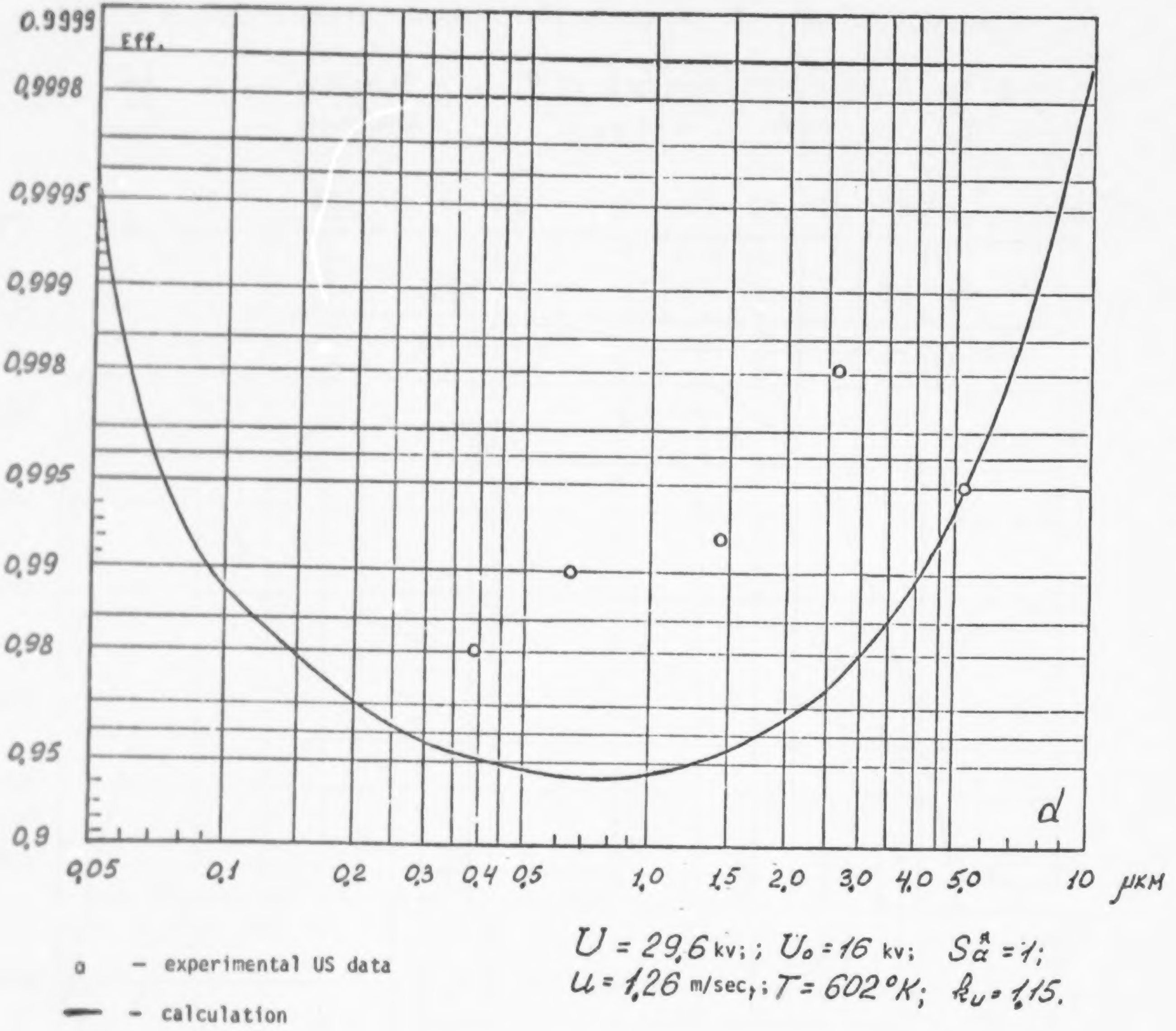

$U = 29{,}6$ kv; ; $U_o = 16$ kv; $S_a^a = 1$;
$u = 1{,}26$ m/sec; $T = 602\,^{\circ}K$; $k_U = 1{,}15$.

Figure 4. Experimental and calculated gas cleaning efficiencies in a high-temperature ESP at the Allen Electric Power Plant.

The value of the fractional coefficient of entrainment $k_{ф}$ (in the formula for fractional degree of cleaning of gas is multiplied by the fractional speed of drift) was found on the basis of the equation of the level of gas cleaning found using $k_{ф}$ and $k_{чн}$. It was found that for all three instruments $k_{ф}$ equals approximately 0.5.

Figures 2, 3, and 4 show the calculated and experimental values for the fractional efficiency of entrainment. As a rule, the calculated values for fractional efficiency are slightly lower for fine fractions and higher for larger ones. Apparently, this shows that during rapping of electrodes coagulation of fine particles takes place which causes the instability of $k_{ф}$.

CONCLUSION

The conducted comparison of calculated values of ESP efficiency with experimental values from industrial ESPs in the U.S.S.R. and in the United States shows that the mathematical model makes it possible to calculate the total gas cleaning efficiency of ESPs with an accuracy acceptable for practice. In order to use the model in designing industrial ESPs it is necessary to supplement the model with methodology for calculating the electrical and dust-gas stream parameters.

REFERENCES

1. A. B. Walker and V. W. Frisch, "Experience in the USA in the Area of Designing and Operating Hot-Side Electrostatic Precipitators on Waste-Heat Boilers Operating on Coal," reports of Symposium on Controlling Particulate Emissions Into the Atmosphere and Related Problems, May 26-28, 1976.

2. W. Deutsch, "Bewegung und Ladung der Elektrizitästräger in Zylinderkondersator," Annalen der Physik, 1922, Bd. 68, N. 12, S. 335-344.

3. M. Pauthenier and M. Moreau-Hanot, "La charge des Particules Spheriques dans un champ jonise," Journal de Physique et le Radium, Vol. 3 (No. 7), 1932, pp. 590-613.

4. V. N. Uzhov, "Industrial Gas Cleaning Using Electrostatic Precipitators," Moscow, Khimiya, 1967, p. 344.

5. H. White, "Industrial Electrostatic Precipitation," London, 1963, p. 337.

6. I. P. Vereshchagin, V. I. Levitov, G. Z. Mirzbekyan, and M. M. Pashin, "Basis for the Electro-gaso-dynamics of Dispersed Systems," Energiya, Moscow, 1974, p. 480.

7. I. V. Yermilov, "Calculating the Gas Cleaning Efficiency of Plate Type Electrostatic Precipitators," Industrial and Sanitary Gas Cleaning, No. 1, 1977, pp. 5-6.

8. I. V. Yermilov, "Calculating the Efficiency of Electrostatic Precipitators for Thermoelectric Power Stations," reports of Symposium on Controlling Particulate Emissions Into the Atmosphere and Related Problems," May 26-28, 1976, Kishinyov.

9. S. Oblesby and J. Gooch, "Mathematical Electrostatic Precipitator Model, Analysis of Parameter Functions Which Have an Effect on ESP Operating Efficiency," reports of Symposium on Controlling Particulate Emissions Into the Atmosphere and Related Problems, May 26-28, 1976, Kishinyov.

10. G. Z. Mirzabekyan, "Aerosol Particle Charging in a Coronal Discharge Field," collection of works: Strong Electric Fields in Technological Processes, Moscow, Energiya, 1969, p. 240.

11. I. V. Yermilov, "Dust Concentration Distribution in the Coronal Field of an Electrostatic Precipitator," Elektrichestvo, No. 7, 1974, pp. 27-31.

12. I. V. Yermilov and G. Z. Mirzabekyan, "Calculating the Gas Cleaning Efficiency in ESPs," Elektrichestvo, No. 3, 1976, pp. 36-40.

13 "Particulate Collection Efficiency Measurements on Three Electrostatic Precipitators," Environmental Protection Technology Series, EPA-600/2-75-056, October 1975.

14. Report on Joint Soviet/American Tests of Dust Removal and Measurement Equipment in Order to Study the Physical and Chemical Properties of Aerosol Conducted in the U.S.S.R. and the U.S. in 1976 (Topics A-4 and A-6), Moscow, NIIOGAZ, 1976.

15. I. Ye. Idel'chik, "Atlas of Gas Air Distribution Devices of Various Industrial Units. Industrial and Sanitary Gas Cleaning," No. 6, 1976, pp. 11-12.

MATHEMATICAL MODELING OF ELECTROSTATIC PRECIPITATORS IN THE UNITED STATES

Jack R. McDonald*

Abstract

Recent work in the United States toward the development of a mathematical model of electrostatic precipitation is discussed. This work includes the calculation of electrical conditions in wire-plate geometries and the calculation of particle charging rates. A mathematical model is described that calculates collection efficiency in an electrostatic precipitator as a function of particle size and operating conditions. The model determines the electric field, particle charge, and removal efficiency as functions of position along the length of the precipitator. Procedures for estimating collection efficiency losses caused by nonuniform gas velocity distributions, gas bypassage of electrified regions, and particle reentrainment are discussed. Model predictions of fractional collection efficiency are compared with field data from a hot-side precipitator used to collect fly ash.

INTRODUCTION

The approach to modeling precipitator performance in the United States has been to theoretically describe the individual processes involved in electrostatic precipitation and to incorporate them into a complete and comprehensive model. Although the model still contains empirical relationships, an objective of the modeling research has been to eliminate the use of such relationships, since it is difficult to establish their validity over the wide range of conditions found in precipitators. Due to the large number of high efficiency precipitators in use in the United States and increasingly more stringent particulate emissions standards, the collection of fine particles (0.1 to 2.0 μm in diameter) has been of great interest. In support of the modeling research, a large number of fractional efficiency measurements have been made under essentially idealized conditions in a laboratory precipitator and under conditions existing in full-scale industrial precipitators, particle charging experiments have been performed, and data relevant to electrical operating conditions have been obtained. The most recent modeling research has involved the development of mathematical descriptions of the electrical conditions in wire-plate geometries and particle charging by unipolar ions.

DESCRIPTION OF THE MATHEMATICAL MODEL

Calculation of Electrical Conditions

The electrical conditions in wire-plate geometries are calculated by using a technique developed by McDonald et al. (ref. 1). In this numerical technique, the appropriate partial differential equations that describe the electrodynamic field are solved simultaneously and subject to a suitable choice of boundary conditions existing in a wire-plate geometry. The procedure yields the voltage-current curve for a given wire-plate geometry and determines the electric potential, electric field, and charge density distributions for each point on the curve. Figures 1 through 6 show comparisons of the predictions of this technique with available experimental data (refs. 2 and 3). The agreement between theory and experiment is within 15 percent.

---

*Southern Research Institute, Birmingham, Alabama.

Calculation of Particle Charge

Particle charge is calculated from a unipolar, ionic-charging theory formulated by Smith and McDonald (ref. 4). In this approximate theory, particle charge is predicted as a function of particle diameter, exposure time, and electrical conditions. The charging equation is derived based on concepts from kinetic theory and determines the charging rate in terms of the probability of collisions between particles and ions. The theory accounts simultaneously for the effects of field and thermal charging and accounts for the effect of the applied electric field on the thermal charging process. For large particles and high applied electric fields, the theory predicts essentially the same charging rate as the classical field charging equation. For low applied electric fields the charging equation reduces to the classical diffusion equation.

The agreement between the results predicted by the theory and experimental data (refs. 5 and 6) for cases where electron-charging can be ignored is within 25 percent over the entire range of available data and is within 15 percent for practical charging times in precipitators. Figures 7 through 10 show comparisons between the theory and experiment. The theory agrees well with experimental data on the charging of fine particles where particle charging is difficult to describe physically and mathematically.

Ideal Calculation of Particle Collection Efficiency

The details of the mathematical model for electrostatic precipitation and a computer program, which performs the various operations, are described elsewhere in the literature (refs. 7, 8, and 9). In the following paragraphs, the mathematical framework of the model is briefly outlined.

Using probability concepts and the statistical nature of the large number of particles in a precipitator, particle collection efficiencies can be expressed in the form of an exponential-type relationship. In the model, the collection fraction ($\eta_{i,j}$) for the ith particle size in the jth increment of length of the precipitator is given by

$$\eta_{i,j} = 1 - \exp\left(-w_{i,j}A_j/Q\right) , \qquad (1)$$

where $w_{i,j}$ (m/s) is the migration velocity of the ith particle size in the jth increment of length, A_j(m^2) is the collection plate area in the jth increment of length, and Q(m^3/s) is the gas volume flow rate. The derivation of equation (1) is based on the simplifying assumptions that (1) the gas is flowing in a turbulent pattern at a constant mean forward velocity; (2) turbulence

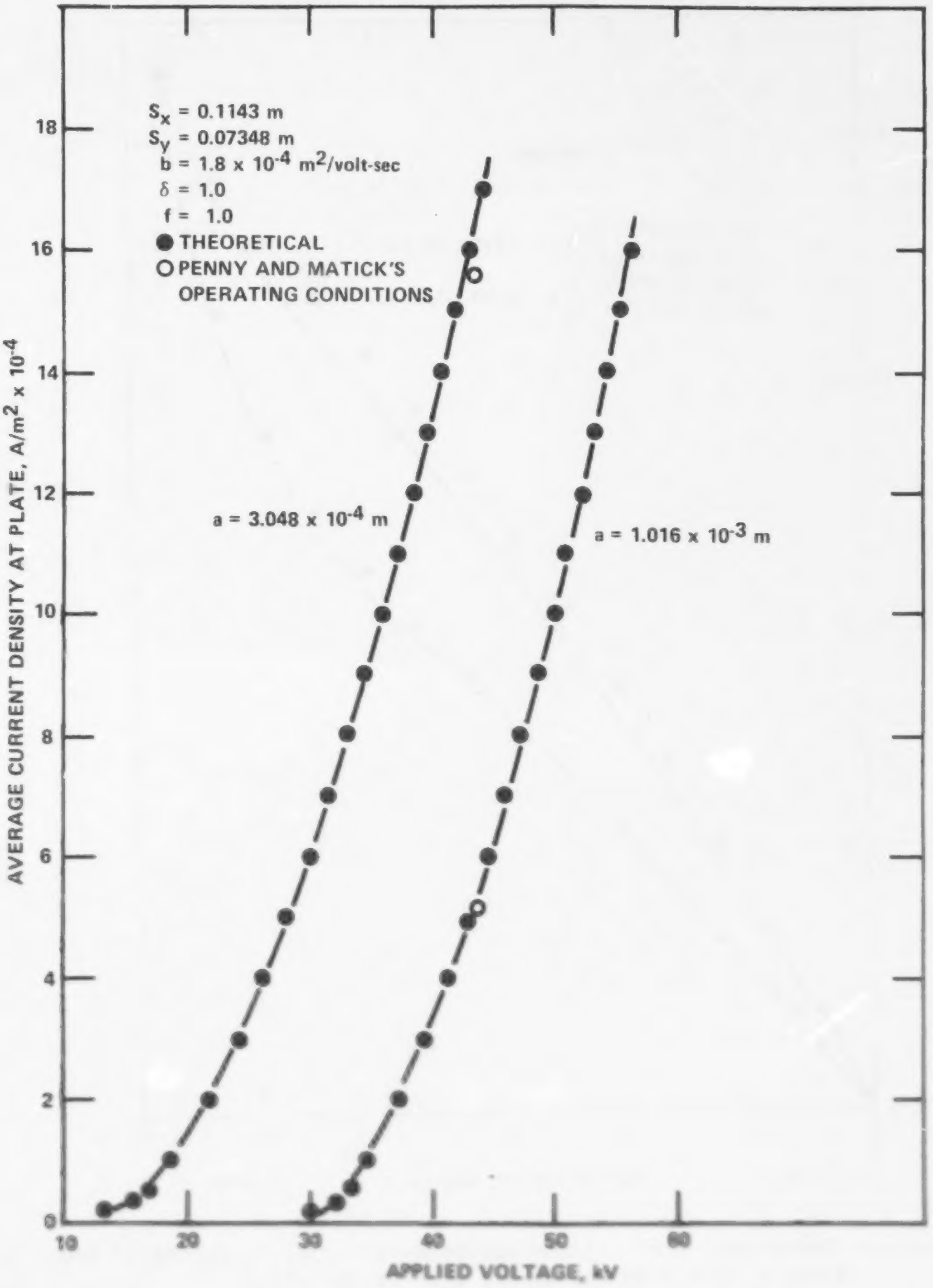

Figure 1. Theoretical (ref. 1) voltage-current characteristics for the geometries used by Penney and Matick (ref. 2).

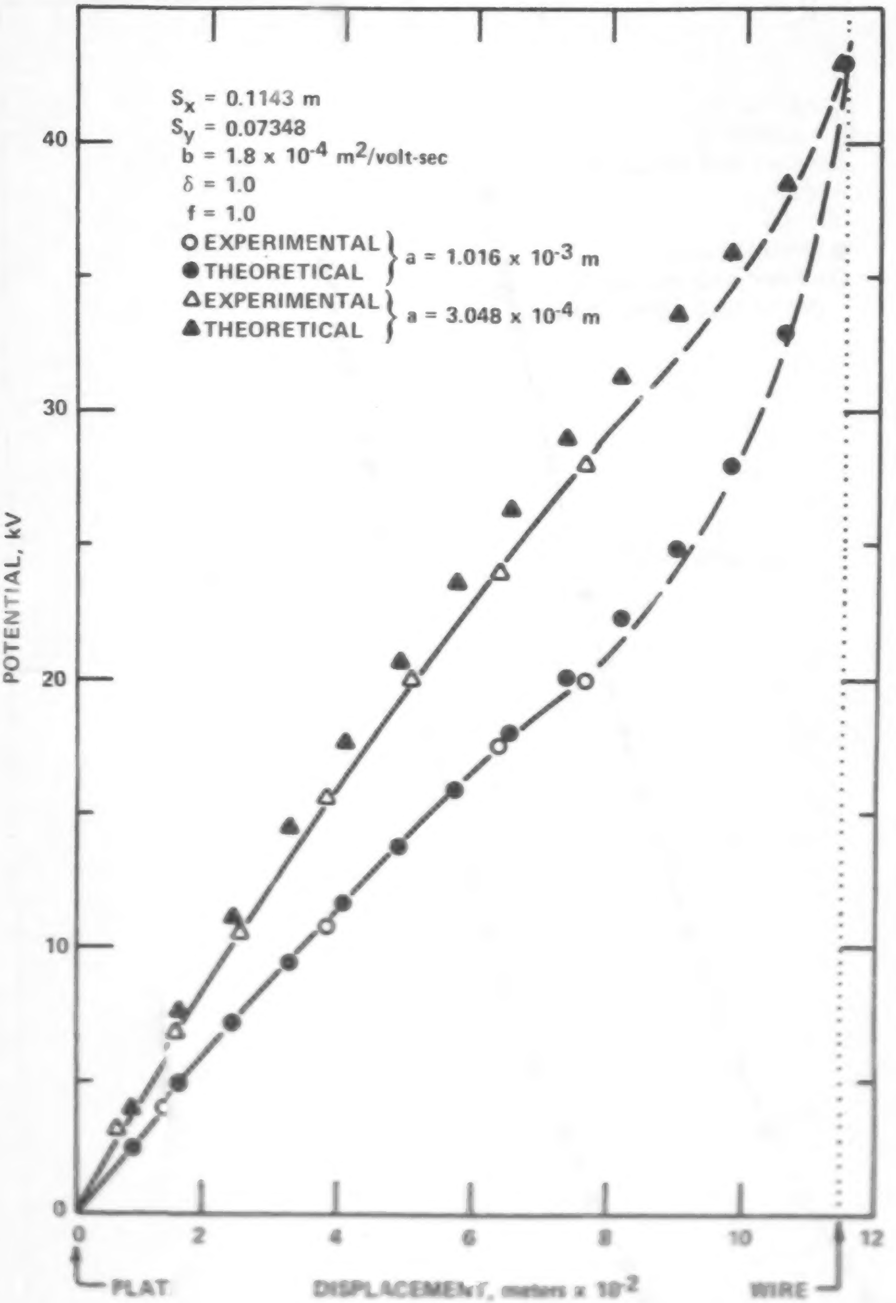

Figure 2. Theoetical (ref. 1) and experimental (ref. 2) potential profiles alon a line from the corona wire to the plate.

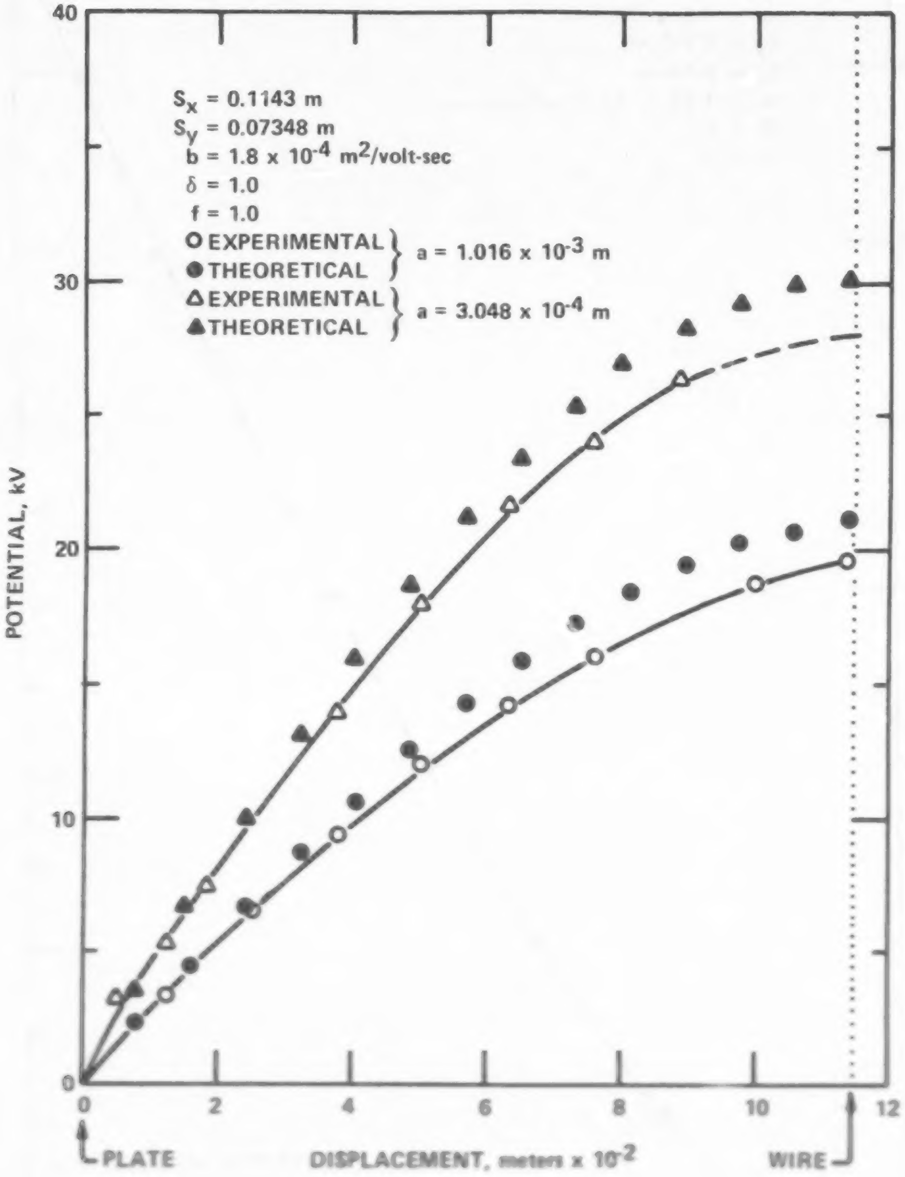

Figure 3. Theoretical (ref. 1) and experimental (ref. 2) potential profiles along a line from a point midway between the wires to the plate.

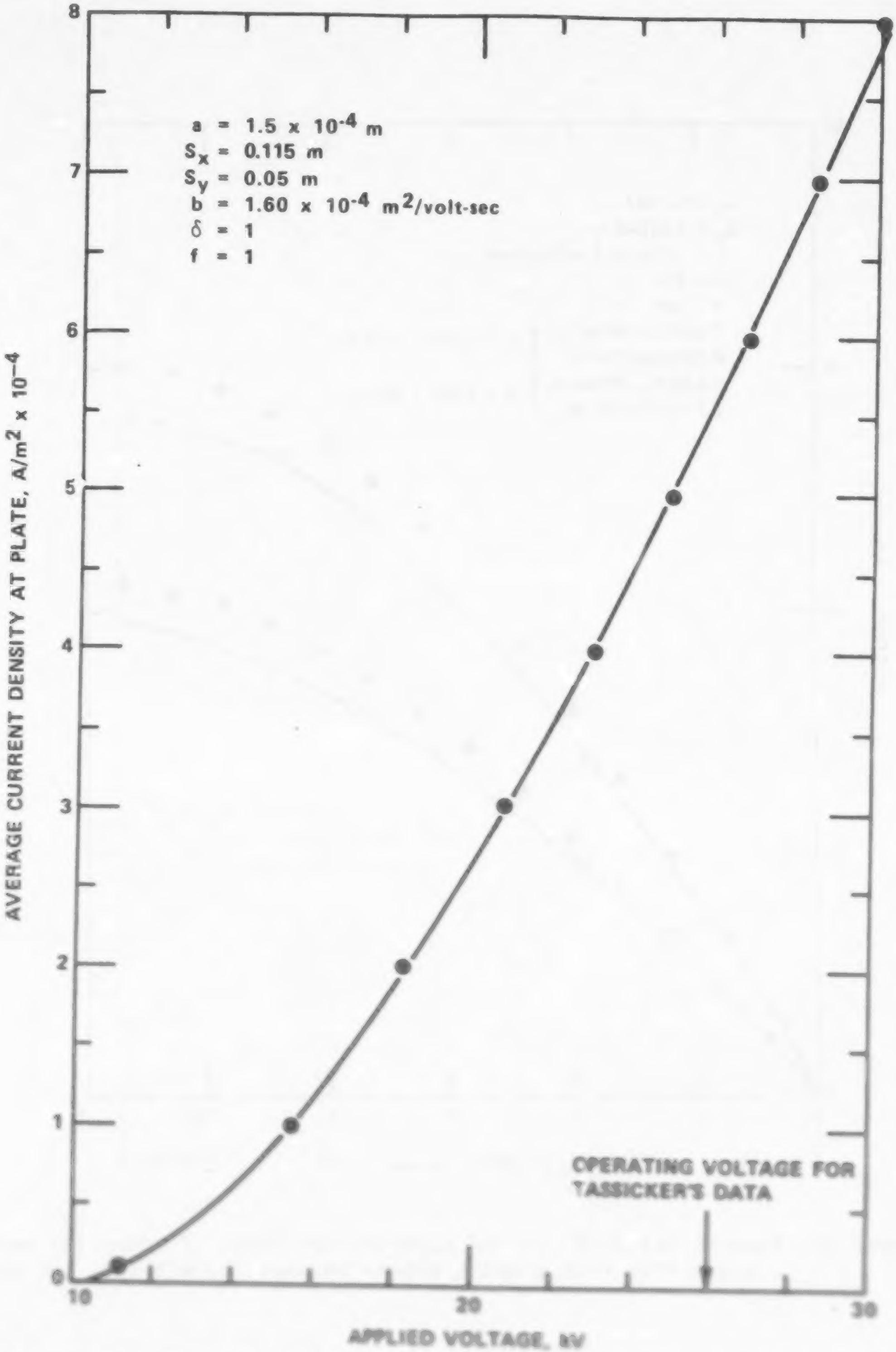

Figure 4. Theoretical (ref. 1) voltage-current characteristic for the geometry used by Tassicker (ref. 3).

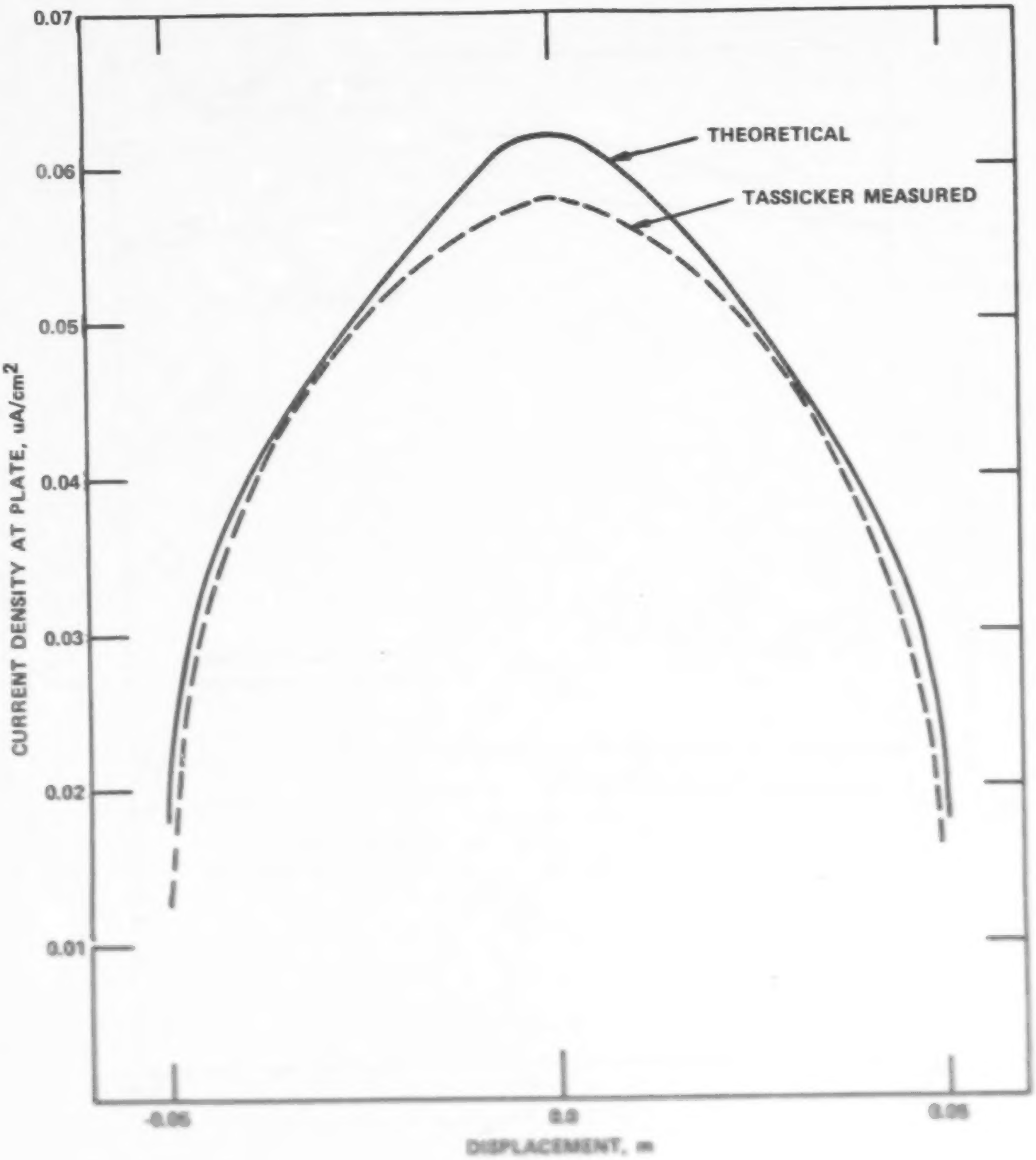

Figure 5. Theoretical (ref. 1) and experimental (ref. 3) current density at the plate as a function of displacement.

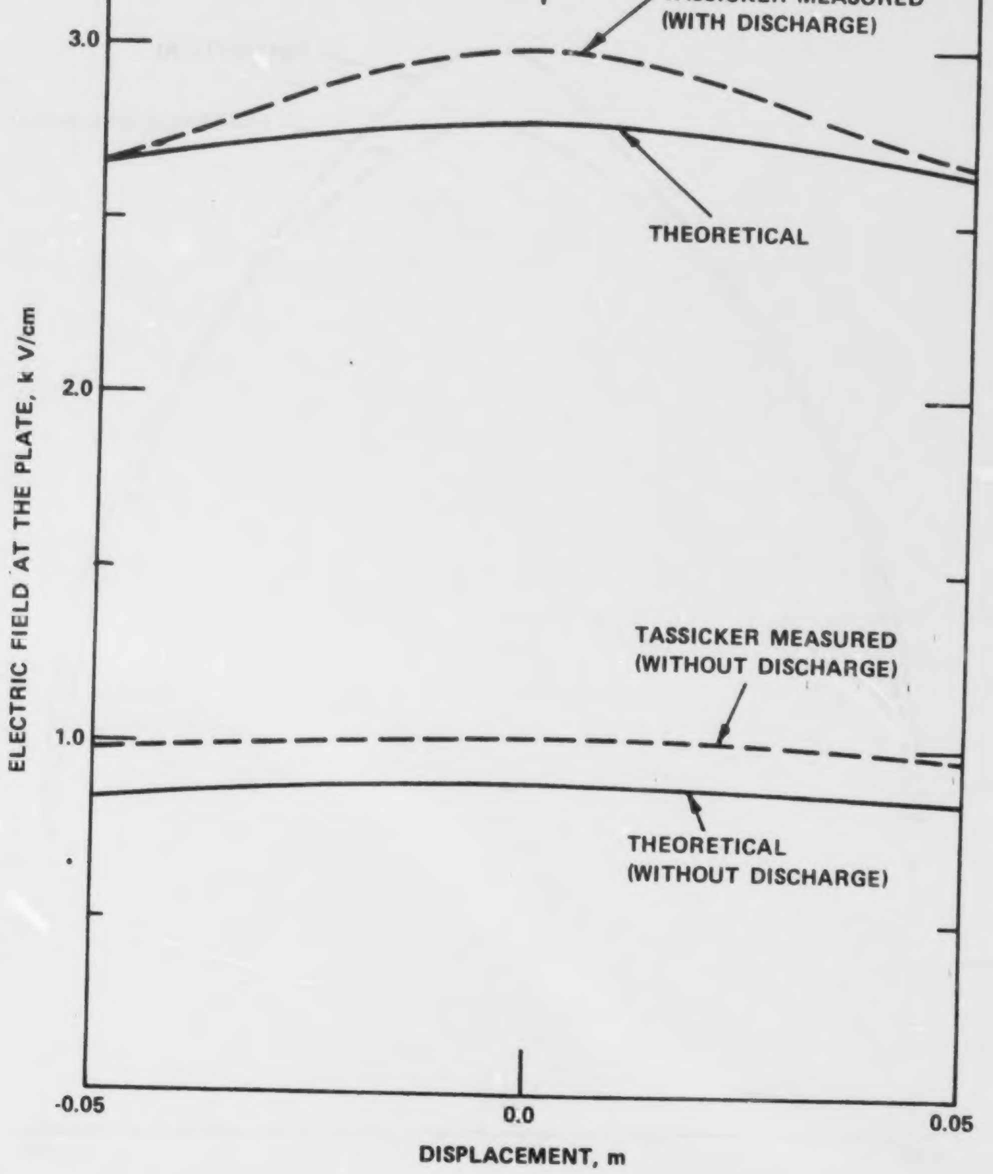

Figure 6. Theoretical (ref. 1) and experimental (ref. 3) electric field at the plate as a function of displacement.

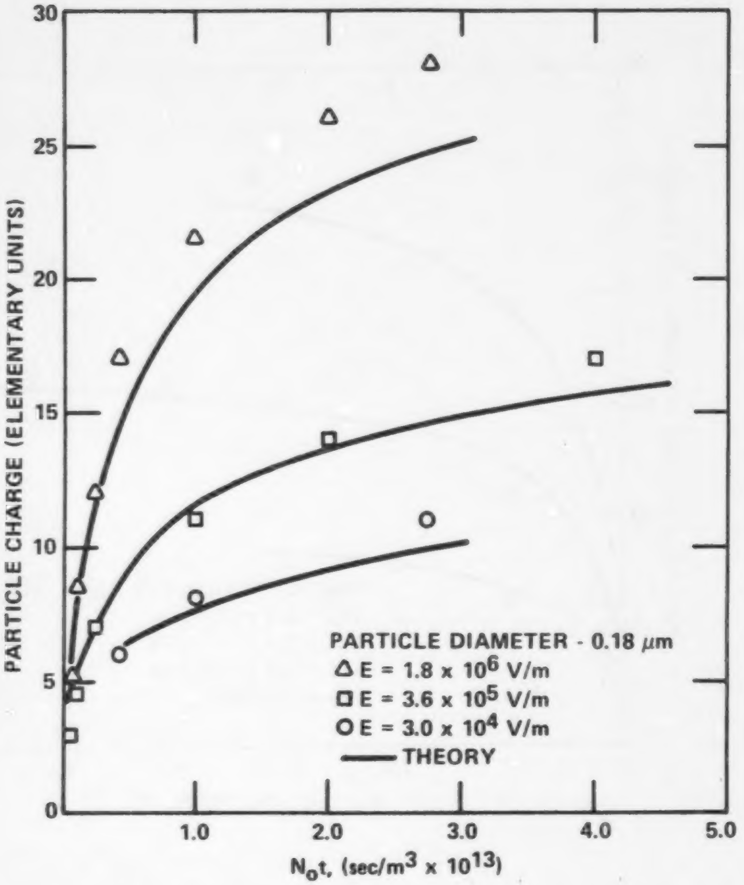

Figure 7. Theoretical (ref. 4) and experimental (ref. 5) particle charge as a function of "exposure time" for a 0.18 μm diameter particle.

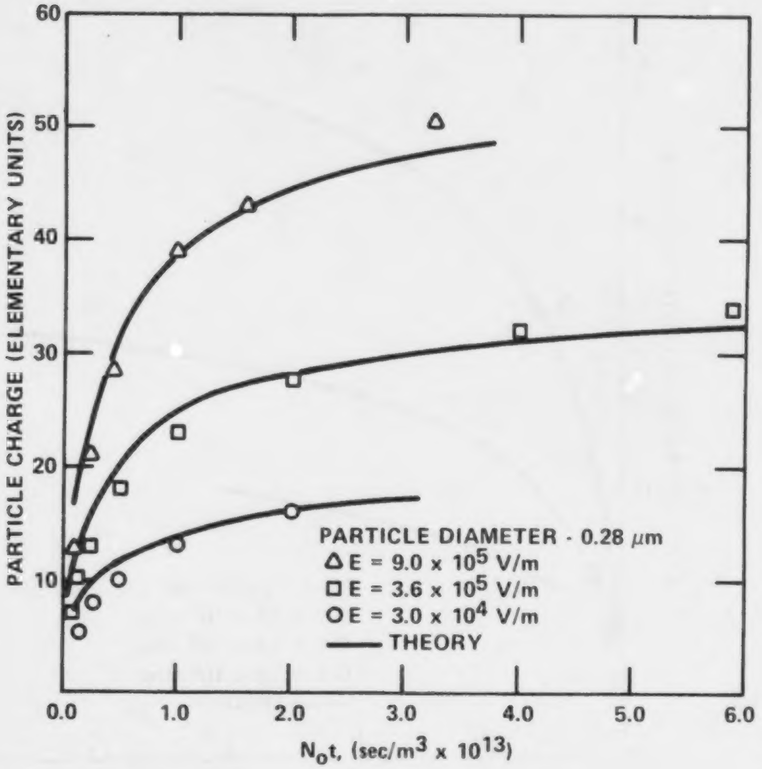

Figure 8. Theoretical (ref. 4) and experimental (ref. 5) particle charge as a function of "exposure time" for a 0.28 μm diameter particle.

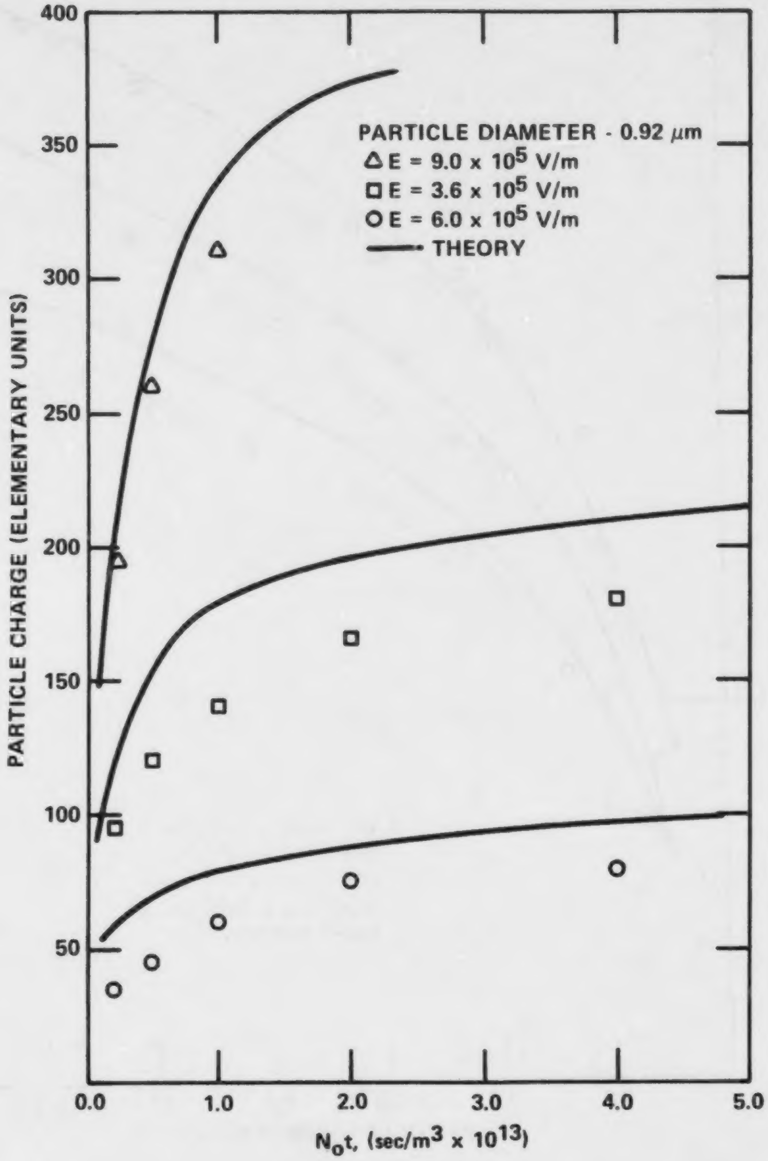

Figure 9. Theoretical (ref. 4) and experimental (ref. 5) particle charge as a function of "exposure time" for a 0.92 µm diameter particle.

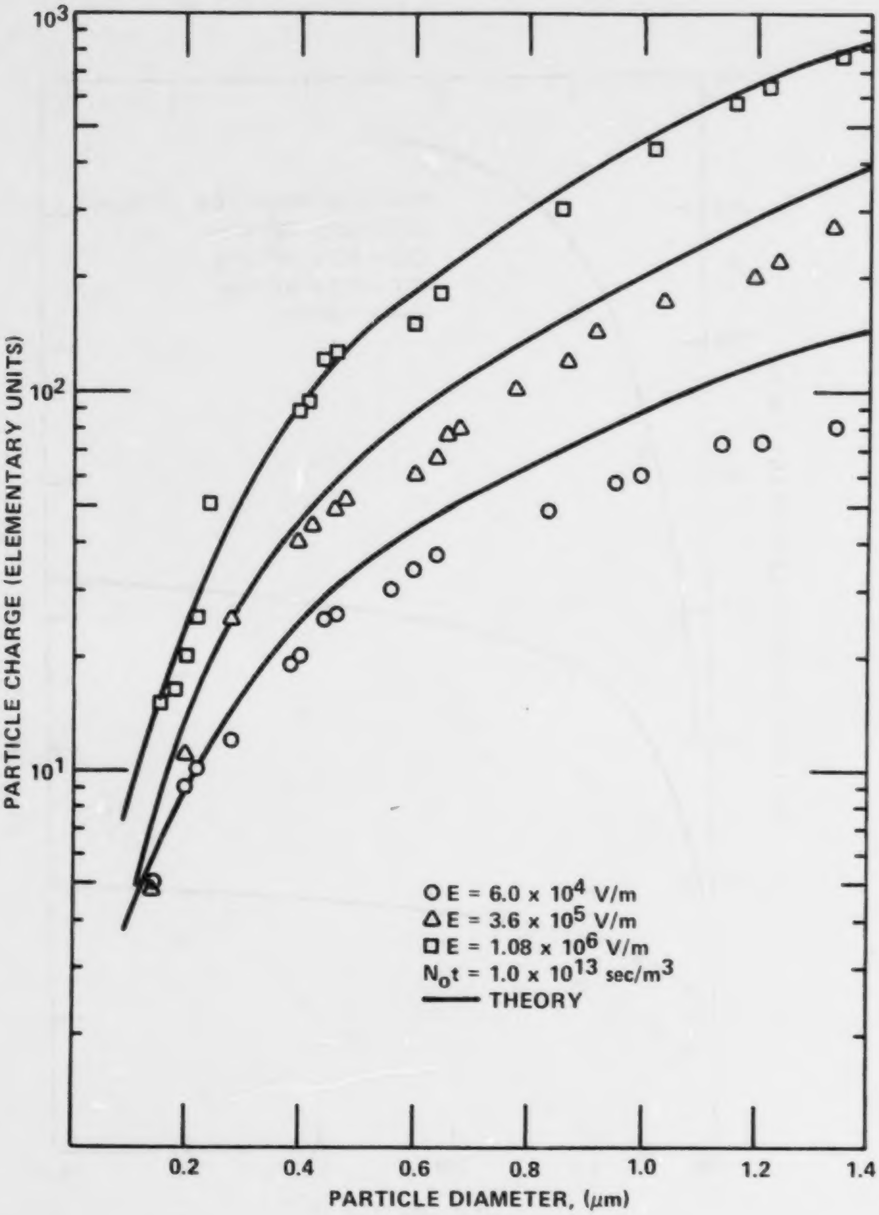

Figure 10. Theoretical (ref. 4) and experimental (ref. 5) particle charge as a function of particle size for low, moderate, and high electric fields.

is small scale, fully developed, and completely random; and (3) particle migration velocities are small compared with the gas velocity.

Equation (1) gives a reasonable representation of fine particle collection provided that the migration velocities can be determined accurately. The migration velocities are calculated from

$$w_{i,j} = q_{i,j}E_jC_i/6\pi a_i\mu \quad , \tag{2}$$

where

$q_{i,j}$ = charge on the ith particle size in the jth increment of length (coul),

E_j = electric field adjacent to the collection electrode in the jth increment of length (V/m),

C_i = Cunningham correction factor for the ith particle size,

a_i = radius of the ith particle size (m), and

μ = gas viscosity (kg/m.s).

The collection fraction η_i for a given particle size over the entire length of a precipitator is given by

$$\eta_i = \left(\sum_j \eta_{i,j}N_{i,j} \right) /N_{i,1} \quad , \tag{3}$$

where $N_{i,j}$ is the number of particles of the ith particle size per cubic meter of gas entering the jth increment.

The overall mass collection efficiency η for the entire polydisperse aerosol is obtained from

$$\eta = \sum_i \eta_i P_i \quad , \tag{4}$$

where P_i is the percentage by mass of the ith particle size in the inlet size distribution.

Recent field tests conducted in the United States, where particle emissions and size distributions were obtained with and without rapping, indicate that the ratio of the measured migration velocity without rapping to that ideally calculated from the model is nearly constant for particle sizes from 0.2 to 4.5 μm in diameter. The measured migration velocities are higher than those calculated from the model and the experimental data provide correction factors given in figure 11, which are used as multipliers on the ideally calculated migration velocities.

Methods for Representing Nonideal Effects

The nonideal effects of major importance are: (1) gas velocity distribution, (2) gas bypassage of electrified regions, and (3) particle reentrainment. These nonideal effects will reduce the ideal collection efficiency that may be achieved by a precipitator operating with a given specific collecting area. Since the model is structured around an exponential-type equation for individual particle sizes, it is convenient to represent nonideal effects in the form of correction factors which apply to the exponential argument. These correction factors are used as divisors for the ideally calculated migration velocities. The resulting "apparent" migration velocities are empirical quantities.

A numerical measure of the degradation of precipitator performance can be obtained by calculating the ratio of the migration velocity determined by the summation of point values of penetration to that determined by equation (1). An expression for this ratio may be obtained by setting the penetration based on the average velocity equal to the corrected penetration obtained from a summation of the point values of penetration and solving for the required correction factor, which will be a divisor for the migration velocity given in equation (1). A limited number of traverse calculations which have been performed indicate a correlation between the correction factors (F_i) and the normalized standard deviation (σ_g) of the velocity traverse. Based upon a pilot plant study (ref. 10), the following empirical relationship between the F_i, σ_g, and the ideal collection efficiencies (η_i) has been obtained:

$$F_i = 1 + 0.766\, \eta_i \sigma_g^{1.786} + 0.0755\, \sigma_g \ln (1/1-\eta_i) \quad . \qquad (5)$$

As of the present, relationships of the form $F_i = F_i\ (\eta_i, \sigma_g)$ have not been established for full-scale precipitators.

The effect on precipitator performance of gas bypassage of electrified regions can be estimated if the simplifying assumption is made that perfect mixing occurs following each baffled section. An expression for the penetration (P_{N_s}) of a given particle size from the last baffled section, which is corrected for gas bypassage, can be derived in the form

$$P_{N_s} = \left[S + (1-S)(1-\eta_i)^{1/N_s} \right]^{N_s} \quad , \qquad (6)$$

where S is the fractional amount of gas bypassage per baffled section and N_s is the number of baffled sections. Correction factors (B_i) are obtained by taking the ratios of the effective migration velocities under ideal

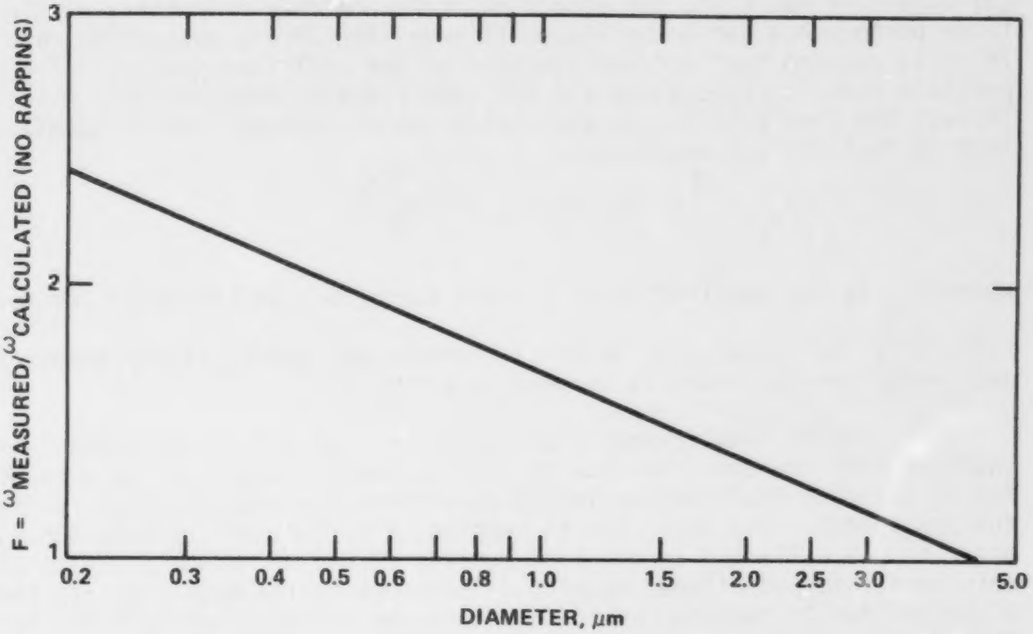

Figure 11. Empirical correction factors for the ideal migration velocities.

conditions to the "apparent" migration velocities under conditions of gas seepage so that

$$B_i = \frac{\ln (1-\eta_i)}{N_s \ln \left[S + (1-S)(1-\eta_i)^{1/N_s}\right]} \quad . \tag{7}$$

Although it is difficult to quantify the complex mechanisms associated with particle reentrainment due to (1) the action of the flowing gas stream on the collected particle layer, (2) sweepage of particles from hoppers caused by poor gas flow conditions or air inleakage into the hoppers, and (3) excessive sparking, the effect of these nonideal conditions on precipitator performance can be estimated if some simplifying assumptions are made. If it is assumed that a fixed fraction of the collected material of a given particle size is reentrained and that the fraction does not vary with length through the precipitator, an expression can be derived that is identical in form to that for gas bypassage:

$$P_{N_R} = \left[R + (1-R)(1-\eta_i)^{1/N_R}\right]^{N_R} \quad , \tag{8}$$

where P_{N_R} is the penetration of a given particle size corrected for reentrainment, R is the fraction of material reentrained, and N_R is the number of stages over which reentrainment is assumed to occur.

The results from several field tests on high efficiency precipitators indicate that the emissions due to rapping reentrainment can be accounted for by assuming that rapping losses come primarily from the last section of the precipitator and that, due to rapping, 5 percent of the mass per cubic meter of gas collected in the last section should be added to the total emissions obtained without rapping. The experimental data indicate that the emissions due to rapping reentrainment can be approximated by a log normal distribution with a mass median diameter of 4.0 μm and a geometric standard deviation of 2.5.

COMPARISON OF MODEL PREDICTIONS WITH FIELD DATA FROM A HOT-SIDE PRECIPITATOR

The mathematical model of electrostatic precipitation has been used to simulate operating conditions for a hot-side precipitator from March 12 through March 19, 1976, during a joint U.S.-U.S.S.R. field test program in the United States. Figure 12 shows the particle size distributions at the inlet that were obtained from measurements with modified Brink cascade impactors on various days. The solid line is a representative curve which was used to obtain an inlet size distribution for use in the model. Table 1 contains all the data that are necessary for use of the model. The individual entries were obtained by averaging all measurements of that variable over the test period.

Figure 13 shows the fractional efficiencies obtained from the experimental data and two theoretical curves predicted by the model. The theoretical overall mass collection efficiency based on σ_g = 0.25, S and/or R = 0.05,

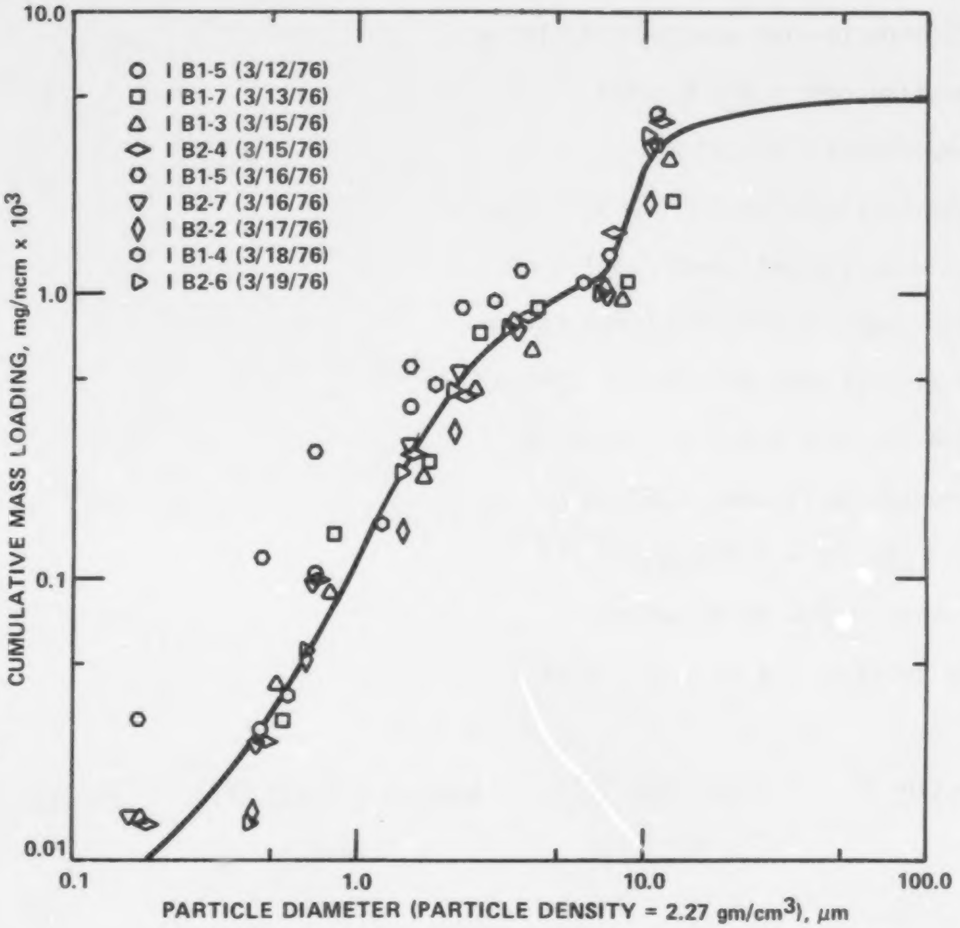

Figure 12. Measured inlet particle size distributions.

Table 1. Data Used in Model Predictions for a Hot-Side Precipitator

Precipitator length = 10.98 m

Particle dielectric constant = 100.0

Estimated efficiency = 99.6%

1/2 wire-to-wire spacing = 0.1143 m

Gas flow rate = 208.5 acm/s

Temperature = 601.7° K

Dynamic viscosity = 2.8×10^{-5} kg/m.s

Ion mean thermal speed = 631.0 m/s

Inlet mass loading = 0.00488 kg/acm

Density of dust particles = 2270.0 kg/m^3

Wire-to-plate spacing = 0.1143 m

Corona wire radius = 0.01384 m

Gas velocity = 1.181 m/s

Pressure = 760 mm of mercury

Ion mobility = 4.85×10^{-4} m^2/V.s

Section #	Plate Area (m^2)	Applied Voltage (kV)	Current (A)
1	3.917×10^3	33.5	1.45
2	3.917×10^3	30.0	1.29
3	3.917×10^3	28.7	1.45
4	3.917×10^3	27.4	1.45

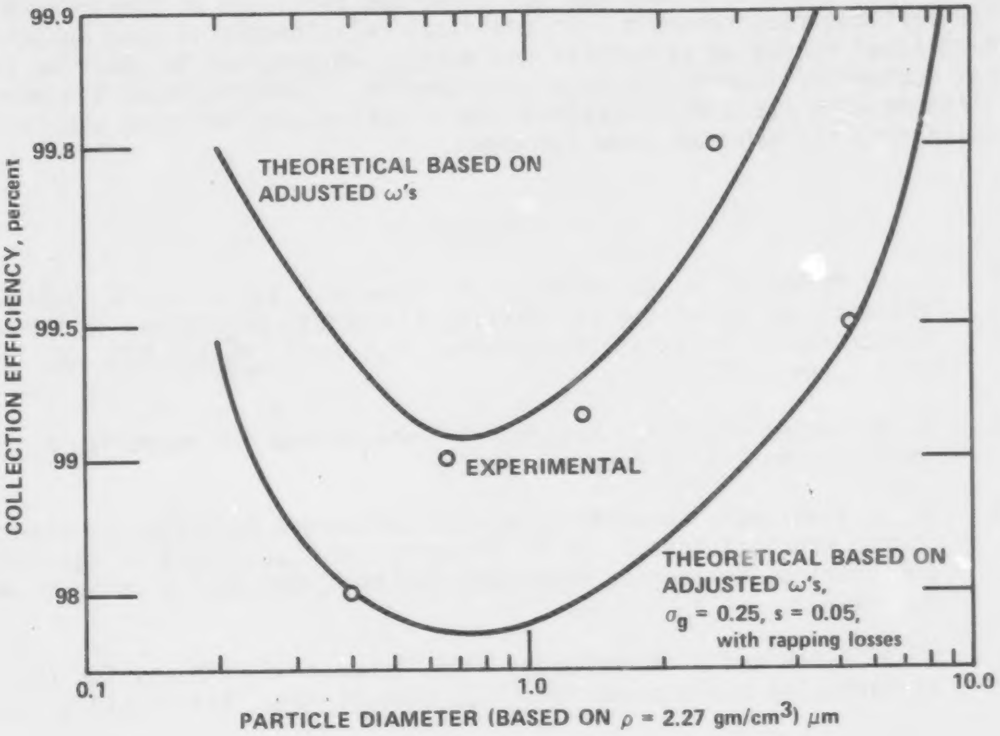

Figure 13. Experimental and theoretical fractional efficiencies.

and rapping losses as described earlier is 99.65 percent as compared with the measured value of 99.67 percent.

SUMMARY

In its present form, the mathematical model for electrostatic precipitation provides a basis for indicating performance trends caused by changes in specific collecting area, electrical conditions, and particle size distribution. Procedures, based on simplifying assumptions, can be used to estimate the effects of nonuniform gas flow, gas bypassage of electrified regions, and particle reentrainment. An empirical relationship is used to better predict ideal migration velocities and work is in progress to describe the physical mechanisms inherent in this relationship. Comparisons of the model predictions with field data obtained from a full-scale, hot-side precipitator collecting fly ash show good agreement.

REFERENCES

1. J. R. McDonald, W. B. Smith, H. W. Spencer, III, and L. E. Sparks, "A Mathematical Model for Calculating Electrical Conditions in Wire-Duct Electrostatic Precipitation Devices," J. Appl. Phys., Vol. 48, No. 6, 2231 (June, 1977).

2. G. W. Penney and R. E. Matick, "A Probe Method for Measuring Potentials in DC Corona," AIEE Preprint (1957).

3. O. J. Tassicker, "Aspects of Forces on Charged Particles in Electrostatic Precipitators." Ph.D. Dissertation, Department of Electrical Engineering, Wallongong University College, University of South Wales, July 1972.

4. W. B. Smith and J. R. McDonald, "Development of a Theory for the Charging of Particles by Unipolar Ions," J. Aerosol Sci., Vol. 7 (1976), pp. 151-166.

5. G. W. Hewitt, "The Charging of Small Particles for Electrostatic Precipitation," AIEE Trans. 76 (1957), p. 300.

6. D. H. Pontius, L. G. Felix, J. R. McDonald, and W. B. Smith, "Fine Particle Charging Development," draft prepared for the Environmental Protection Agency, Industrial Environmental Research Laboratory, Research Triangle Park, North Carolina, Contract No. 68-02-1490.

7. J. P. Gooch, J. R. McDonald, and S. Oglesby, Jr., A Mathematical Model of Electrostatic Precipitation, Environmental Protection Technology Series, Publication No. EPA-650/2-75-037 (April 1975).

8. J. P. Gooch and J. R. McDonald, "Mathematical Modelling of Fine Particle Collection by Electrostatic Precipitation," Atmospheric Emissions and Energy-Source Pollution, AICHE Symposium Series No. 165, Vol. 73 (1977), p. 146.

9. J. P. Gooch and J. R. McDonald, "Mathematical Modelling of Fine Particle Collection by Electrostatic Precipitation," Conference on Particulate Collection Problems in Converting to Low Sulfur Coals, Interagency Energy-Environment Research and Development Series, Publication No. EPA-600/7-76-016, 68 (October 1976).

10. L. Preszler and T. Lajos, "Uniformity of the Velocity Distribution Upon Entry into an Electrostatic Precipitator of a Flowing Gas," *Staub.*, 32 (11) (November 1972), pp. 1-7.

THE STUDY OF THE COMPONENTS OF THE ELECTRIC FIELD IN ELECTROSTATIC PRECIPITATORS*

V. I. Levitov, G. F. Mustafin, V. M. Tkachenko

Abstract

The authors present a research method and derived formulas for determining the intensity vector components in a field of a unipolar coronal discharge, in an electrostatic field, and in their combinations with respect to the trajectory of a freely moving test sphere. A description on the experimental unit and the test equipment is given for registering the motion trajectories of spheres. Results are presented for the experimental treatment of the proposed method for an electrode system (a number of wires between two planes). It is shown that the difference between experimental and theoretical values does not exceed 13 percent in the case of the primary intensity vector component perpendicular to the precipitator electrodes. On the basis of the developed method, the authors studied the electric fields set up by needle-strip electrodes and combination coronal electrodes.

Electric field intensity is a principal factor governing high performance and sizing of electrostatic precipitators (ESP).

By comparison with wire electrodes, needle corona electrodes produce stronger electric fields. Combined discharge electrode assemblies are also known. They induce complex fields with corona discharge and electrostatic field.

Generally accepted environmental methods (refs. 1-3) of determining electric fields using a freely suspended test body (ref. 4) do not provide measurements of the components of these complex fields. Knowledge of these complex fields is of great importance in evaluating electrode assemblies and ESP collection efficiencies.

The developed experimental method (ref. 5) permits one to evaluate the components of intensity in the field with unipolar corona discharge, in the electrostatic field, and in their combination.

The essence of the method is as follows. Freely suspended conducting balls (which have been previously charged) are introduced into the discharge gap. The charge on the balls is high enough to prevent additional charging. The trajectory of the balls should have a peak, where initial velocity affected by the field and gravity are absent. The projected trajectories of ball motion in two mutually perpendicular planes are recorded simultaneously.

---

*For further information regarding the material in this paper, please contact I. K. Reshidov, U.S.S.R. 113105, Moscow, M-105, 1-st Nagatinsky Pass., 6, NIIOGAZ.

Parameters of the trajectory in the proper points are estimated by photograms. Components of electric field for these points are computed from the equation of motion:

$$M \frac{dV}{dt} = q\bar{E} + m\bar{g} + \bar{F}_{df} \qquad (1)$$

where M, q, and $\underline{V}$ = mass, charge, and migration velocity of a ball, respectively;

$\underline{g}$ = gravity acceleration;
$\bar{E}$ = electric field intensity;
$\bar{F}_{df}$ = drag force.

From equation (1), it is clear that the electric field is computed in the simplest way if the mass and the charge of the balls are constant and if the effects of the drag force and the electric wind can be neglected.

Uniform size and density of balls provide mass stability. Constant charge can be obtained by inducing an electric field in the charging region that is stronger than the electric field for the studied corona discharge field. Environmental effects, as test data with a falling ball have indicated, can be ignored if a ball radius is more than 0.3 mm.

Then for the rectangular coordinate system, equation (1) becomes:

$$M_o \frac{dV}{dt} x = q_o E_x \qquad (2)$$

$$M_o \frac{dV}{dt} g = q_o E_y \qquad (3)$$

$$M_o \frac{dV}{dt} 2 = M_o g \pm q_o E_z \qquad (4)$$

where M_o and q_o are constant values of mass and charge on a ball, respectively. Equations (2-4) show that the components of the electric field E_x, E_y, and E_z can be computed when acceleration of a ball moving along the proper axis is known.

Direct double differentiation of the data leads to large errors in calculations. Therefore it is reasonable to find a solution using the angle of arrival.

Let us integrate equation (3) at i+1 and i-1, where i is an arbitrary point of the trajectory:

$$\int_{V_{yi-1}}^{V_{yi+1}} dV_y = \frac{q_o}{m_o} \int_{t_{i-1}}^{t_{i+1}} E_y dt$$

Near the point i in a small segment of the trajectory corresponding to (i - 1) ÷ (i + 1), the E_y value can be assumed constant and equal to E_y.

Then:

$$E_{yi} = \frac{m_o}{q_o} \frac{V_{yi + 1} - V_{yi - 1}}{t_{i + 1} - t_{i - 1}}$$

Using the formula of a free-falling ball, and taking into account that the initial velocity at the peak of the trajectory is absent, i.e., $V_y = V_z Tg\alpha$ (figure 1), we finally have:

$$E_{yi} = \frac{m_o d}{q_o} \frac{\sqrt{hi+1}\ tg\alpha i+1 - \sqrt{hi-i}\ tg\alpha i-1}{\sqrt{hi+1} - \sqrt{hi-1}} \qquad (5)$$

where h = height of falling of a sphere, and
α = angle of arrival in a vertical plane.

For another component:

$$E_{xi} = \frac{m_o g}{q_o} \frac{\sqrt{hi+1}\ tg\alpha i+1\ tg\beta i+1 - \sqrt{hi-1}\ tg\alpha i-1\ tg\beta i-1}{\sqrt{hi+1} - \sqrt{hi-1}} \qquad (6)$$

where β = angle of arrival in a horizontal plane.

For the third electric field component E_z, directed along a corona electrode, the expression will be the simplest when a horizontal position of corona electrodes is considered. Then the expression for E_z will be similar to equation (6).

Widely used horizontal plate ESPs use an electrode assembly with a series of vertical corona electrodes located between two collecting electrodes (figure 1). With this electrode assembly, the electric field component, E_y, is perpendicular to the collecting electrode and mainly accounts for charging and particle collection. Another component, E_x, directed along the gas flow affects particle charging. The vertical component, E_z, parallel to the corona electrode, occurs in three-dimensional fields, for example, in a needle corona electrode apparatus. E_z takes part in charging only those particles passing very closely to corona electrodes.

The present investigation was concerned with the distribution of the first two electric field components, E_x and E_y, in electrode assemblies having a set of cylindrical strip-needle and combined electrodes located between two planes. Experiments were conducted on a laboratory installation, which included a batching and charging device, a model electrostatic precipitator, a high voltage supply, and apparatus to take photos of trajectories of ball motion at pulse illumination of the interelectrode region.

The specially developed batching and charging device blew out separate balls by command and provided stable charging outside the field created in the

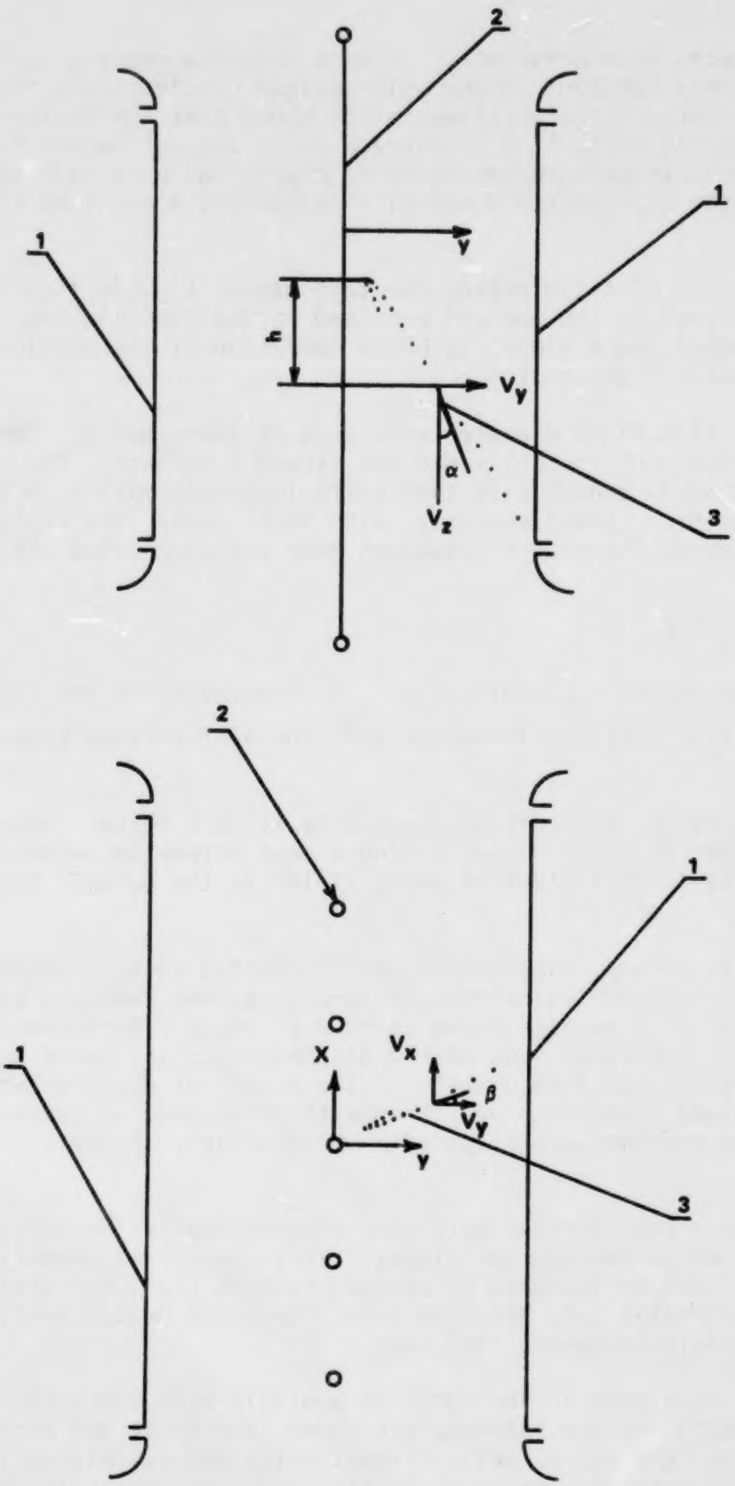
2
1
1
y
h
V_y
α
V_z
3
2
1
1
X
V_x
β
V_y
y
3

Figure 1. Projections of the trajectory of moving the test body in two mutually perpendicular planes.

cylindrical-geometry corona assembly. A more accurate method, i.e., recording trajectories of ball movement in the well-defined electrostatic field, was used to measure charge. The experiments had shown that the maximum deviation of the charges on the balls from an average value did not exceed 6 percent. Therefore, the need to measure the value of charge for each ball before its introduction in the studied field was eliminated. It simplified the task of the investigation.

Synchronization of illuminating the test gap by a pulse light source with movement of particles in the gap was provided in the installation. A start button of the camera fed a signal to begin operation of the particle batching device and the pulse light source.

Steel balls of 0.67-mm diameter were used in experiments. Size instability and nonsphericity of the balls did not exceed 1 percent. The balls selected were of a small enough size that sufficient information on the studied field could be gained. Simultaneously, with small sizes, the fulfillment of the main condition of charging a breakdown body was simplified with small balls:

$$E_o > E_{ch} > E$$

where E_{ch} = intensity of a charging field, E = intensity of the studied electric field, and E_o = critical intensity when the ball surface began to exhibit corona.

For 0.67-mm balls, the critical intensity is 16.5 kV/cm. Therefore, with them it is possible to study fields having a peak intensity value of about 16 kV/cm. This value is sufficient to study fields in the outside region of corona discharge.

With negative corona, experiments were conducted under atmospheric conditions at 50 kV. Cylindrical wires, strip-needle, and combined electrodes were spaced plates with needles being stamped on edges. Arrangement of electrodes and geometrical dimensions of the discharge gap are shown in figure 2. The cylindrical wires had 3-mm diameter. The height of needles for strip -needle and combined electrodes was 12 mm with 40-mm spacing between needles. In all cases, the needles were oriented perpendicularly to the flat collecting electrodes.

The method had been further developed experimentally for an assembly comprising a set of wires between two planes. This electrode assembly is used in plate ESPs and it can be designed by several methods (ref. 6), which had been verified by experimental data obtained both from probe measurements and by the method using a freely-suspended test body.

Experiments were made in the cases of a middle wire along the neutral force line ($x = b/2$), in the intermediate plane ($x = b/4$), and along the central force line ($x = 0$), as well. Experimental and calculated values of E_y for this electrode assembly are given in figure 3. Discrepancies between measured and theoretical values do not exceed 15 percent, which is quite acceptable for practical purposes.

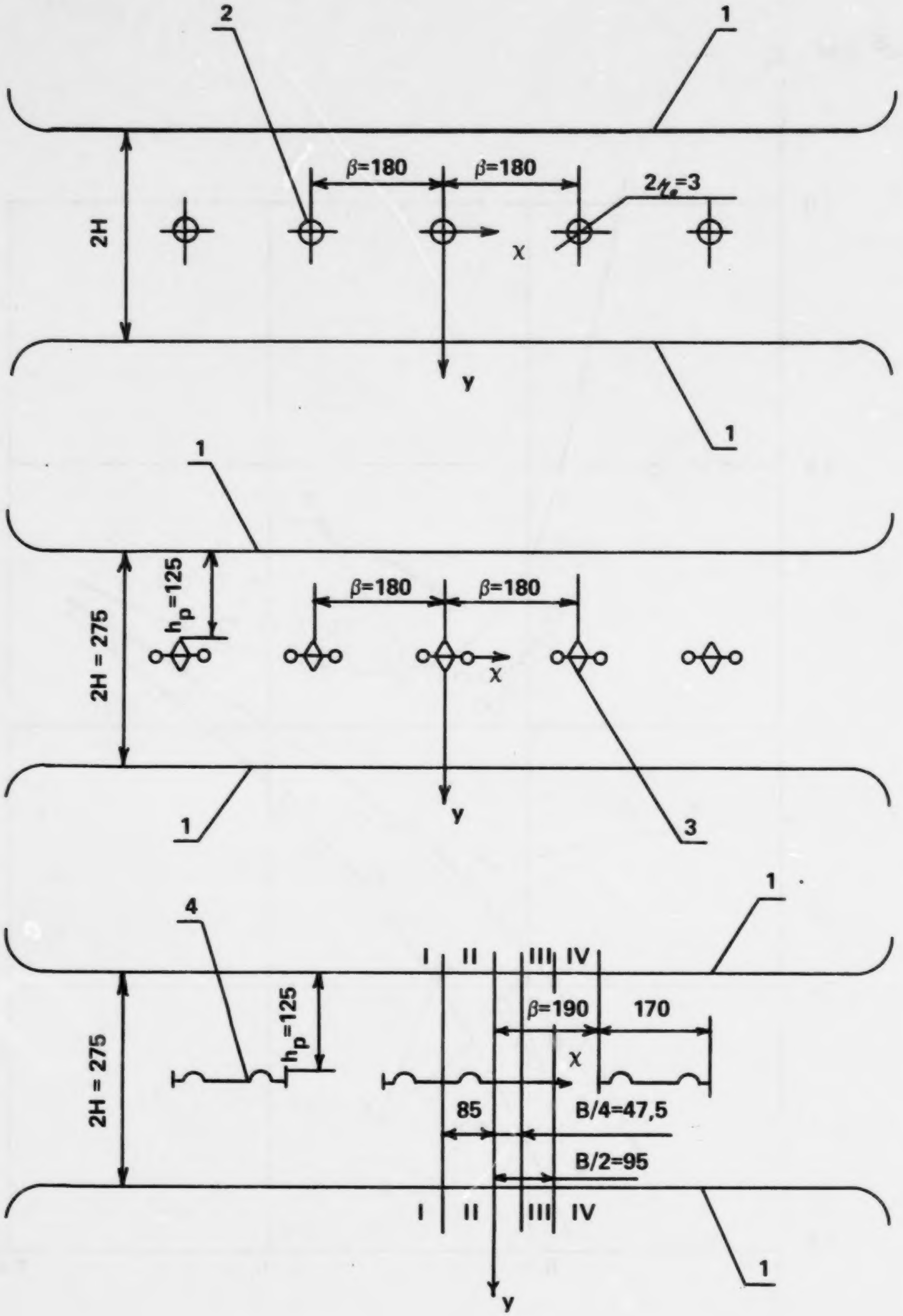
2
1
β=180
β=180
2r₀=3
2H
x
y
1
1
h_p=125
2H = 275
β=180
β=180
x
y
1
3
4
1
I
II
III
IV
h_p=125
2H = 275
β=190
170
x
85
B/4=47,5
B/2=95
I
II
III
IV
y
1

Figure 2. Schemes of electrode position. **1-collecting electrode; 2-cylindrical wire; 3-strip-needle electrode; 4-flat combined electrode.**

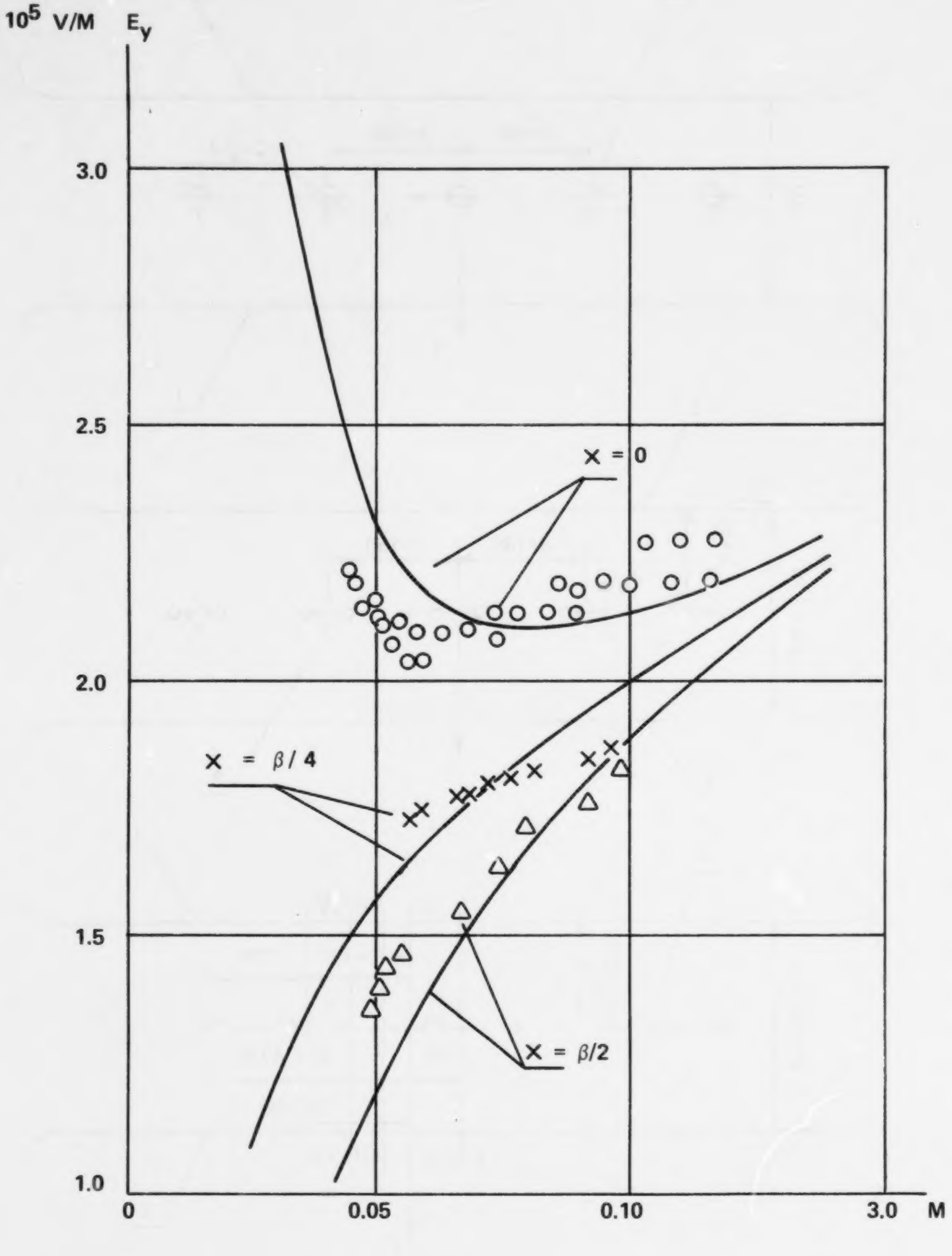

Figure 3. Dependence of E_y component on field coordinates for the electrode assembly including a series of wires between two planes.

2H = 275 mm

Investigation of possible simultaneous estimation of the electric field components constituted the greatest interest. Figure 4 represents experimental and calculated values of E_y and E_x as a function of field coordinates. The data were obtained for the same trajectory of a moving test body.

It is obvious from the figure that the measured data qualitatively agree with the computed data. Deviation of the measured data from the computed data for E_y is less than 13 percent. The E_x component (the field directed along the collecting electrodes) is markedly different.

In the literature, the experimental data for the E_x component are absent. Therefore, its deduction will be of great interest for the qualitative field characteristics. For example, considering that E_x rapidly decreases with increasing the distance from a corona electrode one can establish when the field becomes one-dimensional. For the given case, the field is assumed to be practically one-dimensional at $Y = 2/3\ h_p \div h_p$, i.e., in the region adjacent to the collecting electrode. The region is 1/3 of the discharge gap.

Attention was paid to investigations of the electric field generated by widely used strip-needle electrodes and by combined corona electrodes as well. Figures 5 and 6 represent experimental values of E_y and E_x, respectively, for these electrode assemblies.

Distribution of the E_y component had been obtained for the most typical regions of the discharge gap. With strip-needle electrodes, these were planes (against needles) of the central and neutral force lines and the intermediate plane. With combined electrodes, these were sections passing through the center of a flat portion of the electrode, through needles, along the neutral wire, and in the intermediate region as well.

From figure 5 it is clear that E_y values for planes of neutral force lines (curves 4 and 7) are practically the same for both types of electrodes. With the needle plane (curves 2 and 5) and in the intermediate plane (curves 3 and 6) values in the test region of the discharge gap were higher for combined electrodes than for strip-needle electrodes. In both cases, the difference diminished as the collection electrode was approached.

Highest electric field values were obtained for a flat portion of combined electrodes, i.e., the region with electrostatic field. In this case, E_y values were 1.5-2 times more than the similar values for a plane of neutral force lines in the strip-needle electrode assembly (curves 1 and 7). Therefore, the mean value of E_y within the whole discharge gap would be substantially higher for combined electrodes than for the strip-needle electrodes.

The distribution of the E_x component, figure 6, was obtained for the region closest to the intermediate plane for both combined (curve 1) and strip-needle electrodes (curve II) as well as for a region adjacent to the needle plane of combined electrodes in the electrostatic side (curve III). The

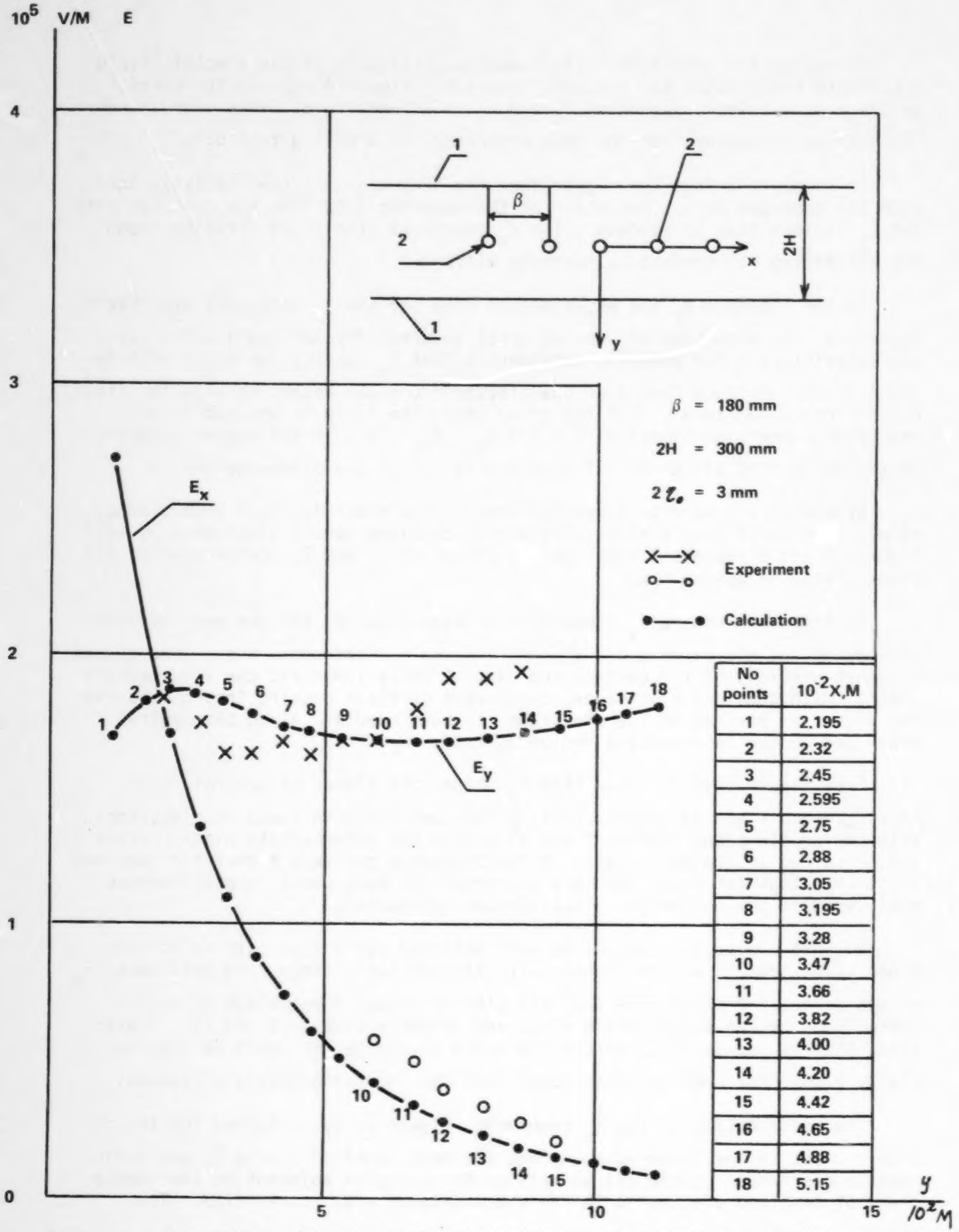

No points	$10^{-2}X, M$
1	2.195
2	2.32
3	2.45
4	2.595
5	2.75
6	2.88
7	3.05
8	3.195
9	3.28
10	3.47
11	3.66
12	3.82
13	4.00
14	4.20
15	4.42
16	4.65
17	4.88
18	5.15

Figure 4. Comparison of test values of simultaneously obtained E_x and E_y components with theoretical data for 50 kV voltage.

1 - plane; 2 - corona wire

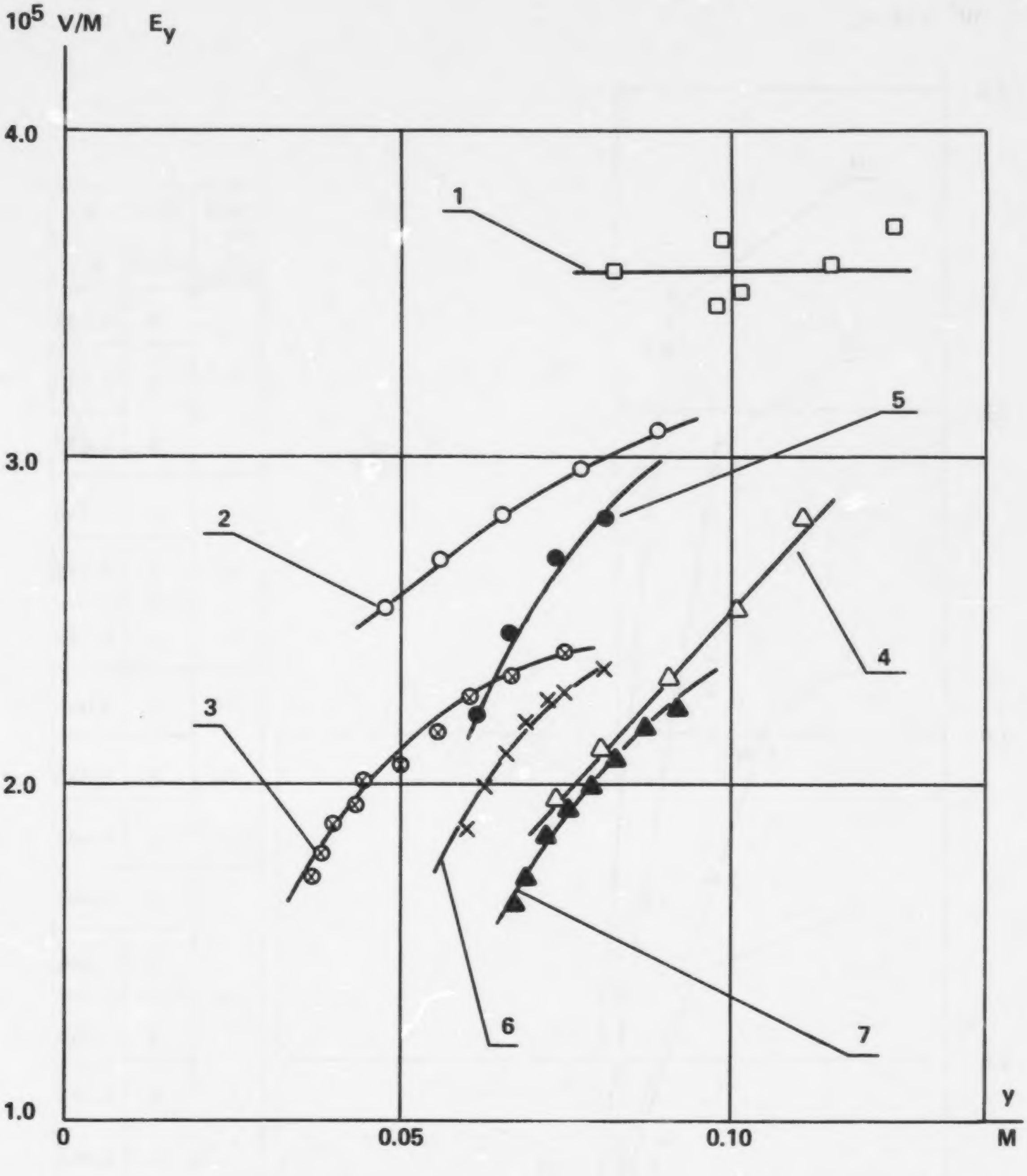

Figure 5. E_y component as a function of field coordinates for electrode assemblies: a series of strip-needle corona electrodes and a series of combined corona electrodes between two planes. **2H = 275 mm.**

Combined Electrodes

1 - plane II; 2 - plane II - II; 3 - plane III - III; 4 - plane IV - IV.

Strip-Needle Electrodes

5 - x = o, 6 - x = b/4, 7 - x = b/2.

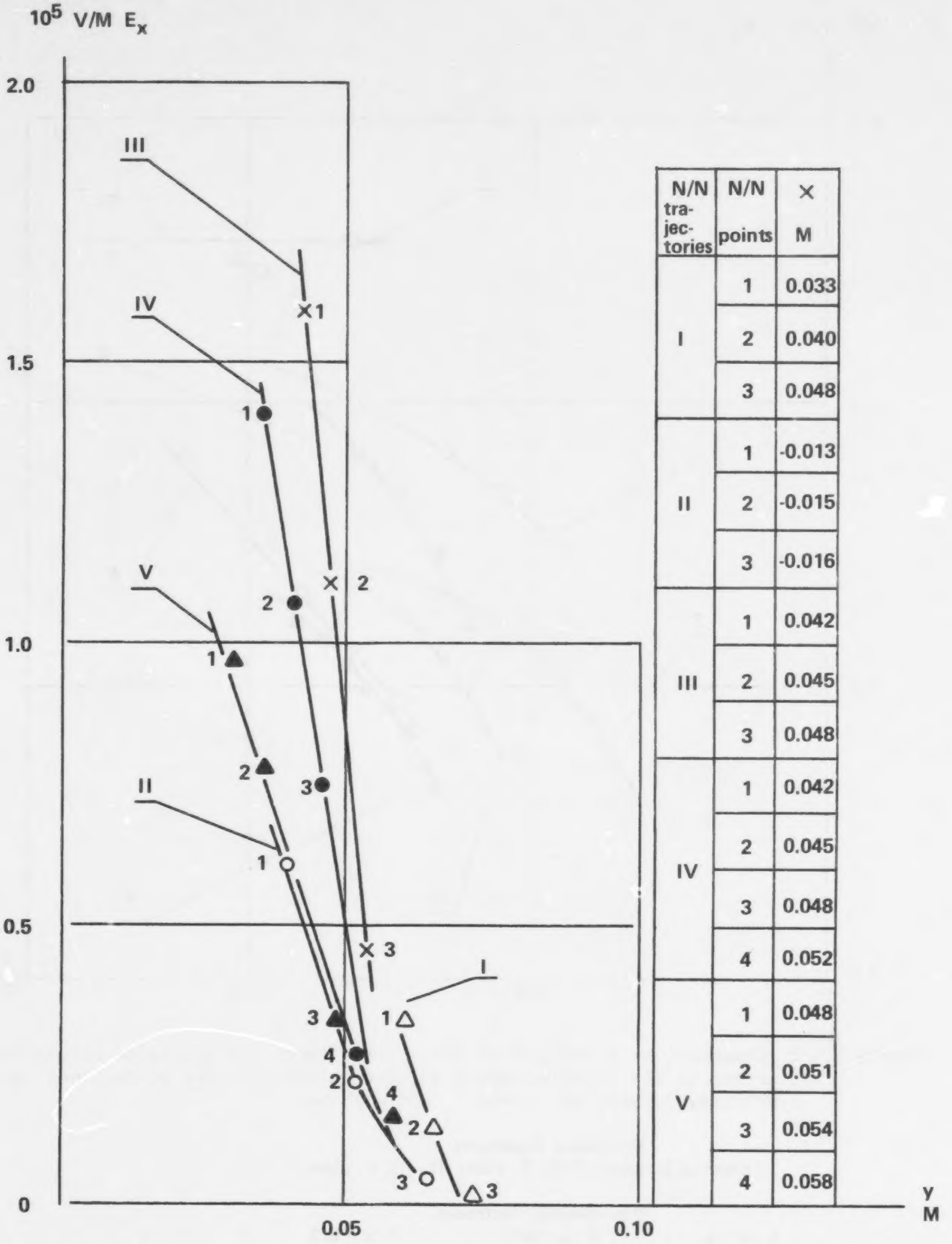

N/N trajectories	N/N points	X M
I	1	0.033
	2	0.040
	3	0.048
II	1	-0.013
	2	-0.015
	3	-0.016
III	1	0.042
	2	0.045
	3	0.048
IV	1	0.042
	2	0.045
	3	0.048
	4	0.052
V	1	0.048
	2	0.051
	3	0.054
	4	0.058

Figure 6. E_x component as a function of field coordinated for electrode assemblies: a series of strip-needle and a series of combined corona electrodes between two planes.

2H = 275 mm.

I, II - combined electrodes; III, IV, V - strip-needle electrodes.

figure shows that for both types of electrodes, the E_x component slowly decreases with increasing the distance from a corona electrode and that it tends to zero approximately in the middle of the discharge gap.

Thus, for both strip-needle and combined electrodes, the electric field is practically one-dimensional in the region spreading from the center of the discharge gap to the collecting electrodes.

CONCLUSIONS

1. The developed method permits one to evaluate the components of the electric field of a complicated configuration including unipolar volume charge, electrostatic field, or their combination.

2. Test data, obtained for electrode assemblies comprising a set of wires located between two planes, are in satisfactory agreement with theoretical values: the maximum deviation for the major E_y component does not exceed 15 percent.

3. With the electrode assemblies studied, the electric field is practically one-dimensional in the region adjacent to the collecting electrode. The field is 1/3 of the discharge gap for the cylindrical wires and a half of the discharge gap for strip-needle and combined corona electrodes.

4. Due to the electrostatic zones, corona electrodes with needles perpendicular to the collection electrode surface provide a markedly higher mean value of the E_y component outside the discharge gap, as compared with strip-needle electrodes.

REFERENCES

1. V. D. Kravchenko and V. I. Levitov, "To the Theory of the Sataugh Probe," Izvestiya of the Acadamy of Sciences, No. 10, 1955.

2. V. I. Levitov, A. G. Lyapin, V. I. Popkov, and Tsin-Izyan-Yan, "Investigation of DC Corona Field With Probe Technique Using an Oscillograph," Izvestiya of the Acadamy of Sciences, OT N, No. 2, 1962.

3. V. I. Levitov and I. K. Reshidov, "Peculiarities of Electric Fields in Plate Electrostatic Precipitators," A collection "Intensive electric fields in technological processes," Energy, 1971.

4. I. P. Vereshchagin and V. A. Babashkin, "Measurement of the electric field of corona discharge by a method using a test body," A Collection "Intensive electric fields in technological processes," Energy, 1971.

5. V. I. Levitov, G. F. Mustafin, and V. M. Tkachenko, Author's certificate No. 481003 "A Method of Estimation of Electric Field," Bulletin Foundings, Discoveries, Industrial Specimen, Brace Marks, No. 30, 1975.

6. I. P. Vereshchagin and V. I. Vasyayev, "Procedures of Calculating Corona Discharge Field," Electricity, No. 5, 1971.

FLUE GAS CONDITIONING IN COAL-FIRED POWER PLANTS IN THE UNITED STATES

Edward B. Dismukes*

Abstract

An overview of flue gas conditioning is given in terms of the reasons for its utilization, the efforts to develop the technology, and the acceptance of the technology by the utility industry. Specific conditioning agents now in use (sulfur trioxide, ammonia, and others) are reviewed. Conditioning mechanisms associated with various agents are discussed; of these, resistivity modification is perhaps most generally important, but others are also significant on occasion. Finally, some of the practical aspects of conditioning are discussed. These matters range from the problem of deciding when conditioning is likely to be beneficial to the various new problems that may be encountered as side effects of conditioning.

OVERALL STATUS OF CONDITIONING TECHNOLOGY

Reasons for Utilization

The primary reason for the utilization of chemical additives for flue gas conditioning in this country is to maintain high efficiency of electrostatic precipitators when they operate with high-resistivity fly ash from low-sulfur coals. Such fuels are being burned increasingly as a means of lowering the emission of sulfur oxides. Older precipitators that were installed to collect ash from medium- to high-sulfur coals as a rule are not efficient enough when the fuel is changed unless some corrective measure is taken.

Use of conditioning is but one of the corrective measures that can be adopted. As one alternative, a so-called cold-side precipitator operating at around 150° C may be replaced with a hot-side precipitator operating at around 350° C. As a second alternative, the gas stream may be cooled below the design cold-side temperature. As a third alternative, the cold-side precipitator may be enlarged to provide a larger ratio of collecting surface to gas volume (ref. 1).

The foregoing statements carry the implication that lowering of the electrical resistivity is the central objective of conditioning. Usually this is true; however, as discussed in this paper, other conditioning mechanisms are sometimes important.

Development of Technology

Private industry, apart from the utility industry, is the main segment of commerce now responsible for the development of conditioning technology. The private industry active in this area consists of chemical manufacturers, precipitator manufacturers, and specialty companies related to the precipitator industry. Chemical companies are interested in exploiting the potential of a wider market for their products, whereas precipitator companies often are interested mainly in making available a corrective measure for precipitators they have installed in the past.

---

*Southern Research Institute, Birmingham, Alabama

Some of the companies installing conditioning systems employ well-known chemical agents such as sulfur trioxide and depend upon engineering expertise in the injection of these agents to gain success in the competitive market. Other companies have proprietary formulations or are attempting to develop such formulations to gain a competitive advantage. As a result of efforts to maintain secrecy insofar as possible about product composition, a full understanding of what can be accomplished with some commercial agents is not available.

Some utility organizations, notably, the Tennessee Valley Authority, provide exceptions to the general rule that outside industry is mainly responsible for technical developments. The TVA organization was a pioneer in the use of ammonia as a conditioning agent (ref. 2).

Acceptance by the Utility Industry

The utility industry, in general, has thus far regarded conditioning as an acceptable way to upgrade the performance of old precipitators, but not as an acceptable design feature of new precipitators. There are few precipitators indeed (maybe only one) that have been built or planned originally with conditioning incorporated in their design. The usual policy for a new precipitator that is to operate on high-resistivity ash is to build a hot-side unit or a cold-side unit of large capacity.

The current degree of utilization of conditioning is indicated by the results of a survey being conducted by the author. A total of about 125 privately owned utility companies were asked about their use of the technology. Out of the companies polled, roughly 25 percent have been identified as current or former users.

It is difficult to describe how the users of conditioning are distributed in terms of location, company size, or other factors. The users include eastern, midwestern, southern, and western companies that burn coal from many sources. One large company located in the Midwest and another smaller company in the West have adopted conditioning by sulfur trioxide on a large scale. Other companies throughout the country have similar power units operating side-by-side with only one unit in a series equipped for conditioning. One of the reasons why it is difficult to give an accurate current picture of the use of conditioning is the frequently transitory nature of conditioning facilities. There is evidence that one of the most successful vendors of a chemical system has had about 50 percent of its installations discontinued after initial trials.

CONDITIONING AGENTS AND MECHANISMS

Sulfur Trioxide and Sulfuric Acid

Each of these compounds is widely used as a conditioning agent. If sulfur trioxide is the compound used, however, it reacts with water vapor in flue gas at the temperatures of cold-side electrostatic precipitators to produce sulfuric acid. Thus, although the two compounds maintain separate identities up to the point of addition to flue gas, they are effectively the same substance (sulfuric acid) after addition.

Typically, the vapor of sulfuric acid acts as an agent for lowering the electrical resistivity of fly ash as a result of its condensation or adsorption on ash surfaces. It undoubtedly acts jointly with water vapor in this connection because of the high affinity of the substances for each other. Data from the field illustrating simultaneous reductions of the acid vapor concentration and the ash resistivity with decreasing gas temperature are shown in figure 1 (ref. 3).

Sometimes, sulfuric acid may act as a conditioning agent by another mechanism such as increasing the cohesiveness of fly ash and reducing rapping reentrainment of fly ash in the flue gas. Various qualitative indications of this effect have been seen in the field (ref. 3), as might be predicted from the tensile strength measurements made on fly ash in the laboratory (ref. 4).

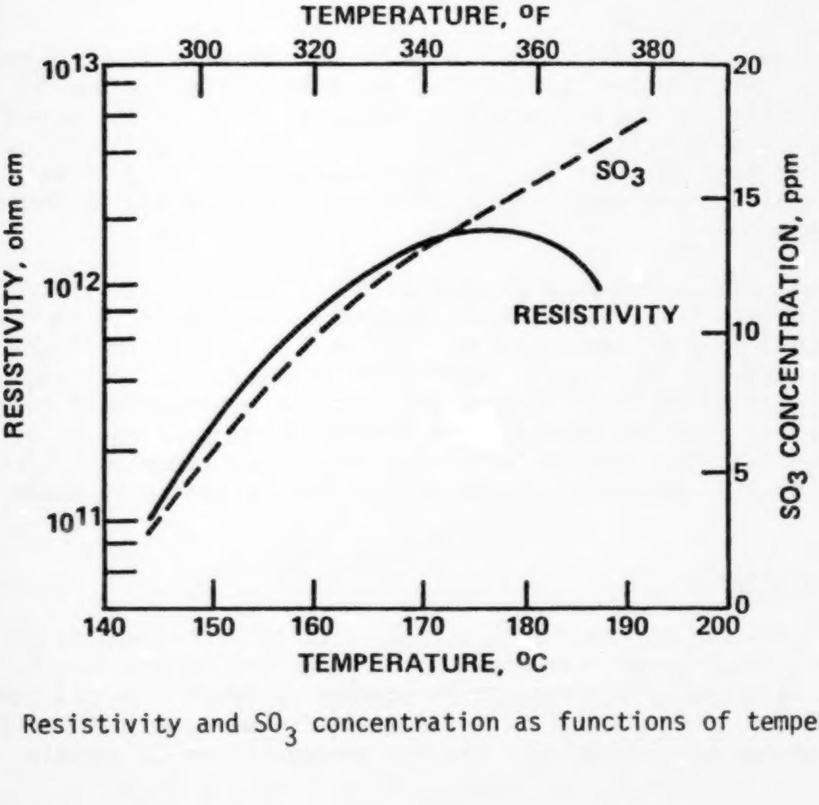

Figure 1. Resistivity and SO_3 concentration as functions of temperature.

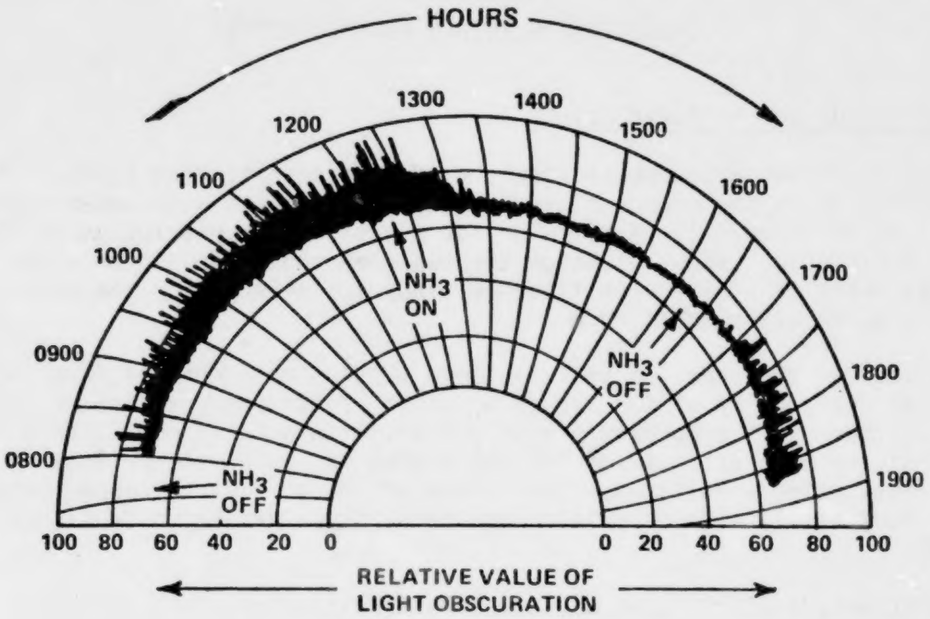

Figure 2. Reduction of rapping reentrainment by ammonia.

Ammonia

This compound is less widely used in this country than sulfuric acid. Major reasons for this are the lack of consistent field results and the lack of a clear indication of the mechanisms by which it acts. With respect to the role of ammonia as a resistivity modifier, in particular, the available data are not consistent. In some applications, a significant resistivity effect is absent (ref. 3); in other applications that involve different reaction environments, a significant effect may occur.

Ammonia conditioning by mechanisms other than resistivity modification sometimes occurs (ref. 3). One alternative mechanism is to increase the cohesiveness of ash and lower reentrainment loss as illustrated in figure 2; this probably involves some type of reaction with naturally occurring sulfuric acid, perhaps producing ammonium sulfate that acts as a binder when collected with ash particles. Another mechanism is through a space-charge effect, again involving a reaction with sulfuric acid to produce ammonium sulfate or bisulfate as a fume of fine particles; evidence for this mechanism is shown in figure 3.

Ammonium Sulfate

There are strong reasons to believe that this compound is the main component of various proprietary commercial formulations that are being widely used. It is normally injected in an aqueous spray at high gas temperatures (around 600° C) even when it is intended to improve precipitator performance at temperatures around 150° C. Thermal decomposition to ammonia, sulfur

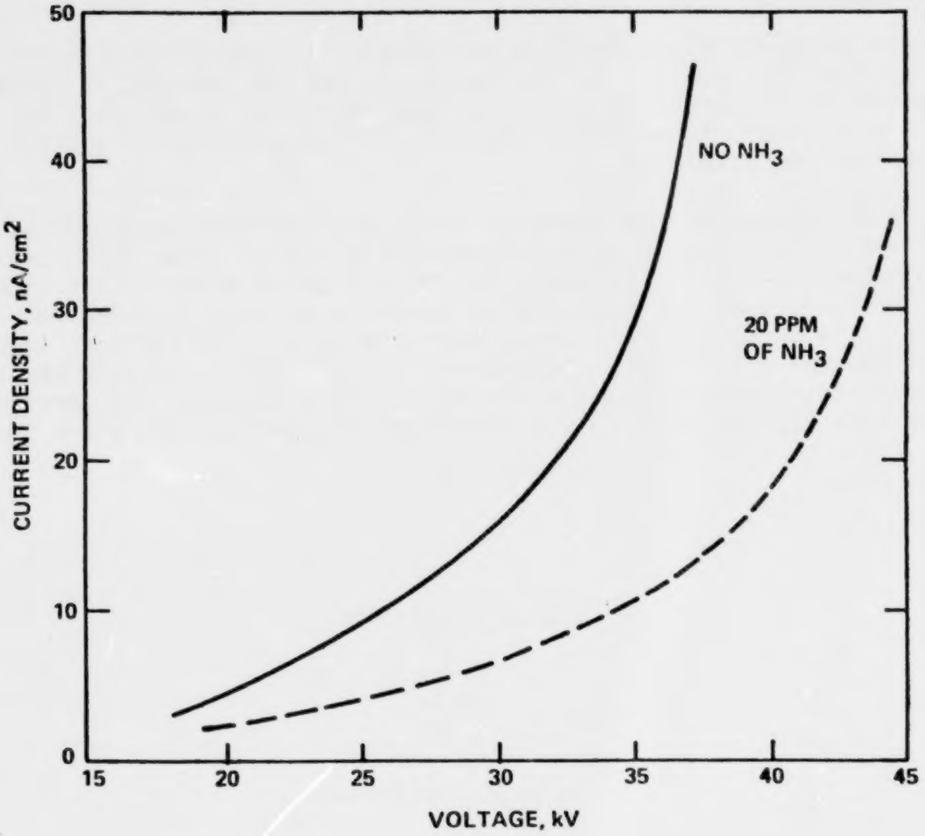

Figure 3. Current-voltage relationship showing space-charge effect by ammonia.

trioxide, and water is to be expected immediately after addition, followed by recombination as the temperature decreases, as is shown by the reaction sequence in figure 4.

Little is known about the mechanisms of action of ammonium sulfate, but claims have been made that the compound can act as a resistivity modifier, an agent increasing cohesiveness, or an agent enhancing space charge. Theoretical consideration indicates that each mechanism may be important, but experimental data to say which mechanism is predominant are lacking.

Triethylamine

This compound is not known to be currently in use in this country. It is worth mentioning, however, for two reasons: (1) the compound is claimed by Australian investigators to act as an "agglomerating" agent (ref. 5), and (2) certain proprietary formulations employed in this country are claimed to act through the same mechanism.

The phenomenon of agglomeration could be a powerful mechanism of conditioning, for it offers the potential of overcoming the relative inefficiency of precipitators for collecting particles below 2 μm in size. There is serious doubt, however, that the mechanism is operative with any chemical now known, whether it is triethylamine or some other compound. The critical experimental test of observing a change in particle-size distribution usually has not been applied to triethylamine; in one instance in this country, the test failed to confirm that agglomeration by a proprietary chemical was operative (ref. 6).

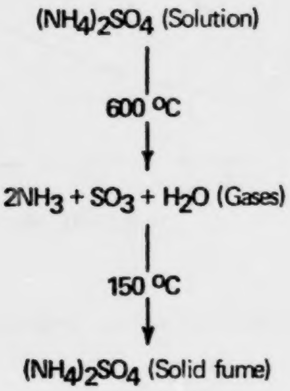
$(NH_4)_2SO_4$ (Solution)
600 °C
$2NH_3 + SO_3 + H_2O$ (Gases)
150 °C
$(NH_4)_2SO_4$ (Solid fume)

Figure 4. Reaction sequence of ammonium sulfate as a conditioning agent.

Compounds of Sodium

Sodium compounds are of particular interest because they are the only agents discussed in this paper that have been used in connection with both hot-side and cold-side electrostatic precipitators. Their potential in both connections is illustrated by figure 5, which shows the importance of the sodium oxide content of the ash in determining both high-temperature and low-temperature resistivity (ref. 7).

The plots in figure 5 indicate the advantages that may accrue by feeding a compound such as sodium carbonate, along with coal, to a boiler. The added compound decomposes and the sodium constituent is incorporated in the fly ash. Conditioning by sodium compounds may also be achieved by feeding a solid powder or an aqueous solution into the gas stream. In this event, a reduction in resistivity may be expected because the more conductive sodium compound is coprecipitated with ash rather than being chemically incorporated in the ash.

Compounds of Transition Metals

Certain compounds of transition metals have been added to flue gas on an experimental basis in the belief that they might catalyze the oxidation of sulfur dioxide and thus make a higher concentration of sulfur trioxide available as a natural conditioning agent. One compound investigated was vanadium pentoxide; it was placed in a bed in a simulated flue gas stream (without suspended fly ash) and found to be an effective catalyst (ref. 8). The activity of this compound would not be remarkable, however, unless it could be shown to have sustained activity despite the threat of poisoning by fly ash. Another compound investigated was ferric sulfate; this compound has the potential both of decomposing to ferric oxide and sulfur trioxide and catalyzing the oxidation of sulfur dioxide. Tests with ferric sulfate do not appear to have given definitive results at this stage.

PRACTICAL ASPECTS OF CONDITIONING

The use of conditioning in this country has been at best a qualified success. There have been numerous trials of conditioning that have not yielded the results hoped for. This has led to abandonment of the technology on occasion; it currently leads to provisional trials of the technology without commitment to its permanent adoption.

A basic practical question that any utility company should face is whether conditioning is a likely remedy for a precipitator that does not operate as efficiently as required. An answer to this question should be obtained by performing certain diagnostic tests. Suppose that high resistivity is assumed to be a source of difficulty. This should be confirmed by making resistivity measurements directly or by drawing reasonable inferences about resistivity from voltage-current data on the precipitator power units. It is unfortunately true that such questions have not always been answered, and it is not surprising that conditioning has given disappointing results on occasion.

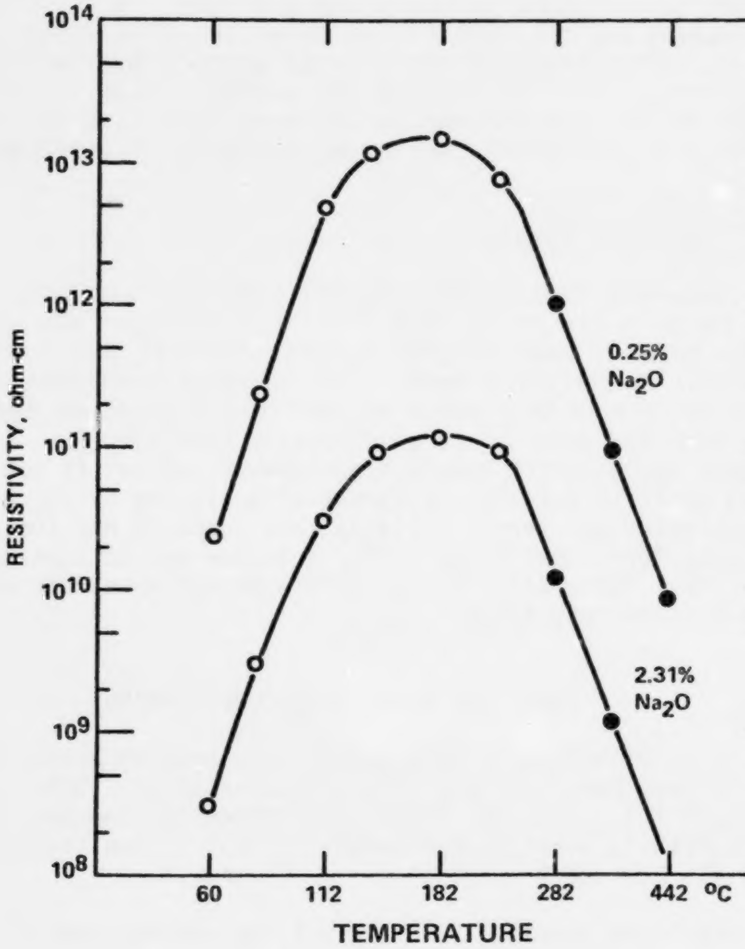

Figure 5. Resistivity of fly ash of different sodium contents in an atmosphere containing 9 percent water vapor.

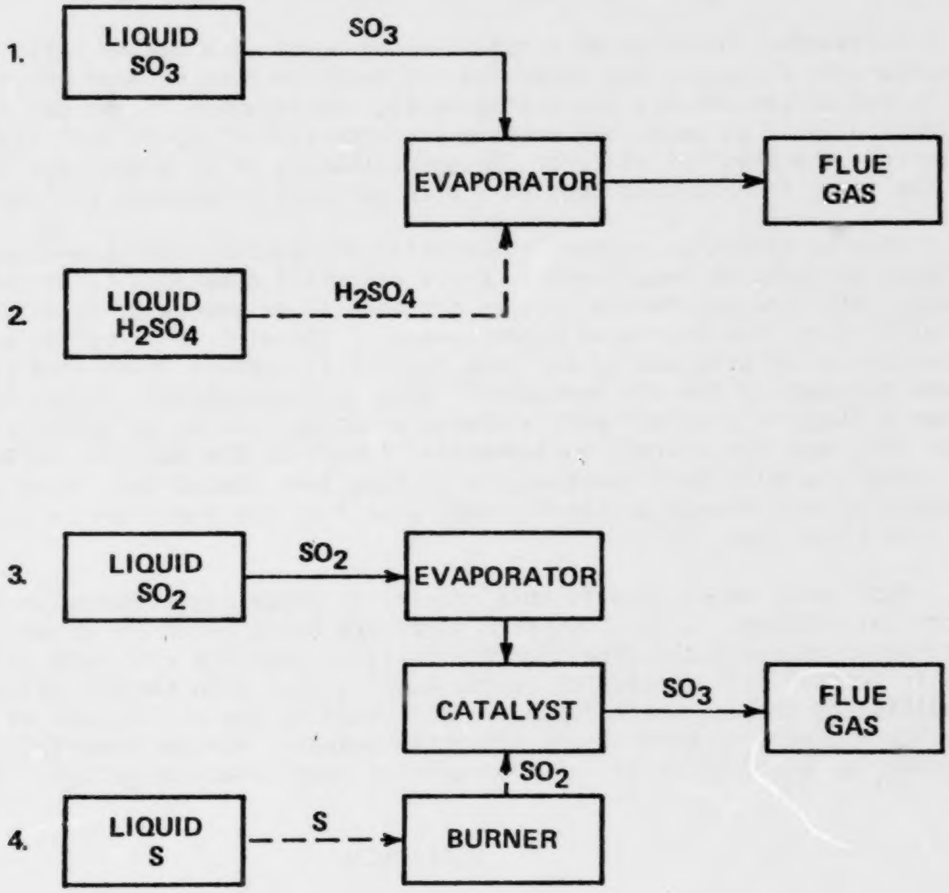
1.
LIQUID SO3
SO3
EVAPORATOR
FLUE GAS
2.
LIQUID H2SO4
H2SO4
3.
LIQUID SO2
SO2
EVAPORATOR
CATALYST
SO3
FLUE GAS
SO2
4.
LIQUID S
S
BURNER

Figure 6. Options for injecting SO_3 or H_2SO_4.

Suppose that a problem of high resistivity has been definitely established. A utility company must then make a choice about the type of agent to be employed. Sulfur trioxide or sulfuric acid is probably the agent of choice from the point of view of expected efficiency. But this choice means the commitment of considerable capital and the disadvantages of handling noxious materials. An alternative choice is an agent that is less certain to work but that requires a lower investment in equipment and that can thus be discontinued more readily if it is unsuccessful. Ammonia surely falls into this category; some of the proprietary formulations probably fall into this category as well.

Successful injection of a conditioning agent is a matter that calls for considerable ingenuity and expertise. A decision must be made about the types of injection systems available (figure 6), the location in the gas train where injection is to be made, the maximum concentration of agent that will be required, the physical state of the agent that is to be added, and the design of the injection manifold that will give adequate uniformity of injection.

Once an injection system is installed and satisfactorily meeting its primary performance requirements, there are still questions to be concerned about. Will the ash removal system continue to be adequate, or will it suffer in efficiency from increased cohesiveness of the ash? Will sulfur trioxide cause corrosion problems in the long run? Will ammonia or related compounds cause blockage of the air preheater? Will sodium compounds in the boiler cause a slagging problem? Will a chosen additive lead to emissions of a new type that make the overall environmental impact of the additive unfavorable? In connection with this question, it is sometimes stated that injected SO_3 appears quantitatively on the fly ash; data from the field are in opposition to this claim (ref. 3).

Much needs to be done in this country to place conditioning on a sound technical footing. Signs that such steps are being taken are given by the systematic research and development activities underway with both private and public funds. Still, research is not keeping pace with the proliferation of conditioning trials, which often are motivated by the willingness of the utility industry to examine any potential measure, however uncertain the outcome, to avoid citation for unacceptable particulate emissions.

REFERENCES

1. L. E. Sparks, "Electrostatic Precipitator Options for Collection of High Resistivity Fly Ash," Symposium on Particulate Control in Energy Processes, Report EPA-600/7-76-010, September 1976.

2. J. T. Reese and J. Greco, "Experience with Electrostatic Fly-Ash Collection Equipment Serving Steam-Electric Generating Plants," J. Air. Pollut. Contr. Assoc., Volume 18, 1968, pp. 523-528.

3. E. B. Dismukes, "Conditioning of Fly Ash with Sulfur Trioxide and Ammonia," Report EPA-600/2-75-015 or TVA-F75 PRS-5, August 1975.

4. J. Dalmon and D. Tidy, "The Cohesive Properties of Fly Ash in Electrostatic Precipitation," Atm. Environ. Volume 6, 1972, pp. 81-92.

5. E. C. Potter and C. A. J. Paulson, "Improvement of Electrostatic Precipitator Performance by Carrier-Gas Additives and Its Assessment Using an Extended Deutsch Equation," Chem. Ind., 1974, pp. 532-533.

6. L. E. Sparks, "Effect of a Fly Ash Conditioning Agent on Power Plant Emissions," Report EPA-600/7-76-027, October 1976.

7. R. E. Bickelhaupt, "Surface Resistivity and the Chemical Composition of Fly Ash," J. Air Pollut. Contr. Assoc., Volume 25, 1975, pp. 148-152.

8. S. Kanowski and R. W. Coughlin, "Catalytic Conditioning of Fly Ash Without SO_3 from External Sources," Environ. Sci. Techn. Volume 11, 1977, pp. 67-70.

THE PROBLEM OF COLLECTING DUSTS THAT CAUSE REVERSE CORONA FORMATION IN ESPs*

S. N. Panev, V. M. Tkachenko, and T. Y. Chelombitko

Abstract

Significant difficulties arise in removing high resistance dust by electrical means due to the manifestation of back corona in the electrostatic precipitator. NIIOGAZ has conducted a number of studies on developing a system for cleaning flue gases from rotary magnesite roasting furnaces where the dust has a resistivity of 10^{12} *to* 10^{13} *ohm/cm. In order to eliminate the harmful effect of back corona, a solution has been adopted that involves increasing the trapping efficiency of high resistance magnesite dust in electrostatic precipitators by reducing the gas velocity in the active zone of the unit. In designing this new dust trapping system, TsN-24 type NIIOGAZ group cyclones were used for the first stage, and the universal horizontal type electrostatic precipitator as the second stage, with a flow velocity in the active zone of 0.5 to 0.7 m/sec. Results are given from the study of the above system. It is shown that the harmful effect of back corona can be eliminated without gas conditioning by increasing the residence time in the electrostatic precipitator by 17 seconds. Under these conditions the cleaning efficiency is 99.9 percent. It is also shown that the optimization of precipitator electrode rapping sharply decreases dust entrainment from the electrostatic precipitator.*

In the process of electrical cleaning of gases from high-resistivity dust, considerable difficulties can arise particularly when there is reverse corona that causes a reduction of collection efficiency of the apparatus.

There are various methods to eliminate the harmful influence of reverse corona. Among them are conditioning, lowering or elevating the gas temperature in order to reduce dust specific resistivity, application of needle corona electrodes, and optimization of electrodes rapping mechanisms.

NIIOGAZ has undertaken studies to develop a system for removal of high-resistivity dust from flue gases of rotary furnaces calcining $MgCO_3$ (refs. 1 and 2). It was found that MgO dust at 100° to 200° C has a specific resistivity of about 10^{12} to 10^{13} ohm/cm and at 400° C of about 5 to 10^{10} ohm/cm respectively. Conditioning of gas with water vapor at 120-1° by increasing the moisture content from 54 g/m^3 to 75 g/m^3 allowed practically complete elimination of reverse corona and increased collection efficiency in an electrostatic precipitator (ESP) with needle corona electrodes.

Thus, in a three-field horizontal plate ESP with total active length of fields of 8.61 m and gas velocity equal to 1.2 m/s, gas conditioning by vapor made it possible to increase collection efficiency from 87 percent to 98.6 percent and to reduce residual dust concentration from 1.3 to 0.5 g/nm^3.

---

*For further information regarding the material in this paper, please contact I. K. Reshidov, U.S.S.R. 113105, Moscow, M-105, 1-st Nagatinsky Pass., 6, NIIOGAZ.

But lack of vapor in the plant caused abandonment of such method of gas conditioning, and increased collection efficiency of the high-resistivity MgO dust was obtained by reducing gas velocity in the active zone of the apparatus.

Application of hot-side ESPs is the other way to solve this problem, but this method is also associated with an additional increase of cross section of the apparatus. Thus, for example, installation of an ESP at 400° C instead of 140° C could cause an increase of active cross section of the apparatus of 1.6 times for the same gas velocity. In addition, the capacity of utility boilers where flue gas is cooled from 600° to 700° C to 230° to 250° C would decrease.

The foregoing reasons were responsible for a new design of dust collection system for six rotary furnaces (dimensions 90 m x 36 m) on the "Magnezit" plant. The following apparatus were applied for each furnace: a group of six NIIOGAZ TCHN-24 type cyclones, diameter 1,600 mm, as a first stage and two UG2-4-37 ESP type as a second stage.

The Type UG2-4-37 ESP is horizontal, of uniform cross section, and is equipped with precipitating electrodes with C-shape elements, belt-needle corona electrodes with 40-mm spacings between the needles and needle length of 12 mm, and has the following specifications (ref. 3).

1.	Number of fields	4
2.	Active cross section, m^2	37
3.	Active length of field, m	2.51
4.	Active height of electrodes, m	7.46
5.	Space between single field electrodes, mm	275
6.	Total precipitating area of precipitating electrodes, m^2	3,150
7.	Total active length of corona electrodes, m	8,467
8.	Gas temperature, °C	250

Dust is removed from the electrodes by means of rappers.

During testing of the dust collection system, power for each ESP field was supplied from separate type AUF-400 power supplies each having double half-wave rectification and a nominal value of rectified (peak) voltage of 80 kV and mean current value of 400 mA.

Units of AUF type allow control of the electrical regime of an ESP by three methods, i.e. to achieve extreme, spark, and periodical control. Under the conditions of extreme control, maximum mean voltage is automatically maintained on the ESP electrodes. Spark control provides a definite frequency of sparkover of the electrostatic precipitator. Optimum frequency of sparking is determined experimentally.

When the last method of control is used, periodic evaluation of voltage up to a sparkover level and subsequent lowering of operating voltage to a given value take place.

The above-mentioned system of removal of high-resistivity MgO dust from process gases has been tested by NIIOGAZ specialists on the "Magnezit" plant with the aim of determining the ESP efficiency and optimizing the operation of electrode rapping and electric power supply. The rotary furnace, in this case, utilized natural gas as fuel, and besides raw materials for the purpose of secondary calcination, the furnace was fed with dust from hoppers of the dust collecting apparatus.

Tests of the group of cyclones showed that at a gas velocity of 3.3 m/s and mean inlet particulate size of 18.5 m, gas cleaning efficiency was 77 percent. Particulate concentration at the outlet of the cyclones was 8 to 10 g/nm^3 with a mean particulate size of 12 m.

Table 1 shows mean values of the results of type UG2-4-37 electrostatic precipitator tests when two electrode rapping regimes and extreme principles of voltage control are involved.

In the first regime, each electrode of all the fields was rapped every 15 min. In the second regime the intervals of electrode rapping were: for the first field, 3.5 min; for the second field, 15 min; for the third field, 45 min; and for the fourth field, 110 min. This schedule was calculated with methods developed by the Semibratovo branch of NIIOGAZ for determining rapping intervals of ESP precipitating electrodes. When the ESP was tested, moisture content of the gas was 43 to 48 g/m^3 of humid gas and dust resistivity was at the level of 10^{12} ohm/cm. Dust resistivity was measured directly in a duct by using a transducer on which a layer of dust was formed in bulk and later compressed.

The ESP under test was operated with back corona. This indicates not only high dust resistivity but also allows the immediate detection of back corona by means of measuring volt/ampere characteristics when the voltage is elevated or lowered (ref. 4).

All ESP fields showed a considerable excess of corona currents during voltage reduction (fig. 1).

The table shows that when the gas velocity in the apparatus is 0.5 to 0.6 m/s (gas stays in the apparatus 17 to 20 s) and the temperature is 140° C, the type UG2-4-37 ESP provides high efficiency cleaning of process gas with high-resistivity MgO dust. When a nonrational schedule of electrode rapping

Table 1. Mean results obtained when a type UG2-4-37 ESP was tried for MgO_2 dust collection

Rapping Cycle	Gas temperature ESP (°C)	Particulate loading inlet (g/nm^3)	Particulate loading outlet (mg/nm^3)	Gas velocity (m/s)	Collection efficiency (%)	Particles drift velocity (cm/s)
1	140	8.03	55	0.52	99.21	3.48
2	142	9.60	16	0.57	99.81	4.87

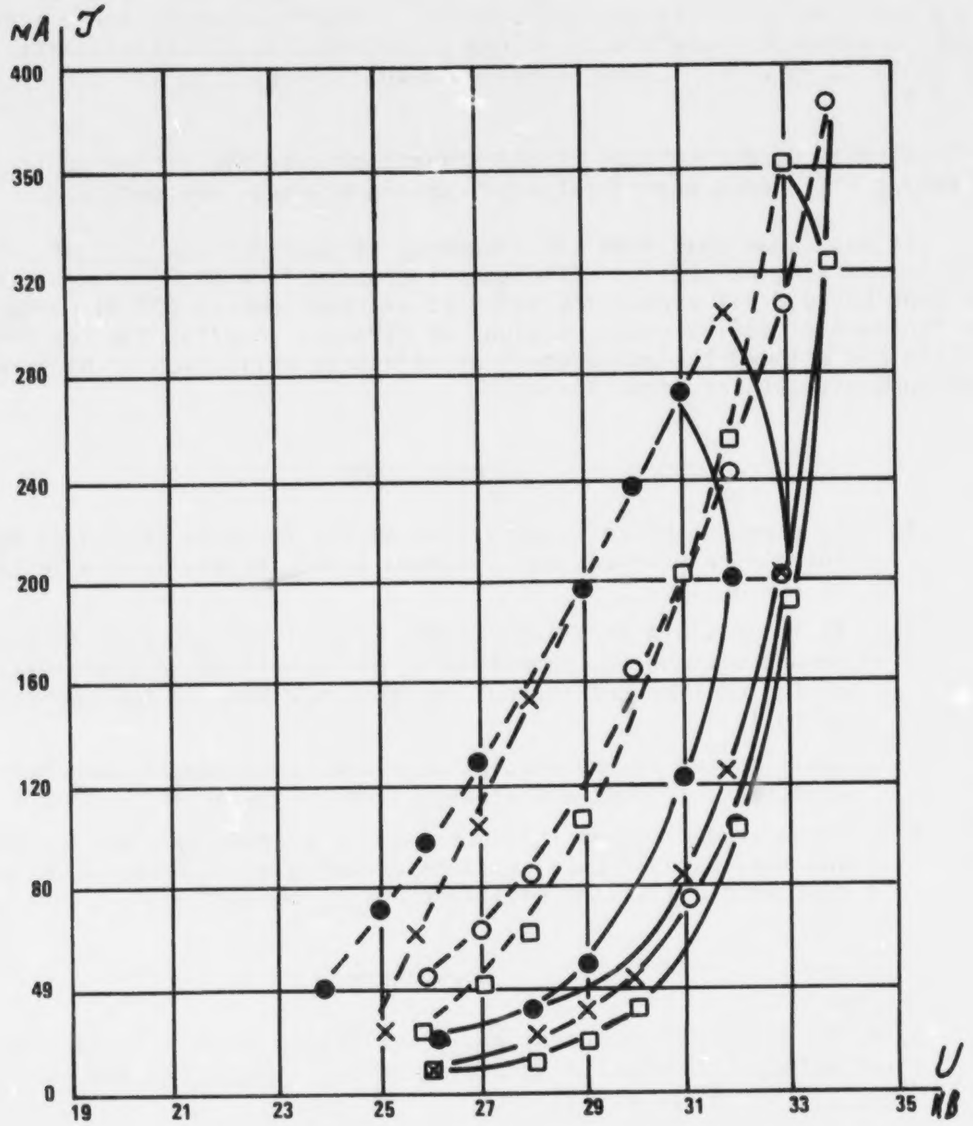

Figure 1. Corona volt-ampere characteristics in an electrostatic precipitator type UG2 -4-37 during cleaning of magnesite dust from gas.

○- field 1, ● - field 2, × - field 3, □ - field 4

_______ voltage increase, - - - - voltage drop is used (schedule 1), cleaning efficiency is 99.21 percent and residual particulate loading of the gas is 55 mg/nm^3. Optimization of the electrode rapping schedule (schedule 2) allows an increase in effective particle drift velocity of 40 percent, and lowers dust entrainment from the ESP by a factor of 3.4.

Studies were also made of the effects of electric regime control on gas cleaning efficiency when a rational rapping schedule was employed.

It was found that when the frequency of sparking was changed from 50 to 150 sparks/min, collection efficiency increased from 99.66 percent to 99.79 percent but did not exceed the value at extreme control (99.81 percent). Thus an increase of active cross sections of ESPs and doubling the residence time in the ESP allowed the achievement of effective collection of high-resistivity MgO dust without gas conditioning.

CONCLUSION

1. In cleaning process gases from rotary furnaces calcining $MgCO_3$, intense reverse corona is formed in electrostatic precipitators of the UG type.
2. It is possible to eliminate the harmful influence of reverse corona without gas conditioning by installing an additional ESP of the UG type and increasing residence time in the apparatus up to 17 s.
3. Optimization of the precipitator electrode rapping schedule allows a decrease in dust entrainment from ESP by a factor of 3.4.
4. A two-staged system that consists of a group of TCHN-24 cyclones and type UG-4937 ESPs provides cleaning of high-resistivity MgO dust with collection efficiency of 99 percent.

REFERENCES

1. G. M. A. Aliev, "Development and Installation of Dust Collecting System after Rotary Furnaces for Calcining $MgCO_3$," Industrial and Sanitary Gas Cleaning, No. 4, p. 2, 1972.

2. G. M. A. Aliev, "Metallurgy," in Dust Collecting in Refractory Production, M, 1971.

3. "Energy," in Reference Book on Dust and Fly Ash Collection, M, 1975.

4. J. Ermilov, B. Zolotarjov, and J. Reshidov, "Method of Detection of Reserve Corona in ESP."

DYNAMICAL BEHAVIOR OF COLLECTING PLATES OF ELECTROSTATIC PRECIPITATORS AND PREDICTION OF RAPPING EFFICIENCY*

V. B. Mescheryakov and A. I. Zavyalov

Abstract

The authors present the state-of-the-art on the dynamic behavior of industrial electrostatic precipitator electrodes. A functional relationship is given that makes it possible to predict electrode rapping efficiency for periodic impact rapping by calculation. The engineering data support the results of experiments conducted with up to date equipment under laboratory and test stand conditions. New designs have been developed based on this study. These designs are undergoing industrial testing.

Performance of industrial electrostatic precipitators (ESPs) depends on dust-collecting efficiency and reliable cleaning of collecting plates. To study the dynamics of collecting plates analytically and experimentally, the investigations were started in 1969 by the Semibratovo branch of NIIOGAZ and the theoretical mechanics chair of the Moscow Institute of Railway Engineers. The program of investigations is described in reference 1. By now it is satisfactorily completed; based on its results the methods have been developed to predict efficient performance of collecting plates; those of the new design are being applied to industrial electrostatic precipitators.

First of all, an individual collecting electrode member, which can be classified as a thin rod of open profile (refs. 2 and 3), was studied analytically and experimentally. The technique of acceleration measurements has been tested with the aid of a specially designed laboratory plant. The next step was to study dynamical properties of a real collecting electrode on the stand.

Analytically, a collecting electrode was considered as a system of thin-walled rods of open profile (fig. 1). During rapping of deposited dust by impact, an impulse of short duration is applied to the collecting electrode. The process of impulse transfer can be considered in steps. During the first step the hammer strikes the anvil of the rapping bar. During the second step the impulse is distributed over the collecting electrode. And, at last, during the third step the impulses distributed over the plates form accelerations in them. To dislodge the dust from the collecting electrodes effectively these accelerations must reach some definite level. To be able to predict the necessary level, one must know the relationship of maximum acceleration in a collecting plate versus the weight of the hammer and the height from which it falls. In solving the problem, the geometry and physical characteristics of all bodies taking part in the transfer of impaction energy play an important role.

---

*For further information regarding the material in this paper, please contact, I. K. Reshidov, U.S.S.R. 113105, Moscow, M-105, 1-st Nagatinsky Pass., 6, NIIOGAZ.

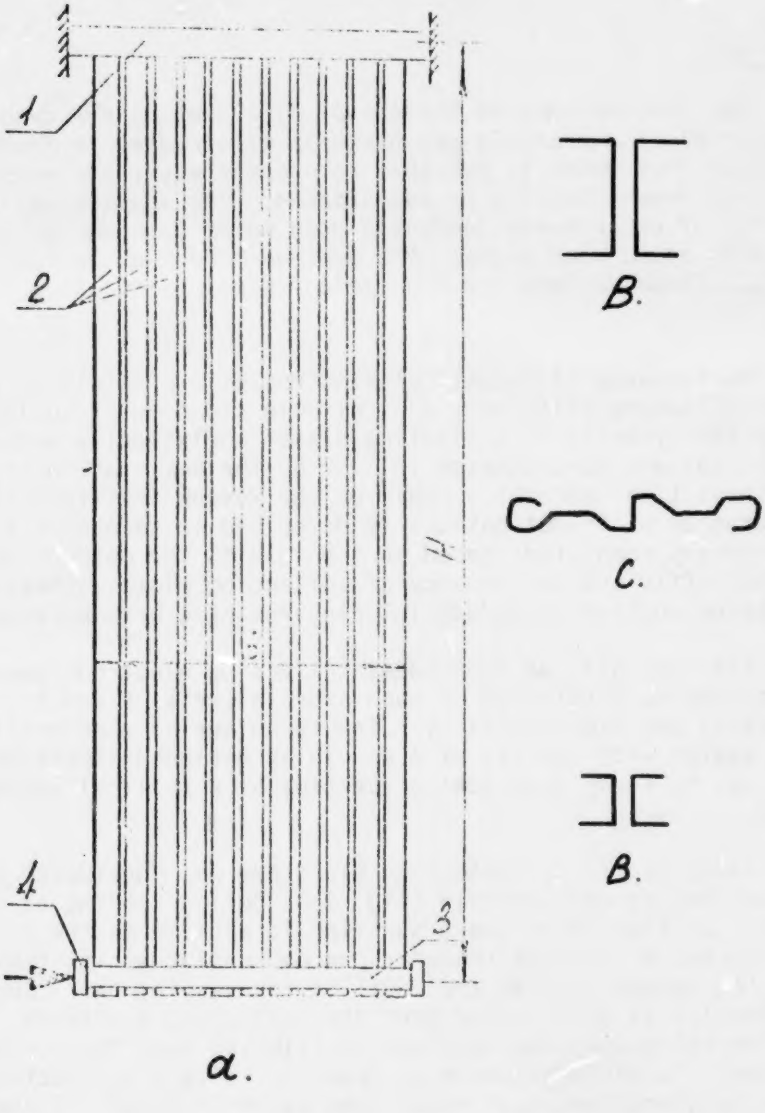

a. Collecting electrode: 1 - suspension bar
2 - collecting electrode element
3 - rapping bar
4 - anvil
b. Profile of rapping bar and suspension bar
c. Profile of collecting electrode element

Figure 1. Collecting electrode.

To determine the contact force acting on the anvil of the rapping bar, a nonlineal integral equation was used:

$$\left[\frac{p(t)}{K}\right]^{2/3} = V_0 t - \frac{1}{m}\int_0^t dt \int_0^t p(t)\,dt \quad \frac{1}{\rho F c}\int_0^t p(t)\,dt, \qquad (1)$$

where $p(t)$ = contact force,

m = mass of the hammer,

V_0 = initial velocity of the hammer,

ρ = density of rapping bar material,

F = cross section area of the rapping bar,

c = velocity of the longitudinal wave propagation in the rod,

K = coefficient depending on the geometry of contacting surfaces.

Equation (1) was solved numerically. Transformation of it to a lineal form results in decreased values for the time of contact (ref. 4).

The impaction impulse, S_0, determined from equation (1) propagates between the tails of collecting electrode members. The impulse values are found from the following equation (ref. 5):

$$S_n = 2 S_0 \alpha (1-\alpha)^{n-1} \qquad (2)$$

Here $\alpha = \frac{m_1 T}{Mtc}$, where m is corrected mass of the collecting electrode member tail (taking into account the mass of that part of the collecting electrode member, which is involved into motion during the time, t_0, when the impulse takes place); M is mass of the rapping bar; and t is time during which the compression wave propagates through the rapping bar. As is seen from equation (2), the values of impulses transferred to the collecting electrode member tails form a decreasing geometric progression. The last collecting electrode member is situated near the end of the rapping bar, that is why one must take into account the back stroke for impulse evaluation. This is done by doubling the value found according to equation (2).

Figure 2 shows impact impulse distribution over the collecting electrode members, the mass of a hammer being 5 kg.

If the collecting electrode members have no tails and are in direct contact with the rapping bar, then the first term in equation (2) is excluded and the parameter α is expressed as

$$\alpha = \frac{-1}{1 + \frac{F}{F_1}\sqrt{\frac{E}{G}}\,K_1}$$

Here F = cross section area of the rapping bar;

F_1 = cross section area of the collecting electrode member;

E,G = elasticity coefficients;

K_1 = form factor for the cross section of a collection electrode member.

To estimate the value of maximum accelerations in cross sections of collecting electrode members, the differential equation was used for swinging of

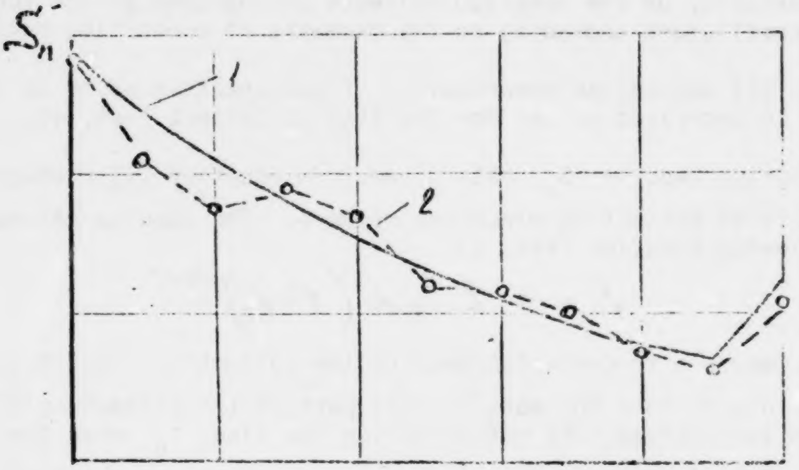

m = 5 kg
1 - calculation
2 - experiment

Figure 2. Distribution of impact impulse over collecting electrode members.

a thin-walled rod taking into account shear distortion and the inertia of longitudinal motion. To estimate energy dissipation, the conception of frequency-independent inner friction in materials was used. The equation was solved with the aid of Fourier transformation. As a result, the following equation for estimation of maximum acceleration (ref. 6) is obtained:

$$a(x) = a_0 \int_0^{\alpha} \varphi(x, \alpha)\, d\alpha ,$$

where

$$a_0 = \frac{S_n r \mu}{2\pi^2 \rho I_y t_0} \qquad \mu = \frac{E}{G} K_1 ,$$

$$\varphi(\alpha, x) = \frac{\exp\left(-\frac{\gamma x}{2} \alpha\right) - \exp\left(\frac{c_1 t_0 - \alpha x}{2} \gamma\right) \mathrm{Cos}\,(\alpha c_1 t_0)}{\sqrt{[1 + \alpha^2 (1 + \mu)]^2 - 4 \mu \alpha^4}}$$

x = coordinate of the collecting electrode member axis;
α = wave coefficient;
α = the limit wave coefficient corresponding to the highest spectre frequency taken into account;
I_y, r = axial inertial momentum and inertial radius of collecting electrode member cross section;
ρ = density of material of collecting electrode member (when the dust layer is present the equivalent density is taken);
c_1 = propagation velocity of high frequency shear wave;
γ = coefficient of inner friction in the material.

The derived functional relationships allow analytical prediction of the level of maximum acceleration in the collecting electrode (ref. 7). The calculations are made on the computer Nairi-2 using a specially compiled program ELOS-3. The time of work for one set of parameters is 5 minutes. The computer types three variables defining the rapping efficiency curve (fig. 3). The acceleration of dust dislodging from the collecting electrode surface given, the curve shows the degree of the electrode cleanliness from the dust in percent.

In experimental investigations, piezoelectric probes and electronic recorders were used. The acceleration measurement technique is described in reference 8. The experiments on the stand confirmed the analytical results. The measured distribution of impulses over the collecting plates is in good agreement with the analysis (fig. 2), though it essentially depends on the size of the gaps that are formed between the collecting electrode member tails and the stoppers on the rapping bar (ref. 9).

Using the experimental results, the statistical characteristics of acceleration fields have been determined. With the aid of formulas for the shortened normal distribution, the degrees of rapping efficiency were calculated. Then the rapping efficiency curves were plotted. As is seen from figure 3, they are in good agreement with the analytical curves. Thus, for the clean electrode the discrepancy is not higher than 5 percent, for the dirty electrode (3 kg of dust per square meter of surface), not higher than 15 percent.

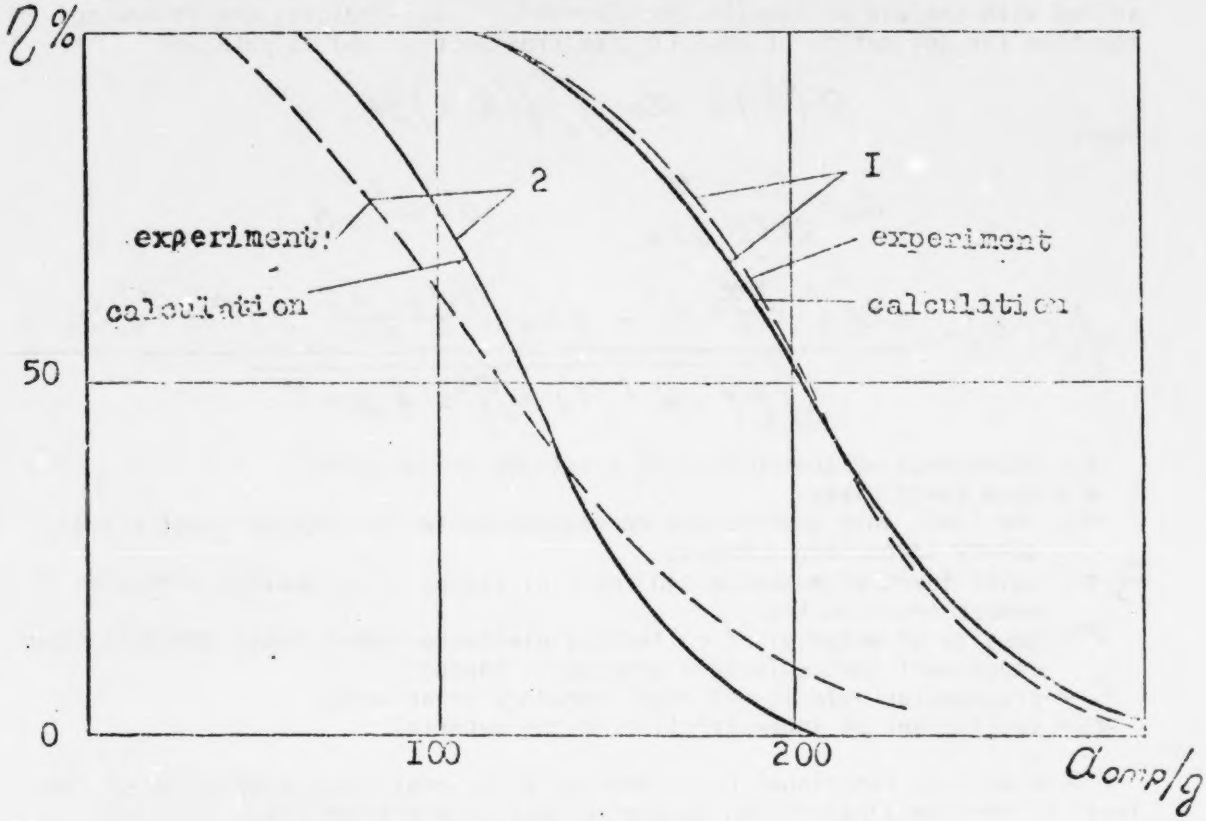

m = 5 kg; *B* = 2.5 m; *H* = 7.9 m
1 - clean electrode
2 - electrode with fixed air-foam rubber simulating dust layer

Figure 3. Comparison of calculated and experimental curves of electrode rapping efficiency.

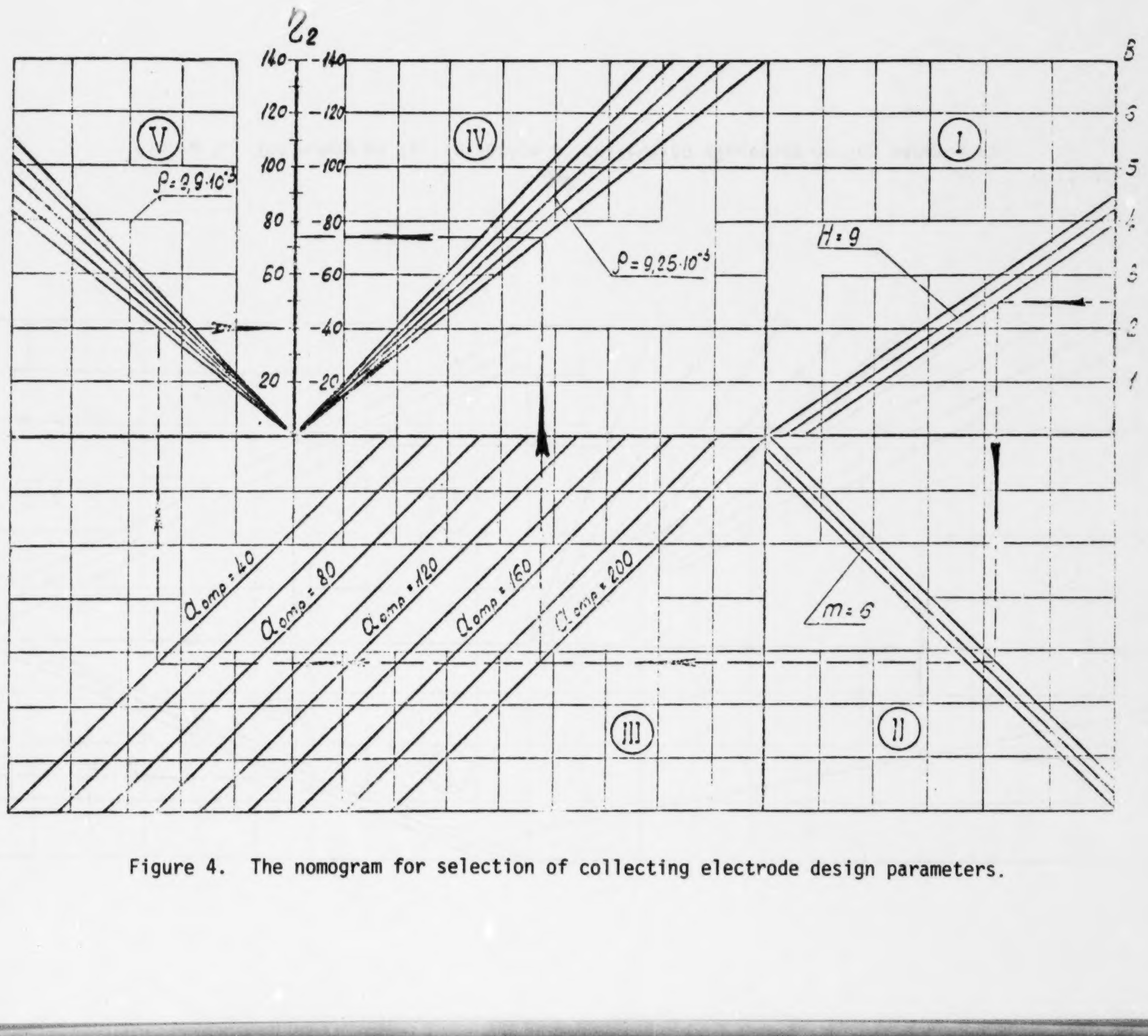

Figure 4. The nomogram for selection of collecting electrode design parameters.

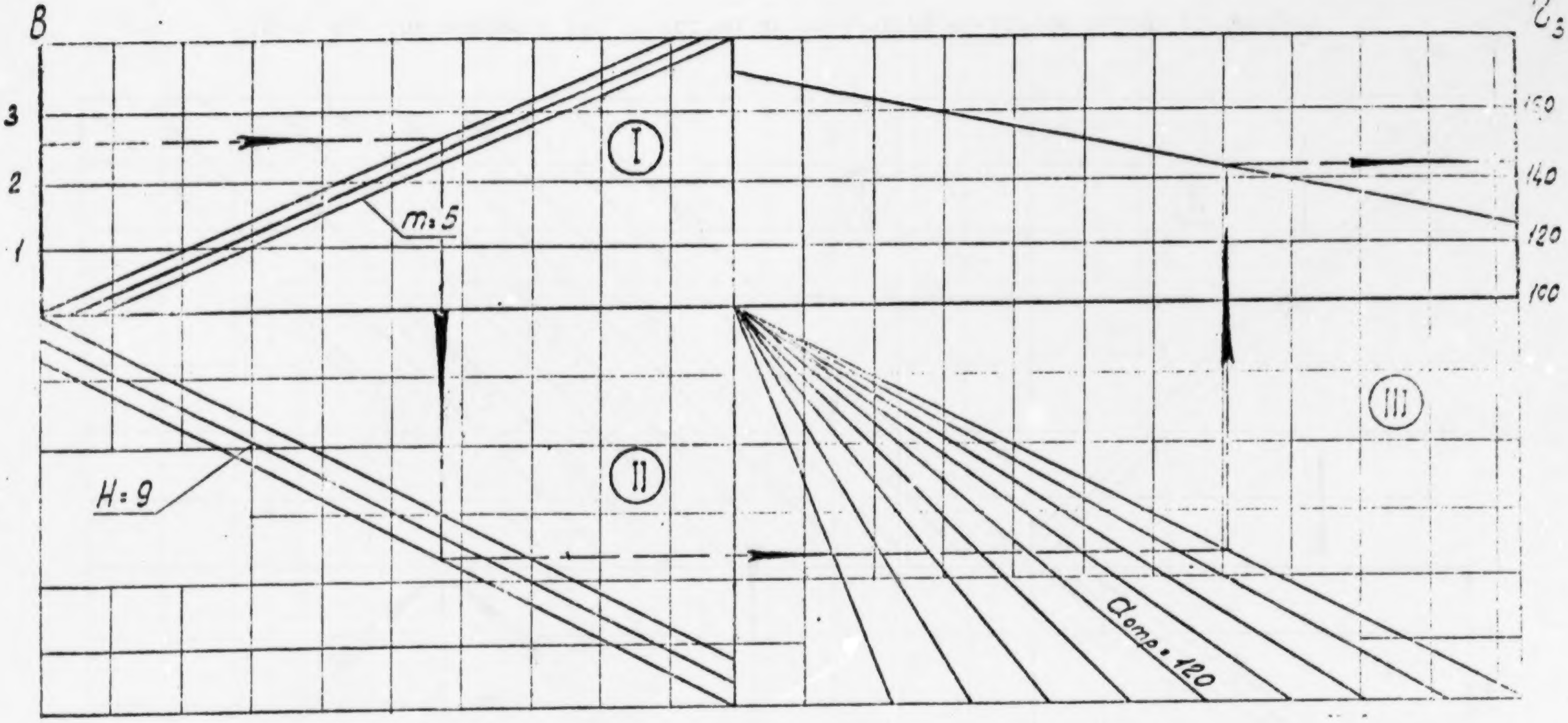

Figure 5. The nomogram for selection of collecting electrode design parameters.

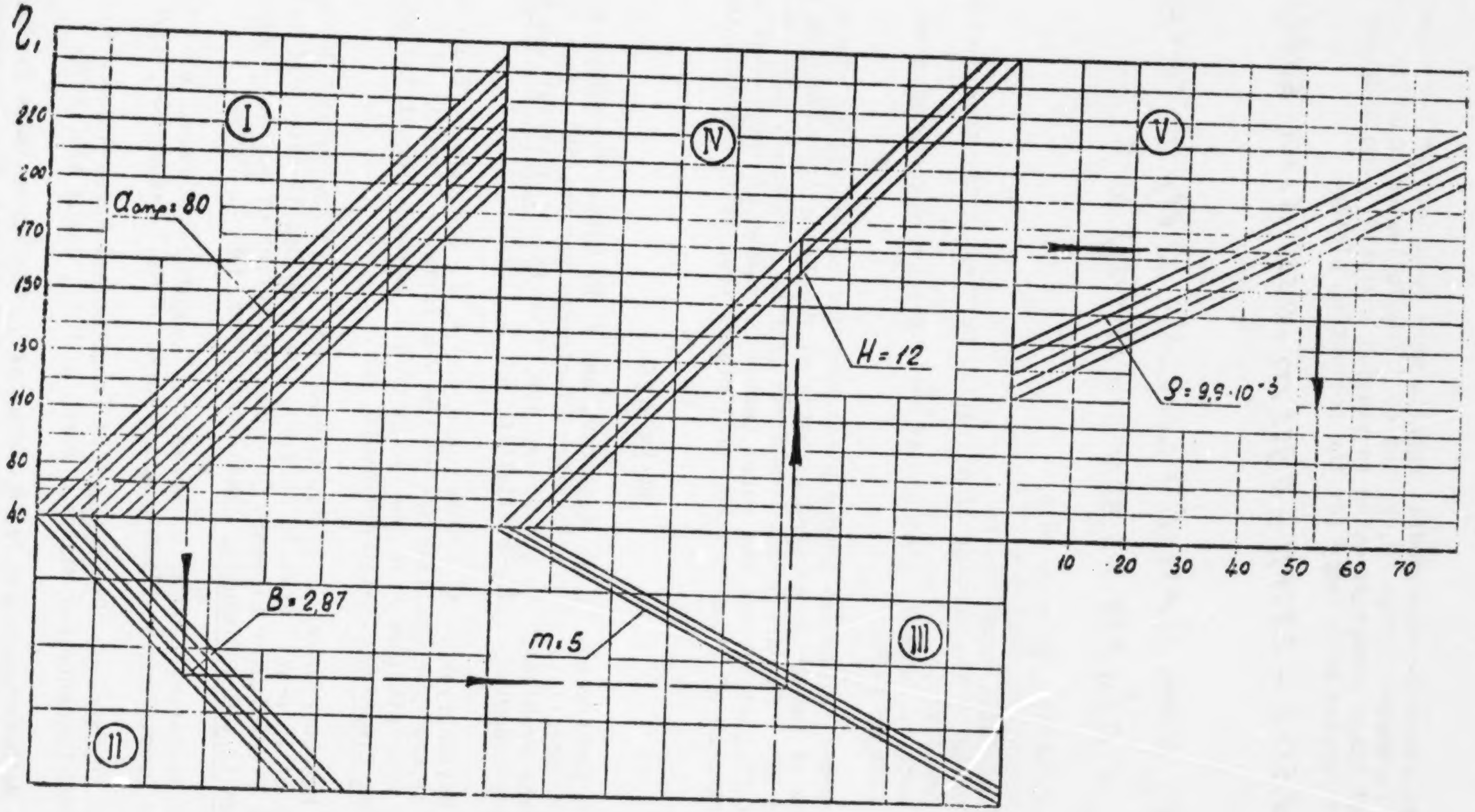

Figure 6. The nomogram for selection of collecting electrode design parameters.

Nomograms based on experimental results were compiled for the selected construction parameters (figs. 4, 5, and 6). The following equation allows compilation of these nomograms using regression analysis. The equation gives the degree of rapping efficiency for the collecting plates:

$$\eta = \eta' - 26.519B - 2{,}826H + 4.912m + 0.539\,\alpha_{omp} - 6{,}956\rho \cdot 10^{-3},$$

where

$$\eta' = 170.4 - \alpha_{omp}\,(0.0492B + 0.0062H - 0.089\rho \cdot 10^{-3} + 0.0072m)$$
$$+ \rho\,(3.04B + 0.33H - 0.445m) \cdot 10^{-3}$$

Here B = width of electrode in m;
H = height of electrode in m;
m = mass of a hammer in kg;
α_{orp} = value of the rapping acceleration related to the acceleration of gravity;
ρ = material density (in case of dirty electrode the equivalent density is used).

The progress in studies of dynamical behavior of collecting plates under the influence of impaction allowed proposal of new types of collecting plates (refs. 9 and 10). Patents were claimed and granted (refs. 11, 12). Specimens of new collecting plates are now under test in a number of industrial ESPs in different branches of industry. The preliminary results are satisfactory.

REFERENCES

1. V. B. Meshcheryakov, I. K. Reshidov, and V. N. Uzhov, "Problems of Reliability and Durability of Precipitator Electrodes and Possible Ways of Solving these Problems," in the collection of works: Industrial and Sanitary Gas Cleaning, TsNIITEneftekhim, No. 2, 1972.

2. V. B. Meshcheryakov, A. S. Arkhipov, and A. I. Zav'yalov, "Experimental Study of the Free Oscillations of the Precipitator Elements of Electrostatic Precipitators," in the collection of works: Industrial and Sanitary Gas Cleaning, TsNIITEneftekhim, No. 5, 1972.

3. V. B. Meshcheryakov, I. I. Ivanchenko, and A. I. Zav'yalov, "Using the Theory of Thin-wall Rods in Studying the Free Oscillation of Electrostatic Precipitator Elements," in the collection of works: Industrial and Sanitary Gas Cleaning, TsNIITEneftekhim, No. 5, 1973.

4. Ye. N. Kurbatskiy and A. L. Shevelev, "Longitudinal Impact of a Concentrated Load Along an Elastic Rod," works of MIIT, issue 509, 1976.

5. Ye. N. Kurbatskiy, "Propagation of Longitudinal Waves Along a Rod With Attached Concentrated Masses," works of MIIT, issue 476, 1975.

6. V. B. Meshcheryakov and Ye. N. Kurbatskiy, "An Approximate Evaluation of Acceleration in a Beam Under the Short Term Effect of a Transverse Force," works of MIIT, issue 509, 1976.

7. V. B. Meshcheryakov, "Computational Evaluation of the Rapping Efficiency of the Industrial Electrodes of Industrial Electrostatic Precipitators," in the collection of works: Industrial and Sanitary Gas Cleaning, No. 1, 1977.

8. A. I. Zav'yalov, "Procedure for Studying the Dynamics of Precipitator Electrodes," Tsement, No. 3, 1975.

9. V. B. Meshcheryakov and A. I. Zav'yalov, "Problems of Improving ESP Precipitator Electrodes," in the collection of works: Industrial and Cleaning of Gases and the Aerodynamics of Dust Trapping Equipment, Yaroslavl', 1975.

10. A. I. Zav'yalov, Selection of Design Parameters for Precipitator Electrodes Which Ensure Efficient Rapping and Reliability in Operation," in the collection of works: Industrial Gas Cleaning and the Aerodynamics of Dust Removal Equipment, Yaroslavil', 1975.

11. A. I. Zav'yalov, V. V. Nagornyy, L. P. Smirnov, and S. I. Sobchuk, "ESP Precipitator Electrodes," U.S.S.R. author certificate, Moscow, Class VOZS 3/40, No. 472690, Announced 06.11.73, No. 1967934/23-26, Published 05.06.75.

12. A. I. Zav'yalov, V. V. Nagornyy, V. I. Panasyenko, and S. I. Sobchuk, "The Electrostatic Precipitator," U.S.S.R. author certificate, Moscow, Class VOZS 3/76, No. 523712, Announced 01.07.74, No. 2039906/26, Published 05.08.76.

ELECTRICAL GAS CLEANING AT HIGHER PRESSURES*

A. Yu. Valdberg, V. V. Danilin, A. G. Ljapin, V. M. Tkachenko

Abstract

A number of branches of industry require high efficiency cleaning of large volumes of gas at higher pressures or at both higher pressures and temperatures. In this report, using blast furnace gas cleaning as an example, the authors study problems associated with the use of dry electrostatic precipitators to meet these objectives. Results are given from studying the electrical characteristics of coronal discharge in air at a pressure up to 0.6 MPa and a temperature of up to 400° C. Test results are also given of a pilot industrial dry-type electrostatic precipitator cleaning furnace gas at a pressure of 0.3 MPa at a temperature up to 25° C.

Within the past few years several industries have been faced with the necessity of treating vast gas volumes at higher pressures or at both higher pressures and temperatures. For example, the construction of large blast furnaces in ferrous metallurgy has resulted in considerable volumes of stack gases at pressures of about 0.35 MPa. This has permitted use of energy from compressed blast-furnace gases in gas turbines. Good performance of these turbines is attainable with fine purification (to 5 mg/Nm^3)[†] of vast gas volumes (to 800,000 Nm^3/hr per furnace) at a minimum decrease of pressure and temperature in the gas cleaning system.

Although modern wet processes provide a desirable, efficient means of gas cleaning, they require large water consumption, a complex and expensive sludge removal system, and additional preheating of purified gas before discharge into a turbine. Development and application of dry cleaning for blast-furnace gases has made it possible to eliminate both the sludge handling system and the gas preheater ahead of the turbine and to increase the turbine capacity well due to gas feed at higher temperature.

Electrostatic precipitators are a most promising device to treat large volumes of hot gases. However, experience in operating dry ESPs to handle blast-furnace gases at higher temperatures is lacking and the literature contains inconsistent data for corona discharge effects on performance of ESPs. Therefore, NIIOGAZ had undertaken an investigation to study electrical characteristics of corona discharge at both higher temperatures and pressures, as well as to evaluate collection efficiencies of dry ESPs as applied to blast-furnace gases.

The investigation has been conducted on an ESP model with an electrode assembly consisting of coaxial cylinders and point-to-plane electrodes. The temperature of a dry process and its pressure varied in the range of 20°-400° C and 0.1-0.6 MPa, respectively. Cylinders with diameters of 65, 99, and 140 mm were used as collecting electrodes. The length of the active part of these cylinders that served as the collecting electrode was 500 mm with a plan of 180-mm diameter, and had edges made in accordance with a profile of the Pogovsky electrode (for $\Psi = \frac{\pi}{2}$ at the discharge gap) of S = 4 cm. End shields of the cylindrical electrodes were separated from the active part by pyroceramic rings. Wires having diameters of 0.5, 1, 2, 3, 7, and 20 mm were used as corona electrodes. In addition, edges were made in the form of a hyperboloid of rotation with a radius of curvature at the tip $\rho = 0.07$ and 0.9 mm. Corona electrodes were also made in the form of rods of 6- and 18-mm diameter and had semispherical ends.

---

*For further information regarding the material in this paper, please contact I. K. Reshidov, U.S.S.R. 113105, Moscow, M-105, 1-st Nagatinsky Pass., 6, NIIOGAZ

[†] Gas volume is henceforth assumed to be under normal conditions.

Rectified voltage of positive and negative polarities was fed to the corona electrodes from a high voltage supply, which provided voltage of up to about 250 kV at current values of 50 mA.

The corona onset voltage (V_0) was determined by smoothly increasing the voltage in the discharge gap by means of stabilizing the voltage at a value corresponding to an average value of corona current on the level of 1 mkA, or it was detected by appearance of current pulses on an oscillograph screen.

The input signal was fed from a resistance connected to the grounded circuit of the measuring part of the collection electrodes. The voltage was decreased and the voltage value, when pulses and corona were disappearing, was measured. The minimum value was assumed to be equal to V_0.

Breakdown voltages (V_{br}) were determined by occurrence of a current spike in the grounded circuit of the measuring part of the collection electrodes, as well as by voltage decrease in the discharge gap when the voltage at the exit of a high-voltage supply was increasing at the rate of about 2kV/s. For each temperature and pressure range, 25-30 measurements of V_{br} values were made.

Ion mobility, k, and critical voltage, V_{cr}, were estimated through treatment of voltage-current characteristics by the reduction method. The characteristics were measured for coaxial cylindrical electrodes. The method is based on the following expression (ref. 3):

$$i = B \frac{8\pi \varepsilon_0 K}{R^2 \ln R/r_0} v(v - v_{\kappa p}), \tag{1}$$

where i = corona current per unit length of a discharge electrode;

ε_0 = permittivity of free space;

R = radius of a collecting electrode;

r_0 = radius of a discharge electrode;

v = applied voltage;

$$B = \frac{v_{\kappa p}}{v} f(\alpha); \quad f(\alpha) = \frac{\alpha/4}{\ln\frac{2}{\sqrt{\alpha+1}+1} + \sqrt{\alpha+1} - 1}$$

$$\alpha = \frac{2 \cdot i \cdot S \cdot 10^{11}}{K} \left(\frac{R/r_0}{E_{\kappa p}}\right)^2$$

Ion mobility is described by equation (2) in accordance with the two-cylinder method (ref. 4):

$$K = \frac{i(R_2 - R_1)^2}{2\pi \varepsilon_0 (v_2 - v_1)^2} \tag{2}$$

where $V_2 - V_1$ = difference in potential applied to two cylinders under the developed corona. R_2 and R_1 were assumed to be radii of the cylinders at the similar corona current. r_0 = radius of the corona electrode.

THE POSITIVE CORONA

There is much evidence in the literature that operation under positive corona at higher temperatures is more effective than operation under negative corona mainly due to the increased puncture voltage of the former (ref. 5). Therefore, by investigating corona characteristics, one could demonstrate the possible applicability of positive corona in ESPs.

At temperatures of 20 to 400° C, and at pressure of 0.1 to 0.6 MPa, two forms of positive corona may occur: continuous (avalanche type) and pulse (streamer type). The pulse corona is characterized by the absence of current pulses and it has an image of a uniform luminescent sheath at the surface of the anode. A slight glow, created by numerous streamers, spreads towards the cathode. Pulses of corona current are very strong. At normal (atmospheric) conditions, the continuous corona exists at polished tips and at fine wires with d = 2 mm diameters as well. An increased air density (δ) results in conversion of a continuous form into a pulse one (figure 1). At the increased temperatures, the transition of a continuous corona to a pulse one occurs at a higher density than that at a normal temperature. Pulse corona generation is accompanied by a sharp decrease of breakdown voltage (by a factor of 2). Further increase of air density to a critical value (δkp) leads to disappearance of pulse corona discharge and gap breakdown starts without preceding corona discharge. δkp values increase with decreasing radius of the discharge electrode.

Ion mobility was evaluated by reduction (K_1) and two-cylinder methods (K_2). For the temperatures and pressures studied, it was found that the product of air density and ion mobility was approximately a constant value ($\delta K_1 \approx \delta K_2 \approx$ const).

Breakdown voltages in the region under positive pulse corona were much lower than the values corresponding to negative corona discharge. Therefore, the electric field attainable in the active zone of the ESP was also weaker.

Migration velocity of particles affects ESP collection efficiency, which is proportional to the electric field and charge on a particle. Available data (ref. 6) indicate that a charge acquired by a particle in fields of continuous and pulse coronas having the same value of voltage in the gap has nearly the identical charge value. Therefore, the collection efficiency of ESPs operating under positive pulse corona will be lower than those with negative discharge electrode polarity.

Under continuous positive corona, breakdown voltages (V_{br}^{+}) are nearly equal to those of negative corona (V_{br}^{-}) at normal temperature. With rising temperature, the value of V_{br}^{-} decreases more than that of V_{br}^{+}. At a high temperature, V_{br}^{+} substantially exceeds V_{br}^{-}. Figure 2 shows that V_{br}^{-} is 30 percent less (24 kV) than V_{br}^{+} at P = 0.14 MPA and T = 400° C.

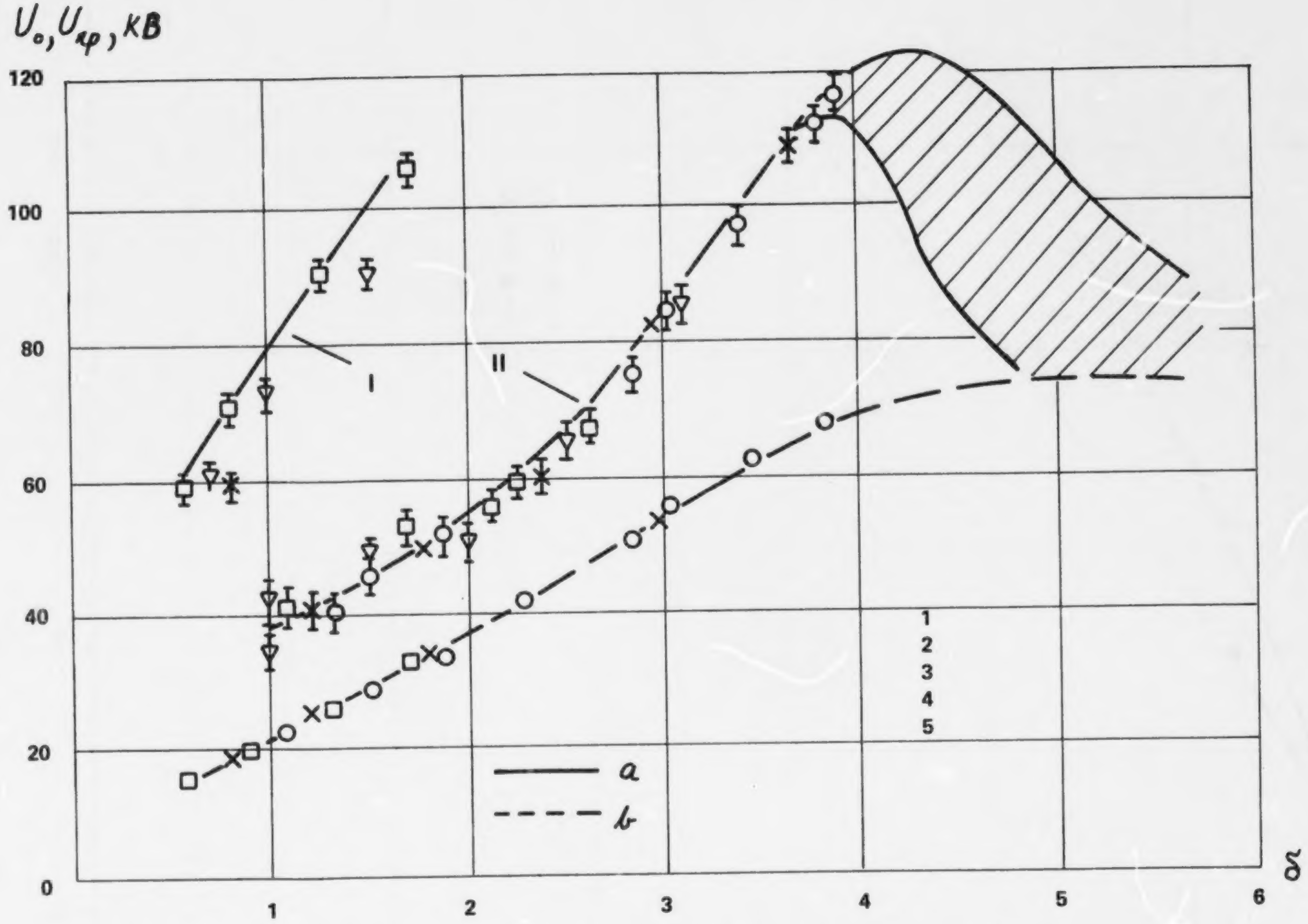

Figure 1. Breakdown and initial voltages at positive corona in the gap of the "point-to-plant" electrode assembly (p = 0.9 mm, S = 4 cm).

a – breakdown voltage (I – continuous corona, II – pulse corona),
b – initial voltage;
1 – 20° C, 2 – 100° C, 3 – 200° C, 4 – 300° C, 5 – 400° C.

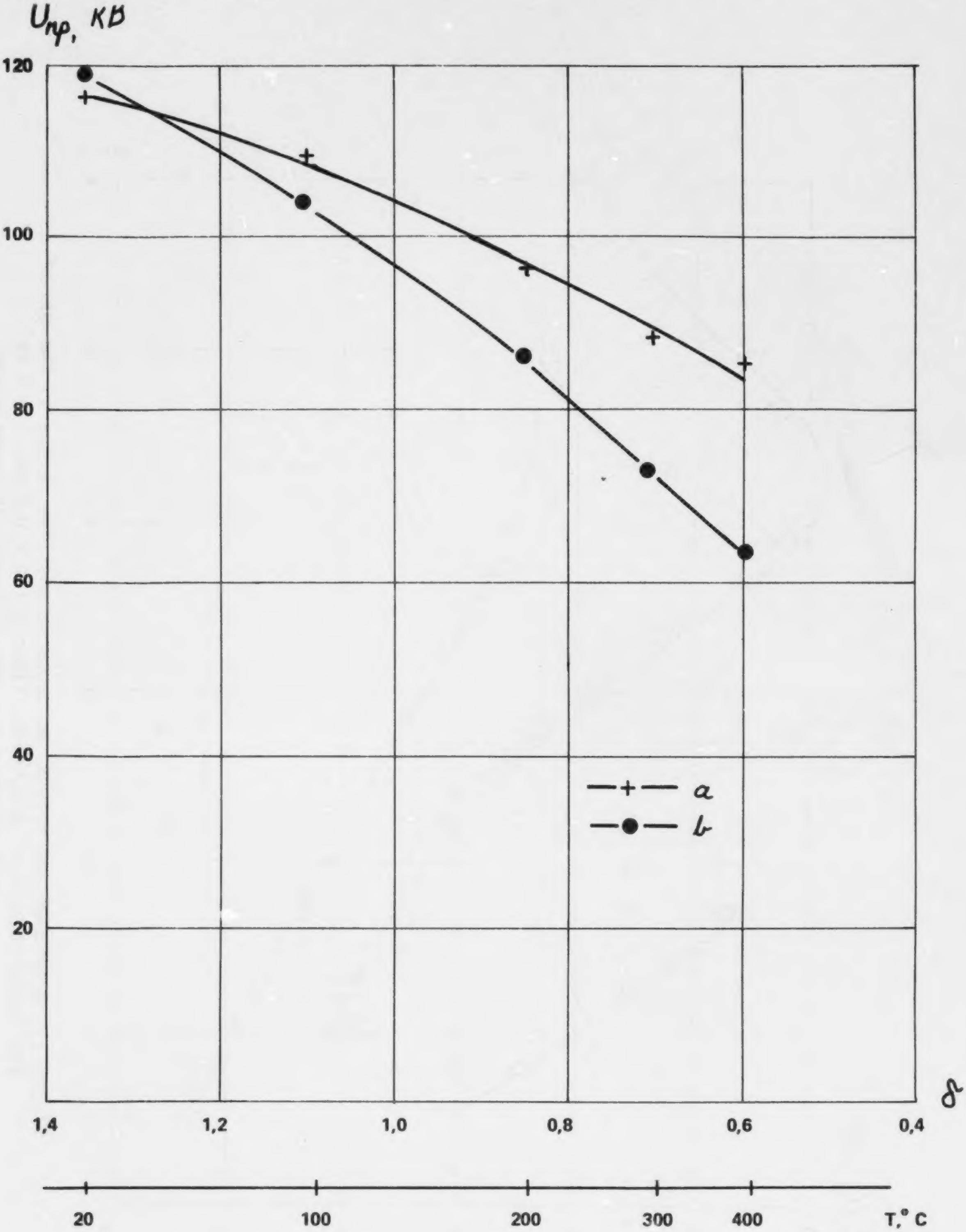

Figure 2. Breakdown voltages in the "coaxial cylinders" electrode assembly at P = 0.14 mPa, D = 140 mm.

d = 0.5 mm.

a – positive; b – negative polarity.

Meanwhile, it has been found that a stable, continuous corona exists only at fine polished wires with a 2-mm or smaller diameter or at edges with a fixed radius of curvature. Mechanical damage on the surface of a discharge electrode (scratches, scores) or erosion due to breakdown of electrodes leads to creation of pulse corona discharge and a sharp decrease in breakdown voltage.

Available data allow one to conclude that application of positive corona in industrial ESPs, particularly for blast-furnace gas control at P = 0.35 and T = 250°, is not reasonable.

THE NEGATIVE CORONA

For an electrode assembly consisting of coaxial cylinders, the value of averaged ion mobility (K_1) within the whole gap was estimated by the method of reduced characteristics. The K_2 value, corresponding to the region of the discharge gap between R_1 and R_2, was estimated by the two-cylinder method.

For the range of P and T studied, it was established that the product of air density and ion mobility δK_1 increases substantially with rising temperature. So, at T = 400° C and P = 0.14 MPa for D = 99 mm and d = 3 mm, the value of δK_1 is equal to 6.55 $cm^2/V/s$, which is 2.5 times more than δK_1 under positive corona.

The values of K_2 determined by the two-cylinder method, for R_1 = 50 mm and R_2 = 70 mm are lower at high temperatures than the corresponding values of K_1. So, at T = 400° C and P = 0.14 MPa, we obtained $\delta K_1 = 5.4$ for d = 0.5 mm as compared with $\delta K_2 = 2.5$ $cm^2/V/s$. This means that the averaged ion mobility along the discharge gap is not constant and it can be associated with decreased adherence of electrons at a higher temperature and subsequent penetration of these electrons far inside the discharge gap.

An increase in δK_1, with raising the temperature, results in much steeper voltage-current curves at the same air density, but at higher temperatures. Current pulses exist at the wires until gap breakdown occurs. With edges of a small radius of curvature, pulses disappear and charge takes a pulseless form when the critical value of current Ikp is exceeded. At the same time, with disappearance of pulses, the form itself is sharply changed. Discharge takes a characteristic shape of a brightly shining cord or several cords at high T zone. The lower end forms a diffusional zone.

A change in radius curvature of the edge from 0.077 to 3mm, and an increase of the discharge gap and temperature from 3 to 6.5 cm and from 20 to 400° C, respectively, both result in a slight variation of I_{cr} value from 120 to 200 mkA. For edges with $\rho < 0.9$ mm, the pulse corona, which has been generated at $I = I_{cr}$, exists until gap breakdown occurs. The breakdown voltage under negative corona, as well as under positive corona, depends on the form of corona discharge preceding breakdown. For the point-to-plane gap, the peak value of V_{br} is observed in the presence of pulseless corona.

If the pulse corona precedes breakdown then the value of V_{br} depends on the radius of curvature of the edge and decreases with increasing values of ρ.p.

Figure 3 shows V_{br} as a function of varying air density, δ. It is apparent that in the range of temperatures and pressures investigated the peak values of V_{br} are obtained with an edge at $\rho = 0.077$ mm. With cylindrical-geometry corona electrodes, the breakdown voltages also have peak values for wires with a small radius of curvature ($d < 2$mm).

Analagous behavior is found in industrial electrode assemblies. Let us consider a strip-needle corona electrode assembly with 40-mm spacing between 12-mm high needles, and 170-mm collector plate spacing. A 90° turn of the discharge electrode reduced puncture voltage from 143 to 121 kV with an increase in the discharge gap from 72.5 to 75 mm. This behavior may be related to corona onset and development of breakdown because of the electrode base having a larger radius of curvature than that of the needles.

Therefore, strip-tooth electrodes having needles with 0.1-mm radius of curvature are recommended for ESPs designed to treat blast-furnace gases.

APPLICATION OF DRY PLATE ELECTROSTATIC PRECIPITATORS FOR BLAST-FURNACE GAS CLEANING

Efficiency of blast-furnace gas cleaning in a dry ESP was investigated on a pilot-plant scale. The installation tested included a dry plate ESP and devices to cool gases before they entered the ESP, a hollow scrubber, or a scrubber with a converging gas feed.

The dry plate ESP was a cylindrical horizontal apparatus with a 1.2-m^2 active section and a 2.5-m long field. C-shaped collection electrodes and strip-tooth discharge electrodes having 5-mm high needles with 40-mm spacing between them were used. Space between collecting electrodes was 275 mm. Rappers to clean discharge and collecting electrodes utilized heavy hammer blows. Gases from a blast furnace of 2,700 m^3 working volume was introduced into the installation at 0.28-0.29 MPa and 210-280° C. Chemical composition of the gas (volume, percent) was as follows: CO = 25. 4 to 27.7; CO_2 = 16.3 to 18.2; H_2 = 6 to 6.9; N_2 = 48 to 51. Moisture content was about 50 g/kg of dry gas.

Cooling of blast-furnace gases (to 120° C) in a hollow scrubber located ahead of the ESP, as well as in a scrubber with converging gas feed (to 150° C), had been investigated. In both cases, carryover of water drops into the ESP and build-up of unshaked dust layers on surfaces of the discharge and collecting electrodes had not been observed. Blast-furnace gases entered the ESP at 120 to 230° temperature. Gas velocity in the active section varied from 0.5 to 1.85 m/sec. High operating voltage was continuously maintained at 85 to 90 kV with cooling gases in a hollow scrubber or in the scrubber with converging gas feed, as well as without water consumption in the scrubber.

Inlet and outlet dust loading in the feed gas was measured by filtration through glass extractors packed with fiberglass. Inlet dust loading was at 10 to 12 g/Nm^3. Dust dispersion was measured by a jet separation method using a 10-stage impactor developed in NIIOGAZ. A mass medium diameter of particles at the ESP exit was 10 m. Chemical composition of dust is as follows (percent by weight): SiO_2 = 7; Al_2O_3 = 7; CaO = 7.2; MgO = 1.1; the total Fe = 45.5; FeO = 58; Fe_2O_3 = 55; MnO = 0.3; S = 0.45; C = 10. Dust resistivity varied between 10^7 and 10^8 ohm/cm.

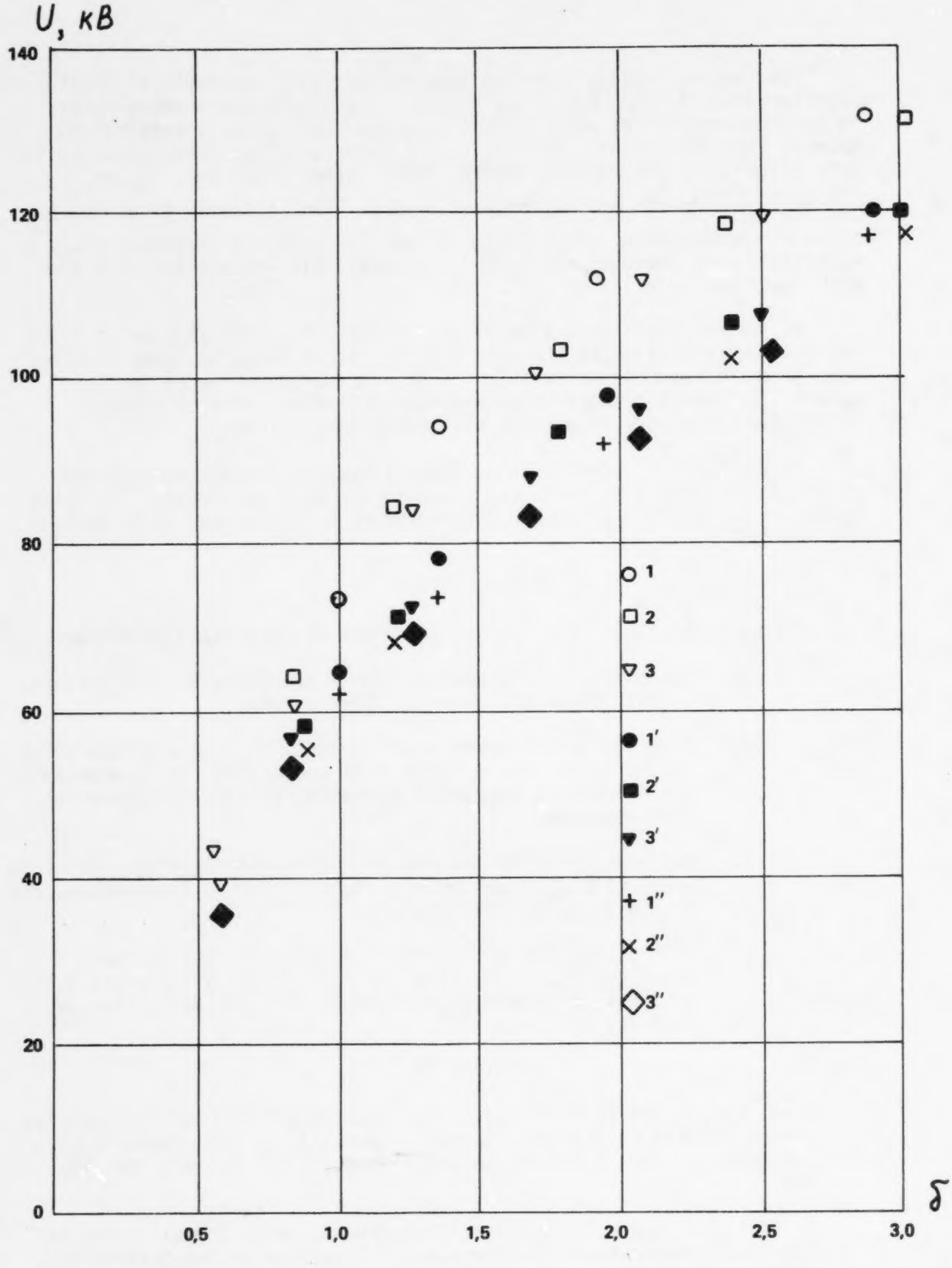

Figure 3. Breakdown voltage at negative corona in the "point-to-point" electrode assembly for edges with varying radius of curvature.

1,2,3 – ρ = 0.077 mm; 1′, 2′, 3′ – 0.9 mm, 1″ 2″, 3″ – 3 mm; I, I′, I″ – T = 20° C; 2,2′,2″ – 200° C and 3,3′,3″ – 400° C.

The rapping systems operated intermittently at intervals of 18 min. Duration of a cleaning cycle was 6 min. To evaluate the reentrainment, factor measurements of dust content were made during the operation and between cleaning cycles. At 0.5 - 1.2 m/s gas velocity through the active zone of the ESP, the rapping reentrainment factor given by: $K_{yh} = \frac{\log(1\eta\ c\ fcmp)}{\log(1-\eta\delta ez\ fcmp}$ was in the range of 0.93 to 0.96, slightly exceeding the value of reentrainment obtained for industrial ESPs. This behavior may be associated with improved electrical characteristics of the test ESP and with lower gas velocity as well.

At 1.2 m/s (residence time of gas in the ESP active zone was t = 2.1 s), dust concentration at the exit did not exceed 60 mg/Nm^3 when shakers were in operation. At 0.5 m/s (t = 5 s), the value decreased to 13.1 mg/Nm^3. Exit dust concentration averaged 9.2 mg/Nm^3 at 99.8 percent collection efficiency regardless of rapping reentrainment.

On the basis of the available data, a preliminary design of a dry plate ESP for high-efficiency gas cleaning had been developed. The installation is designed to treat 200,000 Nm^3/hr of blast-furnace gases at 0.35 MPa and 250° C.

CONCLUSIONS

The main results of the investigation may be summarized as follows:

1. Operation of ESPs both at higher pressures and temperatures is not reasonable under positive corona.

2. Cooling blast-furnace gases to 120-150° C in a hollow scrubber, or also in a scrubber with converging gas feed ahead of the dry ESP is possible. Operating difficulties have not been observed.

3. Application of strip-tooth discharge electrode assemblies to treat blast-furnace gases at both increased temperatures and pressures is recommended.

4. High collection efficiency of a dry plate ESP has been demonstrated. At 0.3 MPa and 230° C, the pilot-plant ESP has shown 99.8 percent efficiency when residence time was 5 seconds.

REFERENCES

1. A. G. Ljapin and V. V. Danilin, "Application of the Unipolar Positive Corona for Electrical Gas Cleaning," Izvestija of the Academy of Sciences, U.S.S.R., Energetics and Transport, No. 6, 1975. pp. 155-160.

2. A. G. Ljapin and V. V. Danilin, "Negative Unipolar Corona in Air at Increased Temperatures and Pressures," Izvestija of the Acadeny of Sciences, U.S.S.R., Energetics and Transport, No. 5, 1976. pp. 148-154.

3. V. I. Popkov, "To the Theory of DC Current Unipolar Corona," Electricity, No. 1. 1949. pp. 33-42.

4. V. I. Levitov, "A. C. Current Corona, M," Energy, 1969.

5. C. C. Shale, "Progress in High-Temperature Electrostatic Precipitation," Contr. Assoc., Vol. 17. No. 3 (1967), pp. 159-160.

6. N. B. Bogdanova and B. I. Popkov, "The Form of Corona Discharge and Breakdown of Air Gaps," Electricity, No. 8, 1973, pp. 27-33.

AIR POLLUTION CONTROL OF EMISSIONS FROM KILNS AND COOLERS UTILIZING FABRIC FILTERS IN THE CEMENT INDUSTRY

Frank R. Culhane*

Abstract

This paper covers the application of fabric filters within the cement industry to control particulate emissions from the cement kilns and clinker coolers.

The subject matter is presented in two parts: Part I - Cement Kilns, and Part II - Clinker Coolers.

PART I - CEMENT KILNS

Particulate emission from rotary cement kilns has long been a difficult problem, but has increased in severity as our air pollution codes have become more stringent with the passing of time. From a gas cleaning standpoint, the difficulties have been due to the large volume of gas involved, heavy dust loading, fine particle size, high dust resistivity on dry-kiln applications, and high moisture on wet-kiln applications.

The standard multicyclone collector is capable of removing a high percentage of dust by weight, but for nearly complete collection of the particulate, the only practical device, until recently, has ~~been the electrostatic~~ precipitator and, to a much lesser extent, the wet scrubber. The fabric filter, which is one of the oldest and simplest collectors capable of a high degree of stack gas cleaning, for a long while was considered unsuited for cleaning kiln flue gases because of the temperature limitations of the filter fabric and generally accepted, but poorly understood, fear of moisture. However, in the 1950's, development of silicone-finished fiberglass, and later graphite- and Teflon-coated fiberglass, raised the operating temperature limits to 288° C (550° F) and provided a fiber with extremely low water absorbancy. As a result, the cement industry in the United States tested a fabric filter utilizing fiberglass filter bags on wet-process kiln gas in 1956, and in October, 1957, the first full-size kiln baghouse went into operation. Today, some 20 years later, there are over 385 cement kilns in the United States, of which it is estimated that over 33 percent are equipped with baghouses, testifying to the acceptance of the fabric filter in this industry.

Portland Cement Process

In order to have an appreciation of the variables involved in the proper application of fabric filters for the cement industry, we should first briefly review the processes involved in the manufacture of Portland cement. Stated briefly, the raw materials utilized in the manufacture of Portland cement consist of argillaceous* and calcareous† materials that are quarried, crushed, ground, and thoroughly mixed in either a wet or a dry state. The mix is fed as a slurry into a rotary kiln in the wet-process plant, and as a dry powder in the dry-process plant. The kilns in the United States vary between 2.5 m (8.2 ft) and 5.5 m (18 ft) in diameter, and are from 30 m (98.4 ft) to 230 m (754.6 ft) in length. The kilns are installed horizontally, refractory lined, rotate slowly between ½ and 1 rpm, and are set at a slight incline in the range of 3 cm/m. The raw materials are fed into the upper end of the kiln and travel downward toward the firing end of the kiln. The kilns are either fired with powdered coal, fuel oil, or natural gas, with the burner located at the lower end of the kiln. At the firing end, the kiln gas temperature ranges from 760° C to 871° C (1,400 to 1,600° F).

---

*Wheelabrator-Frye Inc., Air Pollution Control Division, Pittsburgh, Pennsylvania 15219.

As the feed moves along the upper part of the kiln, it is exposed to increased gas temperatures as it flows slowly toward the lower end. As the raw material is heated, the water is evaporated, the organic material burns away, and the carbonates lose their carbon dioxide and the sulfate is decomposed, liberating SO_3. In addition, chlorides and alkali salts are partially volatized. About a third of the original weight of the raw mix is lost in the burning process due to volatilization.

Chemical reactions take place between the materials in the raw mixture at the elevated temperatures within the kiln. In the course of these reactions, new compounds are formed and some melt to partially fuse the charge into clinker. The resultant clinker is then discharged into a cooler. When cool, the clinker is mixed with a carefully controlled quantity of either calcined or uncalcined gypsum and the mixture is ground to a very fine powder as Portland cement.

Wet Kiln

It is estimated that within the cement industry in the United States, there are some 385 cement kilns in operation today. Of these 385 kilns, a total of 214 are wet-process kilns and 171 are dry-process kilns, which means that 56 percent of the kilns in the United States are of the wet process type. As stated previously, the first fabric filter installed in the United States was installed on a wet-process kiln. Generally speaking, the gas conditions from a wet kiln are readily suitable for electrostatic precipitation without gas conditioning. Therefore, the electrostatic precipitator has been widely accepted in the United States within the cement industry as a suitable and economic solution to kiln emission control. However, wherever the plant operations are: (1) concerned with "snowflaking" from electrostatic precipitators, (2) in localities wherein high availability has been a demand of local air pollution control authorities, or (3) where plant operations have had a preference for fabric filters because of their inherent simplicity and consistent high efficiency, then fabric filters have been installed on kiln exhaust gases with a high degree of success.

---

*Typical sources of argillaceous materials are: clay, shale, slate, slag, silica, ashes, sand, and iron ore.

†Typical sources of calcareous materials are: limestone, sea shells, chalk, and marble.

The application of fabric filters in wet kilns does necessitate operating the baghouse dry. Therefore, special design features must be incorporated into the equipment in order to keep the recovered dust in a dry, free-flowing state and to minimize corrosion and wetting of the filter bags.

As a recognition to sound application engineering and good design, the following installation is cited as typical of many successful installations of fabric filters effectively handling wet kiln emission in the cement industry.

Figure 1 shows a typical wet kiln installation utilizing a fabric filter to control kiln emissions. The kiln is 3.05 m (10 ft) in diameter and 91.4 m (300 ft) long, and produces 324 tons (1,800 bbl) per day of clinker. A 14.6 m (48 ft) section of the feed end of the kiln contains chains that serve to preheat the feed. The slurry feed contains 35 to 40 percent water by weight. The kiln is gas-fired.

In 1965, a 10-compartment Wheelabrator baghouse was installed between the existing multicyclone and the existing kiln fan on the kiln described above. Operating details are as listed below:

Data	Metric Units	English Units
Gas Volume	70,688 m^3/hr	80,000 ACFM
Gas Temperature	254° C	490° F
Gas Dew Point	73° C	163° F
Dust Load	1.37-2.29 g/m^3	0.6-1.0 gr/ft^3
Dust Size	50-10% μm	50-10% μm
Pressure Drop	152.4 mm	6" WG
Efficiency	99.9%	99.9%

The baghouse is operating extremely well and is performing beyond expectations of the customer. The unit has been in service since the spring of 1965, and maintenance has been low. Bag life has been good, availability of the equipment has been excellent, and the efficiency has been consistently high. The stack discharge has been optically clear, enabling the plant to discharge the kiln gases 20 m (65.6 ft) above grade, eliminating the need and expense of a tall stack.

Dry Kiln

Of the 385 kilns in the United States, 171 are operating on dry process systems that represent 44 percent of the total kiln number. Even though the number is not as great as the number of wet-process kilns, the dry kilns remain a dominant factor in the American cement industry production because on a kiln-for-kiln basis, they are by far larger.

In addition, from the standpoint of air pollution control, a dual problem of higher dust loadings and higher resistivity necessitates the employment of large water conditioning towers ahead of the electrostatic precipitators when-

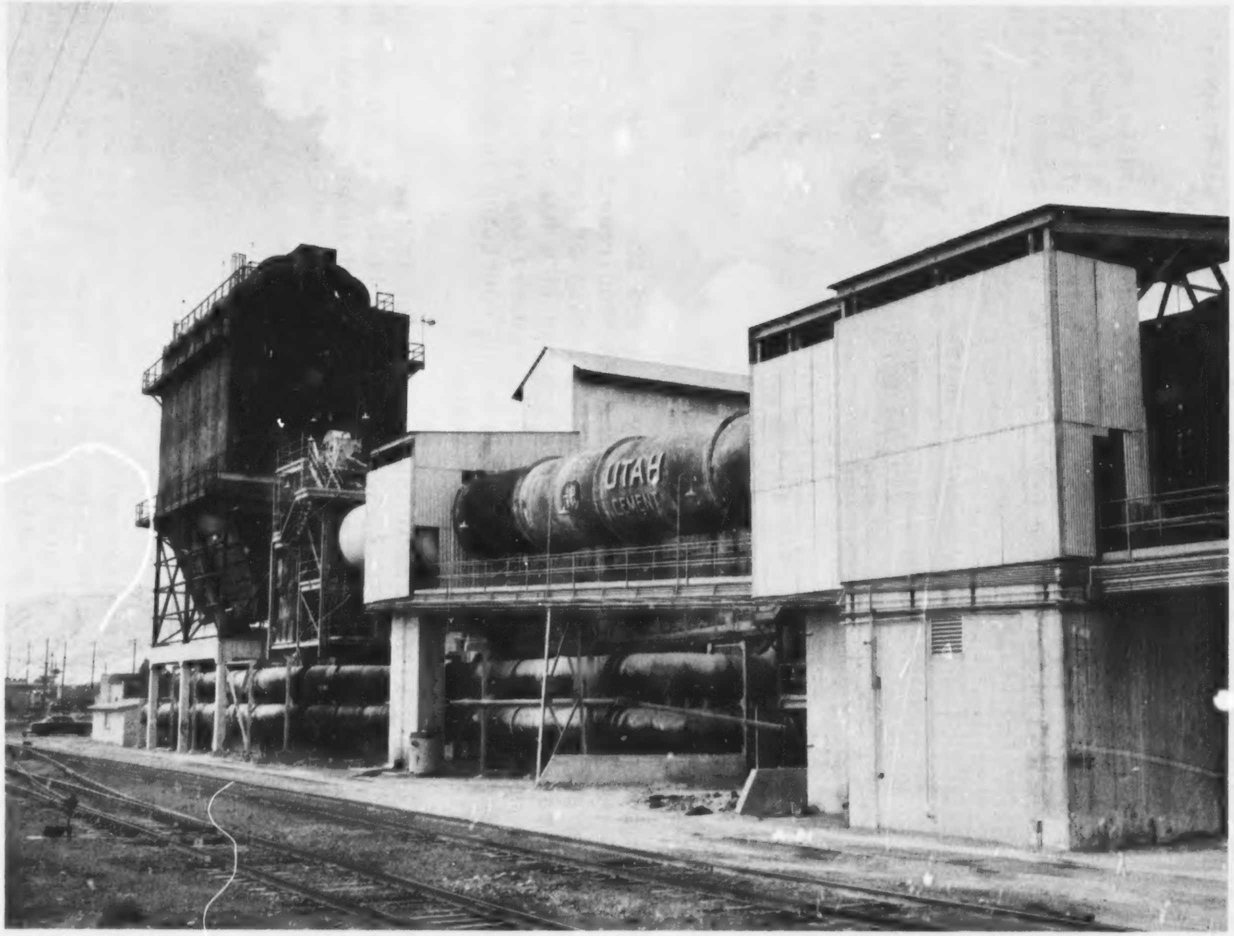
UTAH
CEMENT

Figure 1. Baghouse shown at left controlling emissions from a wet kiln.

ever high-efficiency electrostatic precipitators are specified for emission control. Of the many baghouse installations in the cement industry on dry kilns, a typical installation is represented in the photograph listed herein as figure 2.

This kiln has a nominal diameter of 4.9 and 5.3 m (16 and 17.5 ft), is 179.8 m (590 ft) long, and produces 1,620 tons (9,000 bbl) per day of clinker. The kiln is coal-fired and the exit gases are cooled by water sprays in the final section of the kiln.

In 1964, a 16-compartment Wheelabrator baghouse was installed immediately after the kiln and before the kiln fan. This approach was unique as it represented the first installation of a baghouse on kiln exit gases without a mechanical collector to serve as a precleaner for the baghouse. Operating details are as listed below:

Data	Metric Units	English Units
Gas Volume	249,788 m^3/hr	300,000 ACFM
Gas Temperature	288° C	550° F
Gas Dew Point	53° C	127° F
Dust Load	25.15 g/m^3	11 gr/ft^3
Dust Size	40-10% μm	40-10% μm
Pressure Drop	127 mm	5"
Cloth Baghouse Pressure Drop	222 mm	8.75"
Efficiency	99.9%	99.9%

This baghouse is operating extremely well and the unit has been in service since 1965. The stack discharge meets the EPA requirements of less than 0.15 kg of particulate matter per metric ton (dry basis) of feed (0.3 lb of particulate matter per ton of kiln feed). Average bag life has been 2 years. Recently, the operating temperature has been reduced to 274° C (525° F), resulting in bag life of 2-1/2 years. Previous operating temperature of 288° C (550° F) resulted in bag life of 1-1/2 years.

The usual rotary kiln is notoriously wasteful in fuel consumption, requiring upwards of 1,500 kcal/kg to 2,250 kcal/kg of clinker (1,000,000 Btu to 1,500,000 Btu per barrel of clinker), which has lead to many improvements in the conservation of heat. Heat transferred from the cooling of clinker is recovered as hot secondary combustion air, and the heat leaving the kiln can be used to preheat the incoming raw kiln feed.

Air Suspension Preheater

The air suspension preheater method of preheating the dry kiln feed with the kiln gases was developed in Europe and is known throughout the cement industry today as the Humboldt preheater kiln. The preheating system consists of a number of cyclones through which the kiln exit gases pass before reaching the final gas cleaning equipment. The dry raw feed is introduced into the top chamber and falls by gravity through four cyclones in series. Each cyclone is swept by hot ascending kiln gases countercurrent to the descending raw feed. The kiln gases leave the kiln at about 950° C (1,750° F), and, by direct transfer, the kiln feed is heated to 750° C (1,380° F) during its contact in the suspension kiln gas.

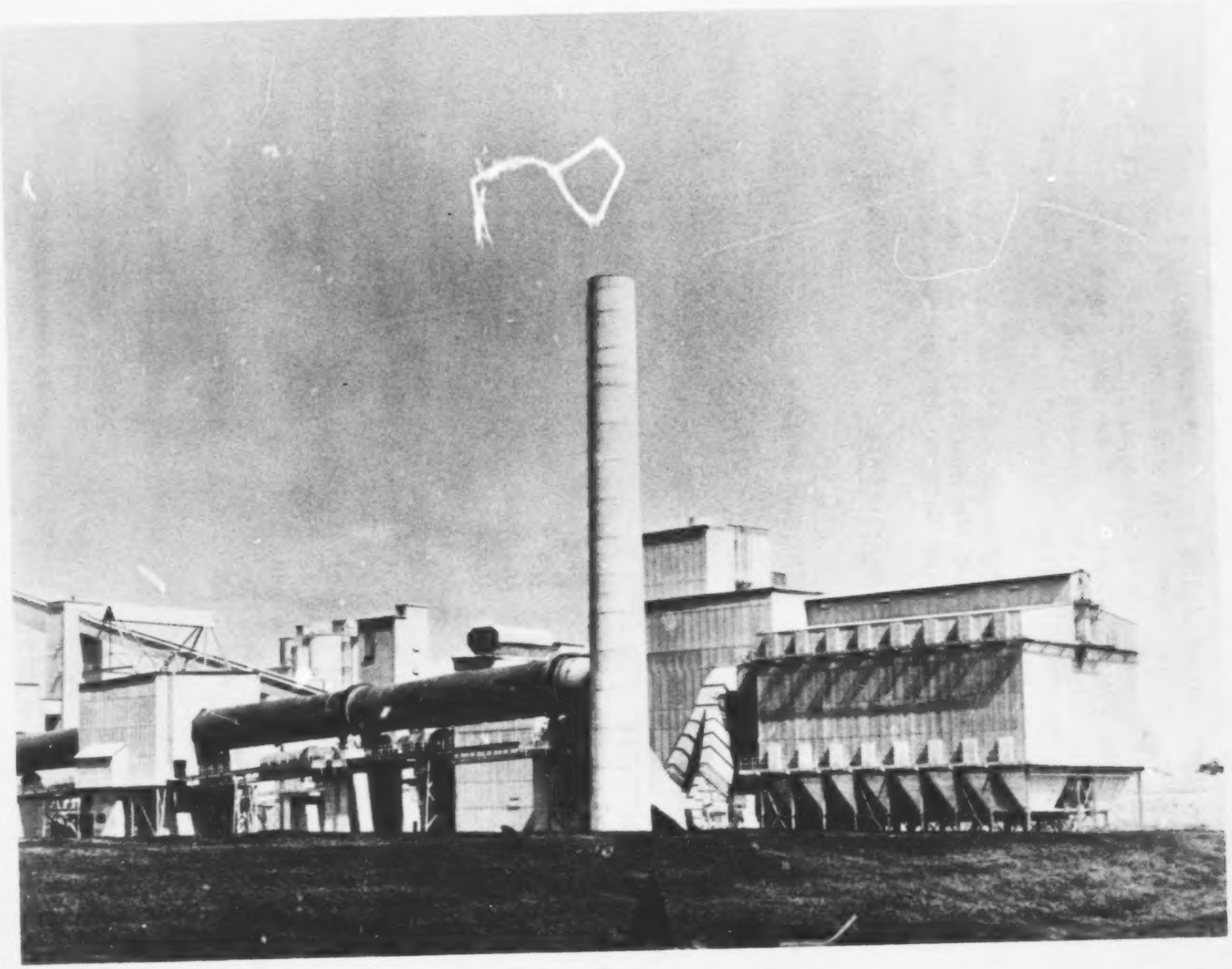

Figure 2. Baghouse shown at right controlling emissions from a dry kiln.

Preheater Kilns

A preheater kiln is a dry process kiln and a typical fabric filter installation handling the emissions from this type of dry kiln is shown in the photograph identified herein as figure 3.

This kiln produces 850 to 950 metric tons of clinker per day (4,722-5,000 bbl/day) from a raw dry feed of 2,100 to 2,200 tons/day. The kiln is 4 m in diameter and 56 m long, and is fired with Bunker oil containing 2.75 percent by weight. Flue gases exit the air suspension preheater and pass through the raw mill before entering the bag filter. There are times, however, when the kiln gases go directly to the bag filter whenever the raw mill is down for maintenance or because the raw mix silos are full.

In 1965, an 8-compartment Wheelabrator baghouse was installed following the final cyclone heater exchange and the raw mill. The process is shown in the flow chart shown in figure 4. The data on the process are as follows:

Data	Metric Units	English Units
Volume of gases passing through raw mill to bag filter	230,000 m^3/hr	136,000 ACFM
Volume of gas direct to bag filter	190,000 m^3/hr	112,000 ACFM
Temperature after heat exchange	330° C	626° F
Temperature after raw mill	200° C	392° F
Moisture by volume	3-6%	3-6%
Dewpoint at B/H inlet with gases passing through raw mill	43° C	109° F
Dewpoint at B/H inlet with gases bypassing raw mill	30° C	86° F
Dust load after raw mill	60 g/m^3	26 gr/ft^3
Size % less than 50 nm	85-95	85-95
Dust recovery	15 tons/hr	

Note: Automatic bypass for temperature surges above 260° C (500° F).

The operation of the baghouse serving this kiln has been outstanding, with the initial set of filter bags lasting 5 years, which has been generally beyond the expectation of both the manufacturer and the operators. Over the past 12 to 13 years, the availability of the fabric filter has been in excess of 99 percent, consistently producing filtration efficiencies of 99.9 percent by weight.

Kiln Emission Code

In considering a fabric filter to control emissions from cement kilns, it is necessary to include consideration of the air pollution code requirements in order to make an equitable economic decision in relationship to other means of control. The EPA Code states that no owner or operator shall cause to be discharged into the atmosphere from any kiln, any gases that:

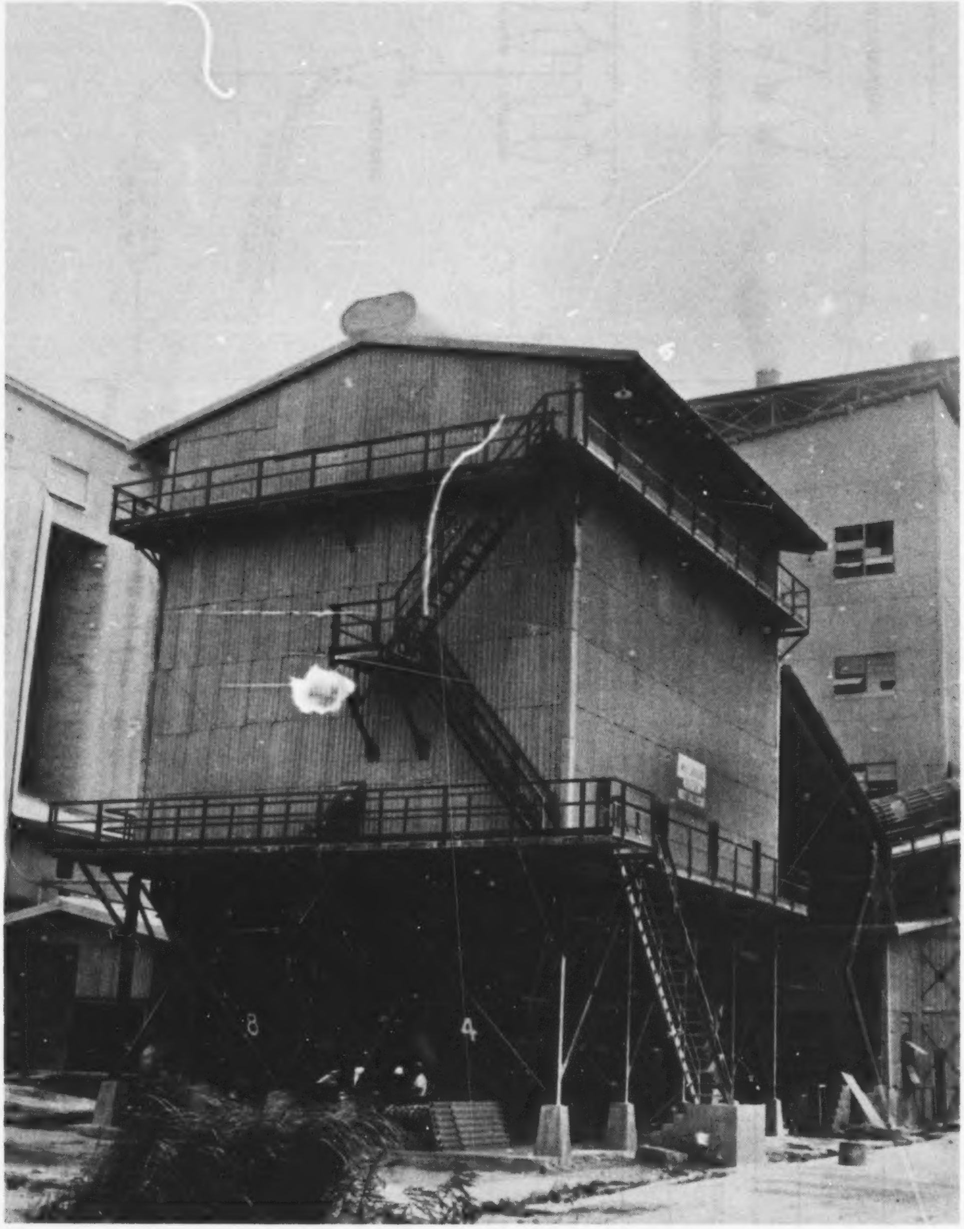

Figure 3. Baghouse controlling emissions from air preheater kiln. Flow diagram for this system is shown in Figure 4.

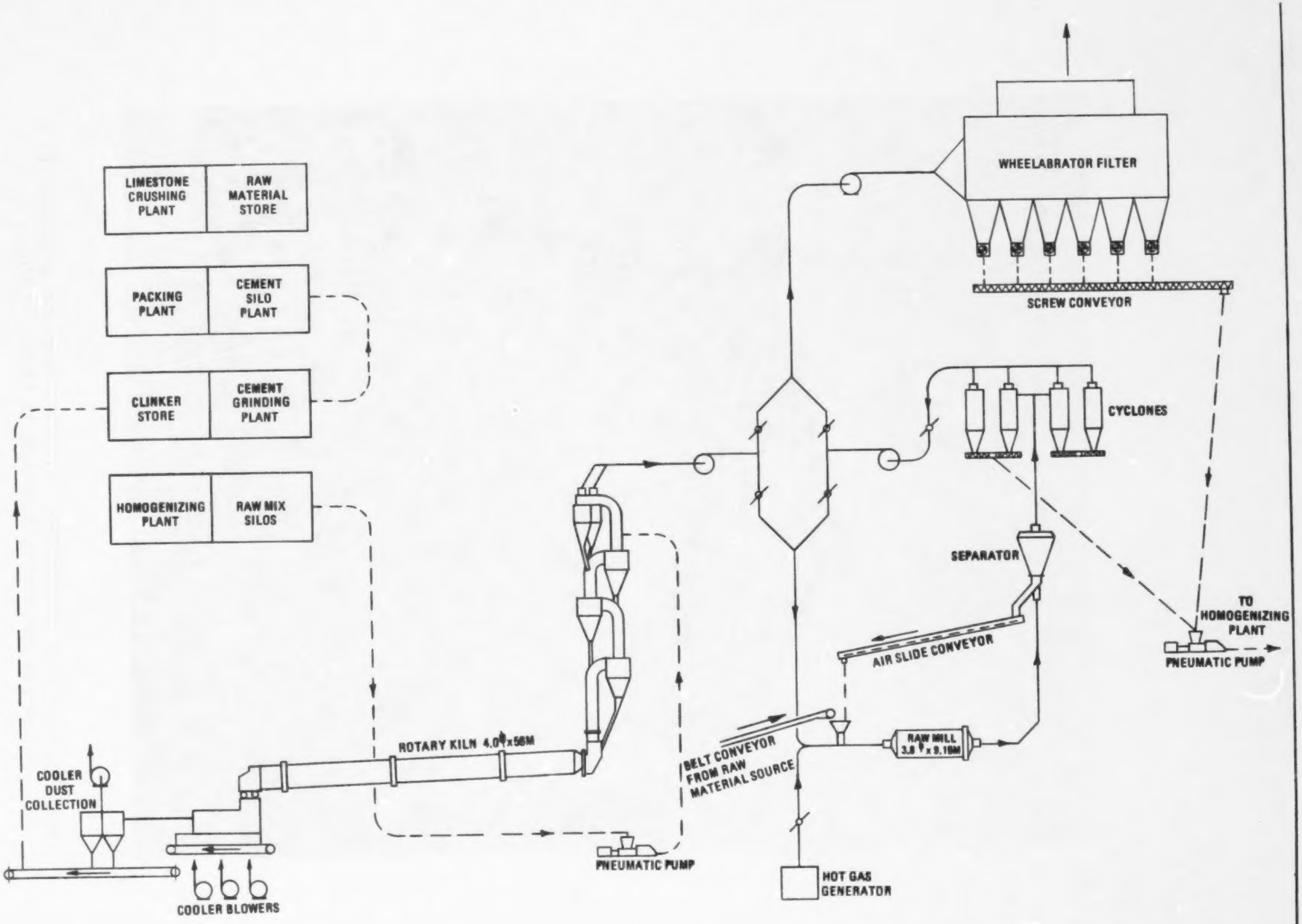
LIMESTONE CRUSHING PLANT
RAW MATERIAL STORE
PACKING PLANT
CEMENT SILO PLANT
CLINKER STORE
CEMENT GRINDING PLANT
HOMOGENIZING PLANT
RAW MIX SILOS
WHEELABRATOR FILTER
SCREW CONVEYOR
CYCLONES
SEPARATOR
TO HOMOGENIZING PLANT
PNEUMATIC PUMP
AIR SLIDE CONVEYOR
BELT CONVEYOR FROM RAW MATERIAL SOURCE
RAW MILL 3.8 ϕ x 9.16M
ROTARY KILN 4.0ϕx56M
COOLER DUST COLLECTION
COOLER BLOWERS
PNEUMATIC PUMP
HOT GAS GENERATOR

Figure 4. Flow sheet for air suspension air preheater kiln.

1. contain particulate matter in excess of 0.15 kg/metric ton of feed (dry basis) to the kiln (0.30 lb/ton), and/or

2. exhibit greater than 20 percent opacity.

Examination of the allowable limits on kiln mass rate of emissions equates to no more than 0.015 percent of the dry kiln feed that can be discharged into the atmosphere. By translating the maximum allowable emission rate to percent of kiln feed on a dry basis, you can readily make a comparison to the emission standards of other countries.

SUMMARY

Comparative analysis of allowable mass emissions from cement kiln gases in the United States to the governmental standards of other industrialized countries demonstrates the high standards and stringency of the US/EPA Code requirements. A code that restricts emissions from cement kilns to no more than 0.015 percent of the kiln feed rate is a stringent code. It is this stringency of the US/EPA requirements that explains the high percentage of fabric filters employed on cement kilns in the United States, as compared with the practice of the cement industry in other countries. The installations described herein demonstrate that the fabric filter properly designed, applied, installed, operated, and maintained can successfully handle the variables of this application and meet the US/EPA Code requirements within a reasonable factor of safety. When comparing the economics of a fabric filter versus an electrostatic precipitator, the selection must be decided on a case-by-case basis because of the number and range of the variables involved.

PART II-CLINKER COOLERS

Some 40 years ago, the cement industry developed the clinker cooler to improve the quality of the Portland cement process. By quenching the clinker with cooling air as the cooler leaves the kiln, the desired improved clinker is obtained. The heated quench air, in terms of quantity, represents some three times as much air as is needed for kiln combustion. This allows 33 percent of the heated quench air to be directed to the kiln as hot air for secondary combustion, and the remaining 66 percent of the quench air to be discharged to atmosphere. As the clinker is air quenched, the quenching air entrains particulate matter in the form of clinker dust, which uncontrolled would create an air pollution control problem.

A typical clinker cooler of the grate type is shown in figure 5. The cooler is designed to air quench 1,420 kg/min (3,130 lb/min) of clinker at 1,370° C to a temperature of 65° C (2,500° F to 150° F). To do this, 93.2 m^3/s at 32° C (197,420 ACFM at 90° F) is blown through a 38-cm thick (15 in) moving bed of clinker utilizing seven forced-draft fans. As stated above, a portion of the higher temperature quench air serves as preheated secondary combustion air. In the example shown in figure 5, 84.5 m^3/s at 760° C (179,000 ACFM at 1,405° F) of quench air is diverted to the kiln. A smaller quantity of quench air is diverted to the coal mill which, in this case, represents 11.3 m^3/s at 420° C (24,800 ACFM at 790° F). The balance of the quench air is vented to atmosphere, which totals 85 m^3/s at 154° C (180,000 ACFM at 310° F). This cooler handles a kiln having a daily clinker production of just over 2,000 metric tons. (12,350 bbl/day).

Cooler Upset Conditions

Within the burning zone of the kiln, a coating of kiln feed builds up on the surface of the refractory and serves as a dam for the feed lying upstream of the burning zone. Under normal operations, the feed spills over the "dam" and quickly forms into moderately sized clinker in the burning zone. In abnormal operations, the "dam" becomes excessive and, as this ring breaks, or is broken, excessive quantities flow through the burning zone uncalcined, and enter the grate cooler as fines. This condition is called a kiln "upset."

Figure 6 shows the gas flows and temperature conditions for the cooler under "upset" operating conditions. During kiln upset, the following conditions exist:

1. The discharge rate increases 50 percent from 1,420 kg/min to 2,136 kg/min (3,130 lb/min to 4,700 lb/min).

2. The clinker temperature from the kiln drops from 1,370° C to 1,200° C (2,500° F to 1,204° F).

3. The automatic controls maintain the same flow through the cooler grates, 93.2 m^3/s (197,420 ACFM).

4. The same weight of secondary combustion air is required and maintained for the kiln.

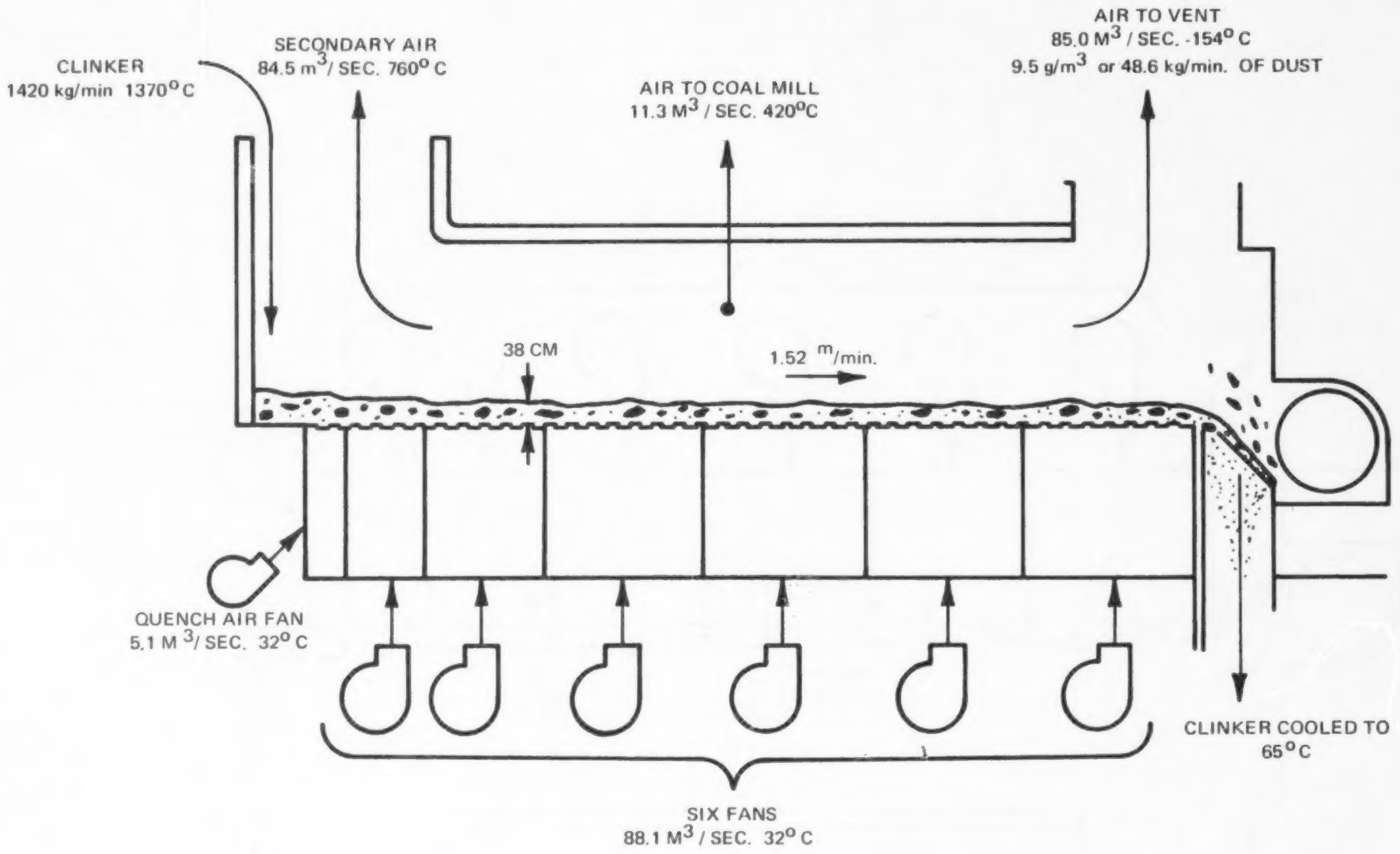
CLINKER
1420 kg/min 1370° C
SECONDARY AIR
84.5 m³/ SEC. 760° C
AIR TO COAL MILL
11.3 M³ / SEC. 420°C
AIR TO VENT
85.0 M³ / SEC. -154° C
9.5 g/m³ or 48.6 kg/min. OF DUST
38 CM
1.52 m/min.
QUENCH AIR FAN
5.1 M ³/ SEC. 32° C
CLINKER COOLED TO
65° C
SIX FANS
88.1 M³ / SEC. 32° C

Figure 5. Clinker cooler under design conditions.

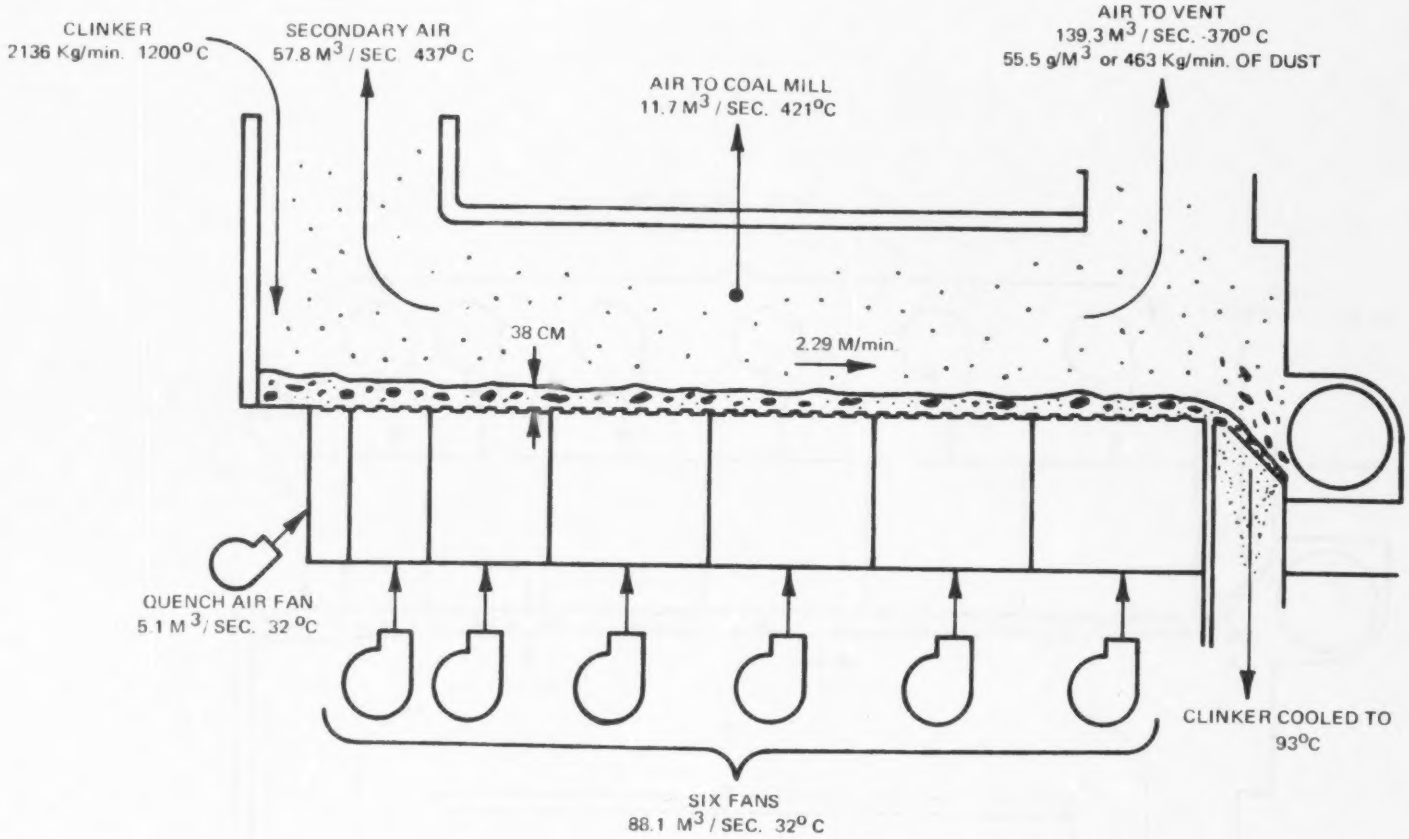
CLINKER
2136 Kg/min. 1200° C
SECONDARY AIR
57.8 M3 / SEC. 437° C
AIR TO COAL MILL
11.7 M3 / SEC. 421°C
AIR TO VENT
139.3 M3 / SEC. -370° C
55.5 g/M3 or 463 Kg/min. OF DUST
38 CM
2.29 M/min.
QUENCH AIR FAN
5.1 M3/ SEC. 32 °C
CLINKER COOLED TO
93°C
SIX FANS
88.1 M3 / SEC. 32° C

Figure 6. Clinker cooler during kiln upset conditions.

5. The same weight of air to the coal mill is required and is maintained.

6. The clinker dust emitted from the cooler is increased from 9.5 g/m^3 to 55.5 g/m^3 (4 gr per ACF to 25 gr per ACF).

7. The quench air out of cooler vent increases from 154° C to 370° C (310° F to 700° F), and

8. The clinker is cooled to only 93° C (200° F).

This upset condition results in a design requirement for the dust collector capacity of 139.3 m^3/s at 370° C (295,000 ACFM at 700° F), a 50 percent increase in gas volume and a tenfold increase in the dust loading.

In summary, based on the above, a clinker cooler pollution control system must handle the following range of conditions:

	Normal	Upset
Air volume	100%	150%
Dust Load	9.15-13.7 g/m^3 (4.6 gr/ft^3)	34.4-57.2 g/m^3 (15-25 gr/ft^3)
Temperature	204° C (400° F)	343° C - 538° C (650° F - 1,000° F)

Thermal Control

The application of a fabric filter makes thermal control of the heated quench air from the cooler vent necessary to prevent damage of the filter fabric during periods of gas temperature surges above design conditions. The design engineers can control these temperature surges by utilizing either: (1) evaporative water cooling, (2) tempering air, (3) blending or mixing of air from adjoining clinker coolers, (4) radiation cooling, or (5) a combination of these four methods. The temperature limitation of the filter fabric is 288° C (550° F) for fiberglass and 218° C (425° F) for Nomex.

Fabric Filters Using Fiberglass

Fabric filters utilizing siliconized fiberglass cloth cleaned by repressuring have proven to be successful in this application. Operating experience has shown that the clinker dust releases very readily from the cloth. The modular design has been used widely with some installations utilizing a single fan on each module, as shown in figure 7. The use of fiberglass minimizes air cooling requirements and, accordingly, is preferred by many of the plant operating personnel.

Fabric Filters Using Nomex

An alternate filter fabric to fiberglass is Nomex, which will handle temperatures up to 218° C (425° F) without damaging the fiber. Nomex is

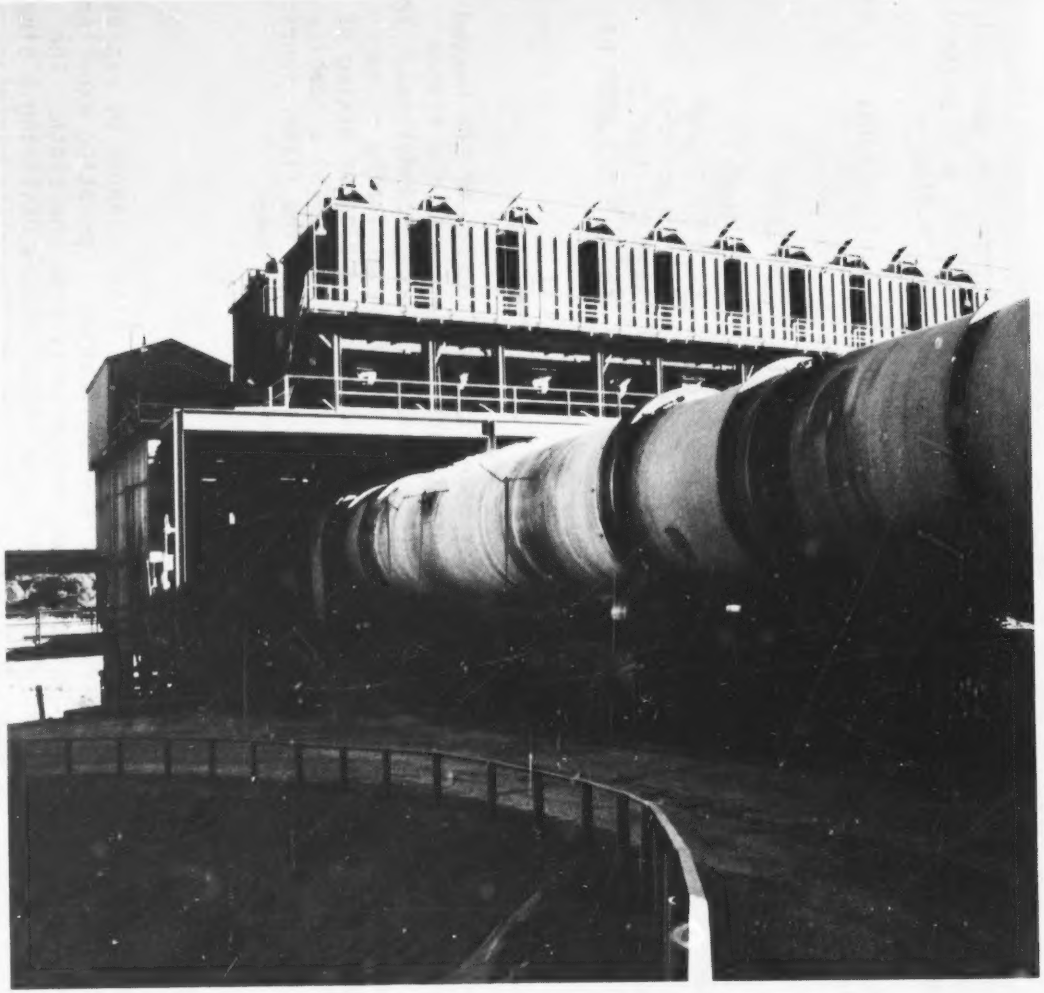

Figure 7. Modular Dustube fabric filter handling emission discharge from clinker coolers.

commonly utilized on fabric filters utilizing a "burst" or "explosion" of compressed air to flex the bag for cloth cleaning purposes. The application of the Ultra-Jet or Pulse-Jet design on clinker cooler emission has been quite common in the United States, with the initial installations dating back to 1965. A typical installation is shown in the photograph identified as figure 8. Because clinker dust is relatively coarse, and releases quite readily from the filter bags, sizing the unit has presented few difficulties. Again, the modular design has been preferred, enabling the plant operating personnel to isolate a single unit for maintenance without affecting continuity of the plant operation.

Inasmuch as the dust is abrasive, special care has been taken in the design of the ductwork and inlet to the units to avoid erosions of the steel and filter fabric. Also, the dust-handling equipment is of special heavy duty design to avoid erosion. Fans should, at all times, be located on the clean side of the filter to avoid erosion of the fan blades and scroll.

In order to meet this requirement, the cement industry in the United States has successfully applied fabric filter to clinker coolers after full evaluation of the economics involved. When properly sized, designed, applied, operated, and maintained, the tubular fabric filter has consistently met the Code requirements and has operated with a high degree of availability requiring minimal and easy maintenance.

Cooler Emission Code

The EPA Code states that no cement plant owner or operator shall cause to be discharged into the atmosphere from any clinker cooler any gases which:

a) contain particulate matter in excess of 0.050 kg/metric ton of feed (dry basis) to the kiln (0.10 lb/ton), and/or

b) exhibit 10 percent opacity, or greater.

The US/EPA Code for kiln emissions, as stated above, represents a stringent requirement for the cement plant operating personnel. However, the US/EPA Code for clinker cooler emissions is more stringent than for the kilns. The kiln allowable emission is up to 0.015 percent of the kiln feed. The cooler emissions are restricted to 0.005 percent of the kiln feed. When the cooler allowable figure is equated to mass rate emissions from the vent stack, the outlet particulate loading oftentimes cannot exceed 10 to 11 mg/m^3. This low outlet residual dust loading requires collection efficiencies of 99.9 percent by weight, which has been successfully achieved by the employment of fabric filters in the United States cement industry, as described within this paper.

SUMMARY

It is essential that the particulate emission control equipment be designed to meet EPA Code requirements during normal and upset operating conditions of the kiln. To do this, the thermal control and particulate control equipment must be designed to handle 50 percent increase in volume, 400 percent increase

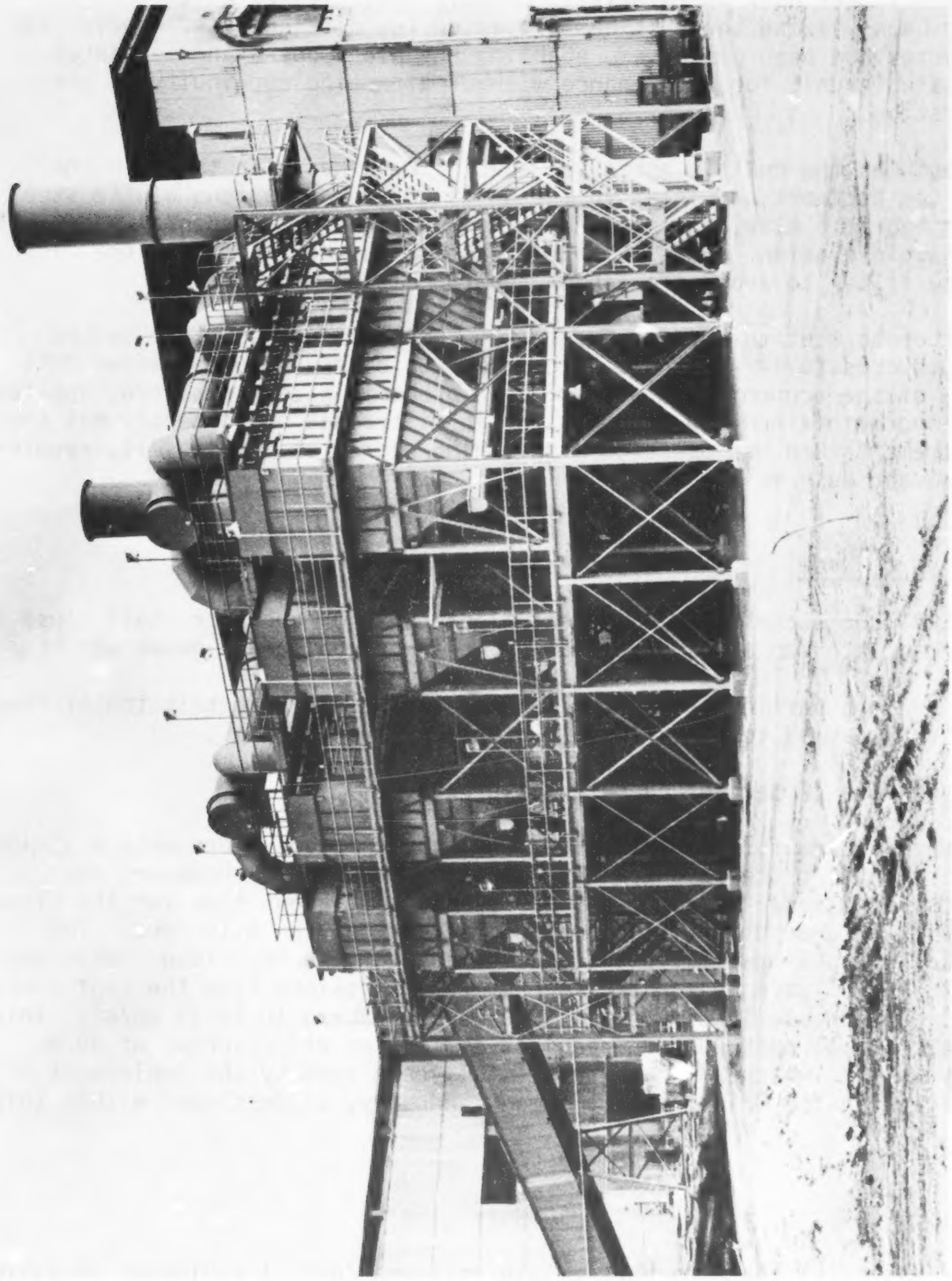

Figure 8. Ultra-Jet modular fabric filter handling emission from clinker coolers.

in dust load, and temperature surges up to 538° C from a 200° C base. The code requirements equate to outlet particulate loadings below a range from 50 to 25 mg/m^3. This low outlet residual dust loading requires collection efficiencies greater than 99.9 percent by weight. The fabric filter has been successfully and widely applied in the United States and Canada on clinker coolers to meet the total conditions of the cooler air pollution control problem and obtain the desired solution. The typical installations described herein demonstrate the viability of the fabric filter to handle the stringency of the U.S. code and the variable operating conditions created by the quench cooling process.

REMOVAL OF HARMFUL PARTICLES FROM THE EXHAUST OF THE CEMENT PLANTS*

G. I. Vodolazskiy

Abstract

At present more than 3,500 pollution control devices are in use throughout the cement industry. Of these, 1,000 are of the electrical type, approximately 1,000 are bag filters, and more than 1,500 are other types of dust collecting units (cyclones, scrubbers, etc.). Design solutions are examined in this report for new process lines for cement plants. Problems associated with rebuilding existing gas cleaning units are also considered. Data are given on the operating conditions of units in use and their cleaning efficiency in removing dust during raw materials processing, clinker calcining and milling, etc.

INTRODUCTION

Today more than 3,500 dust collectors are in service in the cement industry. This dust collecting equipment is represented by 1,000 electrostatic precipitators, about 1,000 bag filters, and by more than 1,500 devices of other types (cyclones, scrubbers, etc.). Every year the number of dust collectors in the cement industry increases by 80-100 units.

Owing to the great deal of development work accomplished in the last years, the value of harmful pollutants to the atmosphere has been reduced. As it is known, dust emissions worsen the sanitary conditions at the plants and in the adjacent areas. They also hasten service wear of the installations, making working conditions worse, and causing occupational diseases adversely affecting labor productivity.

DUST ABATEMENT AT THE RAW MATERIAL PROCESSING AREAS

The great influence on the dust collecting efficiency at the raw material processing areas has the rational technological developments directed to lowering the heights of material overfalls from the conveyors, reducing the sections of the hoppers and the angles of their slopes, and approaching the natural slope of the material in movement, arrangement of baffle plates, and rock cushions in the chutes. In connection with this, the speed of the belt conveyors must not exceed 0.7-1.0 m/s. Nonloaded belts of the conveyors should also be equipped with dust collecting devices.

The obligatory condition of dust collection at the raw material processing areas is the installation of airtight enclosures, their design and sizes, influencing greatly the dust collection efficiency. For the purpose of the dust abatement at all loading points, especially when handling loose material from the upper conveyor to the lower one, it is provided to install an enclosure with air exhaust, the lower enclosure being supplied with double walls. Such enclosures are also installed at the discharge openings of jaw, cone, and hammer crushers. The Institute of NIPIOTSTROM has designed such enclosures with double walls for conveyor transfer points of material and discharge openings of hammer crushers. The similar enclosures are designed by the Institute of NIIRUDVENTILYATSIYA.

---

*For further information regarding the material in this paper, please contact I. K. Reshidov, U.S.S.R. 113105, Moscow, M-105, 1-st Nagatinsky Pass., 6, NIIOGAZ.

Tests conducted at several enclosures with double walls in the crushing departments of the cement plant of "Pzoletariy" in Novorossisk showed that the volume of the aspiring air to be exhausted had been reduced by 1.5-2 times, with the dust content in it being lowered at 30-35 percent, compared with the single-walled enclosures.

According to the analyses, it was stated that about 150-200 m^3 of aspiring air should be exhausted from all the enclosures of the crushing department when processing 1 ton of material.

The dust content of the aspiring air depends not only on physical and chemical properties of the material to be treated, but especially on its humidity. For example, the department for dolomite crushing of the Vitebsk group of enterprises of limestone flour (capacity 3 million t/yr) does not require exhausting because of high moisture content in the raw material, amounting to 8-10 percent.

One of the most important means of dust suppression is wetting the material. Dust content in the aspiring air can be reduced several times by installing sprayers in the enclosures of the places generating dust and by the optimal wetting of the rock. As a result of this, at some plants in southern regions, it turned out to be possible to employ a simplified method of dust collection, consisting of the installation of a hydrosuppression system as the first stage of dust collection, and cyclones as the second stage.

However, the majority of works do not have these highly efficient exhaust systems for crushing departments. In this case, the increase of collection efficiency is attained by means of the wet method of dedusting the aspiring air as well as the dry one.

At the wet process cement plants it is appropriate to utilize the wastes from wet-type systems of dust control by means of feeding them for preparing raw mix. This is the reason for giving preference to the wet-type system of dust control at the crushing departments. Some difficulties and additional expenses connected with the employment of wet dust collectors in the winter time are justified by a simplicity of their design and their efficiency.

Hydrodynamic dust collectors, GDP type, with capacities from 20,000, 30,000 and 50,000 m^3/hr, designed by NIPIOTSTROM, and apparatuses, PVM type, designed by NIISANTECHNIKA, are widely employed by a wet method of dust collection.

For a dry method of dedusting the aspiring air of crushing departments, gravel bed filters type ZF-4, ZF-5, ZF-6 with capacities of 1,500, 4,000, and 5,000 m^3/hr, respectively, are used. The specific capital costs by employment of the gravel bed filters will make up 1.2-1.5 rubles for 1 m^3/hr, collecting efficiency being 98-99 percent.

KILN DUST COLLECTING EQUIPMENT

Reduction of rotary kiln dust emissions is the main task in a general problem of dust collection at the cement plants. All the new present-day operation lines are designed and put into service equipped with standardized 4-field type electrostatic precipitators, typical design data being 1-1.2 m/s gas velocity, 8-10 s retention time. The electrostatic precipitators meet all the requirements of industry and sanitary standards having inlet dust burdens not amounting the optimal values in the range of 10-15 g/m^3.

However, the available electrostatic precipitators 1-, 2-, and 3-fold got completely overburdened with gas and dust as well.

After analyzing the condition of dust collection equipment for dedusting exhausts from the kilns for clinker burning, it was revealed that the dust losses from the kilns were considerably influenced by performance conditions of these kilns.

Dust content at the outlet of kilns of the same type, processing the same raw material at the same plant, may vary greatly depending on conditions of in-kiln preheating devices. Application of the optimal chains allows attainment of dust content at the outlet of the kiln from 2.5-10 g/m^3. This is one of the ways to considerably improve the process of dedusting rotary kiln exhausts. The second way consists of raising the capacity of dust collecting systems by increasing dimensions (volumes) of electrostatic precipitators. So it is known that in order to increase an electrostatic precipitator efficiency from 95 to 99 percent, it is necessary to raise the specific volume (1 m^3 of an electrostatic precipitator per 1,000 m^3 of gas rate per hour) two times, on the average. In the practice of cement manufacture, such a situation takes place when burning mechanisms are intensified, their kilns upgraded, and their capacity raised, causing the amount of gases to be cleaned to be increased. As a result of this fundamental renovation of available operating electrostatic precipitators, it is obligatory to clean the increased volumes of gas. The latter factor entails some difficulties, as successful renovation usually causes complete disassembly of an old unit and installation of a new one.

The most appropriate way to improve the efficiency of the filters, applicable for control of emissions from rotary kilns, can be achieved by keeping in service the available electrostatic precipitators and installation of additional filters with multiple or series connections to the operating units. Design studies show that in most cases, such solutions are quite possible and expedient. This is one of the ways of improving dust collecting systems for control of kiln exhausts.

When choosing one of two possible alternative methods of installation of additional electrostatic precipitators, parallel or series connection, one should show a preference to series connection. There are good reasons for such a choice, as the kiln dust contains 40-50 percent of fine particles of about 5 microns or less in diameter. Therefore, to promote dust coagulation and efficient collection of this dust, it is necessary to lengthen a particle path of movement in the electric field. According to the results of tests, the series connection of additional electrostatic precipitators resulted in reduction of a residual dust burden at 3-5 times, compared with multiple connection. So, by series installation, the outlet dust burden was 50 mg/m^3

at a gas velocity in the electrostatic precipitators in the range of 1.2-1.5 m/s. By multiple connection of the same filters, the velocity reduced to 0.5-0.6 m/s, and the dust burden increased up to 150-200 mg/m^3.

One of the alternatives of the installation of additional electrostatic precipitators has been developed for the cement plant of "Proletariy." The specific capital costs by such design solution made up 1.5-2.0 rubles/m^3/hr. But the same costs totalled 2-2.5 rubles/m^3/hr by the installation of electrostatic precipitators without using existing filters.

The additional installation of electrostatic precipitators should be effected parallel with modernization of the existing units, mainly due to gas distribution devices, replacement of electrode systems, improvement of conveyor systems, and more perfect convertor sets for energy supply.

During the last 5-6 years in the cement industry, the equipment of step-up rectifiers substations of electrostatic precipitators has been completely renovated. More perfect semiconductor sets have been installed at all the plants. Automation of all these sets has been carried out due to the introduction into production of about 1,500 controllers of "Tsemes," designed by NIPIOTSTROM. Since 1974, serial production of sets of type ATF has been started and sets are being designed by some institutes and companies with the participation of NIPIOTSTROM. Now these devices (capacity of 250-1, 600 ma) are being produced by Kuybishev Electroworks in Moscow. A distinctive property of these sets is that they have a thyrister controlling device and a system of automatic voltage regulation respecting the intensity of sparking in the electrostatic precipitators.

To ensure that the electrostatic precipitators operate more efficiently, it is important to properly prepare the aerosol before processing. This procedure is being introduced at some dry process kilns. According to the results of tests conducted in May 1974, irreversible dust losses from the kilns of the Katav-Ivanovsky Cement Plant were reduced five times by a conditioning system developed by GIPROCEMENT and the Institute of NIPIOTSTROM.

Dust control of emissions from the kilns requires the installation of dust collectors at cooler vents and at the transfer points of clinker handling. Taking into consideration physical and chemical properties of kilns for clinker burning (high abrasion, high electric resistance), it is most advisable in this case to use filters with filtering media consisting of spherical grains or grains of some other form. For this reason, some pilot designs of filters, types ZF-7 and ZF-8, have been developed. There are plans to test the units as soon as possible.

DUST CONTROL OF MILLING EQUIPMENT

New cement mills and dry mills are designed and put into operation equipped with a 3-stage system of dust precipitation. The system consists of a so-called aspiring shaft, cyclones, and bag filters or electrostatic precipitators. However, most of the existing milling units have no such system.

As a result of this factor, a high inlet dust burden creates unfavorable conditions for operation of electrostatic precipitators and bag filters. This leads to an average dust burden at the inlet of the filters applicable for control of emissions from the mills of up to 50 g/Nm^3.

Hence, the intensification of control of dust emissions from milling equipment should be effected in two ways. In the first place, it is necessary to equip all the milling plants with a 3-stage system. This measure does not require high capital costs, and it can be realized during medium repairs and major overhauls. The great advantages of the application of the above-mentioned developments are confirmed by the results achieved at the mills of the Dushanbe Cement Plant, at the "Proletariy" and "Oktyabr" plants, and other plants where the inlet dust content in the aspiring air before filters was reduced by 2-5 times.

The second stage of improvement of dust collecting systems in milling plants consists of gradual renovation of obsolete equipment, and especially, its replacement by modern equipment. It is first of all the installation of electrostatic precipitators--type UG, bag filters, type SMTS, and other devices.

CONTROL OF DUST EMISSIONS FROM THE SECONDARY SOURCES OF AIR POLLUTION

The level of equipment for the secondary sources of air pollution (cement silos, clinker storages, stations of cement loading to the road, and railway transport) with dust collectors is still low.

Proceeding from the specific character of the secondary sources of air pollution, it is necessary to create simple and highly reliable filters. Cement silos, for example, may be equipped with frameless pressure bag filters without cleaning devices and dust handling facilities. However, such filters require high housings on the silos, which raises the cost of construction, and besides, it cannot be realized at the conditions of the operating works.

The main dust collecting plants of the above-mentioned sources of pollution are bag filters and cyclones. In order to make easier the maintenance work of bag filters for dedusting the aspiring air of silos, it has been proposed for some developments to be made to install the filters at the levels close to the ground. Application of bag filters, type SMTS, allows location in the space between modules of silo bins and also creates the possibility of cutting down the volume of construction work and improving maintenance and operating conditions.

An indispensable condition of cleaning the dust-laden air at the cement loading points is introduction of the appropriate units for ensuring mechanization of the operations parallel with large scale measures of dust control. Taking into consideration the value of dust losses from drying drums, it is necessary to install not less than a 2-stage system of gas cleaning, that is, cyclones and electrostatic precipitators. Dust control at clinker storages is provided by construction silos. The possibilities of dust collection at clinker storages provided with grab-bucket cranes practically comes to dedusting the points of material discharge to the storage. For this purpose, special dust collection chambers are installed. The high efficiency of these units was confirmed in the process of their operating at a lot of cement plants.

Taking into account the experience of maintenance of the existing pneumatic systems of dust elimination (Urals Aluminum Plant, Serovsky Plant of Ferroalloys, Serbryakovsky Cement Plant, and other plants), there have been elaborate designs of central systems for the elimination of secondary dust from some industrial enterprises. As boosters, vacuum watering pumps, type RMK, and sometimes ejectors or double fans are provided for. Cyclones, GTS, and vacuum bag filters are usually employed for collection. Such systems of dust elimination are successfully applied at Novosibirsk Thermal Station-3 and Barabinsk and Belovsk Hydroelectric Stations.

MAINTENANCE OF DUST COLLECTION PLANTS

The great importance in ensuring efficient performance of equipment and raising the engineering level of its maintenance has resulted in the establishment of a special service on dust control.

Controls for efficient work of dust collecting units affect sanitary laboratories of industrial enterprises of the Ministry of Building Materials of the U.S.S.R. As a result of this design, standards have been established for operation of dust collecting plants.

The estimation of the degree of dedusting exhaust gases and dust-laden air arising in the cement making process is effected by checking whether the level of gas cleaning meets the requirements of the health standards that specify the maximum permissible dust concentrations and the content of other harmful pollutants in the nearby layers of the atmosphere and in the working places. While designing a dust collecting plant, this factor is determined by means of special calculations.

Fulfillment of the projected technical measures and strict compliance with all the laws on environmental protection by collectives of enterprises will promote a successful solution of the problem of air pollution control.

EMISSION STANDARDS AND BACKGROUND DOCUMENT ON CONTROL TECHNOLOGY IN THE CEMENT INDUSTRY IN THE U.S.A.

Gary McCutchen,* George E. Weant, III,† and George Walsh*

Abstract

Historically, the Portland cement industry has contributed significantly to local air pollution problems. This paper summarizes the control techniques, emission standards, and compliance with the standards for particulate emissions from Portland cement plants.

New source Performance Standards have been established for kilns and clinker coolers (viz, 0.15 and 0.05 kg/metric ton of feed to the kiln, respectively). Opacity standards have also been applied to kilns (20 percent), clinker coolers (10 percent), and other equipment (10 percent). In a landmark decision, the United States Court of Appeals for the District of Columbia Circuit has upheld the use of opacity standards.

Control devices used on the kilns and clinker coolers have consisted mainly of baghouses and electrostatic precipitators. Baghouses are the most effective. However, at least one scrubber is being successfully used to control particulates from a clinker cooler.

A 1976 unpublished study by EPA examined compliance data collected from EPA regional offices and showed that nearly every facility with adequate control equipment was in compliance with the NSPS's.

INTRODUCTION

Portland cement is produced by sintering calcium carbonate and aluminum silicates to produce a nodule known as a clinker. The clinker is then pulverized and mixed with small amounts of gypsum to form Portland cement. In 1974, 79.5×10^6 short tons of Portland cement, with a value in excess of $2 billion, were produced in the United States. (ref. 1) The largest production districts were in the States of California, Pennsylvania, and Texas.

PROCESSES

The process for producing cement has undergone little modification over the past 2 decades. Limestone from the quarry is introduced into the primary crusher. The secondary crusher further reduces the size. The material then passes to storage silos from which it is proportionally blended with the other raw materials.

---

*United States Environmental Protection Agency, Emissions Standards and Engineering Division, Durham, North Carolina

†Research Triangle Institute, Research Triangle Park, North Carolina

From this point there are two types of cement processes; the dry and the wet. In the former, the mixed material is passed through a dry grinding circuit. A special predryer is used in some cases. In the wet process, the materials are ground with water to form a slurry.

The dry or wet material is fed to a rotary kiln where the clinker is formed. The clinker is removed from the kiln and cooled. The cooled clinker is then mixed with gypsum, sent to the final grinding mill, and then to storage silos.

Perhaps the most important process modification to be implemented in recent years involves the use of suspension preheaters for dry-process operations. (ref. 2) The preheaters utilize a series of gravity-flow cyclones and ducts that provide direct-contact heat transfer between the falling materials and the rising, hot kiln gases. Thus, the temperature of the kiln feed is raised and the required heat-transfer load of the kiln is reduced. The result is that either a shorter kiln is required for the same throughput, or a larger throughput is possible with the same, existing kiln. A shorter kiln means both less energy use and less pollution.

EMISSION POINTS

Emission points within the production process are numerous. The kiln and the clinker cooler receive the most attention. Others include the grinding mill circuits; storage facilities for raw materials, clinker, and product; conveyors; transfer points; bagging operations; and bulk loading and unloading facilities. (ref. 3) Uncontrolled emissions can exceed 150 kg/metric ton of cement (300 lb/ton). In addition, emission of NO_x and SO_x are estimated at 1.3 and 10.9 kg/metric ton, respectively (2.6 and 21.7 lb/ton, respectively). (ref. 4)

EMISSION STANDARDS

Because of the highly visible nature of the particulate emissions and the severe local problems associated with these emissions, the industry was one of the first to have standards applied. Existing plants are regulated by State and local standards, while new and modified plants are regulated by Federal New Source Performance Standards (NSPS).

One of the top producing States is Pennsylvania, where the particulate emission standard is based on process weight rates. This standard allows particulate emissions of 0.69 kg/metric ton (1.37 lb/ton) of cement or 1.10 kg/metric ton (2.20 lb/ton) of feed to the kiln for an average size kiln of 23.4 metric tons/hr (25.8 tons/hr). This is equivalent to 99.5 percent control.

On December 23, 1971, NSPS for particulates were promulgated for Portland cement plants, based on standards proposed in August 1971. (refs. 3,5) These standards were 0.15 and 0.10 kg/metric ton of feed to the kiln for kilns and clinker coolers, respectively. The emission test methods to be employed were also described. In addition, opacity standards of 10 percent were prescribed for kilns, clinker coolers, and other sources.

Table 1. Stages in the Development of New Source Performance Standards for Portland Cement Plants

	Proposed August 1971		Promulgated December 1971		Revised and Upheld November 1974	
Source	Emission (kg/metric ton)	Opacity (%)	Emission (kg/metric ton)	Opacity (%)	Emission (kg/metric ton)	Opacity (%)
Kiln	0.15	10	0.15	10	0.15	20
Clinker Cooler	0.10	5*	0.05	10	0.15	10
Other	----	5*	----	10	----	10

*Proposed standard reads "Visible emissions shall not be released to the atmosphere." (pg. 28, reference 2). Under the paragraph on particulate matter from other equipment it says, "For the purposes of this standard, visible emissions are considered to be any emission of greater than 5 percent opacity...."

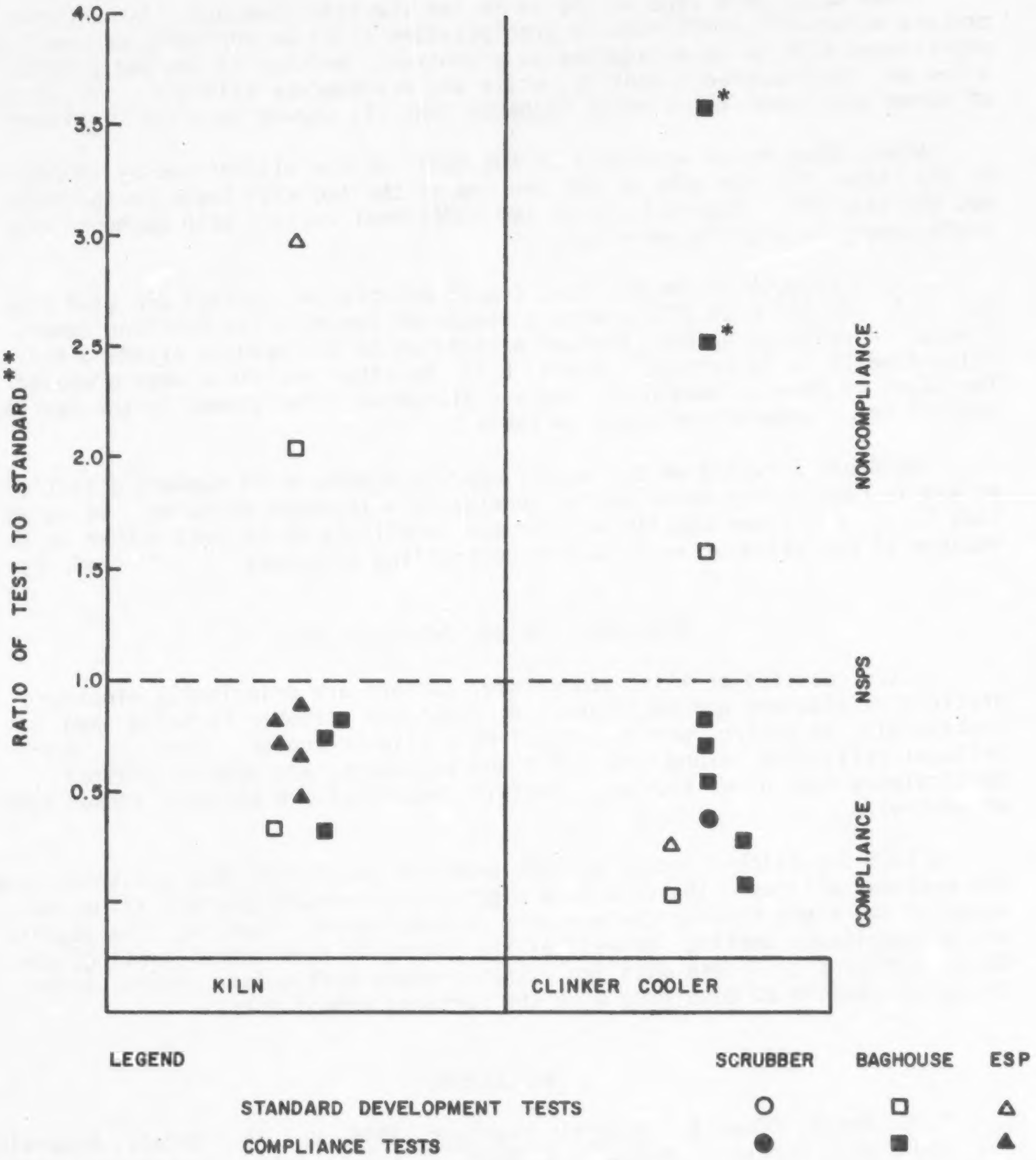

*** SAME FACILITY - LOWER RESULT OBTAINED AFTER BAGHOUSE ADJUSTMENT.**

**** FOR EXAMPLE, A RATIO OF 1.0 INDICATES THAT THE FACILITY EXACTLY MET THE NSPS AND A RATIO OF 0.5 INDICATES THAT THE EMISSIONS ARE 1/2 THE AMOUNT ALLOWED BY THE STANDARD.**

Figure 1. Results of compliance and standards development tests.

Three tests were used as the basis for the kiln standard: two on wet-process kilns with electrostatic precipitators (ESP) as controls, and one on a dry-process kiln using a baghouse as a control. Neither of the wet-process kilns met the proposed standards, while the dry-process kiln did. Inspections of three additional kilns using baghouse controls showed no visible emissions.

Also, three tests were used as the basis of the clinker-cooler standard. Of the three, the one with an ESP and one of the two with baghouse controls met the standard. Observations at two additional coolers with baghouse controls showed no visible emissions.

A suit brought by the Portland Cement Association against EPA (158 U.S. App. D.C. 308,486 F.2d 375) sought a review of the NSPS for Portland cement plants. A response by EPA proposed a revision in the opacity standard for kilns from 10 to 20 percent. (refs. 6,7) No other revisions were proposed. The Court of Appeals upheld the revised standards. The stages in the development of the standards are shown in table 1.

The Court's ruling on the use of opacity standards to measure pollution or aid in controlling emissions is considered a landmark decision. It ruled that ". . . (3) plume opacity was not too unreliable to be used either as a measure of pollution or as an aid in controlling emissions . . ." (ref. 8)

EMISSIONS CONTROL AND COMPLIANCE

Control devices on kilns and clinker coolers are principally electrostatic precipitators and baghouses. At least one scrubber is being used successfully to control particulates from a clinker cooler. (ref. 9) Centrifugal collectors, along with ESP's and baghouses, are used to control particulates from other sources. Overall, baghouses are the most common type of control.

A 1976 unpublished report by ESED examined compliance data collected from EPA regional offices. The data from eight plants showed that all kilns and seven of the eight clinker coolers were in compliance. (ref. 9) The results of the compliance testing, as well as the standards development testing, are shown in figure 1. These data imply that present particulate control technology is capable of complying with the Portland cement NSPS.

REFERENCES

1. B. C. Brown, "Cement," Minerals Yearbook, 1974, Vol. 1 - Metals, Minerals, and Fuels, Bureau of Mines, U.S. Dept. of the Interior, Washington, 1976.

2. N. R. Iammaitino, "Cements' Changing Scene," News Features, Chemical Engineering, June 24, 1974, pp. 102-106.

3. Office of Air Programs, "Background Information for Proposed New Source Performance Standards: Steam Generators, Incinerators, Portland Cement Plants, Nitric Acid Plants, and Sulfuric Acid Plants," Tech Report No. APTD-0711, U.S. EPA, August 1971.

4. T. G. Hopper and W. A. Marrone, "Impact of New Source Performance Standards on 1985 National Emissions From Stationary Sources," U.S. EPA 450/3-76-017, in print.

5. Federal Register, Vol. 36, No. 247, Part II, December 23, 1971.

6. Emissions Standards and Engineering Division, "EPA Response to Remand Ordered by U.S. Court of Appeals for the District of Columbia in Portland Cement Association V. Ruckelshaus (486 F.2d 375, June 29, 1973)," U.S. EPA 450/2-74-023, November 1974.

7. Federal Register, Vol. 39, No. 219 (November 12, 1974).

8. District of Columbia Circuit Court, "Portland Cement Association V. Russell E. Train," U.S. Court of Appeals, 158 U.S. App. D.C. 308, 486 F.2d 375, decided May 22, 1975.

9. Ed McCarley, EPA, ESED, Durham, N. C., June 20, 1977, personal communication.

STATE-OF-ART SURVEY OF MIST ELIMINATION IN THE U.S.A.

Seymour Calvert*

Abstract

Mist or drop entrainment is generated by most types of gas scrubbers and must be removed from the gas. Mist eliminators, or entrainment separators, are incorporated into the scrubber body or in vessels downstream from the scrubber. Major types in use are cyclones, radial baffles, zigzag baffles, flow directional change, beds of massive packing, beds of fibrous packing, and tube banks. Primary drop collection efficiencies for several types are given in the form of an A.P.T. cut/power plot. Reentrainment sets the upper limits on gas and liquid flow capacity. Solids deposition is discussed and a quantitative relationship for predicting suspended solid deposition rate is given.

This paper is a review of the state-of-the-art of mist elimination for scrubbers. Mist eliminators or entrainment separators are generally necessary to prevent undesirable rates of liquid drop emission from the scrubber. An unfortunate consequence of the achievement of thorough and vigorous liquid-gas contacting in the scrubber is that some of the liquid is atomized and carried out of the scrubber (entrained) by the gas that has been cleaned.

The liquid entrainment or mist, as it is commonly referred to, will generally contain both suspended and dissolved solids. Entrainment drops can cause corrosion, erosion, and mechanical failure of the fan blades or housing. Liquid or residual solid entrainment can also be deposited in the ductwork, heat exchange surfaces, and smokestack and cause eventual plugging and/or corrosion. It can cause problems in the area immediately surrounding the point of emission due to "rain-out" of liquid drops.

Stack emissions in the atmosphere will include the solid residues of the dried entrainment drops. The particulate composition can be quite different than that entering the scrubber, especially where reactive solutions or slurries are used for gas scrubbing. Thus, a bizarre consequence of excessive entrainment from a scrubber system can be that more pollutant is emitted either in total or within a certain size range than entered the scrubber.

In many cases excessive entrainment imposes a limitation on the capacity of the scrubber. That is, while the scrubber itself might be capable of handling a larger gas flow rate, the rate at which entrainment is considered excessive will dictate a limit on gas flow rate.

---

*Air Pollution Technology, Inc., San Diego, California 92117

GENERAL PRINCIPLES

The flow rate and drop size distribution of the entrainment will depend greatly on the nature of the gas-liquid contacting within the scrubber. The drops entrained from the scrubber contacting zone may be separated from the gas by a number of mechanisms, the most important of which will be discussed below. The initial collection of the drops is referred to as "primary collection" and the main mechanisms for this are as follow:

1. Sedimentation due to gravitational force.
2. Centrifugal deposition caused by changes in the main gas flow direction.
3. Inertial impaction upon collection bodies placed in the flowing gas stream.

After the liquid drops have been collected, they will coalesce into a sheet of liquid, unless the velocity of impact is so high that some of the drops shatter. In a properly designed and operated entrainment separator, the liquid should drain out of the entrainment separator. The capacity of the entrainment separator is limited by the reentrainment and/or flooding that will occur when the gas velocity is too high. The mechanisms by which reentrainment and flooding occur are as follow:

1. Liquid holdup in the separator increases, the cross-sectional area for gas flow decreases, and the resulting aerodynamic forces cause massive bodies of liquid to be blown out.
2. At high gas flow rates, the aerodynamic drag forces can cause tearing of liquid from the films flowing downward in the entrainment separator.
3. Drops may shatter due to collision with one another or with solid bodies and form smaller drops that are carried out by the gas.

The deposition of solids within the entrainment separator can be a major source of difficulties. The most important mechanisms by which this occurs are as follow:

1. Settling to nonvertical surfaces.
2. Deposition by inertial impaction caused by changes in liquid flow direction and turbulence.
3. Liquid loss from slurry on the entrainment separator surface leaves a residue of solid particles.
4. Precipitation of dissolved solids.

APPARATUS TYPES

The apparatus used for entrainment separation can be described in general terms as shown in the categorical list below:

A. Gravitational sedimentation

    1. Within the scrubber and its outlet ducting, sedimentation is always active and important.

GENERAL PRINCIPLES

The flow rate and drop size distribution of the entrainment will depend greatly on the nature of the gas-liquid contacting within the scrubber. The drops entrained from the scrubber contacting zone may be separated from the gas by a number of mechanisms, the most important of which will be discussed below. The initial collection of the drops is referred to as "primary collection" and the main mechanisms for this are as follow:

1. Sedimentation due to gravitational force.
2. Centrifugal deposition caused by changes in the main gas flow direction.
3. Inertial impaction upon collection bodies placed in the flowing gas stream.

After the liquid drops have been collected, they will coalesce into a sheet of liquid, unless the velocity of impact is so high that some of the drops shatter. In a properly designed and operated entrainment separator, the liquid should drain out of the entrainment separator. The capacity of the entrainment separator is limited by the reentrainment and/or flooding that will occur when the gas velocity is too high. The mechanisms by which reentrainment and flooding occur are as follow:

1. Liquid holdup in the separator increases, the cross-sectional area for gas flow decreases, and the resulting aerodynamic forces cause massive bodies of liquid to be blown out.
2. At high gas flow rates, the aerodynamic drag forces can cause tearing of liquid from the films flowing downward in the entrainment separator.
3. Drops may shatter due to collision with one another or with solid bodies and form smaller drops that are carried out by the gas.

The deposition of solids within the entrainment separator can be a major source of difficulties. The most important mechanisms by which this occurs are as follow:

1. Settling to nonvertical surfaces.
2. Deposition by inertial impaction caused by changes in liquid flow direction and turbulence.
3. Liquid loss from slurry on the entrainment separator surface leaves a residue of solid particles.
4. Precipitation of dissolved solids.

APPARATUS TYPES

The apparatus used for entrainment separation can be described in general terms as shown in the categorical list below:

A. Gravitational sedimentation

    1. Within the scrubber and its outlet ducting, sedimentation is always active and important.

2. Entrainment separators using sedimentation are rarely used following a scrubber.

B. Centrifugal deposition

1. Cyclone separators of various designs are common. "Anti-creep" skirts to prevent liquid flow into the gas outlet tube and bottom baffles to prevent liquid swirl at the liquid outlet are recommended (Nonhebel 1972) (ref. 1). (See figure 1.)
2. Radial baffles and other types of guide vanes are used to induce a rotary motion of the gas stream within scrubber shell. As in the cyclone separator, this causes drop deposition on the scrubber shell and the baffles, and from there the liquid film runs down into the scrubber.
3. Zigzag baffles, chevrons, corrugated sheets, and similar devices are used to cause one or more abrupt changes of gas flow direction. Drops are deposited on the baffles and the collected liquid film either runs down the baffles (if their major axis is vertical) or drips off as large drops (if axis is horizontal). There are many proprietary designs employing shapes that are claimed to give better liquid drainage (Conkle et al., 1976) (ref. 2). Figure 2 shows an example.
4. A directional change in the gas duct causes considerable deposition of large drops. This is commonly used with venturi scrubbers that can be oriented with flow downward into a duct that turns 90° to cause flow in the horizontal direction.

C. Inertial impaction

1. Beds of massive packing elements (such as saddles, rings, and other gas absorption or distillation tower packings) are used in either vertical or horizontal gas flow configurations.
2. Fibrous packings are used in beds comparable to massive packed systems. Knitted wire mesh, screen, metal wool, felted fibers, open-celled polymeric sponge, and glass fiber have been used for this purpose.
3. Banks of round tubes, streamlined struts, and other shapes have been used in vertical and horizontal orientations.
4. Trays (or plates) such as perforated plates, valve trays, impingement plates, and others have been used for special purposes. Because there are scrubbing devices, they generate entrainment and their use following another type of scrubber may be redundant and should be carefully analyzed.

PRIMARY EFFICIENCY

The overall collection efficiency for drops is dependent on primary collection and on reentrainment. In most cases, the overall efficiency is low at gas velocities because the primary efficiency is low, then it increases with velocity. At higher velocities, reentrainment begins and causes a decrease in overall efficiency even though the primary efficiency is high.

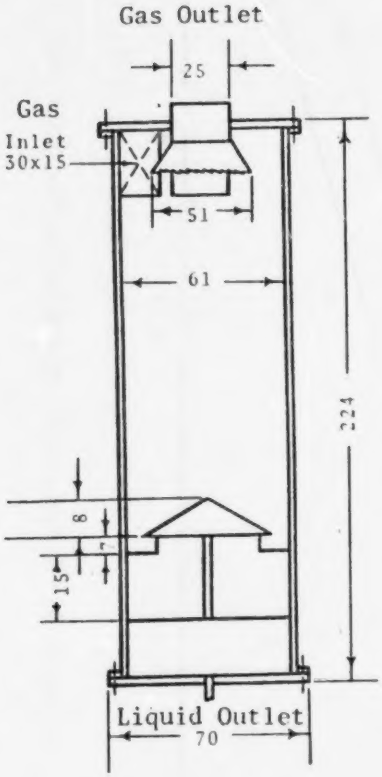
Gas Outlet
25
Gas
Inlet
30x15
51
61
224
8
15
Liquid Outlet
70

Figure 1. Cyclone separator. All dimensions are in cm.

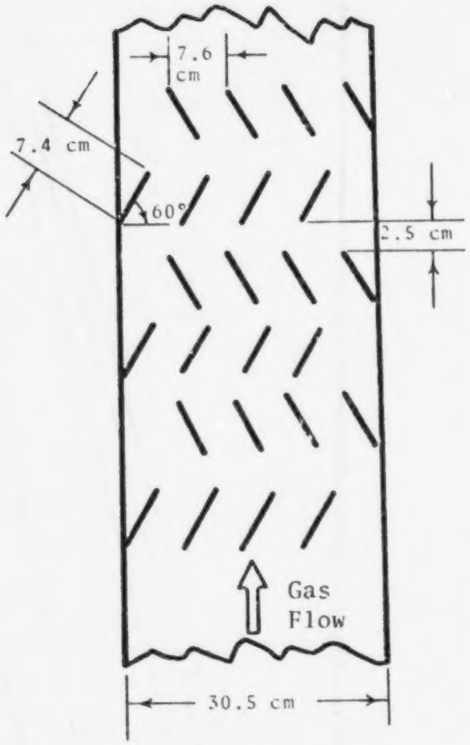
7.6
cm
7.4 cm
60°
2.5 cm
Gas
Flow
30.5 cm

Figure 2. Top view of zigzag baffle arrangement.

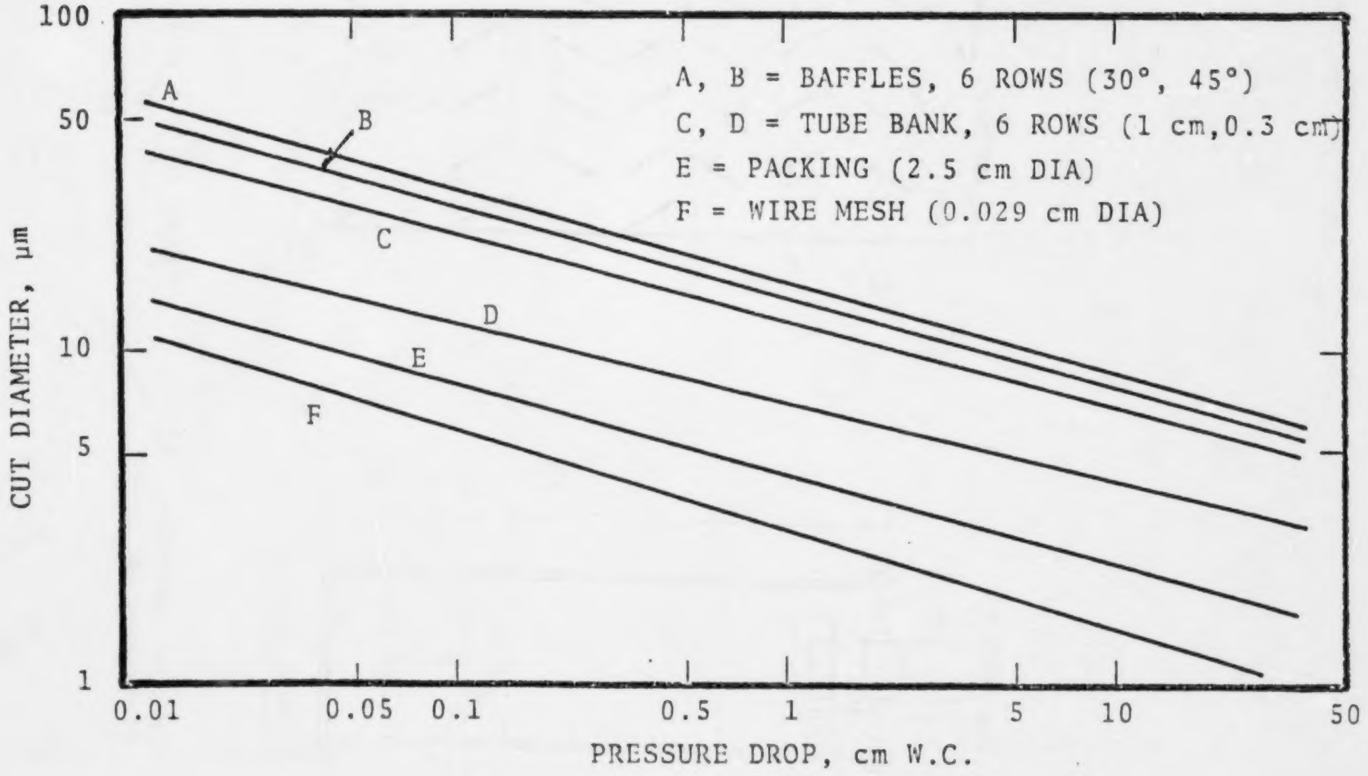

Figure 3. Entrainment separator performance cut diameters.

Methods for predicting primary collection efficiency for various types of separators were reported by Calvert et al. (1974, 1975, and 1977) (refs. 3, 4, 5). A concise representation of the primary efficiency capabilities of several types of separators is given by the "cut/power" relationship developed by Calvert (1974) (ref. 6). This relationship is shown in a plot of the drop diameter collected at 50 percent efficiency (i.e., the cut diameter) against the gas-phase pressure drop or power input for the separator (see figure 3).

Figure 3 was drawn based on design equations and experimental correlations. It shows curves for baffles at two angles of attack to the flow direction (not inclinations to the horizontal), curves for tube banks with two different spacings between tubes with a row, packing of one particular size, and knitted mesh with a certain wire diameter. The curves would be different for entrainment separators of other collection element dimensions, but are not much affected by the extent of the separator. For instance, the position of the lines changes with the wire diameter--it is not affected by the thickness of the knitted mesh pad over a reasonable range.

REENTRAINMENT

The liquid and gas flow capacity of an entrainment separator is limited by the occurrence of reentrainment. Experimental data on collection efficiency for several types of separators have been taken by Bell and Strauss (1973) (ref. 7), Calvert et al., (1975), and Houghton and Radford (1939) (ref. 8). A summary of reentrainment characteristics is given below for several types of separators.

Cyclone

Cyclone separator performance was measured for a straight cylindrical cyclone 61-cm i.d. and 224 cm long. A serrated anti-creep skirt was used on the 25-cm i.d. central outlet tube. Figure 4 is a plot of percent

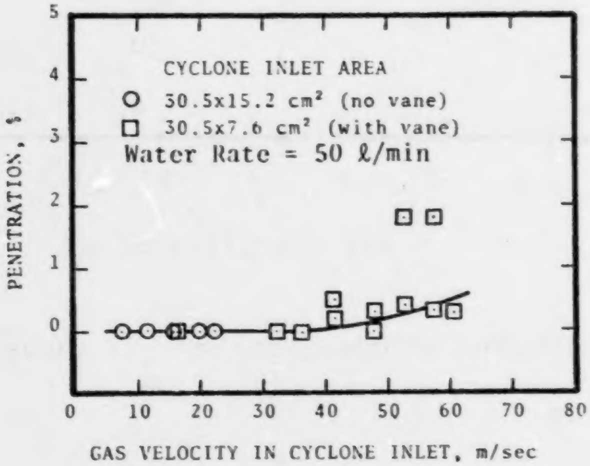

Figure 4. Experimental penetration in cyclone.

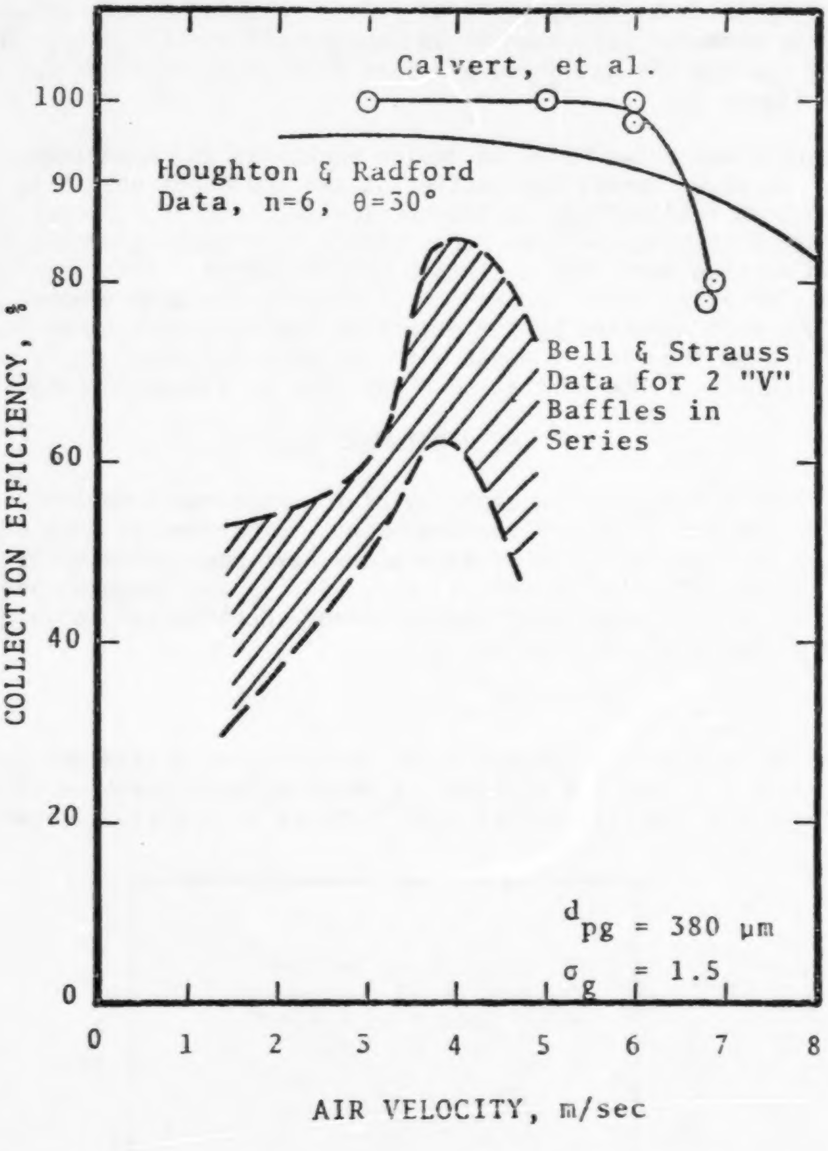

Figure 5. Collection efficiency for vertical zigzag baffle.

penetration (of drops) versus inlet gas velocity. It can be seen that no reentrainment occured below 40 m/s and that less than 0.5 percent was observed between 40 m/s and 60 m/s.

Zigzag Baffles

Several variations of zigzag baffle arrangements were studied by Calvert et al., (1975) for 7.4 cm wide baffles set 7.6 cm apart in rows normal to the gas flow and 2.5 cm between rows. The arrangement included horizontal gas flow with vertical baffles (having attack angles of 30° or 45°) and vertical, upward gas flow with baffles inclined 0° (horizontal), 30°, and 45°.

Figure 5 shows a comparison of collection efficiency versus air velocity data by three investigators. Figure 6 is a plot (for the horizontal gas flow arrangement) of the liquid/gas ratio entering the separator versus the superficial (empty cross sectional) gas velocity in the separator with reentrainment rate as a parameter. The indication of zones is approximate and it indicates that above the shaded area some slight reentrainment was noted.

Figure 7 is a plot of the approximate curves above which heavy reentrainment occurred for three baffle inclinations in the upward flow arrangement. It can be seen that the separator capacity increases with the baffle inclination.

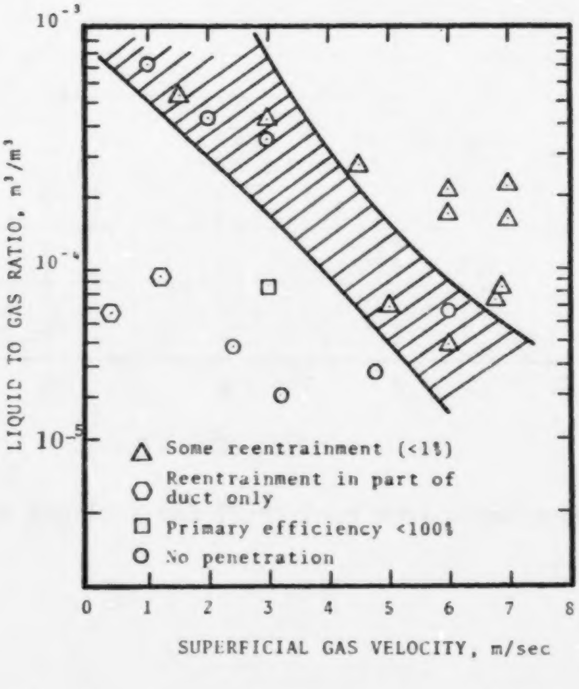

Figure 6. Reentrainment from vertical baffles.
(horizontal gas flow)

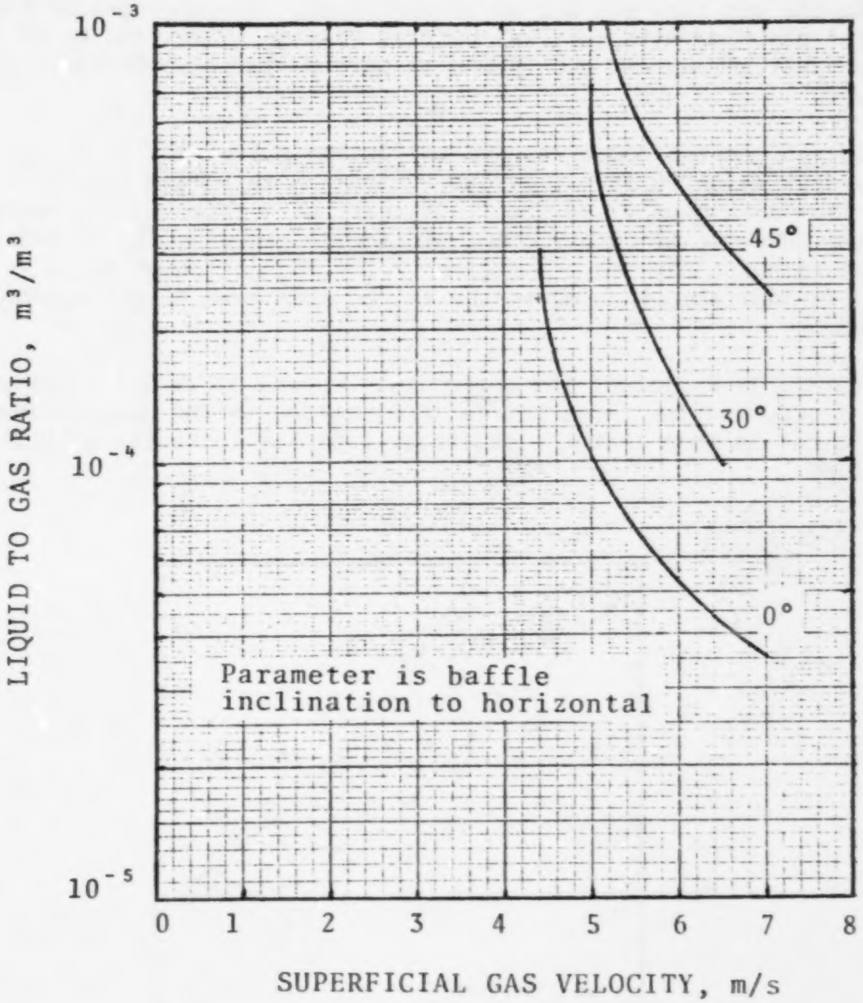

Figure 7. Reentrainment from horizontal and inclined baffles (upward flow).

Massive Packings

Drop collection efficiency data for horizontal and upward flow through beds of 2.5-cm nominal size Pall Rings are shown in figure 8, a plot of penetration versus superficial gas velocity. For horizontal gas flow with liquid/gas ratio ranging up to 1 l/m^3, there is no reentrainment until the gas velocity exceeds 6 m/s. Reentrainment starts at a lower velocity when the gas flow is vertical and it is comparable to the 3.5 m/s flooding velocity predicted for a counter-current packed tower.

Fibrous Packing

Knitted wire mesh pads were studied with horizontal and vertical air flow and figure 9 shows a plot of drop penetration versus superficial gas velocity. Reentrainment started at a velocity of 4.5 m/s and a liquid/gas ratio of 0.4 l/m^3 for the upward flow arrangement. In the case of horizontal flow, reentrainment did not become significant until the gas velocity was about 6.5 m/s, although slight reentrainment was noted in part of the duct at velocities over about 5 m/s.

Tube Banks

Tube banks composed of 6 rows of 1.9-cm o.d. tubes spaced 3.8 cm center-to-center (therefore the space between tubes was 1.9 cm) and with tube centers staggered from row-to-row were studied with horizontal and upward air flow. The measured reentrainment loci are shown in figure 10, a plot of liquid/gas ratio versus superficial gas velocity. Liquid/gas ratio up to 0.22 l/m^3 at 7 m/s gas velocity did not have a significant effect on the horizontal flow arrangement.

Solids Deposition

Industrial experience with entrainment separator fouling and plugging has yielded some empirical observations and guidelines for design. Vertical collection surfaces stay cleaner than horizontal ones due to better liquid drainage. Intermittent washing with sprays is beneficial, but the details of the washing system and procedure depend on the specific case. Precipitation scaling must be controlled through the system chemistry.

Some quantitative experimentation on suspended solids deposition has been done by Calvert et al., (1975), and their findings are summarized below:

1. Deposition rate decreases as the slurry flux on the surface is increased.
2. Deposition rate decreases as the liquid film thickness is increased.
3. Deposition rate is higher on an inclined baffle than on a vertical baffle due to the increase in settling rate of solids suspensions.
4. Small drops are more susceptible to being caught in eddies, which would bring them to the back surfaces of the baffles.
5. Small drops that do hit the baffle surface have a higher deposition rate than larger drops because of their lower localized slurry flux.

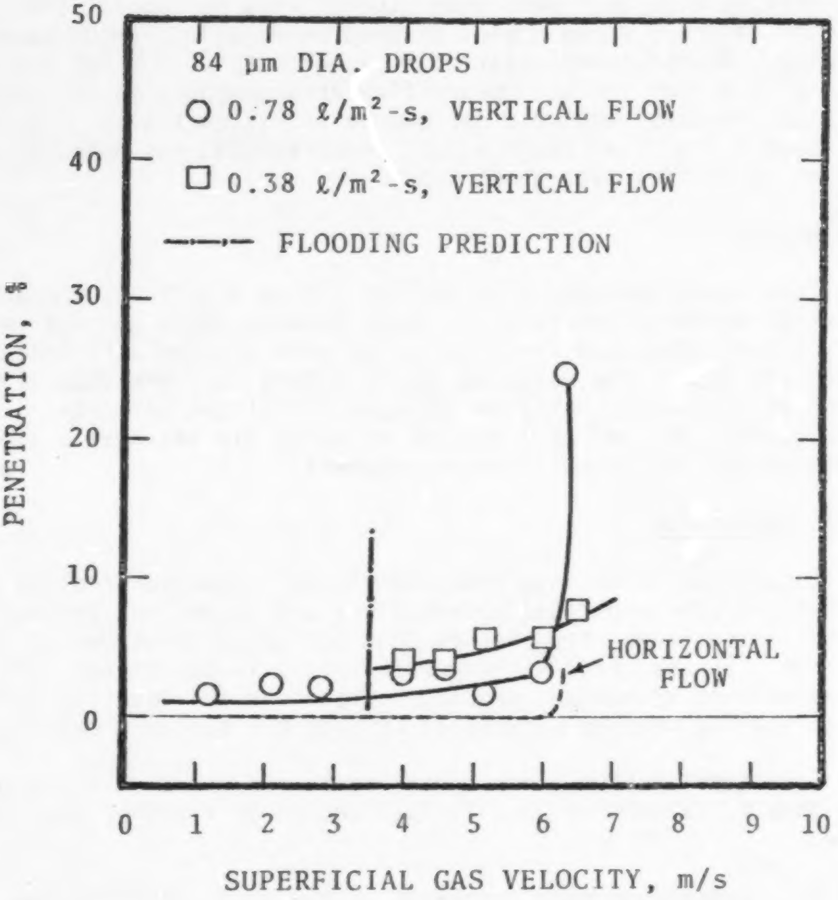

Figure 8. Experimental penetration through packed bed.

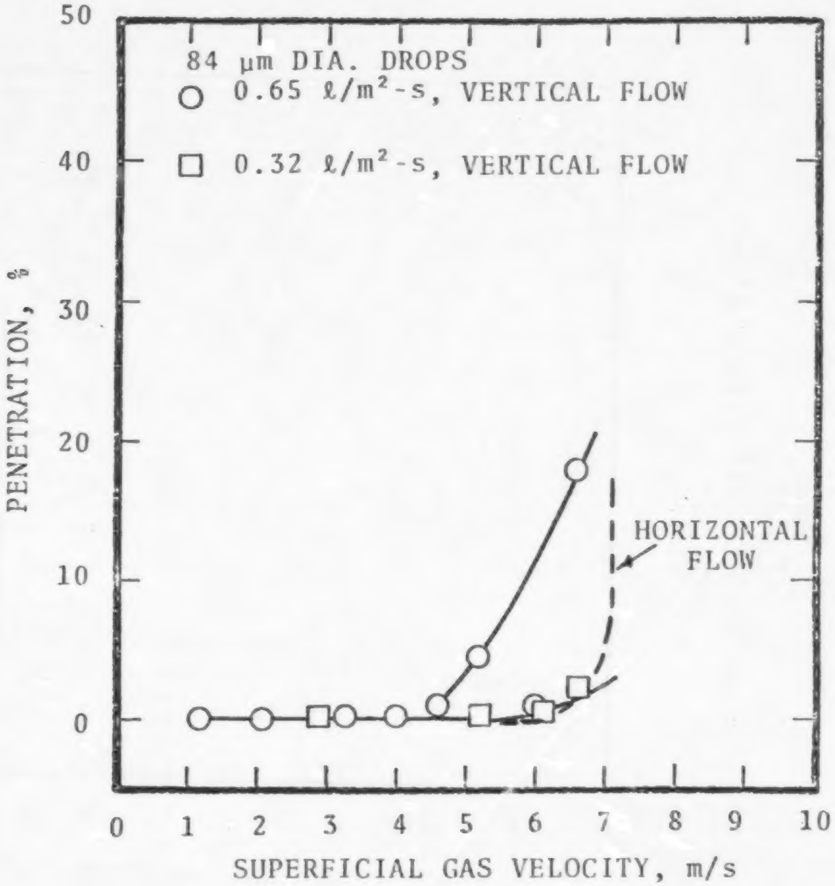

Figure 9. Experimental penetration through mesh.

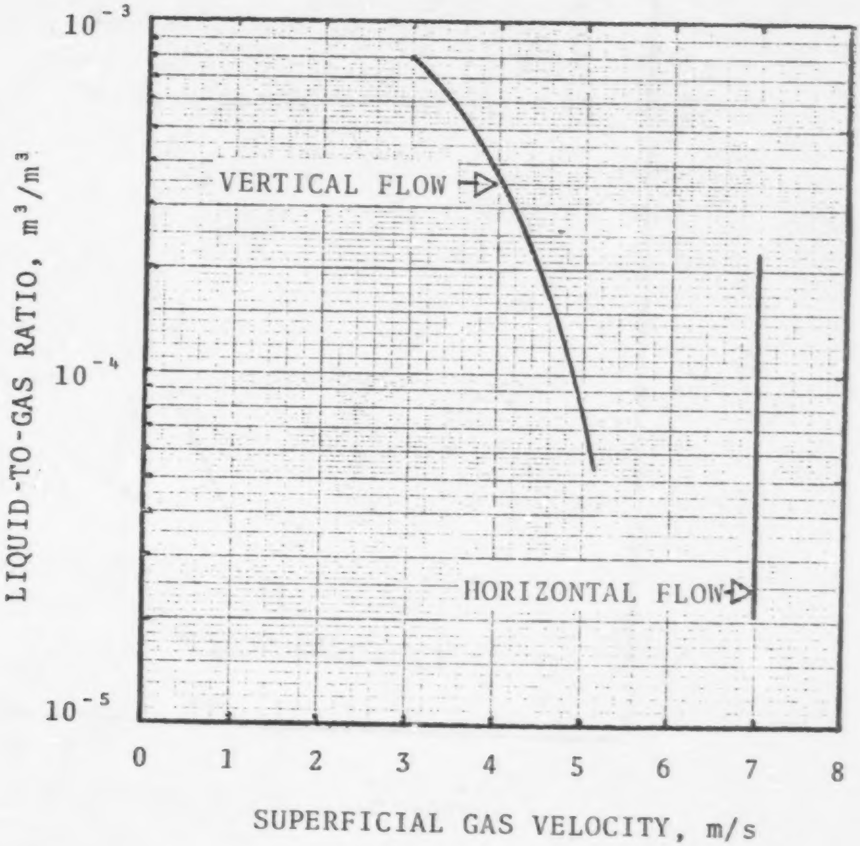

Figure 10. Reentrainment from tube bank.

The deposition data were correlated by the following empirical equation:

$$R_S = W\phi \exp [- (0.13 + 0.53\phi)\delta] \qquad (1)$$

where R_S = deposition rate of $CaCo_3$ on a vertical flat surface, mg/cm^2-s,

W = weight fraction of solids in the slurry,

ϕ = slurry flux, mg/cm^2-s, and

δ = liquid film thickness, μm.

REFERENCES

1. Nonhebel, Processes for Air Pollution Control, 2nd ed., Chapter 16 - "Spray Elimination," CRC Press, Cleveland, 1972.

2. H. N. Conkle, H. S. Rosenberg, and S. T. DiNovo, "Guidelines for the Design of Mist Eliminators for Lime/Limestone Scrubbing Systems," EPRI FP-327, 1976.

3. S. Calvert, S. Yung, and J. Leung, "Entrainment Separators for Scrubbers -Final Report," EPA 650/2-74-119b, NTIS No. PB 248-050, 1975.

4. S. Calvert, S. C. Yung, H. F. Barbarika, and L. E. Sparks, "Entrainment Separators for Scrubbers," presented at the Second Fine Particle Scrubber Sumposium, New Orleans, 1977.

5. S. Calvert, I. L. Jashnani, and S. Yung, "Entrainment Separators for Scrubbers," J. Air Pollution Control Association, Vol. 24, No. 971 (1974).

6. S. Calvert, "Engineering Design of Fine Particulate Scrubbers," J. Air Pollution Control Association, Vol. 24, No. 929 (1974).

7. C. G. Bell and W. Strauss, "Effectiveness of Vertical Mist Eliminators in a Cross Flow Scrubber," APCA Journal, Vol. 23, No. 967 (November 1973).

8. H. G. Houghton and W. H. Radford, Measurements on Eliminators and the Development of a New Type for Use at High Gas Velocities," Trans. American Inst. of ChE, Vol. 35, No. 427 (1939).

MIST ELIMINATOR TESTING AT THE SHAWNEE PROTOTYPE LIME/LIMESTONE TEST FACILITY

John E. Williams*

Abstract

This paper presents the major test results and discusses their significance in respect to practical application to commercial-size units from the mist eliminator testing conducted at the Shawnee prototype lime/limestone test facility over a 5-year period from 1972 through 1977. Much of the early work was conducted at a reduced gas velocity using various combinations of mist eliminator washing techniques and hardware configurations, including a wash tray upstream of the mist eliminator. It was not recognized early in the program that scaling and mud-type solids deposition in the restricted area of the mist eliminator were indeed separate problems, each with separate and distinct solutions. Consequently, it was only after this fact was recognized that methods were developed to adequately control both problems at design gas velocities.

Control of mud-type solid deposits proved to be more difficult than control of scaling. The real key to successful control of mud-type solid deposits was not found until tests were initiated to study methods to improve alkali utilization. A correlation was found between alkali utilization and accumulation of the mud-type solids. Above about 85 percent alkali utilization, these solids can easily be removed even with very infrequent (once per 8-hour shift) washing with fresh makeup water. Tests to confirm this correlation and its significance for both improving operating reliability and in reducing overall scrubbing costs for commercial-size applications are also discussed. Selection of operating parameters (such as liquid-to-gas ratio (L/G), reaction tank residence time, pH, or percent solids in the circulating slurry to maintain a gypsum saturation level in the scrubber below about 130 percent) will normally control scaling.

Recent test results applicable to mist eliminator performance obtained during flue gas characterization testing at Shawnee are also presented.

INTRODUCTION

With dramatic increases in the use of high sulfur coal reserves being a near certainty, the widespread use of flue gas desulfurization (FGD) will play an increasingly important role in near term SO_x control strategies. Expanded coal use must be accompanied by sound air and water pollution control measures to minimize threats to human health and to avoid widespread environmental damage.

---

*Emission/Effluent Technology Branch, Utilities and Industrial Power Division, Industrial Environmental Research Laboratory, U.S. Environmental Protection Agency, Research Triangle Park, North Carolina 27711

As the FGD technology most commonly accepted and used by domestic utilities for coal-fired boiler applications, lime/limestone processes are especially important to the success of a policy to rapidly expand coal use. Based on the most recent estimate, 30 FGD systems are presently installed and an additional 94 are in various stages of planning or construction. Most of these 124 units will be in service by the early 1980's. Of these, 78 have already selected lime/limestone processes and an additional 25 have not yet selected a process type.

For the past 5-1/2 years the Industrial Environmental Research Laboratory-Research Triangle Park (IERL-RTP) has sponsored the operation and testing of a prototype lime and limestone wet scrubbing test facility located at the Tennessee Valley Authority's (TVA) Shawnee power plant near Paducah, Kentucky. This versatile facility allows comprehensive testing of up to three scrubber types under a variety of operating conditions. Bechtel Corporation of San Francisco, as the major Environmental Protection Agency (EPA) contractor, designed the test facility and directs the test program. TVA constructed and operates the facility.

The major concerns of the utility industry to date regarding lime/limestone scrubbing have centered around scaling and plugging potential, the large quantities of byproduct sludge generated, and the high costs (capital and operating) of scrubbing. It is toward these areas of concern that the Shawnee program has been directed.

A summary which describes in more detail the test facility, the test program objectives, the significant test results to date, and the future plans is presented in reference 1. This paper will be directed only to the mist eliminator testing portion of the Shawnee program. The major mist eliminator test results and their significance in respect to practical application to commercial-size units will be discussed.

DISCUSSION OF RESULTS

Throughout the Shawnee program, one of the most persistent problems has been that of scaling and plugging, especially in the relatively restricted area of the mist eliminators. Consequently, much of the early effort was devoted to identifying and learning how to control two separate and distinct operating reliability problems--scaling and soft, mud-type solids deposition, especially in the mist eliminators. In fact, identification of the problems was even more difficult because it was not recognized early in the program that scaling and mud-type solids deposition were indeed separate problems, each with separate and distinct solutions. This fact was not really apparent until methods were found to adequately control both.

In a lime- or limestone-based system, the most frequently encountered scaling problem is due to sulfate (gypsum) crystals which precipitate on scrubber internals rather than outside the scrubber in the reaction tank. Selection of operating parameters (such as liquid-to-gas ratio (L/G), reaction tank residence time, pH, or percent solids in the circulating slurry to maintain a gypsum saturation level in the scrubber below about 130 percent will prevent this type of scaling. The use of very infrequent (once every 4 to 8 hours) top sequential washing with fresh makeup water and low pressure drop nozzles proved adequate at Shawnee for control of scaling in the mist eliminators. However, identification of those operating parameters affecting scaling potential, safe operating ranges, and mist eliminator washing techniques proved time consuming (refs. 2, 3, and 4). This was especially true with the problem of mud-type solids deposition, which was superimposed over the scaling problem.

Solution to the problem of mud-type solids deposition proved even more difficult than control of scaling, especially in the mist eliminators. Much of the early work of Shawnee was conducted at a reduced gas velocity using various combinations of mist eliminator washing techniques and hardware configurations, including a wash tray upstream of the mist eliminator. The use of a wash tray upstream of the mist eliminator to transfer the mud-type deposits to an area where they could more easily be removed by washing was only marginally successful and required reduced gas flow rates. Ultimately, washing techniques for the mist eliminator were found which controlled restriction from the mud-type solids to less than 10 percent of the open area at satisfactory gas flow rates and without the need for a wash tray. This level of solid deposits did not hinder operation or cause shutdown for periodic cleaning. However, the real key to successful control of these mud-type solid deposits was not found until well into the advanced test program.

During tests to study methods to improve alkali utilization, a correlation was found between alkali utilization and the accumulation of these mud-type solids. Above about 85 percent alkali utilization, the solids can easily be removed even with very infrequent (once per 8-hour shift) washing with fresh makeup water. In fact, an entirely clean system was maintained over an extended period using only approximately 25 percent of the available fresh makeup water. (The available makeup water is defined as that added to maintain a closed-loop water balance and represents the water lost through evaporation and that which leaves the system with the purged solids.) This correlation was subsequently confirmed at Shawnee using three different methods for improving alkali utilization (ref. 2) and has also been confirmed on a different system at TVA's 1 MW Colbert pilot plant (ref. 5). The ability to improve alkali utilization then becomes extremely important for limestone scrubbing because:

1. It provides a means for existing installed full-scale systems, at low cost, to solve or to reduce the severity of an operating reliability problem that persisted in many of the early applications.

2. It permits the use of limestone costing about $4 to $6/metric ton rather than lime costing about $30 to $40/metric ton at greater than 90 percent utilization (or about 1.1x stoichiometric quantity), which is comparable to that normally obtained with lime.

3. It further reduces the overall costs of scrubbing by substantially reducing the quantity of byproduct sludge produced.

The methods developed for improving alkali utilization apply equally as well for lime scrubbing as for limestone scrubbing. However, since alkali utilization of greater than 85 percent is normally obtained with conventional lime scrubbing, further improvement of the lime utilization is not as significant as improved limestone utilization.

Scaling and plugging are no longer a major concern at Shawnee. Avoiding these types of problems has become almost routine, although lessons learned are not ignored in selecting the operating conditions for current tests. The detailed discussions contained in references 2, 3, and 4 help to illustrate that finding solutions to these problems was not as simple and straightforward as it may appear from the brief summary presented here. Schematic drawings showing the scrubbers, the overall scrubber systems, the various types of mist eliminators tested at Shawnee, the wash tray, and the various types of wash configurations used are also included in references 2, 3, and 4.

Another important facet of the mist eliminator testing at Shawnee of interest for this paper are the flue gas characterization tests that address the mist eliminator efficiency. In order to maximize the amount of useful data for the funds expended and to obtain long-term continuous data (as opposed to having an outside group come in for one or two spot checks), it was decided to train onsite personnel to conduct mist eliminator emission characterization tests routinely. Through a separate contract, TRW Corporation was chosen to develop the best testing methods for particulate mass loading, particle size distribution, sulfate measurement, and mist eliminator liquid entrainment; to write the appropriate operating manuals; and to train the onsite personnel in the procedures developed. Most of these tests are now being run routinely by the Shawnee onsite personnel.

The test methods and preliminary test results covered briefly here are discussed in detail in references 4 and 6. Initial intensive test series on both the venturi/spray tower and the turbulent contact absorber (TCA) systems were run to determine the effect of major operating variables on particulate mass removal, emitted particle size distribution, and SO_3 removal. Variables investigated on the venturi/spray tower system were gas flow rate, slurry circulation rate, M_gO addition, venturi pressure drop, mist eliminator wash configuration, percent solids recirculated, and inlet particulate mass loading. Variables investigated on the TCA system were gas flow rate, slurry circulation rate, mist eliminator wash configuration, and inlet particulate mass loading.

The limited data available thus far indicate:

1. Outlet particulate mass loading appears to be unaffected by operating variable levels over the ranges investigated except for venturi pressure drop and inlet particulate mass loading. Outlet mass loading was always less than the inlet mass loading even for very low values of the inlet mass loading. Outlet mass loading was directly proportional to inlet mass loading and was inversely proportional to the venturi pressure drop.

2. Scrubber reaction product emission represented only a small percentage of the total mass emission (usually less than 10 percent of the total) with the bulk being fly ash particles that entered with the flue gas. Size distribution results and scanning electron microscope photographs indicated that most of the scrubber reaction product emission was confined to the fractions larger than 5 μ. This also suggests that the type of mist eliminator used at Shawnee is reasonably efficient. However, this is based on a limited number of tests and further tests are planned to verify these observations.

3. Measurement of mass penetration through the scrubbers as a function of particle size indicated that there was no massive generation of particulate in any size fraction (i.e., outlet greater than inlet). Penetration became significant in the range of 1 μ and smaller where penetration varied from 25 to 90 percent. Under comparable operating conditions, the relative mass penetration for the TCA system was greater than for the venturi/spray tower system.

4. The SO_3 removal efficiency of the scrubbers appeared to be fairly constant at about 58 percent over the range of variables tested.

SUMMARY AND CONCLUSIONS

Mist eliminator testing at Shawnee has made a significant contribution toward improved reliability for lime and limestone scrubbing systems. Furthermore, the results have helped in overcoming other major utility and vendor concerns as well. These include equipment and process variations that can lead to substantial reductions in both the quantity of sludge produced and in the costs for installing and operating the lime and limestone scrubbing sytems. The most significant results of the Shawnee mist eliminator tests to date include:

1. Demonstration has shown that conventional lime/limestone systems can be operated reliably. Two separate reliability problems were identified--scaling and soft, mud-type solids deposits, and methods to control each were demonstrated.

2. Soft, mud-type solids deposition was shown to be a strong function of alkali utilization. At high alkali utilization (greater than about 85 percent) these solids are much more easily removed, and very infrequent intermittent freshwater wash is adequate for their complete removal in restricted areas such as the mist eliminator where accumulation can lead to plugging problems.

3. Several equipment or process variations were also demonstrated for improving alkali utilization. This is particularly significant for limestone where alkali utilization is typically about 60 to 70 percent and can be increased to 85 to 95 percent, or comparable to that normally obtained with lime. This not only improves reliability, but also reduces costs by permitting the use of a much less expensive alkali feed material and by substantially reducing the quantity of byproduct sludge produced.

4. Initial results from a limited number of tests indicate that when a reasonably efficient mist eliminator is used, scrubbers do not generate or contribute to either particulate or sulfate emissions in any particle size fraction. Mass emissions were unaffected by changes in operating variables over the ranges investigated except for venturi pressure drop and inlet mass loading. Reaction products were concentrated in those fractions greater than 5 μ and were usually less than 10 percent of the total mass emissions. The SO_3 removal efficiency was relatively constant at about 58

percent over the range of variables investigated. Further tests are planned to verify these observations and to better quantify the initial data.

REFERENCES

1. J. E. Williams, unpublished paper*, "Summary of Operation and Testing at the Shawnee Prototype Lime/Limestone Test Facility," April 1977.

2. Bechtel Corporation, "EPA Alkali Scrubbing Test Facility: Advanced Program - Second Progress Report," EPA-600/7-76-008 (NTIS No. PB 258-783/AS), September 1976.

3. Bechtel Corporation, "EPA Alkali Scrubbing Test Facility: Advanced Program - First Progress Report," EPA-600/2-75-050 (NTIS No. PB-245-279/AS), September 1975.

4. Bechtel Corporation, "EPA Alkali Scrubbing Test Facility: Advanced Program - Third Progress Report," EPA-600/7-77-105, September 1977.

5. Tennessee Valley Authority, "TVA's 1-MW Pilot Plant: Final Report on High Velocity Scrubbing and Vertical Duct Mist Elimination," EPA-600/7-77-019 (TVA PRS-19) (NTIS No. PB 269-850/AS), March 1977.

6. R. G. Rhudy and H. N. Head, paper presented at the Second Fine Particle Scrubber Symposium in New Orleans, Louisiana, "Results of Flue Gas Characterization Testing at the EPA Alkali Wet-Scrubbing Test Facility," May 1977.

*A copy of this paper is included here as Attachment A.

SUMMARY OF OPERATION AND TESTING AT THE SHAWNEE PROTOTYPE LIME/LIMESTONE TEST FACILITY

John E. Williams
Emissions/Effluent Technology Branch
Utilities and Industrial Power Division

Industrial Environmental Research Laboratory
U.S. Environmental Protection Agency
Research Triangle Park, North Carolina 27711

April 1977

ATTACHMENT A

INTRODUCTION

EPA's Industrial Environmental Research Laboratory-RTP and its predecessors over approximately the past 15 years have undertaken a program of research and development to establish the technical and economic feasibility of promising processes for removing sulfur dioxide and particulates from coal-fired boiler flue gases. An important part of this effort involves the operation and testing of a prototype wet lime and limestone scrubbing test facility located at the Tennessee Valley Authority's (TVA) Shawnee power plant near Paducah, Kentucky. This versatile facility allows comprehensive testing of up to three scrubber types under a variety of operating conditions. Bechtel Corporation of San Francisco, as the major contractor, designed the test facility and directs the test program. TVA constructed and operates the facility.

Purposes of this report are to describe the Shawnee test facility, to discuss the test program objectives, and to summarize major test results to date. More detailed information is presented in published EPA reports listed in the reference section at the end of this report. Two additional reports are presently being reviewed and should be published by July 1977. These are: 1) the third progress report covering testing from February through November 1976 under the advanced program; and 2) the second annual report covering the Shawnee field evaluation of the disposal of flue gas cleaning wastes.

The test facility consists of three parallel scrubber systems: a venturi followed by a spray tower, a Turbulent Contact Absorber (TCA), and a Marble-Bed Absorber. Each system is capable of treating approximately 10 MW equivalent (30,000 acfm @ 300°F) of flue gas from Shawnee unit 10 (nominally 150 MW total) containing 1000 to 5000 ppm sulfur dioxide (SO_2) and 0.2-11 gms/m^3 of particulates (fly ash). Operation of the Marble-Bed Absorber was discontinued in July 1973 (see Reference 1 for a discussion of the reasons), and subsequent operation has been limited to the two remaining scrubber systems. Each of the systems can be operated in a variety of configurations. Typical system configurations depicting lime testing with the venturi/spray tower and limestone testing with the TCA scrubber are illustrated schematically in Figures 1 and 2, respectively.

Major goals of the original two-year test program were:

- Characterization of the effect of important process variables on sulfur dioxide and particulate removal.
- Development of mathematical models to allow scale-up to full-size scrubber facilities.

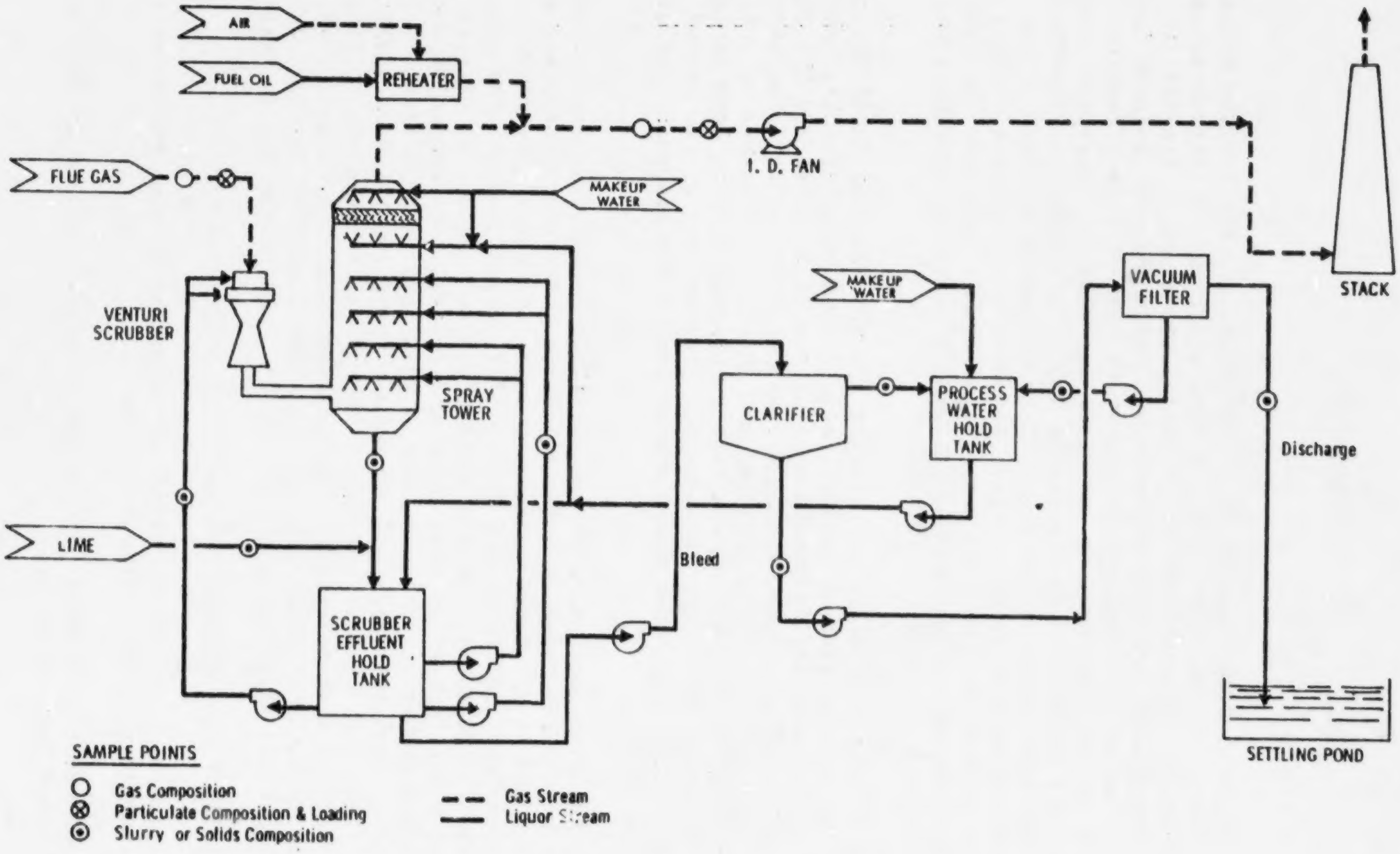
AIR
FUEL OIL
REHEATER
FLUE GAS
I. D. FAN
STACK
MAKEUP WATER
VENTURI SCRUBBER
SPRAY TOWER
MAKEUP WATER
VACUUM FILTER
CLARIFIER
PROCESS WATER HOLD TANK
Discharge
LIME
Bleed
SCRUBBER EFFLUENT HOLD TANK
SETTLING POND
SAMPLE POINTS
○ Gas Composition
⊗ Particulate Composition & Loading
⊙ Slurry or Solids Composition
Gas Stream
Liquor Stream

Figure 1. Venturi/Spray Tower-Typical System Configuration

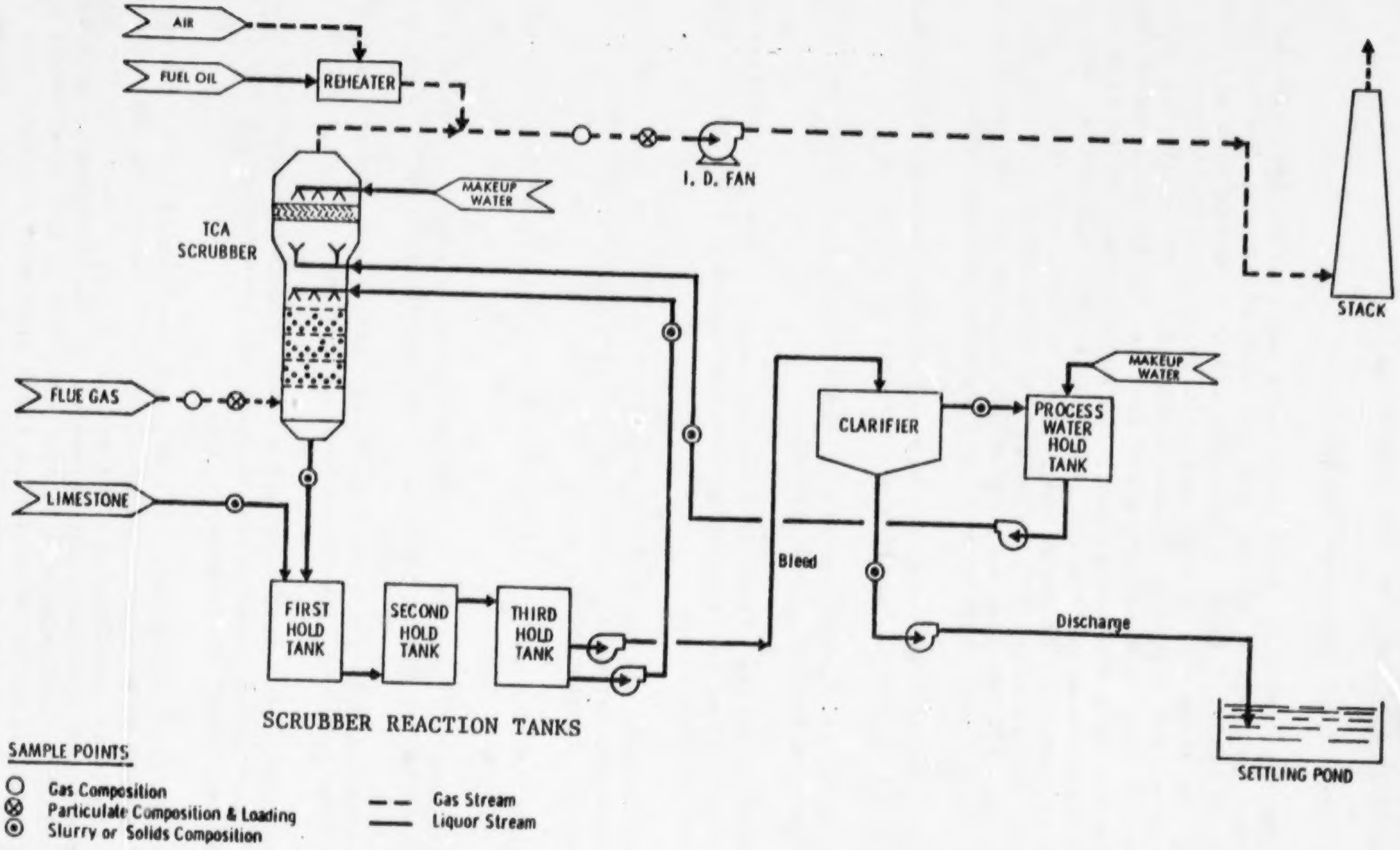
AIR
FUEL OIL
REHEATER
I. D. FAN
STACK
MAKEUP WATER
TCA SCRUBBER
FLUE GAS
LIMESTONE
FIRST HOLD TANK
SECOND HOLD TANK
THIRD HOLD TANK
SCRUBBER REACTION TANKS
Bleed
CLARIFIER
MAKEUP WATER
PROCESS WATER HOLD TANK
Discharge
SETTLING POND
SAMPLE POINTS
○ Gas Composition
⊗ Particulate Composition & Loading
⊙ Slurry or Solids Composition
-- Gas Stream
— Liquor Stream

Figure 2. Turbulent Contact Absorber-Typical System Configuration

- Development of information to study the technical and economic feasibility of lime/limestone scrubbing.

- Demonstration of long-term reliability.

Although for the most part these goals were met at the completion of the original test program, it became apparent that additional Shawnee testing was needed to supply further information and to optimize lime and limestone systems in the areas of: sludge disposal, improved reliability, variable load operation, and improved process economics. This conclusion was based on comments of need from utilities and flue gas desulfurization system vendor representatives, and particularly the encouraging results from IERL-RTP pilot plant support studies which indicated several potentially attractive new scrubber operating concepts and process variations that could favorably affect both the economics and the operating reliability of scrubbing. Therefore, in 1974 the Shawnee program was extended and the scope was expanded. Additional objectives of the expanded program were:

- Investigation of advanced process and equipment design variations for improving system reliability and economics.

- Evaluation of process variations for a substantial increase in alkali utilization for limestone systems.

- Evaluation of the effect of increased magnesium ion concentration or other additives on reducing gypsum saturation and increasing SO_2 removal efficiency.

- Determination of the efficiency and reliability of lime and limestone scrubbers under conditions of widely varying flue gas flow rate and inlet SO_2 concentration.

- Evaluation of system performance and reliability without fly ash in the flue gas.

- Assessment of the effectiveness of forced oxidation or other process variations for producing an improved throwaway sludge product.

- Determination of the practical upper limit of SO_2 removal efficiency for both lime and limestone scrubbing systems.

- Development of a design/economic study computer program for comparison of both initial investment and lifetime operating costs for full-scale lime and limestone systems.

Two smaller scrubbing systems (0.1 megawatt each) have also been operated at the IERL-RTP pilot plant in support of the Shawnee program. These small, pilot-scale scrubber systems are capable of simulating the Shawnee scrubber systems with excellent agreement in the lime/limestone wet-scrubbing chemistry. Preliminary data are generated on the pilot-scale systems to verify and guide the selection of those promising concepts that should logically be investigated on the larger size Shawnee units. Indeed, results obtained from operation of the IERL-RTP pilot plant were very instrumental in the decision to continue testing at Shawnee under the advanced test program.

DISCUSSION OF RESULTS

The test program schedules based on the defined objectives for the initial program and the advanced concept testing are presented in Figures 3 and 4, respectively. As shown by the schedules, much of the early effort was devoted to identifying and learning how to control two separate and distinct operating reliability problems--scaling and soft, mud-type solids deposition, especially in the relatively restricted area of the mist eliminators. Much of the early work was also conducted at a reduced gas velocity using various combinations of mist eliminator washing techniques and hardware configurations, including a wash tray upstream of the mist eliminator. In fact, it was not recognized early in the program that scaling and mud-type solids deposition were indeed separate problems, each with separate and distinct solutions. This fact was not really apparent until methods were found to adequately control both.

In a lime or limestone based system, the most frequently encountered scaling problem is due to sulfate (gypsum) crystals which precipitate on scrubber internals rather than outside the scrubber in the reaction tank. Selection of operating parameters (such as liquid-to-gas ratio (L/G), reaction tank residence time, pH, or percent solids in the circulating slurry to maintain a gypsum saturation level in the scrubber below about 130%) will prevent this type of scaling. The use of very infrequent (once every 4-8 hours) top sequential washing with fresh make-up water and low pressure drop nozzles proved adequate at Shawnee for control of scaling in the mist eliminators. However, identification of those operating parameters affecting scaling potential, safe operating ranges, and mist eliminator washing techniques proved time consuming. This was especially true with the problem of mud-type solids deposition which was superimposed over the scaling problem.

Solution of the problem of mud-type solids deposition proved even more difficult than control of scaling, especially in the restricted area of the mist eliminators. The use of a wash tray upstream of the mist eliminator to transfer the mud-type deposits to an area where they could more easily be removed by washing was only marginally successful and required reduced gas flow rates. Washing techniques for the mist eliminator were ultimately found without requiring a wash tray and at design gas velocities which limited restriction from these mud-type solids to less than 10% of the open area. These solid deposits did not hinder operation or cause shut-down for periodic cleaning. However, the real key to successful control of these mud-type solid deposits was not found until well into the advanced test program.

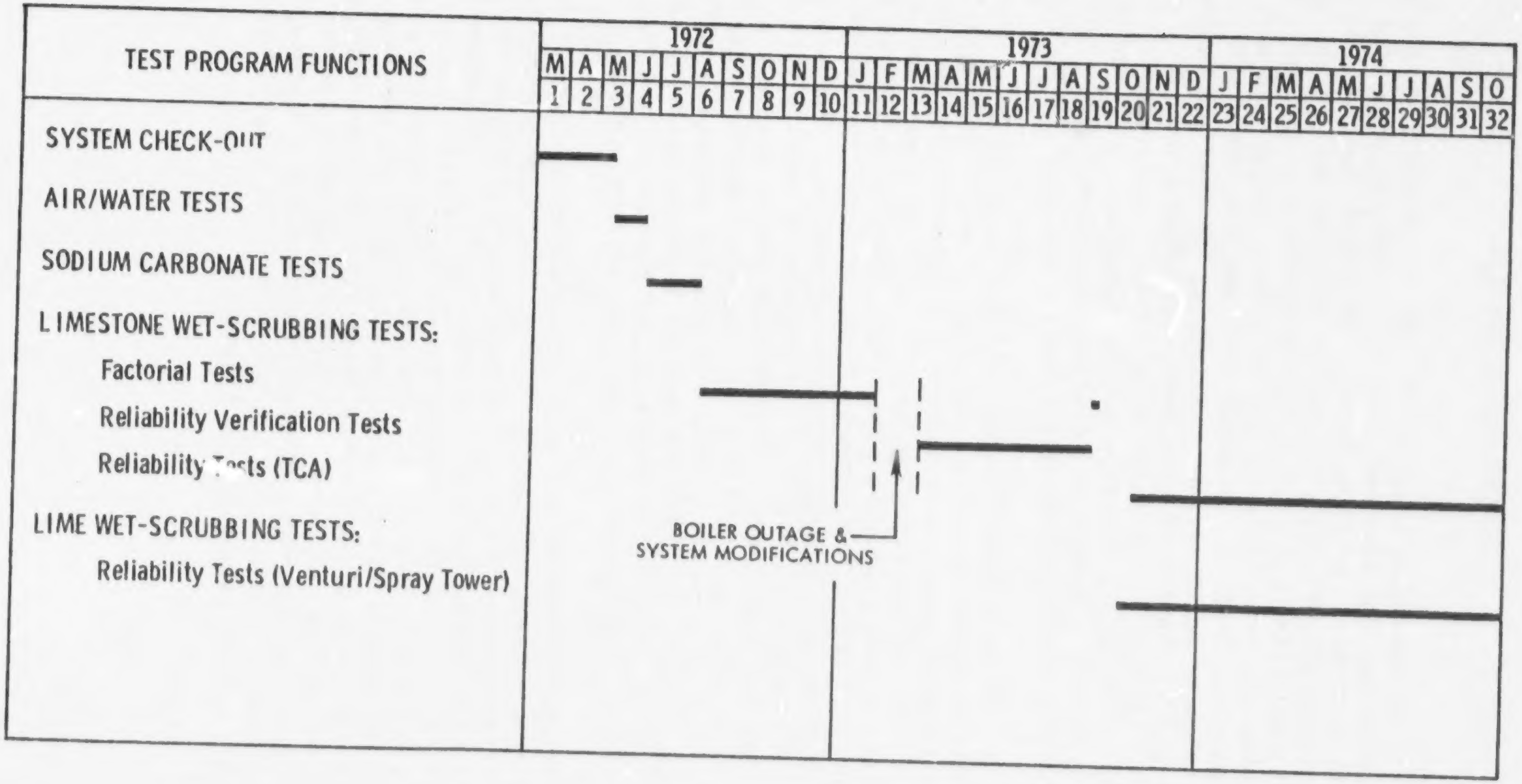

Figure 3. Shawnee Test Program Schedule

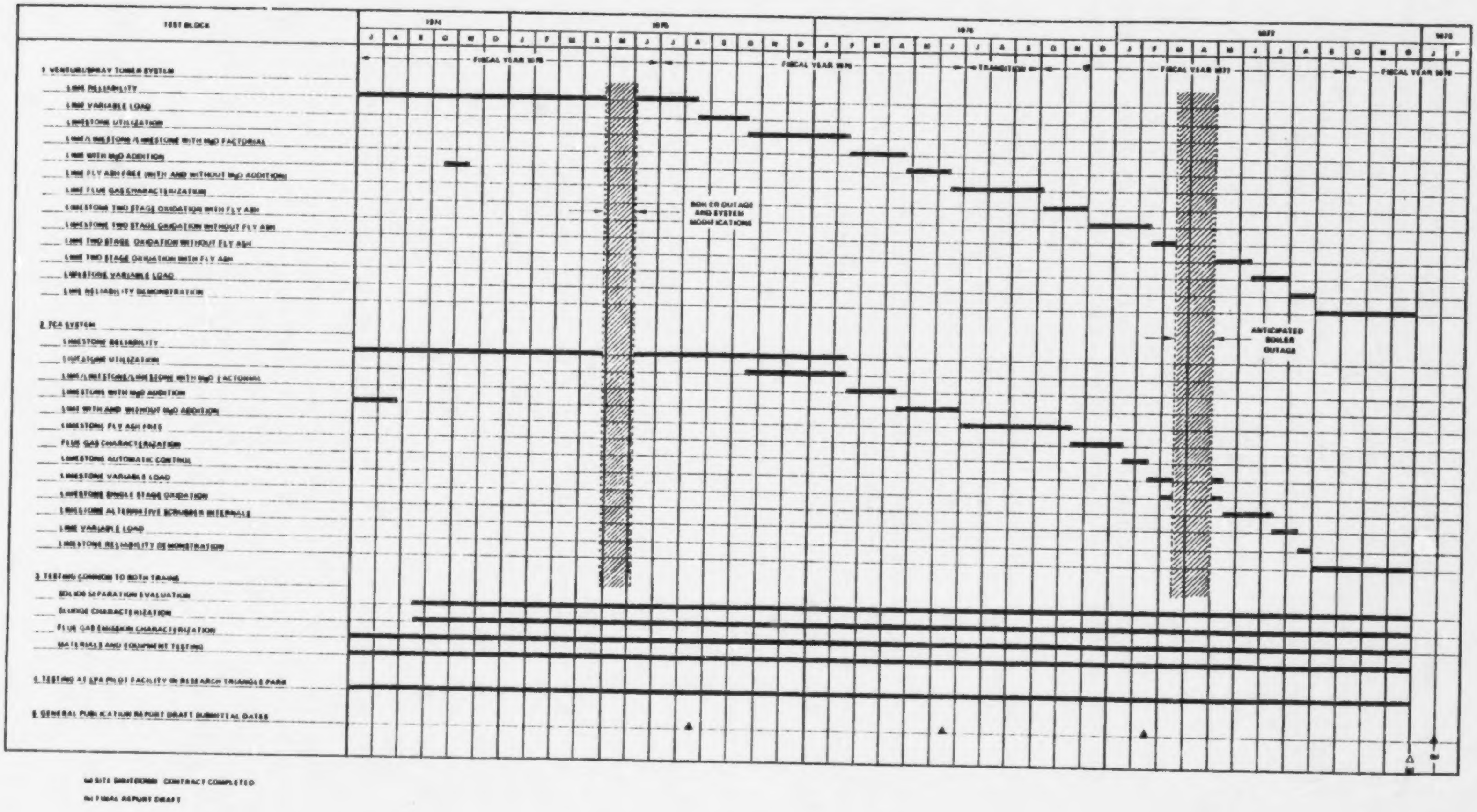

Figure 4. Shawnee Advanced Test Program Schedule

SCHEDULE FOR
ADVANCED TEST PROGRAM
WITH PROPOSED SIX MONTH
EXTENSION - NOVEMBER 1976

During tests to study methods to improve alkali utilization, a correlation was found between alkali utilization and the accumulation of these mud-type solids. Above about 85% alkali utilization, the solids can easily be removed even with very infrequent (once per 8-hour shift) washing with fresh make-up water. In fact, an entirely clean system was maintained over an extended period using only approximately 25% of the available fresh make-up water. (The available make-up water is defined as that added to maintain a closed-loop water balance and represents the water lost through evaporation and that which leaves the system with the purged solids.) This correlation was subsequently confirmed at Shawnee using three different methods for improving alkali utilization and has also been confirmed on a different system at TVA's 1 MW Colbert pilot plant. The ability to improve alkali utilization then becomes extremely important for limestone scrubbing because:

- It provides a means for existing installed full-scale systems, at minimal cost, to solve or improve an operating reliability problem that persisted in many of the early applications.
- It permits the use of limestone costing about \$4-6/metric ton rather than lime costing about \$30-40/metric ton at greater than 90% utilization (or about 1.1x stoichiometric quantity), which is comparable to that normally obtained with lime.
- It further reduces the overall costs of scrubbing by substantially reducing the quantity of by-product sludge produced.

Another major area being studied at Shawnee during the advanced test program is that of forced oxidation of sulfite to sulfate (gypsum). This concept was developed in the IERL-RTP pilot plant and includes both a staged scrubber configuration and forced oxidation within a single scrubber. Both configurations have the potential for obtaining essentially complete oxidation of the solids to gypsum and an accompanying improvement in solids settling characteristics and dewatering properties. However, each method has possible advantages and disadvantages compared with the other, and both will be evaluated further on the larger units at Shawnee. Forced oxidation in a single scrubber is certainly a more simplified approach requiring less equipment than staged scrubbing and can probably be more easily controlled from an operational point of view. However, this method applies only to limestone systems while the staged scrubbing configuration can be used with either lime or limestone. The staged scrubber configuration has the added advantage of also being able to obtain very high (about 95%) alkali utilization simultaneously with the forced oxidation to gypsum. The benefits and significance of high alkali utilization, especially for limestone operation, were pointed out in the preceding paragraph.

It has been estimated that the application of forced oxidation in the staged scrubber configuration (compared to conventional limestone scrubbing) can reduce limestone requirements by roughly one-third and can reduce the volume of by-product sludge generated by more than 50%. An economic sensitivity analysis made earlier in the program by TVA indicated that sludge disposal costs represent a significant portion of the overall costs for lime/limestone scrubbing, and the large quantities of waste sludge that must be disposed of have long been one of the major objections of the utility industry to these types of flue gas desulfurization (FGD) processes. Obviously, reductions of this magnitude in both limestone requirements and waste sludge generation would have a large impact on the economics of scrubbing and, hopefully, on wider acceptance and application by industry of lime/limestone scrubbing.

Other promising areas* which have been or will be studied at Shawnee during the advanced test program include:

1. Addition of MgO to increase the SO_2 removal efficiency and to force operation into the gypsum unsaturated mode. From the test results to date, it appears virtually certain that the SO_2 removal efficiency can be substantially improved by MgO addition using either lime or limestone feed. Higher MgO addition rates are required for limestone than for lime, but the SO_2 removal efficiency can be increased using either alkali from a normal 80% removal to 95% removal or greater, with other operating parameters (L/G, percent solids recirculated, scrubber type, pressure drop, etc.) remaining the same. However, MgO addition did not always result in a gypsum subsaturated operation, and under some conditions the scaling potential was actually increased. The reasons for this, certain other apparent inconsistencies in the data, and how these types of systems can be controlled are not yet fully understood. Efforts are being continued to satisfactorily resolve these important questions.

2. Demonstration of variable load operation on the venturi/spray tower system with lime. The gas rate was adjusted hourly to follow the boiler load over a range of 60-150 MW while the inlet SO_2 also varied from 1400 to 5000 ppm. Sustained runs were made at conditions probably much more severe than would be encountered at most operating plants with no problems of reliability or control of the system. Variable load operation will also be included during the long term reliability runs planned on each scrubber system (one with lime and one with limestone) in which the most promising concepts will be combined for the extended reliability demonstration runs near the end of the current program.

3. Operation with and without fly ash in the system has also been made with both lime and limestone. The major differences noted were in the solids settling rate and the solids dewatering properties. This was true for both lime and limestone operation

---

*These are discussed in more detail in References 1-3.

with filter cake solids averaging 40-50% without fly ash compared to 50-60% with fly ash in the system. When operating without fly ash, there was also a greater tendency for the clarifier overflow to be turbid, and on occasion flocculent addition to the clarifier was even required to maintain a clear overflow for return to the scrubber loop. Some difference was also noted in the pH and SO_2 removal efficiency at a given stoichiometric feed rate. The direction of the difference was opposite to that expected based on the high pH of the effluent from the regular plant fly ash pond which normally has a pH of 10.5-11.0. Without fly ash in the system the pH averaged about 0.2 pH units higher, and therefore the SO_2 removal was also about 5% higher. This is attributed to a higher leaching rate for the acidic components in the fly ash compared to the basic components. In separate tests it was shown that upon standing, Shawnee fly ash/water mixtures first exhibit a lower pH, and with time the pH gradually increases. It is probable that operation without fly ash would lead to lower erosion rates of nozzles, piping, TCA spheres, etc. However, operation has not yet been for extended periods to properly assess this possibility.

4. Factorial tests conducted with both lime and limestone have been very useful in developing and checking the accuracy of the design models for scale-up to full-scale units. The models have also been useful in developing the computerized Shawnee data base and the design/economic study computer program. When completed the design/economic study computer program will be one of the most useful tools for industry, vendors, and engineering firms produced from the Shawnee program. It will readily permit comparisons of capital and lifetime operating costs for essentially all of the equipment and process variations studied during the Shawnee program. The computer program may also be modified to include other types of scrubbers and processes to even further expand its applicability and usefulness.

5. Field evaluation studies to assess techniques for the disposal of power plant flue gas cleaning wastes[4] are also being conducted at Shawnee in parallel with the regular program. Waste material (sludge) produced during operation of the test facility using both lime and limestone as absorbents has been placed in six small disposal ponds on the plant site. Three of the ponds contain untreated wastes; each of the three remaining ponds contain waste that was chemically treated by one of the three contractors (Dravo, Chemfix, and IU Conversion Systems) who presently offer such commercial fixation processes. Test samples of treated and untreated wastes, ground water, surface water, leachate, and soil cores are being analyzed to evaluate the environmental acceptability of current disposal technology.

Results to date indicate that the total dissolved solids in leachate from untreated wastes increase after filling, reaching a peak value equivalent to the input liquor, and then steadily diminish. Leachates from treated wastes exhibit similar characteristics, except the peak value is approximately half the level of the total dissolved solids (TDS) in the input liquor. In addition to a reduction in the leachate TDS, the treated materials also exhibit greatly improved structural stability and, for at least one of the processes, greatly reduced permeability. (These improved physical properties would allow management of disposal operations such that leachate generation can be minimized or eliminated.) Ground water monitoring has shown no change attributable to the ponds. Monitoring will be continued during the balance of the Shawnee program.

6. Peripheral types of studies are also underway or are planned during the Shawnee program. These will not be discussed in detail but include the following (reports listed in the reference section are available for more detail):

   a. A corrosion/erosion study and a mechanical components evaluation program conducted by TVA. (ongoing)

   b. Flue gas characterization study to determine the effect of changes in major operating variables on particulate mass loading and particle size distribution, gaseous and solid sulfates, and on mist eliminator efficiency. (ongoing)

   c. Future studies of alternative scrubber internals, automatic feed control, minimum energy requirements, maximum SO_2 removal efficiency, and variation of limestone type and size. (planned)

SUMMARY AND CONCLUSIONS

With dramatic increases in the use of high sulfur coal reserves being a near certainty in the Administration's developing energy policy, particularly in the eastern half of the country, the widespread use of FGD will play an important role in near term SO_x control strategies. Expanded coal use must be accompanied by sound air and water pollution control measures to minimize threats to human health and to avoid widespread environmental damage.

As the FGD technology most commonly accepted and used by domestic utilities for coal-fired boiler applications, lime/limestone processes are especially important to the success of a policy to rapidly expand coal use. Based on the most recent estimate, 30 FGD systems are presently installed and an additional 94 are in various stages of planning or construction. These 124 units represent almost 50,000 MW of electric generating capacity, most of which will be in service by the early 1980's. Of these, 78 have already selected lime/limestone processes and an additional 25 have not yet selected a process type.

The major concerns of the utility industry to date regarding lime/limestone scrubbing have centered around scaling and plugging potential, the large quantities of by-product sludge generated, and the high costs (capital and operating) of scrubbing. It is toward these areas of concern that the Shawnee program has been directed.

The Shawnee program has made major contributions toward improvement of lime and limestone scrubbing technology in the areas of reliability, variable load operation, system control, sludge disposal techniques, and process economics. The most significant results to date include:

- Demonstration has shown that conventional lime/limestone systems can be operated reliably. Two separate reliability problems have been identified--scaling and soft, mud-type solids deposits, and methods to control each have been demonstrated.
- Soft, mud-type solids deposition was shown to be a strong function of alkali utilization. At high alkali utilization (greater than about 85 percent) these solids are much more easily removed, and very infrequent intermittent fresh water wash is adequate for their complete removal in restricted areas such as the mist eliminator where accumulation can lead to plugging problems.

- Several equipment or process variations were demonstrated to improve alkali utilization. This is particularly significant for limestone where alkali utilization is typically about 60-70% and can be increased to 85-95%, or comparable to that normally obtained with lime. This not only improves reliability, but also reduces costs by permitting the use of a much less expensive alkali feed material and by substantially reducing the quantity of by-product sludge produced.

- The ability to operate during widely varying boiler load and inlet SO_2 concentrations for extended periods was demonstrated on the venturi/spray tower system using lime with no reliability or system control problems. This has long been a major concern of utilities for lime/limestone FGD systems.

- Addition of MgO to either lime or limestone systems has shown that a substantial increase in SO_2 removal efficiency can be obtained, and also indicates a good potential for forcing operation into the gypsum unsaturated mode. However, further work is needed to fully understand how to design and control such a system for subsaturated operation to avoid potential problems.

- The initial results of staged scrubber forced oxidation studies at Shawnee appear very promising. The ability to simultaneously obtain both high alkali utilization (over 90%) and essentially complete oxidation of sulfite to sulfate (gypsum) opens up numerous possibilities for further reducing costs and quantity of sludge produced while maintaining or even improving operating reliability.

- Data generated during the factorial testing have been very useful in developing and checking the accuracy of the design models for scale-up to full-scale lime/limestone systems. The models have also been useful in developing other valuable tools for industry such as the computerized Shawnee data base and the design/economic study computer program. Furthermore, all of these will have increased value as they are expanded to include additional data and other equipment and process variations.

Although substantial progress and significant improvement have been made over the past several years in lime/limestone scrubbing, to be of practical use to industry, results of research and development efforts must be accepted and applied by the utilities and FGD system vendors. Acceptance and application of the Shawnee results by several of the major FGD system vendors has recently been more apparent, but this area of technology transfer to commercial application by utilities has, unfortunately, been sluggish. Consequently, a positive, applications-oriented program involving a higher degree of participation and coordination by EPRI, the utility industry, and FGD system vendors is now being considered as a means of overcoming the apparent reluctance to accept and apply pilot plant and prototype results to commercial size units. The Shawnee prototype test facility will in all likelihood play an important role in this program continuation.

REFERENCES

1. Bechtel Corporation, "EPA Alkali Scrubbing Test Facility: Summary of Testing Through October 1974." EPA-650/2-75-047 (NTIS No. PB 244-901), June 1975. The results of the initial test program from March 1972 to October 1974 are presented in this report.

2. Bechtel Corporation, "EPA Alkali Scrubbing Test Facility: Advanced Program - First Progress Report." EPA-600/2-75-050 (NTIS No. PB 245-279/AS), September 1975. The results of advanced testing from October 1974 through April 1975 are presented in this report.

3. Bechtel Corporation, "EPA Alkali Scrubbing Test Facility: Advanced Program - Second Progress Report." EPA-600/7-76-008 (NTIS No. PB 258-783/AS), September 1976. The results of advanced testing from June 1975 through mid-February 1976 are presented in this report.

4. Aerospace Corporation, "Disposal of Flue Gas Cleaning Wastes: EPA Shawnee Field Evaluation Initial Report." EPA-600/2-76-070 (NTIS No. PB 251-876/AS), March 1976. The results of the field evaluation program from September 1974 through July 1975 are presented in this report.

5. EPA Technology Transfer Capsule Report, "First Progress Report: Limestone Wet-Scrubbing Test Results at the EPA Alkali Scrubbing Test Facility."

6. EPA Technology Transfer Capsule Report, "Second Progress Report: Lime/Limestone Wet-Scrubbing Test Results at the EPA Alkali Scrubbing Test Facility."

7. EPA Technology Transfer Capsule Report, "Third Progress Report: Lime/Limestone Wet-Scrubbing Test Results at the EPA Alkali Scrubbing Test Facility," EPA-625/2-76-010.

FIELD MEASUREMENTS OF PARTICLE SIZE DISTRIBUTION WITH INERTIAL SIZING DEVICES*

N. G. Bulgakova, L. Ya. Gradus, and S. S. Yankovskiy

Abstract

The authors describe the design, principal of operation, and calculation of units used in the U.S.S.R. for determining the dispersion composition of particles under industrial conditions. The following are considered: impactors, two-cyclone separator, and rotational analyzer. Procedure is given for impactor calibration that is based on the graphoanalytic method for determining the parameters of the fractional characteristic of stages starting with the known parameters of polydispersed dust. Results are presented from the comparison of three methods with respect to each other under laboratory and industrial conditions. These are also compared with the classical methods for dispersion analysis involving samples taken beforehand. It is shown that the error of inertial methods in determining particle size under industrial conditions does not exceed ± 15 percent with respect to the average median diameter. A method is recommended for evaluating the reproducibility of the results obtained with one unit under identical conditions.

Efficiency of dust collection by electrostatic precipitators is influenced by particles having a diameter less than 5 μm. Traditional methods of particle sizing use a dust sample on a filter and then disperse it in a liquid media (sedimentation column or in Coulter counter) or in a gas stream (in Gonnel device or BAHCO centrifuge). In the course of these processes aggregates may disintegrate into component particles and this distorts test results. On the contrary, very small particles (less than 1 or 2 μm) may aggregate in the liquid media in the course of analysis, which leads to overestimating of real particle sizes.

In order to avoid the above-mentioned faults of the traditional particle sizing methods, several devices have been developed recently. In these devices an aerosol is fractionated during the sampling itself. These devices include: impactors, in which separation process takes place in the space of small dimensions, each stage consisting of a nozzle with deposition surface placed opposite it; cyclone separators, which allow considerable amount of fractional particulate to accumulate; and the rotary dust analyzer, in which aerosol sample is separated into fractions when passed through rotating cylinder, with particles depositing on the inner walls of this cylinder.

There are two main types of impactors: the first has converging nozzles (Brink impactor) and the second has nozzles in the form of openings in a thin plate (Andersen impactor and NIIOGAZ impactors used in the U.S.S.R.).

The advantage of the Andersen Impactor lies particularly in the fact that according to Stokes Law, particles are exposed to a considerably lesser blowing effect of flow due to the small opening diameter. On the other hand, these devices are suitable only for low dust concentration (up to 1 g/m³) because of the clogging of small diameter openings by particulate matter. The Brink impactor permits sampling at dust concentration up to 10 g/m³.

---

*For further information regarding the material in this paper, please contact I.K. Reshidov, U.S.S.R. 113105, Moscow, M-105, 1-st Nagatinsky Pass., 6, NIIOGAZ.

The construction of the NIIOGAZ impactor is based on the Andersen principle of a set of perforated disks provided with openings serving as nozzles for the next stage and with substrate-filled grooves relating to the previous stage to minimize dimensions of the device and to minimize the weight of the particulate settled, both opposite the nozzles and on the internal surfaces.

In order to retain particles deposited opposite a nozzle, the surface is usually greased with a thin silicon oil layer. In NIIOGAZ impactors a layer of lubricant (ref. 1) consisting of a mixture of fine powder with highly-distilled oil (an allowable temperature of heating is 60° to 70° C) is used. Under higher temperatures a layer of thermostable fibrous material (ref. 2) able to retain deposited particles is inserted in the groves on the plates.

A particle size distribution is determined from the deposit mass on different stages of a device. When calculating this distribution a fractional efficiency curve for each stage is approximated by a vertical line passing through cut-off diameter d_{50}. Value of d_{50} is determined from Stokes relation (ref. 3):

$$d_{50}^2 = \frac{MD}{V} StR_{50} = \frac{MD^3}{Q} StR_{50}$$

where StR_{50} = value of Stokes number referred to d_{50},

V = velocity of gas flow in the nozzle,

P = density of particles,

M = gas viscosity,

D = nozzle diameter,

Q = gas flow rate through the device.

As d_{50} is constant for impactor stages of a fixed geometry, equation (1) can be used for caluclation of $(d_{50})_{exp}$, referred to experimental conditions, by the formula using a value of $(d_{50})_{cal}$ being found as a result of calibration:

$$(d_{50})_{exp} = (d_{50})_{cal} \, A \, \frac{M}{QP}$$

where $A = \frac{Qcal.Pcal}{Mcal}$ = const.

(Here Q_{cal}, M_{cal}, and P_{cal} are gas flow rate, its viscosity, and density particles under calibration conditions.)

Fractional characteristics and d_{50} values for separate impactor stages, which were obtained by calibration and with the use of a thin grease layer, cannot immediately coincide with that obtained for impactors provided with glass fiber substrate or oil-impregnated powder. A method for comparing the calculated and experimental values of d_{50} was developed. According to this method particles are deposited on the same substrate and in the same amount as during field tests. The method is based on placing two identical calibrated disks in pairs and on the assumption that both fractional characteristics and particle size distribution curve are governed by lognormal law.

Two parameters of fractional characteristic (i.e., cut-off diameter d_{50} and standard deviation σ_{fr}) can be obtained with the aid of two parameters of particle size distribution (i.e., mass median diameter dp and standard deviation σ_p) and of the efficiency values found for the first (η_1) and second (η_2) identical stages. For this a special nomogram is used. On this nomogram two families of curves corresponding to equal values of (η_1) and of (η_2), respectively, are plotted and with abscissa and ordinate axes values of $lg\sigma_p llg\sigma_{fr}$ and $lg(d_{50}/dp/)lg\sigma_p$, respectively, placed. The unknown parameters of the fractional characteristic d_{50} and σ_{fr} are found as the abscissa and ordinate values of the crossing point of two curves corresponding to η_1 and η_2 measured during experiments.

The cyclone separator includes two impactor stages for preliminary collection of the coarsest particles and two cyclones of 32 and 16 mm diameter respectively with a filter at the outlet. For the calculation of particle size distribution presented as two parameters of the lognormal distribution (d_p and σ_p), three nonograms with equiefficiency curves for each separation stage are used (ref. 4). On the nomogram axes, corresponding values of d_p and σ_p are put. Parameters of the particle size distribution can be found as an abscissa and an ordinate of the crossing point of the three curves corresponding to the values of the efficiency for each stage, being measured in the course of experiment.

Nomograms were plotted by calibrating the device stages.

The rotationary dust analyzer consists of the rotating cylinder enclosed in a casing. For convenient usage, cylindrical thin-walled sections whose length increases downstream are inserted. These sections, made of aluminum foil, are to be weighed before and after sampling. Coarse particles are settled on the first stages and the smaller ones on the next stages.

At the device outlet a fiberglass filter is placed. Particle size distribution is calculated using the weight gains of the dusted sections with the aid of the Avdoev method (ref. 5). Rotational device calibration was performed by passing monodispersive glass spheres of different diameters through the device.

The comparison of results obtained by the different inertial devices as well as by common methods based on preliminary dust sampling was carried out under laboratory and field conditions.

In one series of such investigations the inertial devices were placed into stack and, in another one, the sample was air-suspended by a fluidized bed laboratory dust feeder followed by an orifice. The feeder is filled with a mixture of sand and powder. Air-suspended dust was additionally disaggregated when passing through the narrow slit orifice with the velocity of 150 m/s to 200 s/s. The unbranched aerosol stream flowed through the fractionating device.

Under field conditions, samples were taken by impactor, cyclone separator, and/or rotationary analyzer simultaneously. The inlet sections of sample probes placed in a duct were situated approximately on the same plane at the distance of 100 mm from one another. The results of comparative measurements of particle size distribution are presented as points with coordinates corresponding to mass median diameter d_p and standard deviation σ_p (in all cases size distribution was approximated by lognormal law).

Cyclone separator, impactor, rotating analyzer, air separation (in Gonnel apparatus), and liquid sedimentation (including pipette method) were compared; the results are shown in figure 1.

Four illustration points referring to the same sample having been analyzed by different methods are connected by straight lines.

As can be seen in figure 1 there is a good agreement between mass median diameter and standard deviation values, which was measured by inertial sizing devices and air separation method (in Gonnell device for fly ash of Cherepetskaya GRES (power station) and for magnesite dust).

On the other hand, disagreement between mass median diameter values for dolomite and zinc oxide dusts having approximately the same values of standard deviation is large. The agreement in the first two cases can be explained by the fact that the dust is loose and its mean particle size is greater than 10 μm. Such dust easily disaggregates during the air separation.

The mentioned disagreement between the analyses resulting for the dust sampled directly from the stack and for resuspended dust confirms the assumption that coarse dust moves in ducts in aggregated form. The disagreement of the result for zinc oxide and dolomite dust is explained by the particle aggregate in Gonnell apparatus. Thus, the Gonnell method gives overestimated particle sizes. This confirms a well-known fact that only particles larger than 5 to 7 μm may be processed by Gonnell separation.

An agreement between results obtained by liquid sedimentation and cyclone device in Nizhne-Turinskaya GRES is explained by the fact that coarse fly ash particles with diameters of more than 40 μm remain unagglomerated both in the gas stream and in liquid sedimentation.

For carbide furnace dusts, sedimentation analysis for equal geometrical mean size leads to more narrow particle size distribution (the small standard deviation value) than three cyclone separators and impactor. The narrowing of distribution of the finest and coarsest fractions reflects an underestimating. Underestimated content of the smallest fraction can be explained by its coagulation in the course of sedimentation and the underestimated content of the

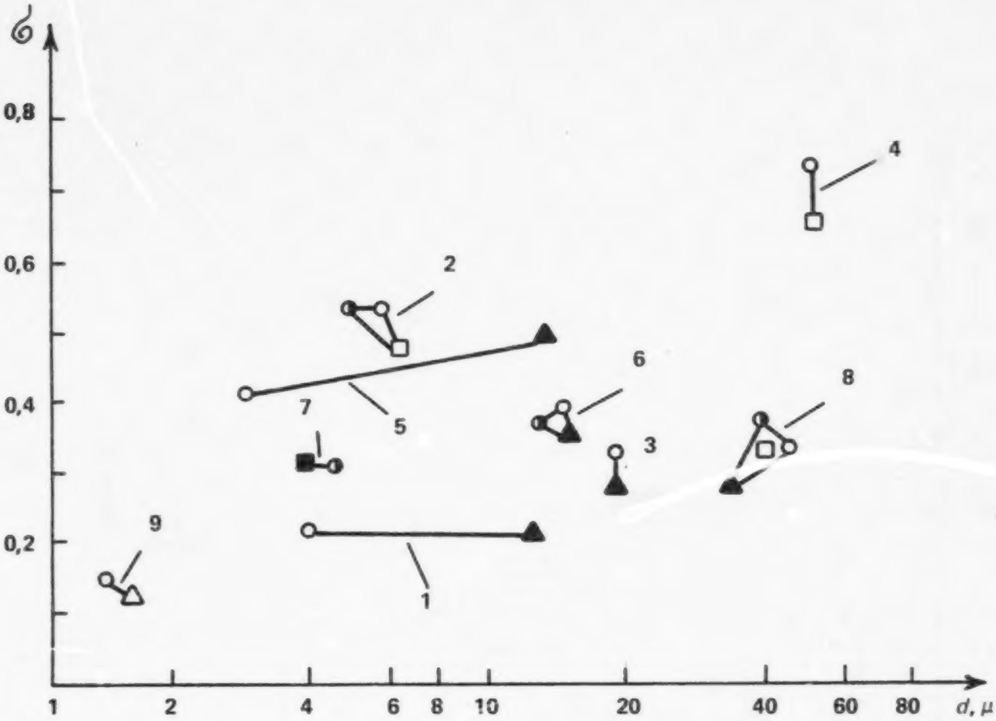

Figure 1. Comparison of size distribution data for particulates and mists by several methods.

1 – dolomite dust (at ESP outlet)
2 – particulates of blast-furnace gases
(at carside furnace outlet)
3 – Cherepetsk power station ash
4 – Lower-Turin power station ash
5 – zinc particulates of sulfur acid production
6 – magnesia dust (at cyclone outlet)
7 – quartz particulate matter
8 – coal dust
9 – tarry mist

o – cyclone separator
Δ – air separation
– pipette method
o – NIIOGAZ impactor
– liquid sedimentation
Δ – microscopy

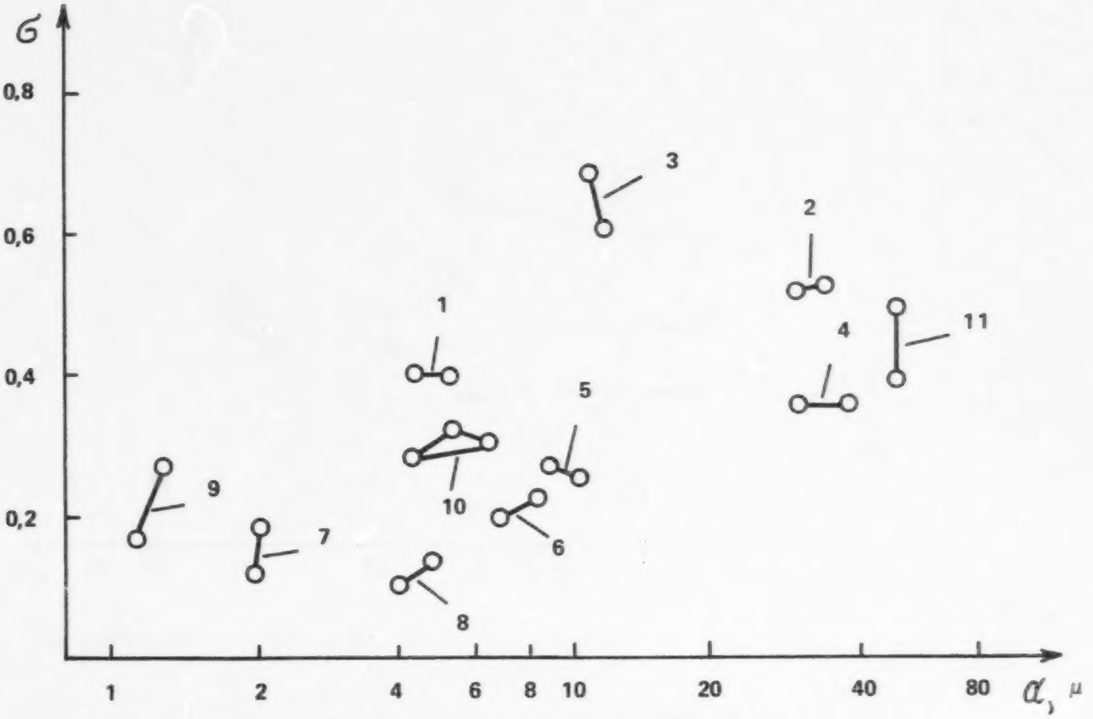

Figure 2. Comparison of results of aerosol particle size distribution using inertial devices.

1 – electrolysis particulates
2 – dolomite dust (at the ESP inlet)
3 – Baltic power station ash
4 – hydrophobic chalk
5 – corund M10
6 – mixture of spores and likopodia
7 – dried droplets of sodium salt solutions
8 – mist of transformator oil
9 – dioctilphtalate mist
10 – corund M7
11 – corund M20

o – cyclone separator
o – rotary analyzer
o – impactor

largest fractions is due to the destruction of the aggregates in the course of sedimentation. In cyclone separator and impactor these aggregates remain unchanged.

In figure 2 the results of simultaneous measurements of particle size distribution by impactor, cyclones, and rotary analyzer conducted in ducts are shown. According to the results obtained, mass median diameters differ from one another by not more than ± 15 percent. The disagreement in standard deviation is not more than 20 percent.

In order to evaluate the reproducibility of results obtained by the same inertial device, measurements with the corund powder were conducted under laboratory conditions. As an example, the results of five impactor measurements are presented in figure 3. A scattering area can be limited by two straight lines having the same angle of incline. In this case a scattering zone can be presented by only one parameter, i.e., d_p (σ = const). The latter can be considered as a measure of results scattering. Thus, an error can be presented as a deflection ± Δdp from the mean value d_p. For example, according to figure 3, we have $d_p \pm \Delta d_p = 5.7 \pm 0.5$ μm. This method can be used for evaluation of reproducibility of results obtained by the same device under the same conditions.

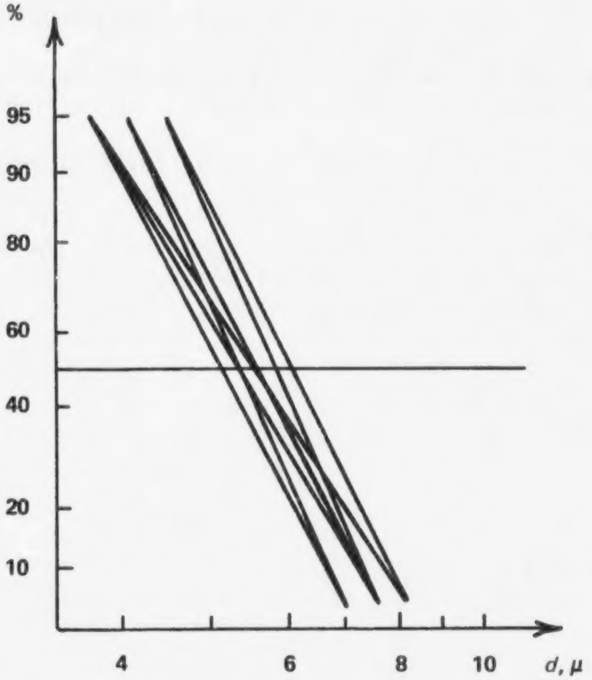

Figure 3. Variation of results for 5 size corund powder distributions obtained under equal conditions using the NIIOGAZ impactor.

REFERENCES

1. A. A. Rusanov and S. S. Yankovskiy, "Greasing in Order to Hold Particles on a Hard Surface," Author Certificate No. 197344 issued 17,04,67.

2. Yu. V. Abrosimov, A. A. Rusanov, and S. S. Yankovskiy, "Multistage Impactor for Weight Dispersion Analysis," Author Certificate No. 261772 issued 28,06,68.

3. A. Berner, "Staub-Reinhalt," Luft, 1972, No. 8.

4. N. G. Bulgakova and S. S. Yankovskiy, "Graph Method for Determining the Fractional Efficiency Curve of Cyclones and Dispersion of Dust," Theoretical Bases of Chemical Technology, Moscow, 1971, No. 5.

5. A. A. Rusanov and S. S. Yankovskiy, "Impactors for Determining the Dispersion Composition of Industrial Dust," Literature Survey of TSNIITEneftekhim, Moscos, 1970.

BIBLIOGRAPHY

Bulgakova, N. G., and S. S. Yankovskiy, "Cyclone Separator for the Dispersion Analysis of Industrial Dust, Express-Information," Series KhM-14, No. 2, TSINTIkhimneftemash, Moscow, 1976.

Skryabin, G. M., "Rotational Analyzers of the Dispersion Composition of Industrial Dust," Literature Survey of TSINTIkhimneftemash, Moscow, 1973.

Yankovskiy, S.S., and L. Ya. Gradus, Calculating and Calibrating NIIOGAZ Impactors with Flat Stages, Scientific Technical Collection of Works

"Industrial and Sanitary Gas Cleaning," Moscow, TSINTIkhimneftemash, 1975, No. 3.

Bulgakova, N. G., L. Ya. Gradus, and S. S. Yankovskiy, Low Rate Dust Feeder, Scientific-Technical Collection of Works, "Industrial and Sanitary Gas Cleaning," Moscow, TSINTIkhimneftemash, 1973, No. 3.

SIZING TECHNIQUES FOR SUBMICRON PARTICLES

Wallace B. Smith and D. Bruce Harris*

Abstract

The size distribution of submicron particles suspended in process streams can be measured with cascade impactors, electrical mobility analyzers, or diffusion batteries and condensation nuclei counters. If samples are to be taken for analysis of composition, then the impactor would be used. On sources where the size distribution is stable, the electrical mobility analyzer yields data quickly and conveniently. If temporal variations in the particle-size distribution are of interest, the diffusional system is most useful.

The electrical mobility analyzer and diffusional system both require that most process streams be cooled and diluted before the sample is taken. The sample conditioning procedure is difficult and special care must be taken to avoid serious errors. Line losses due to diffusion and turbulent deposition limit the useful size range to 0.01 to 2 μm diameter.

Data are shown for several pollution sources where these methods were used in conjunction with ordinary cascade impactors to obtain particle-size distributions from 0.01 to over 10 μm diameter.

INTRODUCTION

The size distribution of submicron particles suspended in process streams can be measured with cascade impactors, electrical mobility analyzers, or diffusion batteries and condensation nuclei counters. If samples are to be taken for analysis of composition, then the impactor would be used. On sources where the size distribution is stable, the electrical mobility analyzer yields data quickly and conveniently. If temporal variations in the particle-size distribution are of interest, the diffusional system is most useful.

The electrical mobility analyzer and diffusional system both require that most process streams be cooled and diluted before the sample is taken. The sample conditioning procedure is difficult and special care must be taken to avoid serious errors. Line losses due to diffusion and turbulent deposition limit the useful size range to 0.01 to 2 μm diameter.

In this paper, each of the three sizing methods is described; a sample extraction and dilution system is also described; and some experimental results are shown.

---

*Dr. Smith is with the Southern Research Institute in Birmingham, Alabama, and Mr. Harris is with the Environmental Protection Agency, Industrial Environmental Research Laboratory, Research Triangle Park, North Carolina.

SAMPLING PROCEDURES

Cascade Impactors

It is possible to extend the sizing capability of cascade impactors to submicron particles by operating the device at pressures of 0.01 to 0.1 atmospheres. If all operating parameters except the pressure are held constant, the cut point, or D_{50}, is inversely proportional to the slip correction factor:

$$D_{50} \alpha L - \frac{1}{2}.$$

Since C increases rapidly with pressure, cut points of 0.02 μm or less can be obtained. Pilat (ref. 1) has developed and tested a low pressure impactor for sampling from process streams.

Figure 1 shows the sampling train used by Pilat in his experiments. Two impactors are operated in series. The first impactor is a conventional design with cut points from about 0.3 to 20 μm diameter. The second impactor is operated at reduced pressure with cut points from about 0.03 to 0.2 μm diameter. The sampling train contains a low pressure drop condenser; a double vane, leakless, high vacuum pump; a control box with pressure gauges, thermocouple pyrometers, and valves; and a dry gas meter. A 90-mm diameter filter holder is used downstream from the second impactor. The maximum flow rate is approximately 50 l/min.

Figure 2 shows typical data reported by Pilat for tests made at the outlet of an electrostatic precipitator installed on a coal-fired electric generating plant.

Sample Extraction and Dilution

Although in situ sampling is preferred, this is not possible with the electrical and diffusional apparatus, which are designed for laboratory use. Figure 3 is a schematic diagram of an aerosol extraction-dilution system which has been used successfully on several field tests. A 15 l/min sample flow is removed nonisokinetically from the process stream through a rigid probe, and a heated, flexible hose into a heated chamber that contains a cyclone, sample metering orifices, and diffusional adsorbers. Large particles are removed by the cyclone and the excess air is vented to atmosphere. The low flow rate sample, which is to be diluted, passes through a calibrated orifice into the diluter. If the formation of a fine aerosol by condensation is observed, the sample must first be passed through a series of diffusional absorbers containing activated charcoal. A Polonium-210 (500 mC) ionizer is used in the diluter to neutralize any electric charge that may exist on the particles. The sample gas enters the dilution chamber at the apex of a perforated cone into which clean, dry air is pumped through the perforations, creating a turbulent mixing zone. At a downstream point, after adequate mixing has occurred, the diluted sample is extracted and conveyed to the sizing instrument. Sample and dilution airflow rates are controlled by means of two bleed valves.

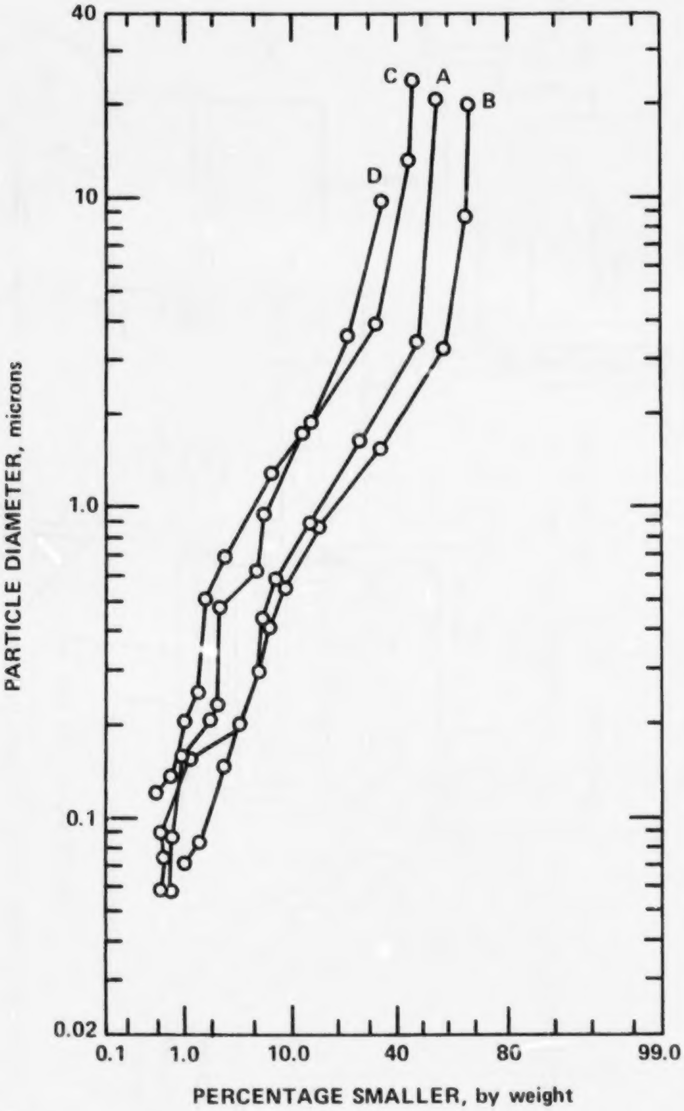

Figure 1. Impactor sampling train for sampling from 0.02 to 20 μm diameter particles (ref. 1).

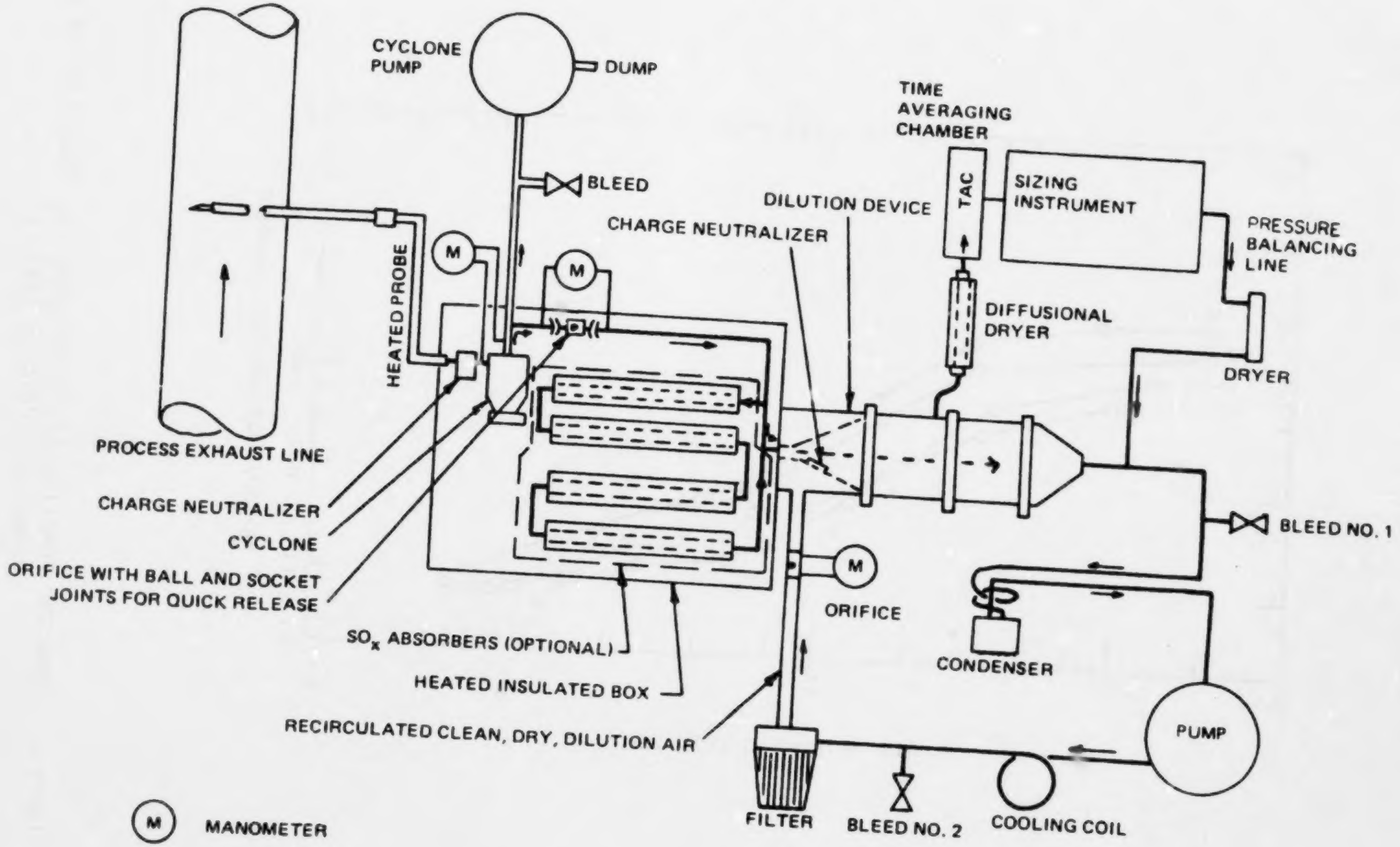
CYCLONE PUMP
DUMP
BLEED
TIME AVERAGING CHAMBER
TAC
SIZING INSTRUMENT
PRESSURE BALANCING LINE
DILUTION DEVICE
CHARGE NEUTRALIZER
DIFFUSIONAL DRYER
DRYER
HEATED PROBE
M
PROCESS EXHAUST LINE
CHARGE NEUTRALIZER
CYCLONE
ORIFICE WITH BALL AND SOCKET JOINTS FOR QUICK RELEASE
BLEED NO. 1
ORIFICE
CONDENSER
SO$_x$ ABSORBERS (OPTIONAL)
HEATED INSULATED BOX
RECIRCULATED CLEAN, DRY, DILUTION AIR
PUMP
FILTER
BLEED NO. 2
COOLING COIL
M MANOMETER

Figure 2. Size distributions measured at outlet of electrostatic precipitator on 175 MW coal-fired utility power generating plant (ref. 1).

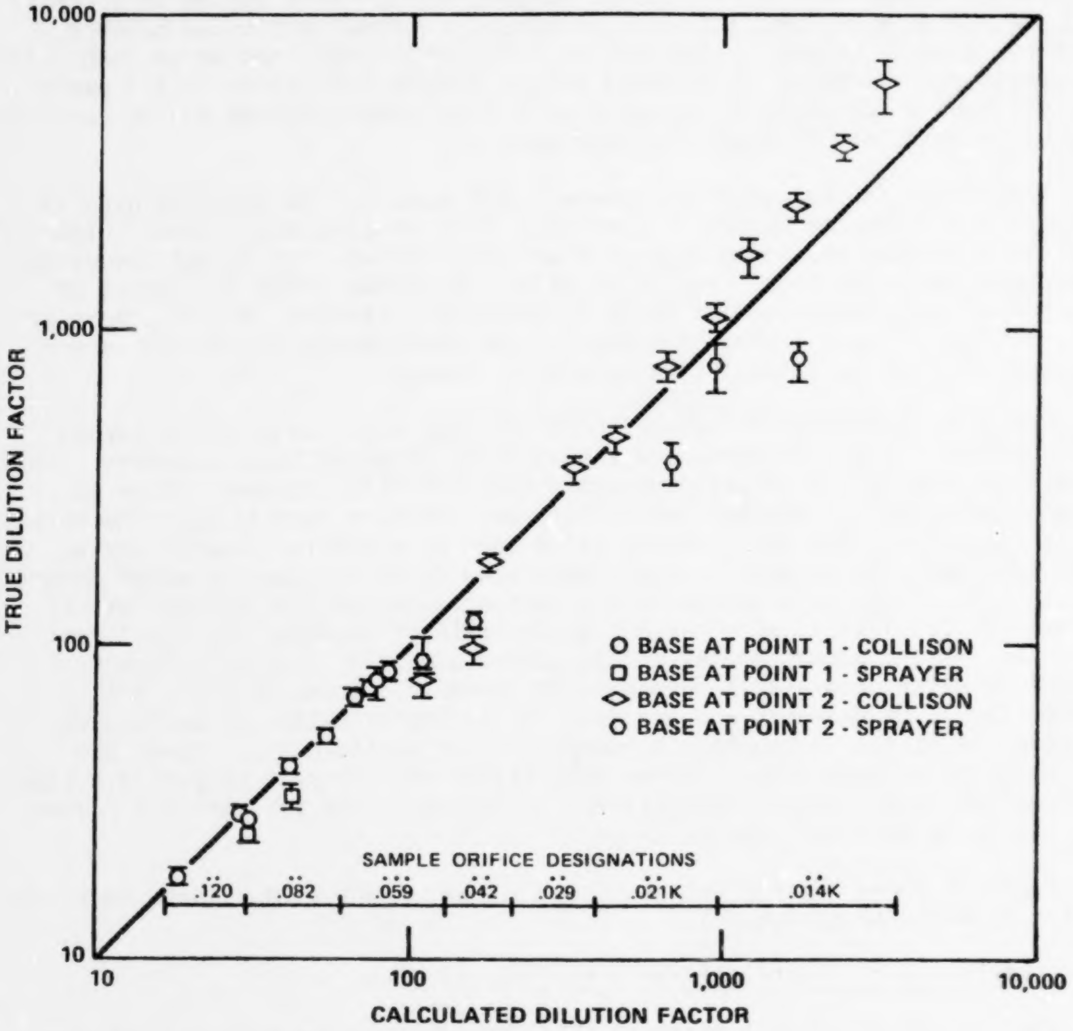

Figure 3. A sample extraction-dilution system for submicron particles.

Figure 4 is a graph showing calibration data for the sample extraction-dilution system. It can be seen that the calculated and measured dilution agree very well for 0.15 µm diameter particles. Aerosol dilution is required for both the diffusional and electrical mobility systems described in the following paragraphs.

Sizing Particles by Diffusion

Diffusion bateries may consist of long, narrow, rectangular channels in parallel, a cluster of small diameter tubes (ref. 2), or a series of screens (ref. 3). Figure 5 shows a typical rectangular channel diffusion battery which contains 98 channels, each 0.1 cm wide, 10 cm high, and 48 cm long. As the sample aerosol moves in streamline flow through the channels, the particles diffuse to the walls at a predictable rate, which depends on the particle size, flow rate, and diffusion battery geometry.

Variations in the number of channels and aerosol flow rate are used as means of measuring the number of particles in a selected size range. Figure 6 is a block diagram showing a typical field test system. It is only necessary to measure the total concentration of particles at the inlet and outlet of each diffusion battery configuration in order to calculate the particle-size distribution. Figure 7 shows the theoretical performance curves for several configurations at an aerosol flow rate of 6 l/min.

Particle concentration measurements are made with condensation nuclei (CN) counters. These counters are essentially automated cloud chambers. They operate by drawing the aerosol through a humidification chamber, where it becomes saturated for ambient temperature and pressure conditions. The aerosol is then pulled through a rotary valve into an expansion chamber where adiabatic expansion produces a super-saturated condition causing water droplets to grow on the particulate in the aerosol. The droplet growth rate of the smaller droplets is more rapid than the rate of increase for the larger particles. Thus, after several milliseconds, a more or less monodisperse aerosol of water droplets is formed in the chamber. These droplets are greater than 1 µm diameter and are detected by light scattering techniques. The response of the CN counter is independent of particle size; thus, the instrument is said to have a linear sensitivity with respect to particle size. This uniform sensitivity is also linear in concentration for particle concentrations up to about 10^5 particle/ cm^3.

Figure 8 shows typical data taken at a power plant with cascade impactors and the diffusional system.

Sizing Particles by Electrical Mobility (ref. 4)

The electrical aerosol analyzer (EAA) operates on the concept that there is a monotonic decrease in electrical mobility with increasing particle size for submicron particles that are exposed to a homogeneous ion field.

The EAA is shown schematically in figure 9. As a vacuum pump draws the aerosol through the analyzer, a corona generated by a high voltage wire within the charging section gives the sample a positive electrical charge.

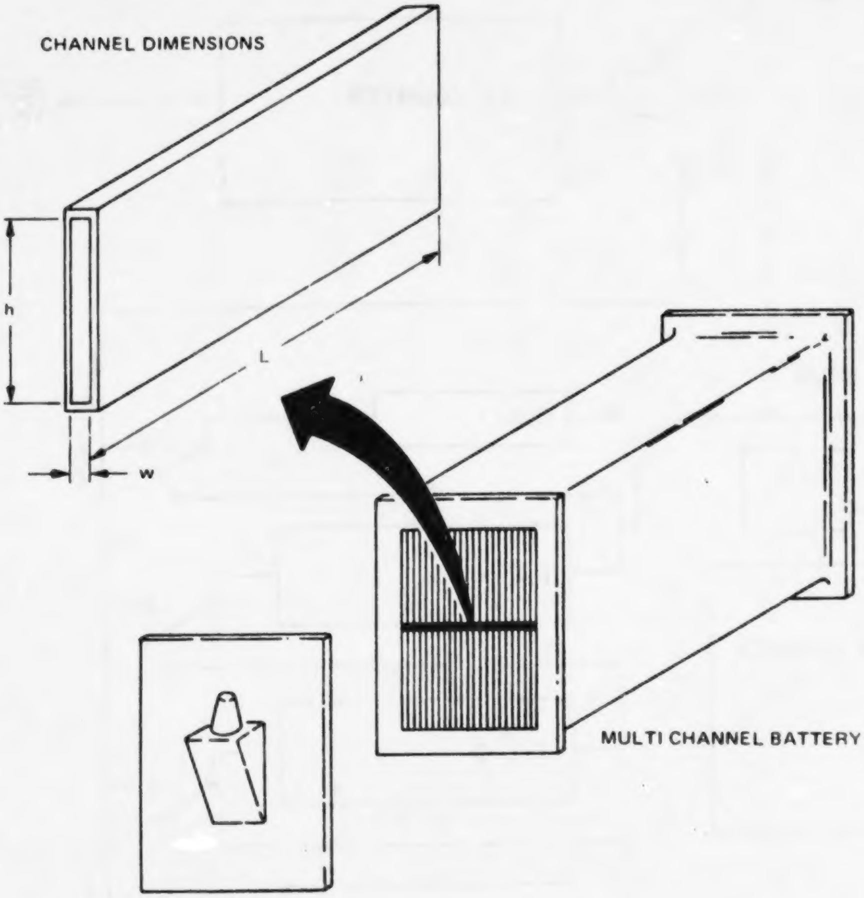
CHANNEL DIMENSIONS
h
L
w
MULTI CHANNEL BATTERY

Figure 4. Calculated dilution versus true dilution for the sample extraction-dilution system, 0.15 μm diameter particles.

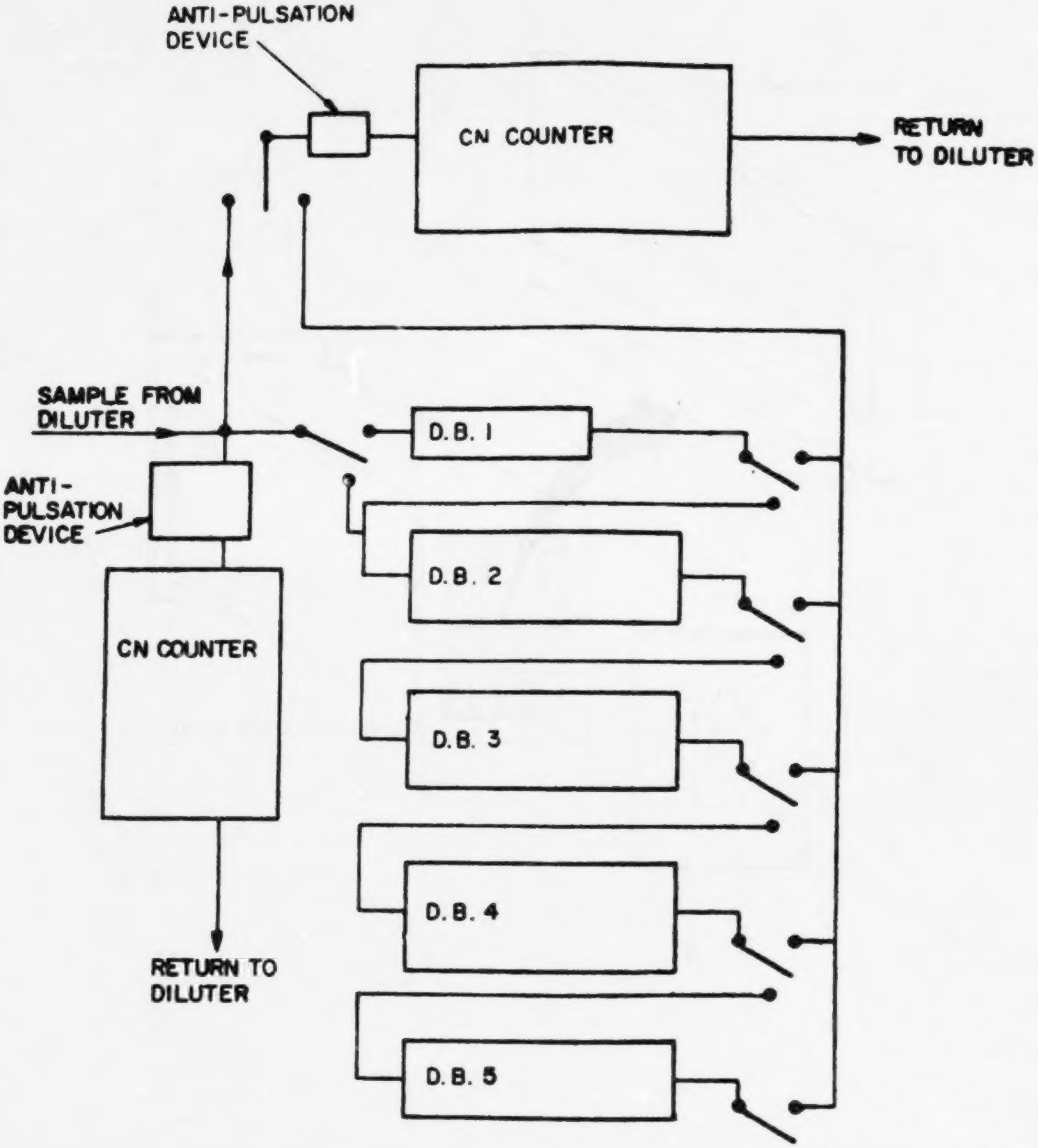
ANTI-PULSATION DEVICE
CN COUNTER
RETURN TO DILUTER
SAMPLE FROM DILUTER
D.B. 1
ANTI-PULSATION DEVICE
D.B. 2
CN COUNTER
D.B. 3
D.B. 4
RETURN TO DILUTER
D.B. 5

Figure 5. A typical rectangular channel diffusion battery.

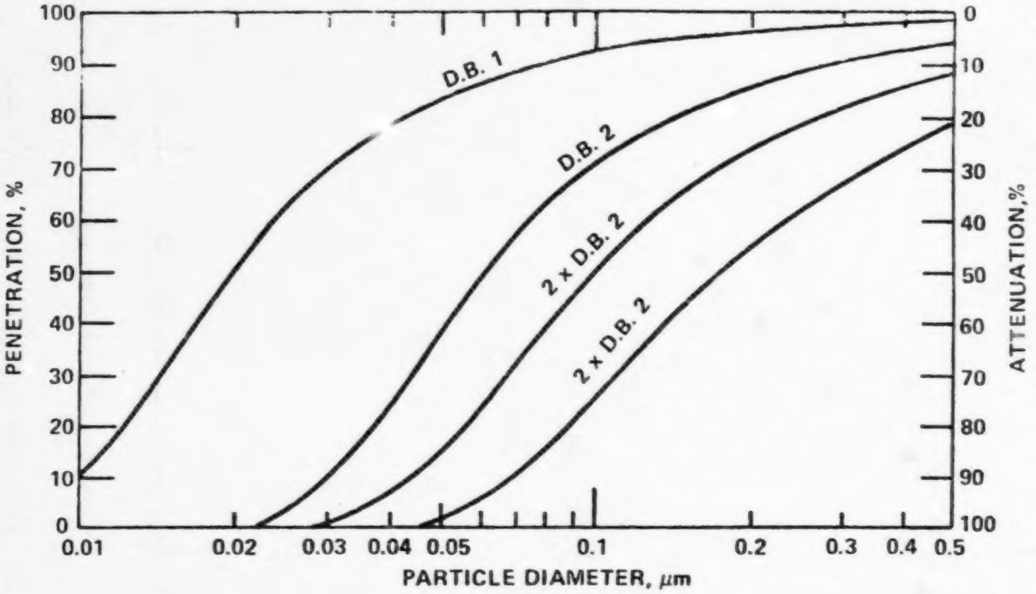

Figure 6. Block diagram of a diffusional sizing system.

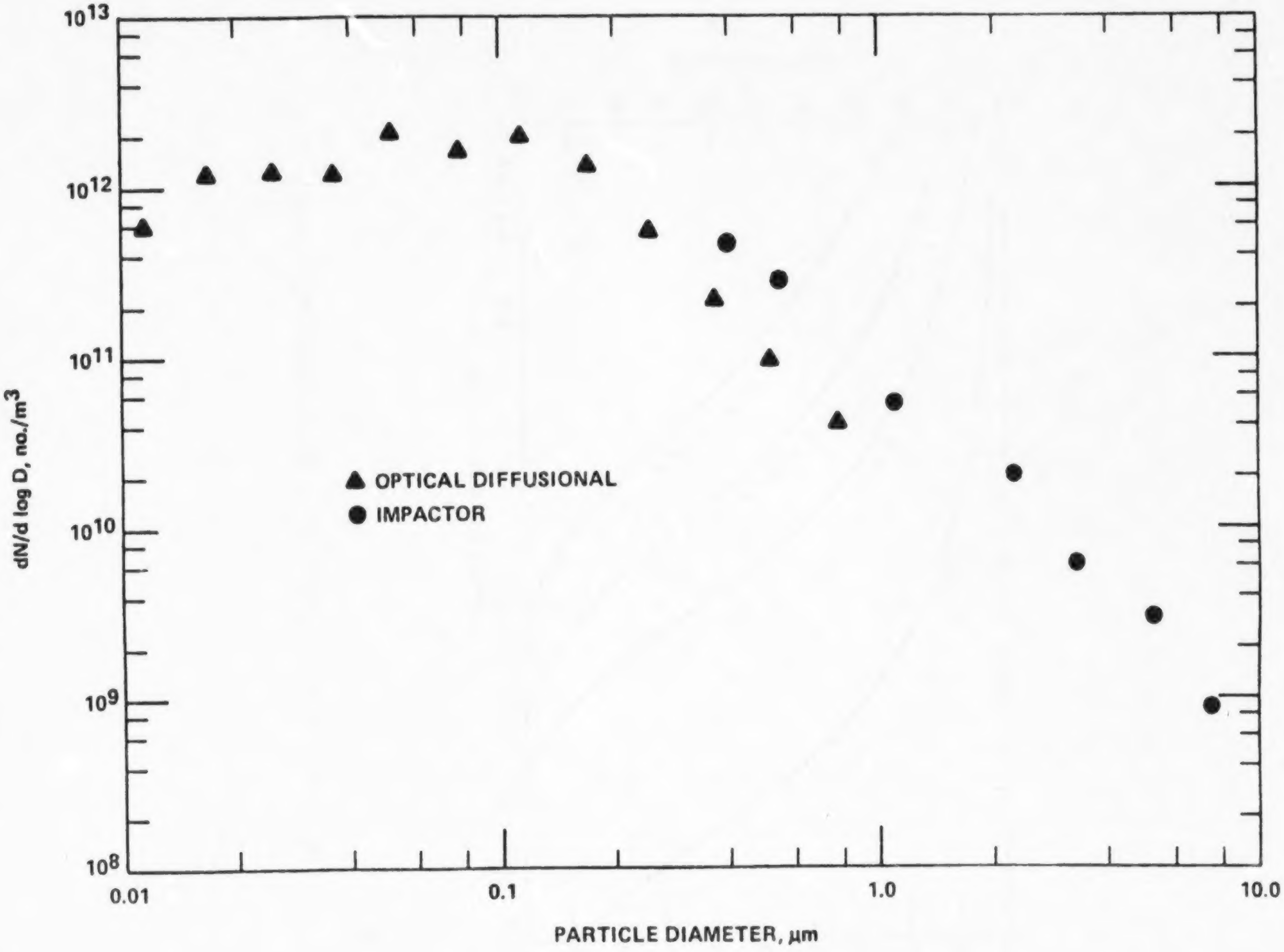

Figure 7. Theoretical diffusion battery penetration curves. D.B. 1 consists of 13 channels, 0.1 × 10 × 48 cm. D.B. 2 consists of 98 channels of the same dimensions.

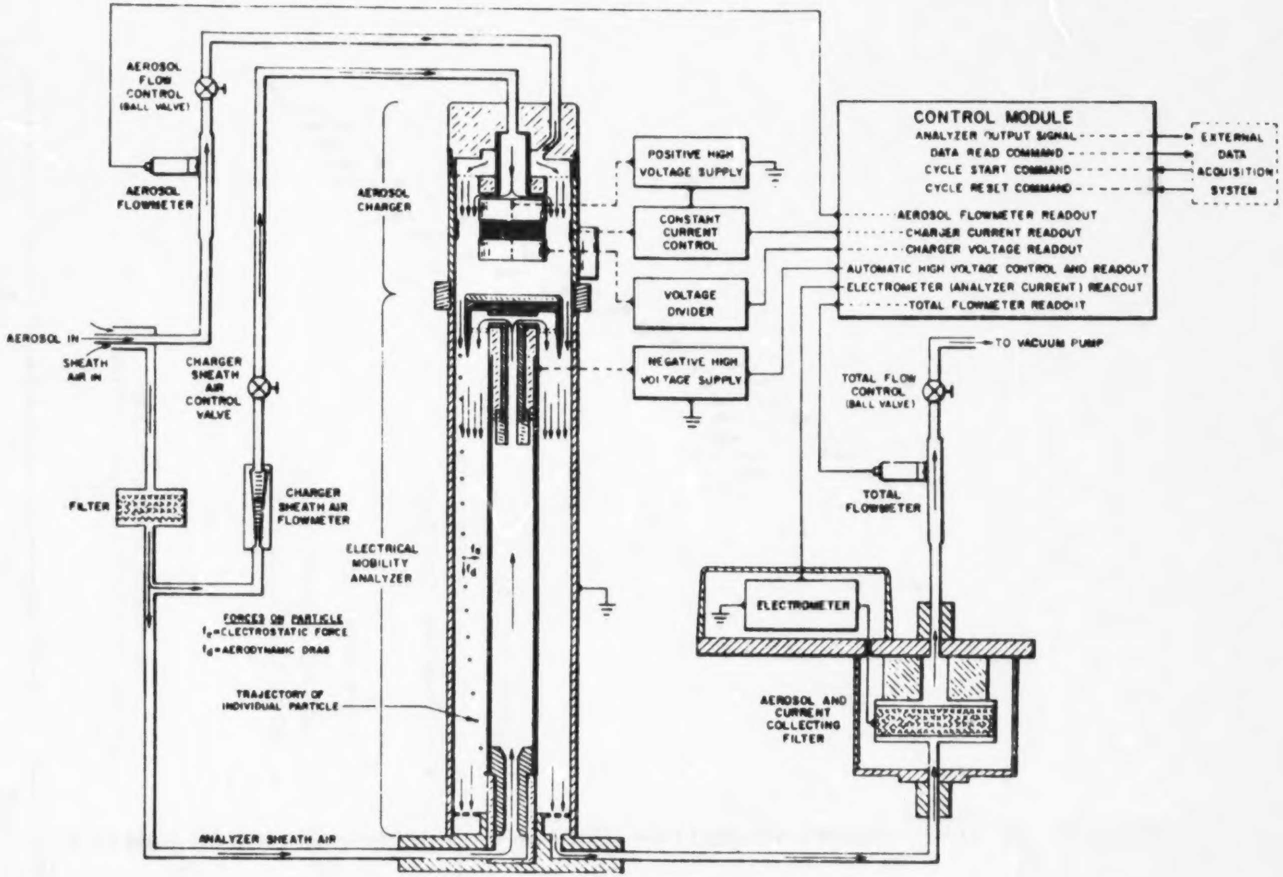
AEROSOL FLOW CONTROL (BALL VALVE)
AEROSOL FLOWMETER
AEROSOL IN
SHEATH AIR IN
CHARGER SHEATH AIR CONTROL VALVE
FILTER
CHARGER SHEATH AIR FLOWMETER
AEROSOL CHARGER
ELECTRICAL MOBILITY ANALYZER
FORCES ON PARTICLE
f_e=ELECTROSTATIC FORCE
f_d=AERODYNAMIC DRAG
TRAJECTORY OF INDIVIDUAL PARTICLE
ANALYZER SHEATH AIR
f_e
f_d
POSITIVE HIGH VOLTAGE SUPPLY
CONSTANT CURRENT CONTROL
VOLTAGE DIVIDER
NEGATIVE HIGH VOLTAGE SUPPLY
CONTROL MODULE
ANALYZER OUTPUT SIGNAL
DATA READ COMMAND
CYCLE START COMMAND
CYCLE RESET COMMAND
AEROSOL FLOWMETER READOUT
CHARGER CURRENT READOUT
CHARGER VOLTAGE READOUT
AUTOMATIC HIGH VOLTAGE CONTROL AND READOUT
ELECTROMETER (ANALYZER CURRENT) READOUT
TOTAL FLOWMETER READOUT
EXTERNAL DATA ACQUISITION SYSTEM
TO VACUUM PUMP
TOTAL FLOW CONTROL (BALL VALVE)
TOTAL FLOWMETER
ELECTROMETER
AEROSOL AND CURRENT COLLECTING FILTER

Figure 8. Particle-size distribution measured at a power plant by diffusional analysis and cascade impactors (E.S.P. Outlet).

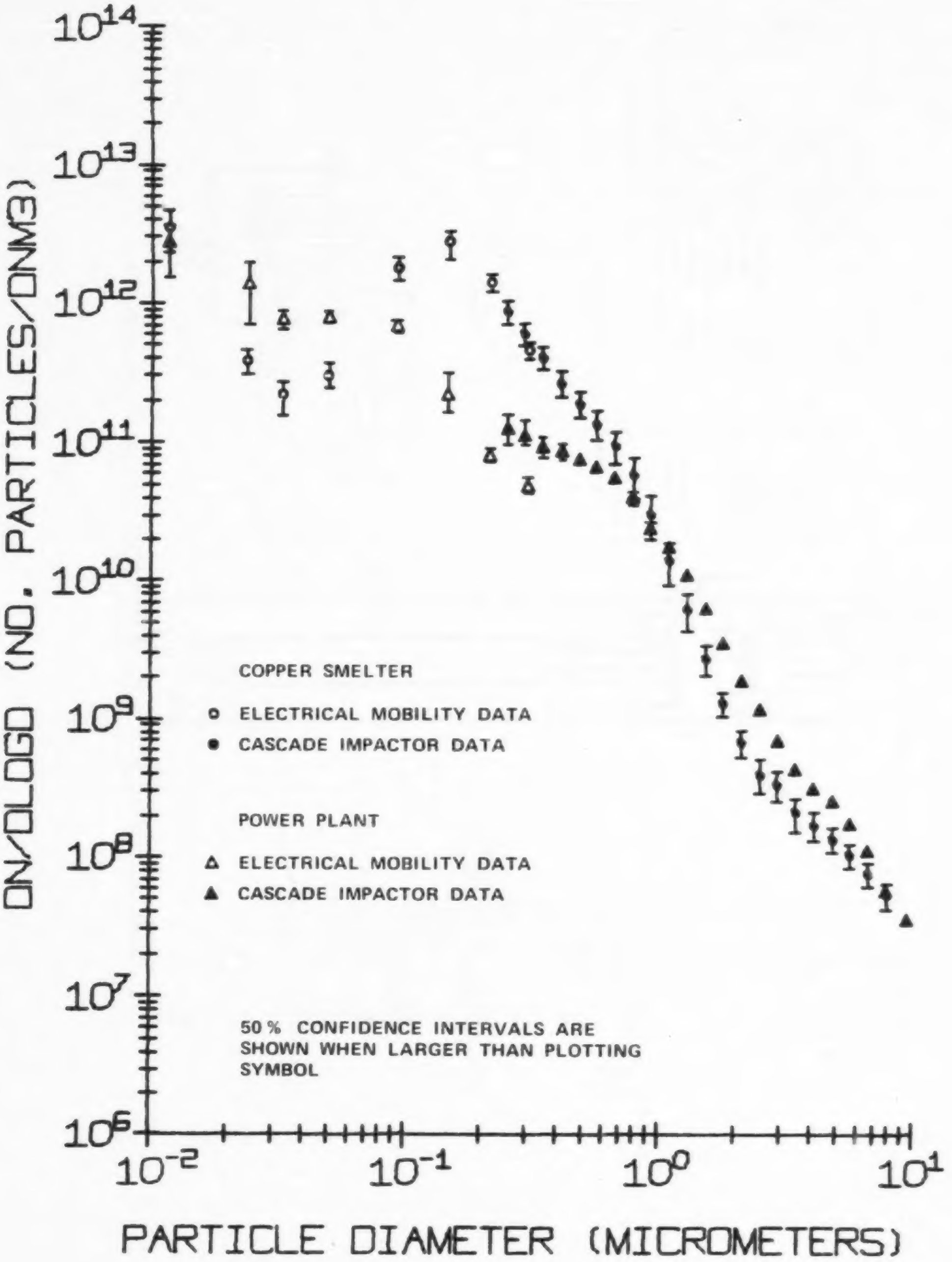

Figure 9. Schematic of the electrical aerosol analyzer (ref. 4).

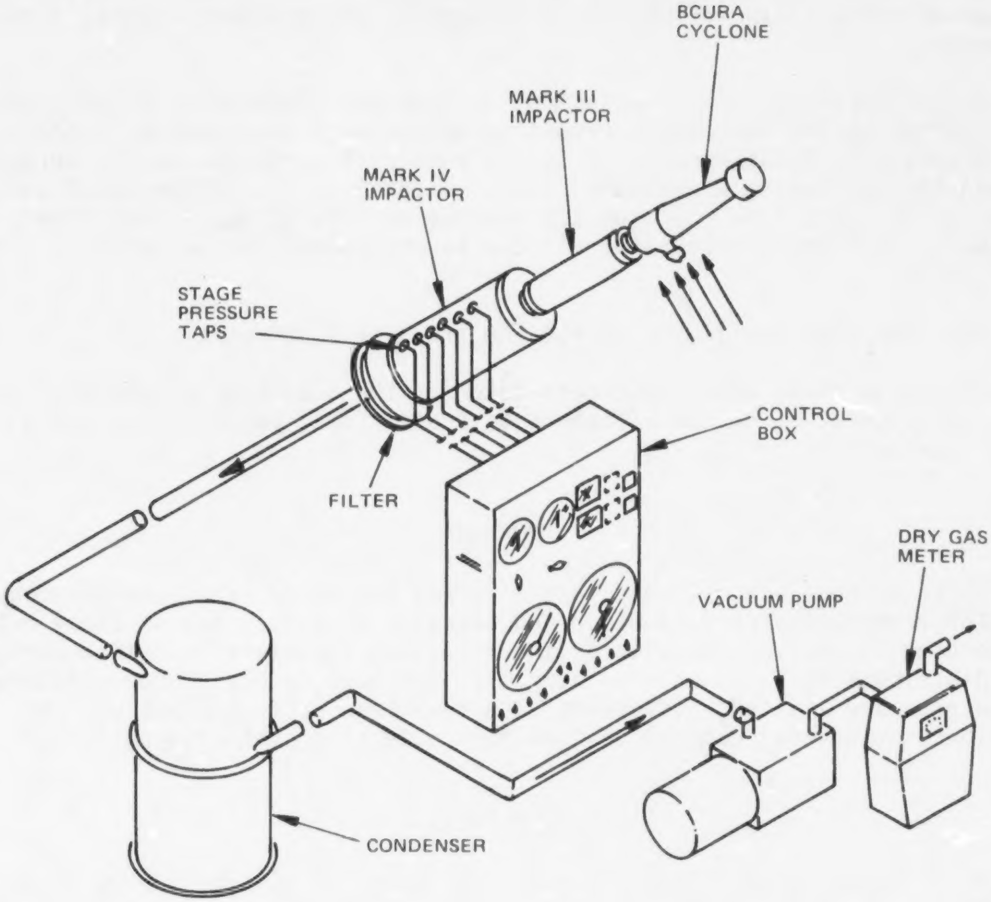
BCURA CYCLONE
MARK III IMPACTOR
MARK IV IMPACTOR
STAGE PRESSURE TAPS
CONTROL BOX
FILTER
DRY GAS METER
VACUUM PUMP
CONDENSER

Figure 10. Particle-size distributions measured by the electrical mobility method and cascade impactors (E.S.P. Outlet).

The charged aerosol flows from the charger to the analyzing tube section, which is an annular volume of aerosol surrounding a cylinder of clean air. A metal rod, to which a variable, negative voltage can be applied, passes axially through the center of the analyzer tube. Particles smaller than a certain size, with highest electrical mobility, are drawn to the collecting rod when the voltage corresponding to that size is on the rod. Larger particles pass through the analyzer tube and are collected by a filter. The electrical charges on these particles drain off through an electrometer, giving a measure of current.

A step increase in rod voltage will cause particles of a larger size to be collected by the rod with a resulting decrease in electrometer current. This decrease is related directly to the number of particles in the aerosol between the two discrete particle sizes. A total of 11 voltage steps divide the 0.032 to 1.0 μ size range of the instrument into 10 equal logarithmic size intervals. Different size intervals can be programmed via an optional plug-in memory card.

The concentration limits of the EAA are 1 to 1,000 $\mu g/m^3$.

Figure 10 shows field test data taken at the outlet of electrostatic precipitators operating on the effluents of a coal-fired power boiler and a copper smelter.

SUMMARY

Three methods are now used in the United States to size submicron particles for control device evaluation and emission studies. Any of these methods can be used in conjunction with ordinary cascade impactors to define particle-size distributions in industrial aerosols from 0.01 to over 10 μm. Although the methods are limited, sufficient data have been obtained to study the efficiency of several control devices for collecting submicron particles.

REFERENCES

1. M. J. Pilat, G. M. Fioretti, and E. B. Powell, "Sizing of 0.02 to 20 Micron Particles Emitted From Coal-Fired Power Boiler With Cascade Impactors," presented at APCA-PNWID Meeting, November 20, 1975, Vancouver, B. C.

2. A. J. Breslin, S. F. Guggenheim, and A. C. George, "Compact High Efficiency Diffusion Batteries," Staub (in English), 31(8), 1971, pp. 1-5.

3. D. Sinclair. "A Portable Diffusion Battery," Am. Ind. Hygiene Assoc. J., 36(1), 1975, pp. 39-42.

4. B. Y. H. Liu, K. T. Whitby, and D. Y. H. Pui, "A Portable Electrical Aerosol Analyzer for Size Distribution Measurements of Submicron Aerosols," presented at the 66th annual meeting of the Air Pollution Control Association, Paper No. 73-283(1973).

DUST RESISTIVITY AND REVERSE CORONA FORMATION IN ELECTROSTATIC PRECIPITATORS*

I. K. Reshidov, Yu. I. Sanayev, I. A. Kizim

Abstract

In this paper the authors study the reasons for the appearance of back corona in electrostatic precipitators. Procedures are described for measuring dust resistivity under industrial conditions. Two modifications are given of a device for measuring resistivity developed at the Semibratov branch of NIIOGAZ that make it possible to form a dust layer in the clearance between comb-type electrodes in a gas duct or directly on the precipitator electrode. Basic methods are studied for reducing back corona intensity by using design factors and conditioning.

One of the major problems in electrical gas cleaning is to increase collection efficiency of high resistivity dust. A great number of studies are being undertaken by Soviet and foreign scientists in this respect.

It is known that passing of corona current through an electrode covered with a high resistivity dust layer is accompanied by a voltage drop across the layer U_1. U_1 can be approximately expressed as:

$$U_1 = E_1 \cdot d = P_\nu \cdot J \cdot d \qquad (1)$$

where E_1 = field intensity, v/m
d = thickness of ash layer, m
P_ν = ash specific resistivity, ohm/cm
J = density of corona current passing through ash layer, a/m^2.

Due to the voltage drop in the dust layer, the voltage in the interelectrode space decreases. This results in a reduction of the corona current and in a deterioration of dust precipitation. When dust specific resistivity is high enough, E_1 reaches such a value, at which sparkover occurs and corona discharge of the reverse sign appears in the layer.

A method to detect reverse corona in ESP was suggested in the U.S.S.R. (ref. 1). It lies in comparing volt/ampere characteristics taken by increasing and decreasing of the voltage on the electrodes.

Criterium for the existence of back corona is the excess of corona current of descending curve over the current of ascending curve. Reverse corona time lag can account for the hysteresis character of volt/ampere characteristics.

---

*For further information regarding the material in this paper, please contact I. K. Reshidov, U.S.S.R. 113105, Moscow, M-105, 1-st Nagatinsky Pass., 6, NIIOGAZ.

This method is now widely used when industrial electrostatic precipitators collecting high resistivity dust are investigated.

Because back corona is highly dependent on dust specific resistivity, it is very important to study factors influencing the value of specific resistivity. Besides, investigations of high resistivity dust precipitation aimed at forecasting ESP performance efficiency require the true value of specific resistivity to be known.

The value of dust specific resistivity is influenced by the particle size distribution and the density of the ash layer, the electric field intensity, and conditions of taking measurements.

Presently, there are several methods to measure specific resistivity value that basically differ in the way the dust layer is deposited. Dust layer is brought on the electrode usually by hand or in the field of corona discharge. There are installations where dust deposition is done mechanically by filtration through metailceramics or by high-efficiency cyclones of small diameter.

To measure dust specific resistivity under industrial conditions, an apparatus of the "cyclone" type is applied (ref. 2). It consists of a small-sized, high-efficiency cyclone and resistivity transducer located in cyclone's hopper. The transducer's measurement system consists of coaxial cylindrical electrodes. An instrument for measuring resistivity is used as a secondary one.

It was found experimentally that the value of specific resistivity is considerably dependent on the degree of dust layer packing, level of applied voltage, and density of corona current that passes through the dust layer (ref. 3).

Simm (ref. 4) thinks that dust specific resistivity should be measured at currents preceeding sparkover of the layer. Experimental data relating the specific resistivity of an ash from near-Moscow coal to the corona current density passing through a layer (ref. 5), shows that high measurements errors can appear when the value of P_V is determined by the instrument for resistivity measurements when the electrode is put on the ash layer. Such measurements do not allow one to judge the critical value of specific resistivity, in the best case they can give an idea about the order of magnitude of the measured value. That is why measurement to determine the critical value of P_V, at which reverse corona can appear, should be conducted at current densities close to values typical for industrial ESP.

As a method to determine specific resistivity of dust, the one dealing with dust deposition due to electric field in corona discharge is preferable. To reduce measurement errors connected with the fact that electrodes are put on the layer and the layer packs, the layer should be of a given thickness, as is done, for example, in a Lurgi instrument (ref. 6).

For research purposes, NIIOGAZ is using two modifications of the instrument for dust resistivity measurements.

The measuring part of the instrument for specific resistivity measurement (figure 1) consists of two electrodes located in one plane forming a comb-type gap. When high voltage is supplied, the gap is filled with dust. The value of specific resistivity is measured when high voltage is cut off.

The second modification of the instrument (figure 2) allows one to measure specific resistivity of the dust layer formed directly on the precipitating electrode of the ESP under investigation.

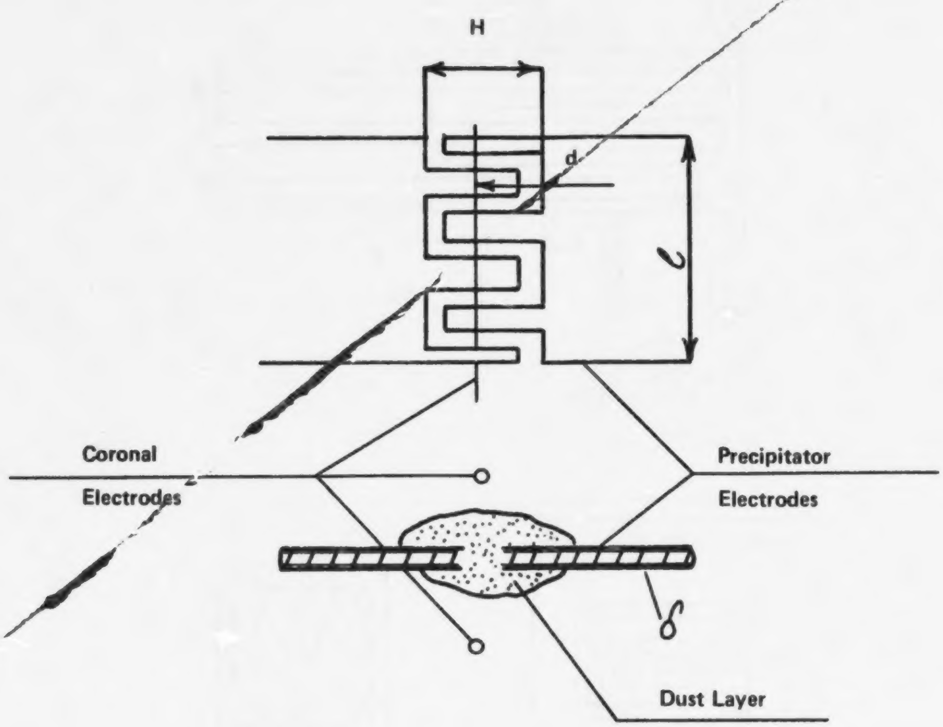

Figure 1. The measuring part of the device for evaluation of electrical dust resistivity.

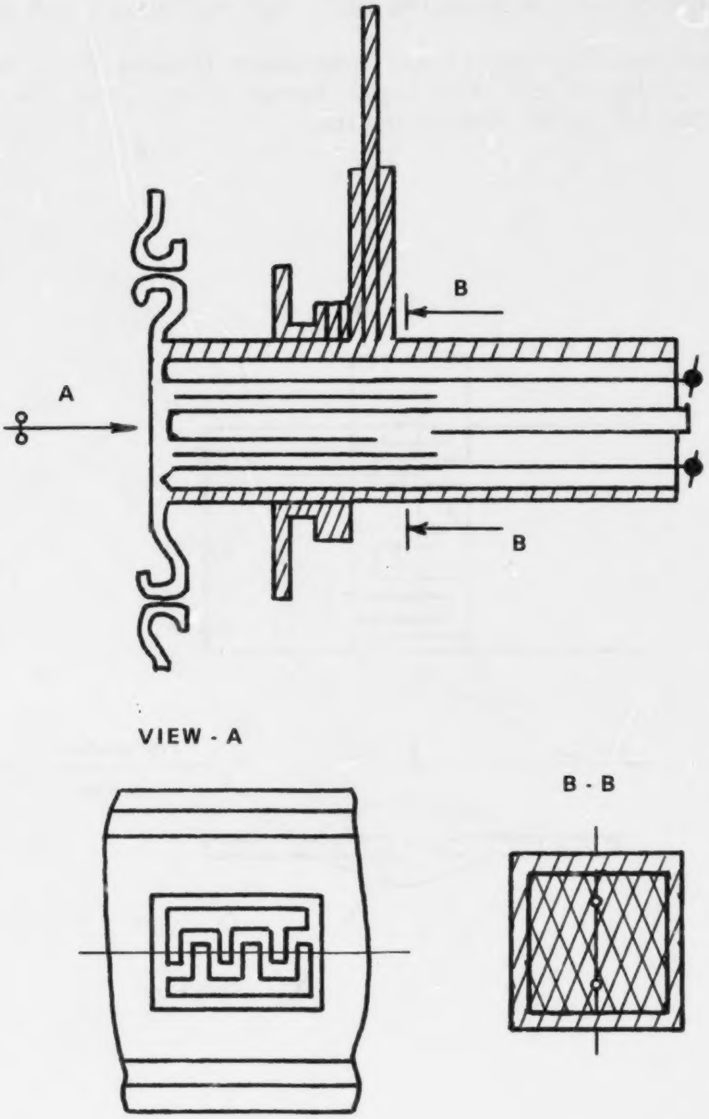
B
A
B
VIEW - A
B - B

Figure 2. A scheme of the device for measuring electrical resistivity in the active zone of the ESP.

Application of these instruments allowed us to obtain comparable data when the electrostatic precipitators utilized in various industry branches were tested. Table 1 gives an example of measuring specific resistivity.

It was found out experimentally that the most intense reverse corona occur in the last electric fields of ESP. This can be connected with the fact that the largest or conductive particles (underburnt matter) are collected in the first ESP fields. That is why it is very interesting to see the relationship between particles size distribution or other physical and chemical properties of dust and its conductivity. For that purpose, experiments were undertaken to determine dust conductivity at the outlet of pilot-commercial ESP where reverse corona is not formed and at the outlet of ESP DGPN-55-2 type under the conditions of reverse corona.

Comparison of data given in table 1 shows that dust resistivity at the outlet of pilot precipitator (OPE) exceeds the ash resistivity at the inlet by more than an order of magnitude.

Table 1. Measuring Specific Resistivity

Place and conditions of measurements	Mean specific resistivity value, ohm/m	Mean-square error, ohm/m	Coefficient of variation, %
At the inlet to the pilot ESP (OPE) t = 135° C	2.87×10^9	0.25×10^9	8.9
At the outlet of the pilot ESP (OPE) t = 130° C	4.4×10^{10}	0.37×10^{10}	8.4
At the inlet to ESP DGPN-type t = 150° C	8.3×10^9	0.7×10^9	8.5
At the outlet of ESP DGPN-type t = 145° C	2.8×10^{10}	0.3×10^{10}	10.7

Figure 3 gives particle size distribution at the outlet and inlet to ESP. Here one can see considerable difference in particle size. But in this case it is rather difficult to account for the difference in dust resistivity due only to the difference of particle size distribution while it's known that there is a considerable quantity of underburnt matter in ash A-III-type. The measurement gave such values of underburnt matter:

at the inlet - 16.9 percent,
collected - 20 percent,
at the outlet - 24 percent.

Since there is a considerable difference in the underburnt matter content at the inlet and outlet of the apparatus, conductivity of ash could not be identically connected with particle size distribution.

From this point of view, interesting data is found with the measurements of resistivity of ash from near-Moscow coal. The content of underburnt matter in this ash at the inlet is 0.78 percent, in the collected portion it is 0.8 percent, i.e., practically the same and very small. Mean values of ash resistivity at the inlet and outlet of ESP were respectively 8.3×10^{11} ohm/cm and 2.8×10^{12} ohm/cm.

From the above data, one can see a clear connection between granulometric composition of dust and the value of its specific resistivity. Thus, change of particles' median diameter from 20 to 5 μm caused more than a threefold growth of dust resistivity.

Let us consider the main methods to reduce reverse corona intensity. Critical field intensity E_{cr} in the dust layer is determined by the product of ash specific resistivity and corona current density. Therefore, there are two main ways to reduce E_{cr}, and thus reverse corona intensity: (1) reduce ash specific resistivity, or (2) reduce corona current density.

The value of ash specific resistivity is greatly influenced by temperature, humidity of gases, and SO_3 content. It is seen from the relationship of ash specific resistivity to temperature of exhausted gases (relationship has a steep maximum), that ash resistivity can be reduced both by lowering and elevating temperature.

Figure 4 shows how the temperature influences gas cleaning efficiency when the ash from Ekibastuzsk coal is collected. This method is not always suitable in the industrial conditions, since the optimal temperature of the gases exhausted from the boiler is not determined only by ESP performance. Therefore, it is expedient to consider other methods intensifying ESPs' performance when high-resistivity ash is collected.

Conditioning can be provided by feeding steam, spraying water, or moistening raw material, and also by introducing chemical agents. Gas conditioning by moistening is widely spread for the cases when natural moisture content in the gas is low and the gas temperature is relatively high. It was found out that introduction of moisture increases the electrical stability.

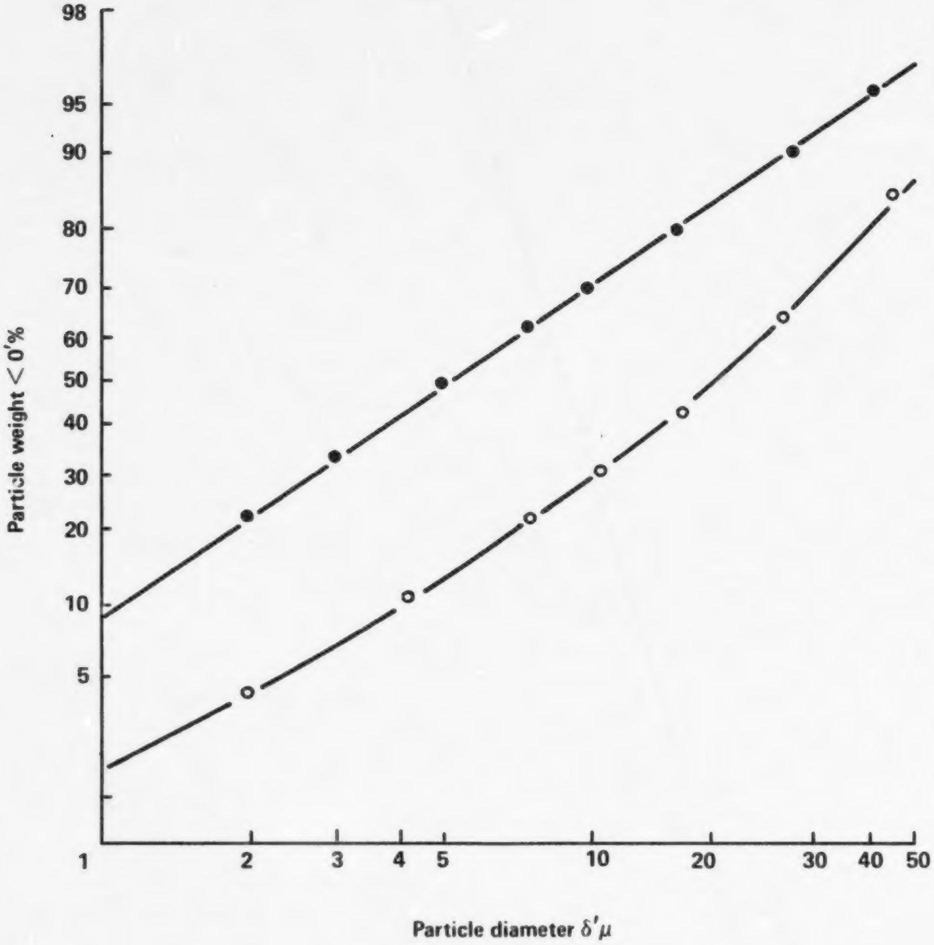

Figure 3. Size distribution of ash particles in the pilot ESP.
1 - at inlet/ 2 - at outlet

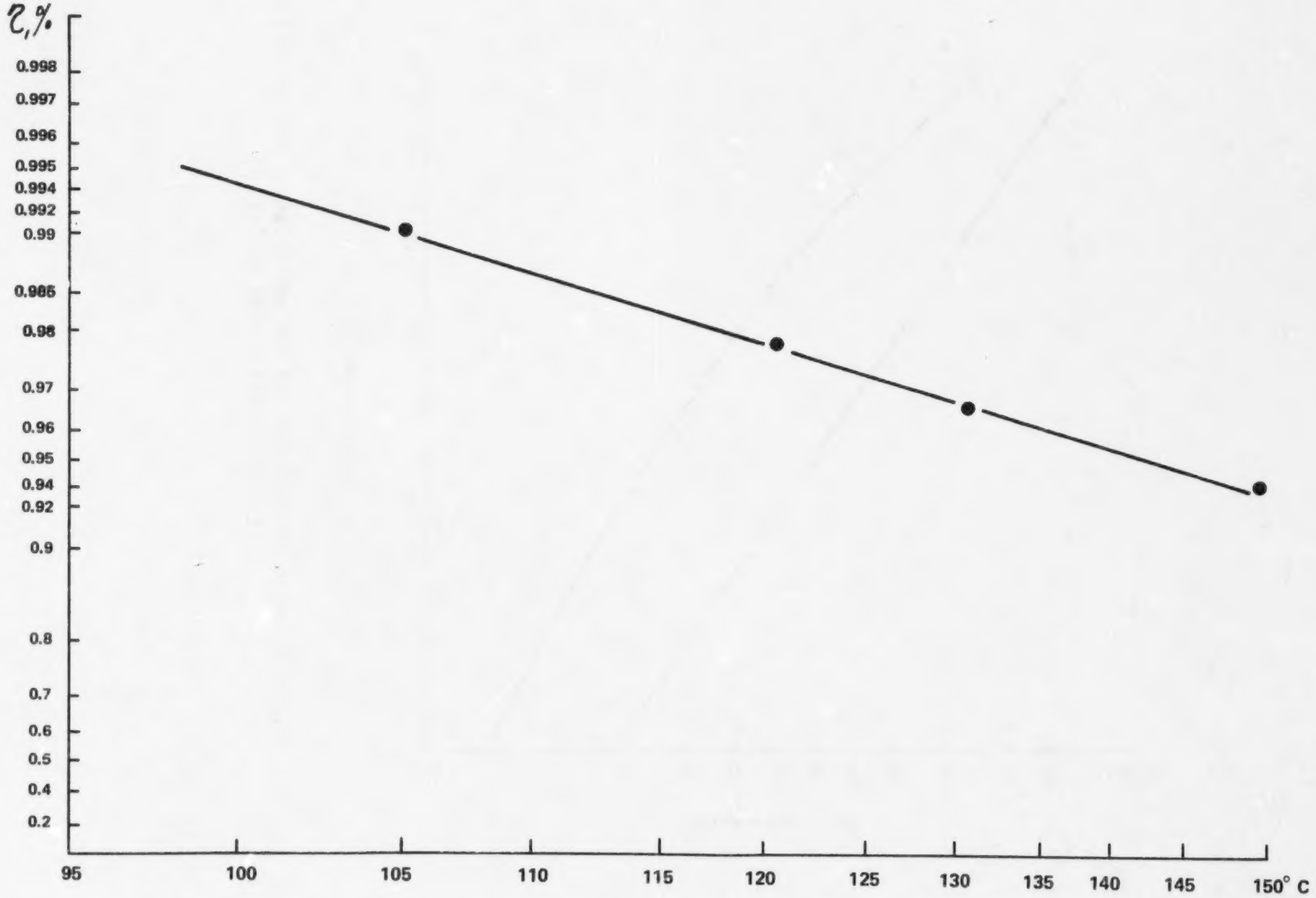

Figure 4. Gas cleaning degree as a function of temperature at collection of ekibastuzsk coal ash.

But conditioning by moistening at power stations causes difficulties because it requires a considerable consumption of steam or water. Besides, at the power stations at sufficiently low temperatures of exhaust gases it is impossible to obtain complete evaporation of water. That causes fallout of liquid droplets in gas ducts, ESPs, fume pumps, and sealing of their surfaces, causing corrosion.

An effective means to increase gas cleaning efficiency is to use chemical conditioning to reduce specific resistivity value. The way that an electrostatic precipitator operates to remove ash from Ekibastuzsk coal when gas is conditioned with ammonia was investigated. When gas velocity was 2.45 m/sec and 30 ppm of ammonia was introduced, cleaning efficiency increased from 96.5 to 98 percent and outlet dust concentration decreased 1.6 times. When in flue gases before the pilot ESP, 8-32 ppm of ammonia was added at a gas velocity of 1.5 m/sec and cleaning efficiency was raised from 88.4 to 94.4-98.3 percent (figure 5).

Experiments have shown that beyond 20-25 ppm, a further increase in ammonia concentration does not lead to an increase in ash precipitation efficiency, i.e., that this concentration should be optimal to condition flue gases for ESP that remove high resistivity ash of Ekibastuzsk coal.

At this ammonia concentration, outlet dust concentration decreased more than sixfold from the normal 0.8 g/m^3. Gas cleaning efficiency increased due to reduction of reverse corona intensity. That can be confirmed by the change of electrical parameters of ESP and by the ash specific resistivity measured in the course of tests. When ammonia was introduced, ash resistivity at the inlet to the ESP reduced by three orders to 6×10^7 ohm/m. Gas conditioning by ammonia allowed a twofold increase in the precipitation rate parameter.

Economic expendiency of ammonia conditioning was proven at the electrostatic precipitators on a 300-MW unit of Troitzkaya Power Station.

Performance of precipitators for removal of high-resistivity dust from clinker kilns for dry cement production is accompanied by intense reverse corona. Conditioning of gases by water was applied to increase collection efficiency. When the gases' humidity increased from 4 to 10 percent, voltage in the ESP became 10-12 kV higher. Specific resistivity measured by an instrument of ICP-type/dust precipitation on a comb-shaped electrode in the electric field decreased, when moistened by 1-1.5 orders, to 9×10^8 ohm/m.

Reverse corona intensity that is indirectly determined by loop square between ascending and descending volt/ampere characteristics decreased. Gas cleaning efficiency increased from 93 to 98.5 percent.

Although gas conditioning was effective in increasing gas cleaning efficiency in this case, the required efficiency was not obtained. To increase collection efficiency of high resistivity dusts, design methods were studied, alongside the above mentioned ones, that could be called technological.

An investigation of belt-needle electrodes with various needle lengths was conducted at a pilot-commercial ESP. This investigation showed that reduction of needle length caused a decrease of discharge current, elevation of working voltage, and reduction of corona discharge power. One of the possible

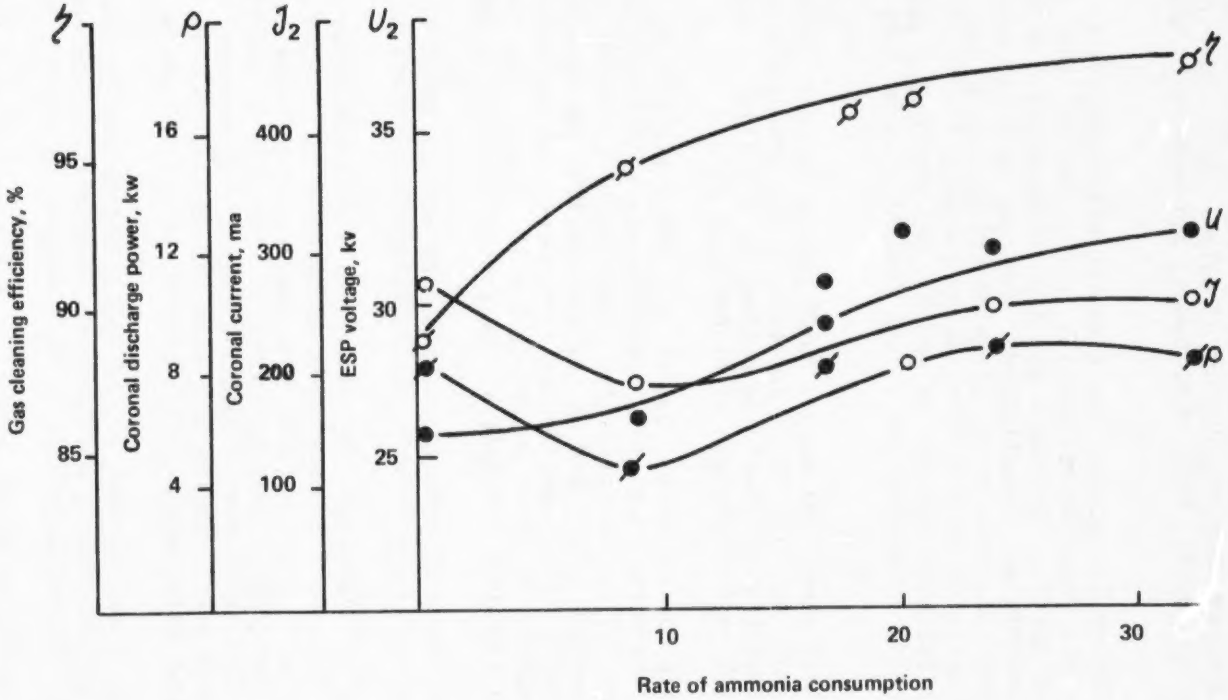

Figure 5. Dependence of gas cleaning degree, corona discharge power, current and corona voltage on ammonia rate.

ways to even the electric field and reduce specific corona currents, besides the above-mentioned, is to turn belt-needle electrodes 90° so that the needles are oriented in the direction of gas flow.

Comparison of field equipotentials shows that when needle elements are turned in the direction of gas flow, considerable decrease of maximal and mean corona current density occurs. That allows reduction of corona current intensity.

Complex application of various methods is an operative measure to increase efficiency of ESPs collecting high resistivity dust.

REFERENCES

1. I. K. Reshidov, I. G. Yermilov, and B. V. Zolotaryev, Author's Certificate No. 284973.

2. A. A. Rusanov, I. I. Urbakh, and A. V. Anastasiadi, "Cleaning of Flue Gases in Industrial Energetics," *Energy*, 1969.

3. I. K. Reshidov, "Peculiarities of Electrostatic Precipitators' Performance for High Resistivity Dust Collection," Proceedings, Scientific Technical Conference on Industrial Gas Cleaning, Yaroslavl', 1969.

4. W. Simm, Untersuchungen Uber das Ruckepruhen bei der elektrischen Staubabscheidung, *Che.-Ing.-Ted.n.*, *No. 1*, 1959, pp. 43-49.

5. V. I. Levitov and I. K. Reshidov, "How to Apply the Automatically Controlled Method of Probe Characteristics to some Problems of Electrical Gas Cleaning," Strong Electric Fields in Technological Processes, Ed.Ac. Popkov, V. I., *Energy*, 1969.

6. H. G. Edshold, Eine Messerrichtung zur Bestimmung des spezifischen elektrischen Staubwiderstands, *Staub*, No. 1, 1966, pp. 11-14.

A REVIEW OF THE INFLUENCE OF FLY ASH COMPOSITION ON RESISTIVITY

R. E. Bickelhaupt*

Abstract

This paper reviews the influence of fly ash composition on surface and volume resistivity. The pertinent literature of the past fifteen years regarding this subject is included in the review. Both practical and academic viewpoints with respect to the resistivity--ash composition relationship are considered.

The author subscribes to the idea that the conduction mechanism for fly ash is analogous to that for silicate glass. Therefore with respect to the ash composition, the alkali metals present are of greatest importance as charge carriers. To emphasize this point and to illustrate that the presence of sulfuric acid in the environment or an adsorbed film containing charge carriers is not required to produce a reasonable level of conduction, additional laboratory data are presented.

INTRODUCTION

Interest in the subject of resistivity is maintained because of the importance of this material property with respect to the dry electrostatic collection of fly ash. It is a key characteristic utilized in sizing precipitators, troubleshooting inefficient operation, and anticipating problems associated with changes in coal supply.

Several factors either independently or in combination affect the magnitude of the resistivity value. These include: specific surface, particle size distribution, ash layer porosity, environmental chemical composition, ash layer field strength, temperature, and ash chemical composition. When considering a general case within a narrow temperature range for ashes produced from low-sulfur coals, the fly ash chemical composition is the dominant factor. For a given set of conditions, a four order of magnitude change in resistivity as a function of fly ash composition has been observed. The relationship between resistivity and ash composition is also important with respect to developing an understanding of the conduction mechanism, the selection of conditioning agents, and in the prediction of resistivity for ashes from heretofore unburned coals and cleaned coals.

In this paper, fly ash is defined as essentially an inorganic, amorphous, chemically heterogeneous substance produced from the fusion and volatilization of the accessory coal minerals. Physically, the material is primarily spherical in shape, has a typical mass median diameter of 5 to 15 μm, and has a pycnometric density value of 2.0 to 3.0 g/cm^3.

---

*Southern Research Institute, Birmingham, Alabama.

Presentation and Definition of Resistivity Data

Data are usually illustrated by the logarithm of resistivity as a function of reciprocal absolute temperature. This is desirable because over a large temperature range, resistivity is very sensitive to this variable and pragmatically one is interested in both cold - and hot-side precipitators. This type of presentation is also suitable for discussion of conduction mechanisms and for distinguishing between volume and surface resistivity. Figure 1 is an example of laboratory resistivity data shown in the above manner.

The linear portion of the curve FE and its extension to D is usually referred to as volume resistivity. That part of the curve AB and its extension to C is defined as surface resistivity, and although plotted as a function of temperature, it is dependent on the combined effect of temperature and environment. Phenomenologically one can accept the segment BE as the resistivity resultant from a parallel circuit comprised of the volume and surface resistivities. Several authors (refs. 1, 2, and 3) have advanced mathematical expressions that define the shape of the curve ABEF. These expressions emphasize the particulate nature of the fly ash, define the effect of environmental partial pressures and temperature, and point out the need to know the fly ash material parameters to be able to calculate the magnitude of resistivity. It was suggested above that the chemical composition of the ash is the most important material parameter. In this paper an attempt is made to review the relationship between resistivity and fly ash composition from a mechanistic as well as an empirical viewpoint.

Volume Resistivity

Until several years ago, the volume conduction mechanism was thought to be electronic and particulates were considered intrinsic semiconductors (refs. 4 and 5) or impure insulators. Efforts were made to identify the specific electronic mechanism and little attention was given to fly ash composition. This viewpoint was probably encouraged by the assumption that the ashes were principally crystalline, by the observation that log ρ vs 1/T is linear and that the numerical value of experimental activation energy is commensurate with semiconduction, and by the tendencies of investigators to explain conduction for all amterials subjected to electrostatic precipitation using one mechanism.

About 1970 there was evidence that investigators (refs. 6, 7, and 8) were observing the pronounced reduction in resistivity for fly ashes containing large amounts of sodium. In late 1971 and early 1972 an effort (refs. 9 and 10) was made to determine the mechanism for volume conduction. It was hypothesized that the conduction mechanism was ionic and that the charge carriers were alkali metal ions.

The high temperature, linear portion of the resistivity-temperature curve can be expressed in terms of an Arrhenius equation,

$$\rho = \rho_0 \exp(\Theta/kT), \qquad (1)$$

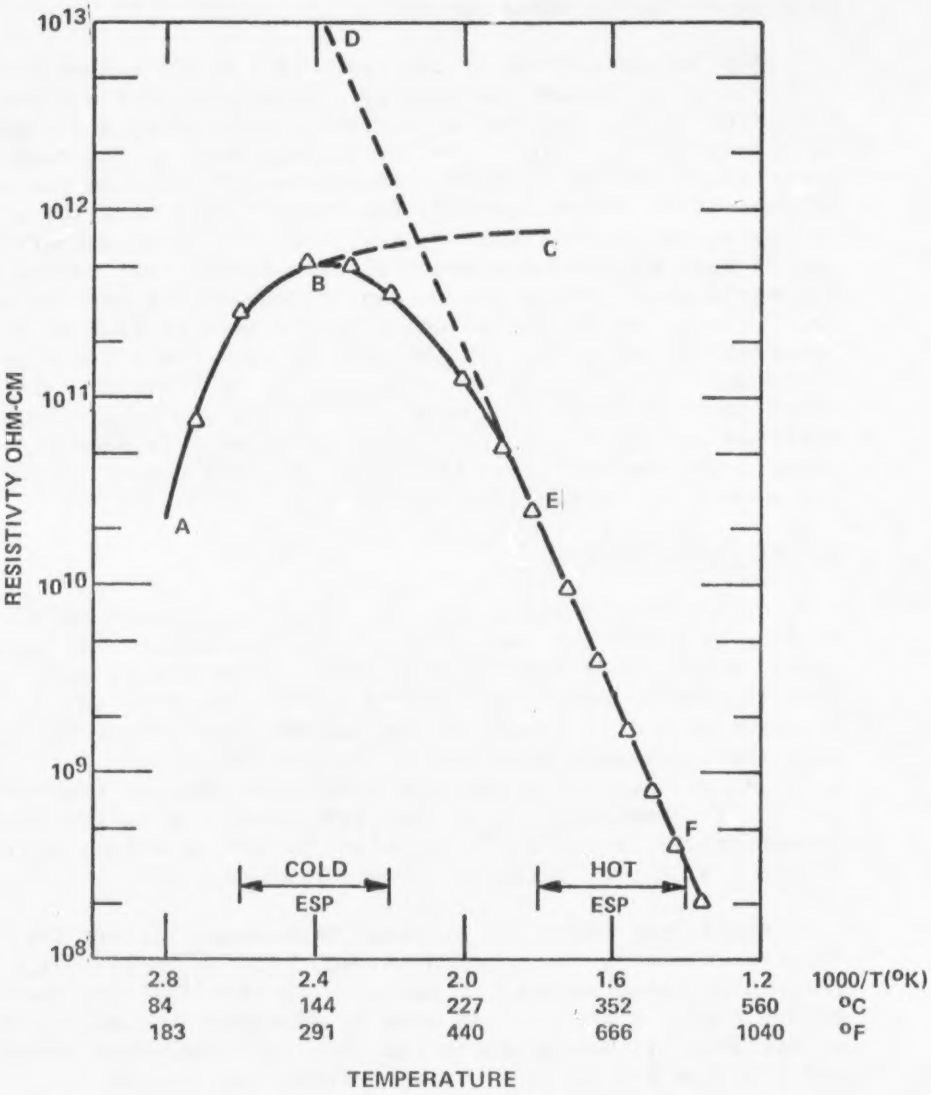

Figure 1. Typical laboratory resistivity--temperature data.

where

ρ = resistivity

ρ_o = a complex material parameter,

Θ = experimental activation energy,

K = Boltzmann constant, and

T = absolute temperature.

The denominator of the expression for the complex material parameter, ρ_o, contains a term for the number of mobile charge carriers. Therefore, it was expected that the resistivity would be inversely proportional to the atomic concentration of alkali metal ions at a specific temperature. Figure 2 shows this relationship to be true. Resistivity was determined at $\sim$350¼ C using several fly ashes having generally similar chemical composition but differing significantly in amount of Na^2O. The best illustration of the data was shown by a plot of log resistivity versus the log of the combined atomic concentration of lithium and sodium.

Transference experiments were used to demonstrate the mass transfer associated with ionic conduction and to identify the charge carriers. Some of the results of these experiments are shown in figure 3. An exuded mass of material collected in the region of the negative electrode was found to contain about 50 percent sodium and crystallographically contained compounds associated with the reaction of sodium and the ambient laboratory environment. Chemical analyses of the individual ash layers qualitatively indicate that the three alkali metal ions migrated. Because of the combined effect of concentration present and mobility, the sodium transfer was most obvious. Gravimetrically it was observed that a weight loss occurred at the anode and a gain at the cathode. The values are of reasonable magnitude for the amount of electrical energy passed, assuming that sodium was the principal migrating species. The data and observations shown in figures 2 and 3 were offered as proof of the hypothesis that the volume conduction mechanism is ionic and that the alkali metal ions, principally sodium, serve as charge carriers. The following mechanism (ref. 11) satisfying electrostatic neutrality was suggested. Alkali metals migrate to the cathode accepting electrons which causes a depletion of these ions at the anode. At the anode in the region of depleted alkali, unbridged and unassociated oxygen ions under the influence of an intense electric field migrate to the anode to form oxygen molecules with the release of electrons.

In the subsequent years, Selle et al., (refs. 12 and 13) and Bickelhaupt (ref. 14) have conducted extensive research programs associated with the resistivity-fly ash composition relationship. Selle has shown the pronounced effect of sodium on resistivity for lignite and subbituminous coals mined in the western United States. These studies have led to the development of a correlation that can be used to determine resistivity from ash composition for these coals.

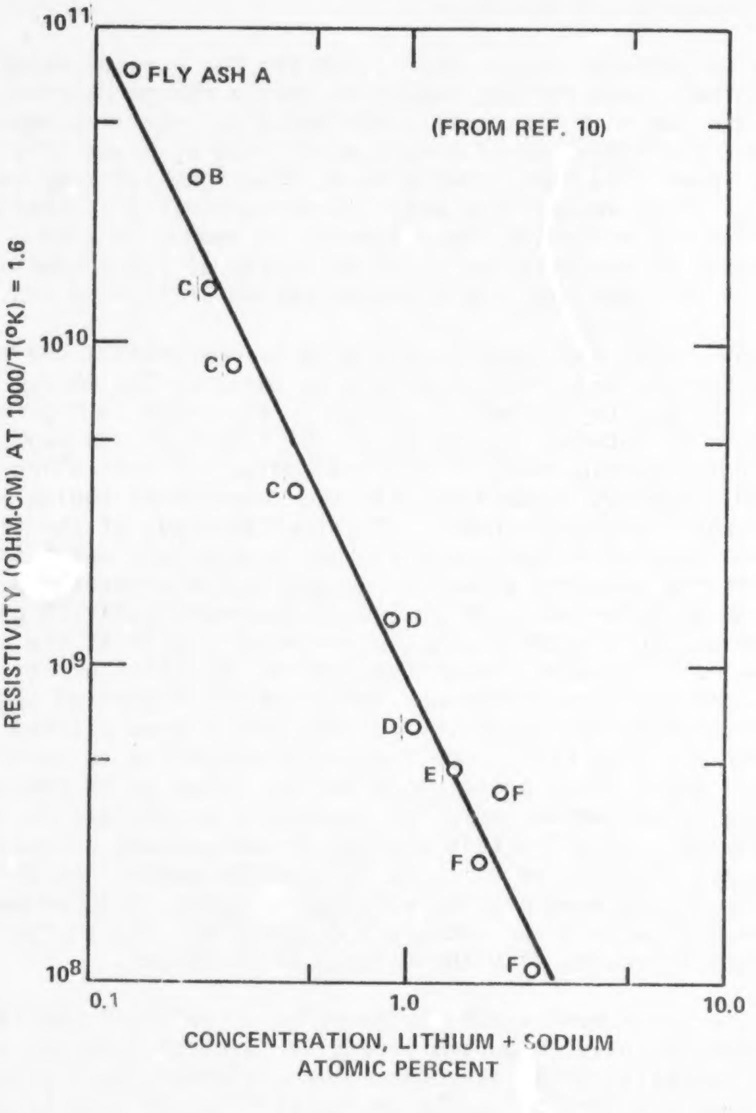

Figure 2. Representation of high temperature--long time transference results.

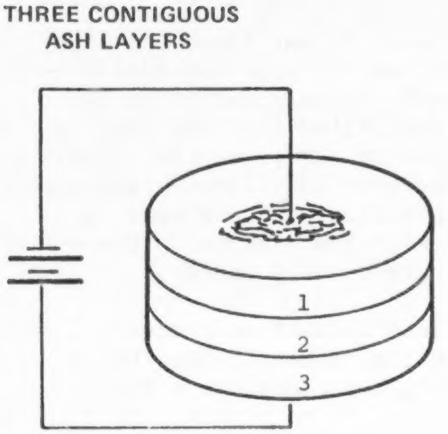
THREE CONTIGUOUS ASH LAYERS
1
2
3

CHEMICAL ANALYSIS

EXTRUDED MASS AT CATHODE - 50% Na

Disk	Li_2O	Na_2O	K_2O	GRAVIMETRIC DATA
1.	0.018	3.0	0.8	+44 mg
2.	0.01	2.3	0.7	− 1 mg
3.	0.006	1.4	0.7	−34 mg

Figure 3. Volume resistivity versus lithium and sodium concentration for ashes of generally similar composition.

Bickelhaupt attempted to expand the earlier work on volume resistivity to include a general cross section of ash compositions produced throughout this country. These results are summarized in figure 4. The data show the resistivity at ~350° C as a function of the atomic concentration of lithium and sodium for a large number of ashes having diverse chemical composition. It was observed that the data in the region near the illustrated curve were produced from ashes having a relatively low and uniform iron concentration. Those data lying well below the line between 0.2 and 0.5 atomic percent sodium were related to ashes of moderate to high iron concentration. If the data were normalized to constant sodium concentration, it was found that an excellent correlation existed between resistivity and iron concentration. Others (refs. 6 and 15) have noted this effect. A number of experiments were conducted to elucidate the effect of iron. The obvious suggestion that iron introduces an electronic contribution to the total conduction process could not be demonstrated. Transference experiments using ashes having four levels of iron concentration yielded useful information. It was found that for a constant amount of electrical energy passed, the ratio of the alkali metal migrated to that amount present in the ash increased with increasing iron concentration. As a result, it was speculated that the iron in the glassy structure of the ash permitted a greater number of the alkali metals ions to be mobile. This point has never been additionally studied. As a result of this research, an empirical expression was developed to estimate resistivity from ash composition for high temperatures. Correspondence has indicated that the expression is reasonably useful.

Emphasizing the role of sodium in the volume conduction process, evidence (ref. 16) has been recently presented that demonstrates the potential for sodium as an injected conditioning agent used in a hot-side precipitator.

Surface Resistivity

Until recent years, the role of ash composition with respect to surface resistivity received little attention. This was true principally because the generally accepted mechanism (ref. 17) for surface conduction does not require the ash composition specifically to be operative. This electrolytic mechanism suggests that conduction takes place through an adsorbed film, one or more molecular layers thick, of water and/or sulfuric acid. In a manner analogous to that for bulk aqueous solutions, conduction occurs by electrolysis of the adsorbed agents or by a proton jump processes (ref. 18). In these cases, the hydrogen ion would be the principal charge carrier. With the exception of the effect a given ash might have on the adsorption process and the availability of the adsorbed species to be functional, the chemical composition of the ash was not considered important to the extent that the material was sometimes described as inert.

Many investigations have shown that the composition of the fly ash has a vital role in the surface conduction process. Included are observations (refs. 7 and 19) of improved precipitator performance when coals high in sodium concentration were burned, tests (refs. 17 and 20) demonstrating the effect of sodium as a conditioning agent, and laboratory studies relating resistivity and ash composition.

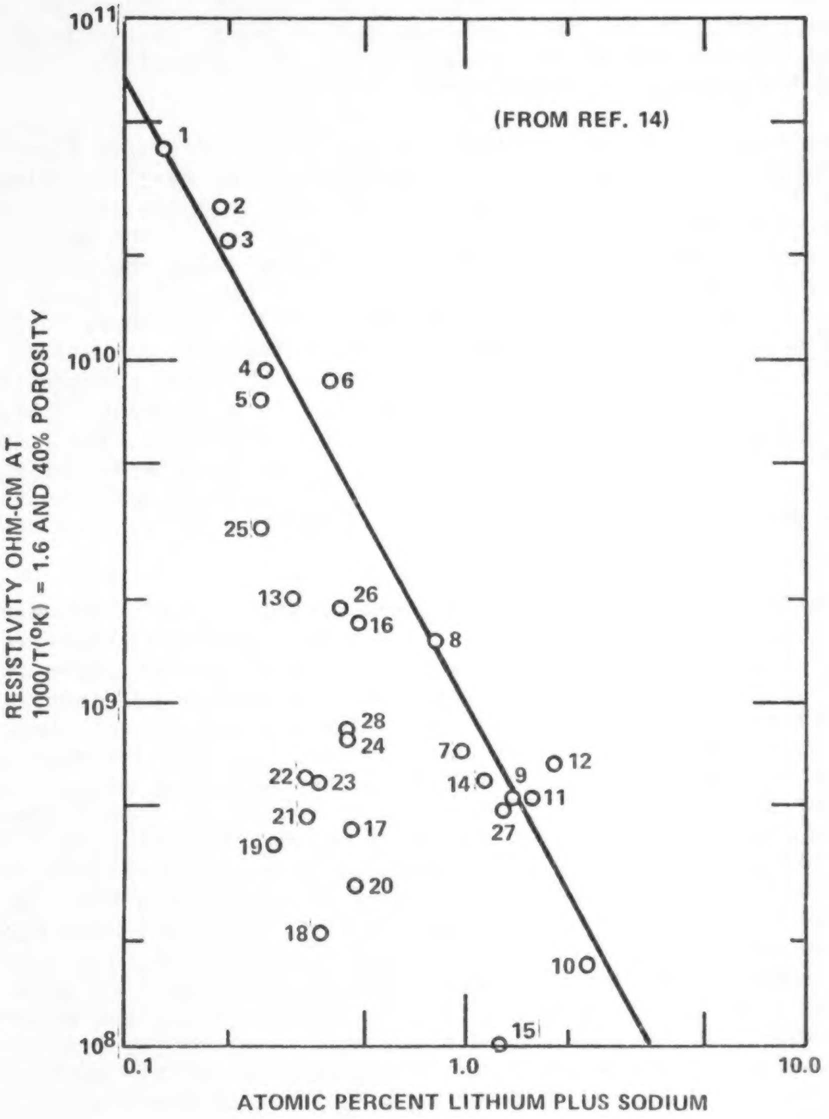

Figure 4. Volume resistivity versus lithium and sodium concentration for ashes of generally dissimilar composition.

The previously cited works of Bucher (ref. 8) and Selle (refs. 12 and 13) et al. are equally applicable to a discussion of the effect of ash composition on surface resistivity. These authors have shown that surface resistivity under constant environmental test conditions decreases over 3 orders of magnitude as the sodium concentration increases within the normal limits for ashes produced from Western coals. High coefficients of correlation were found for relationships between resistivity data and expressions derived to predict resistivity from ash composition. It was pointed out that, in the cases of high sodium coals, volatilized sodium appears on the surface of fly ash as Na_2SO_4 readily available for participation in the conduction process (ref. 20).

Bickelhaupt (ref. 21) studied surface resistivity as a function of a broad range of ash compositions to determine a correlation between these two factors and to establish the role of ash composition with respect to the conduction process. An illustration of the data acquired in this study is shown in figure 5. This figure shows the general dependency of surface resistivity on the atomic concentration of lithium and sodium. Those data points significantly below the curve in the region of 0.3 percent lithium and sodium were found to contain 10 to 25 percent Fe_2O_3 and 2.3 to 3.9 percent potassium. It was subsequently determined that resistivity values normalized to a constant lithium plus sodium concentration could be correlated with either the atomic concentration of iron or iron plus potassium. The choice between these two correlations was dependent on the iron concentration. Based on these data, a graphical method of estimating maximum fly ash surface resistivity was offered.

The effect of iron and potassium was partially clarified using chemical transference experiments. It was observed that after extended periods of time under applied electrical field at a temperature at which only surface conduction was operative, a concentration gradient for the alkali metals lithium, sodium, and potassium had been established. This gradient showed the migration of these ions to the negative electrode. The greater participation of potassium in the conduction process was found to be sensitive to the greater concentrations of iron in the ash. It was speculated that, as in the case of volume conduction, the role of iron is indirect. Ancillary tests revealed an enhanced release of alkali metal ions for aqueous solutions of ash suggesting that the presence of iron may decrease the resistance of the glassy ash to attack by environmental agents. The influence of adsorbed H_2SO_4 and other condensed agents cannot be overlooked, because the high iron ashes also possess the higher concentrations of soluble sulfate and the experimental procedure would not have destroyed these agents. From the transference experiments, it was estimated that the migration of alkali metal charge carrying ions would account for the major portion of the electrical energy passed.

In reference 21, an extended description of a surface conduction mechanism is given that accentuates the role of ash composition. It was suggested that the conduction mechanism for glassy ash is analogous to that recorded for silicate glasses (ref. 22). For the general case, one can visualize an ion exchange process in which a H^+ replaces a Na^+ in the surface structure of the ash thereby freeing the sodium ion to

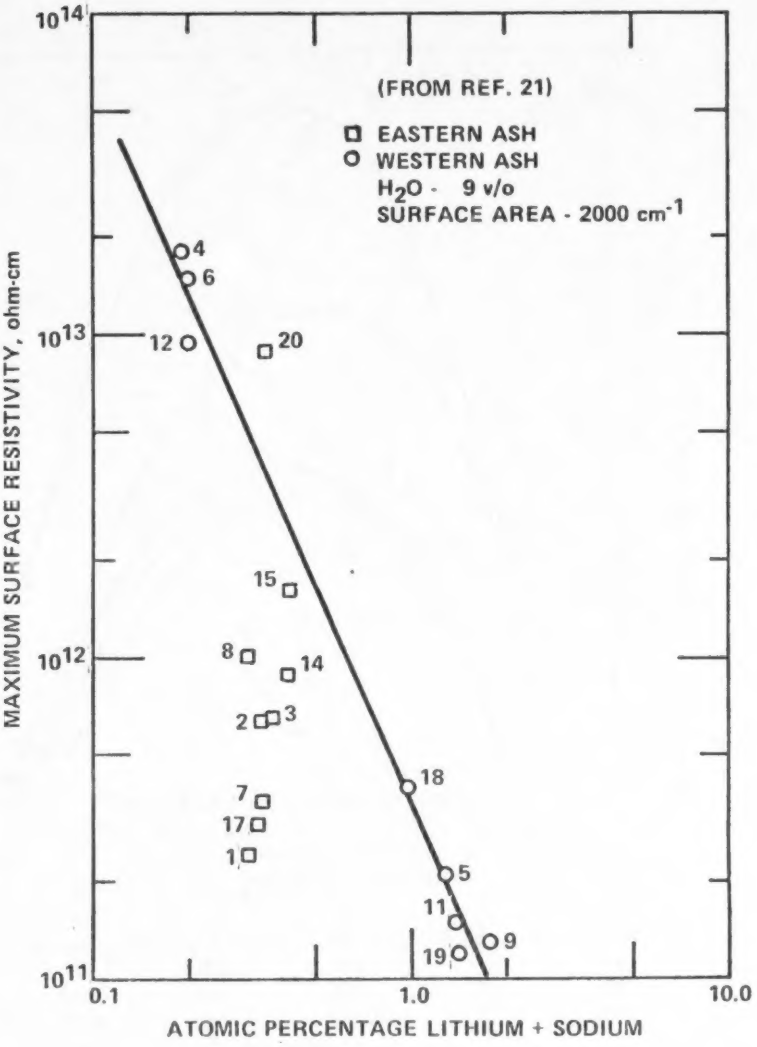

Figure 5. Maximum surface resistivity versus lithium and sodium concentration for ashes of generally dissimilar composition.

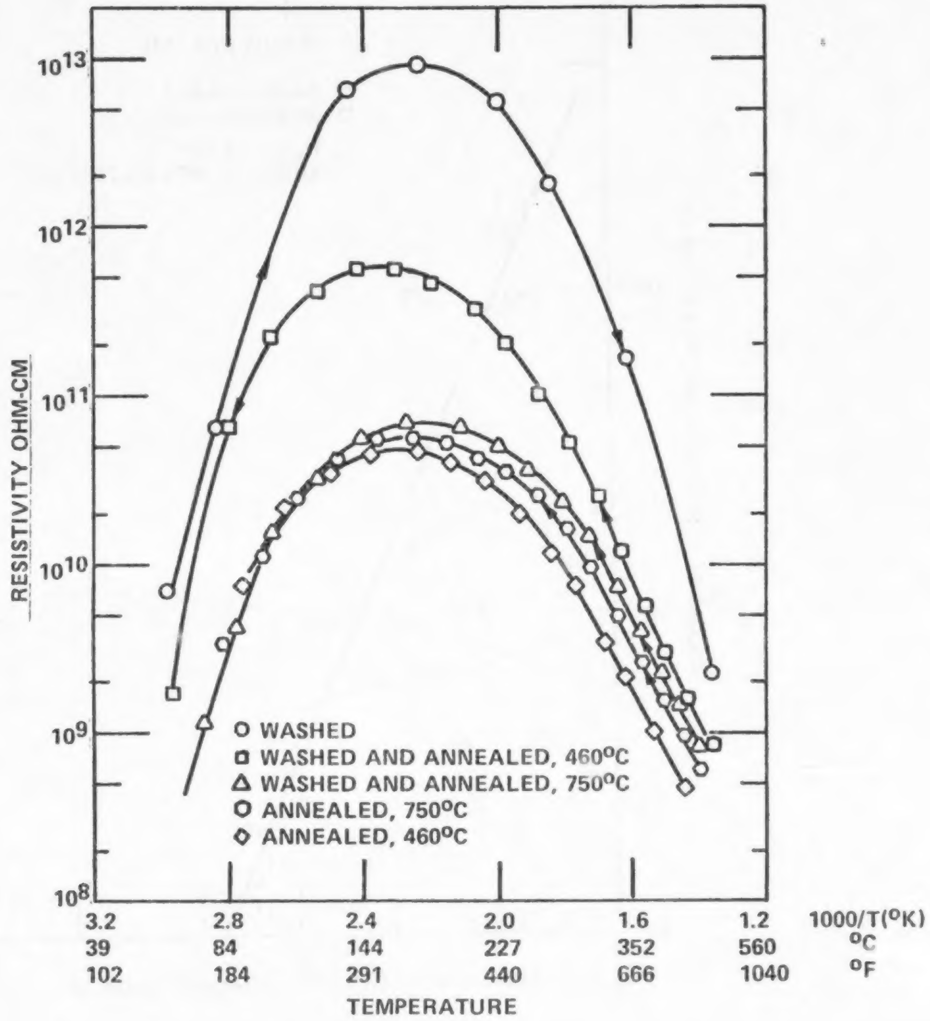

Figure 6. The effect of water washing and/or thermal annealing on the resistivity of an ash.

migrate. Also, any condition that would provide a source of mobile alkali metal ions on the ash surface will enhance conduction. The foregoing does not preclude the role of sulfuric acid in the surface conduction process. However, the role of this natural conditioning agent within in the scope of the conduction process needs additional study.

To support the proposal that surface conduction is principally dependent on the charge carrying alkali metal ions, it was believed necessary to demonstrate the surface conduction phenomenon in the presence of air and water alone and in the absence of any natural or inadvertent surface films or deposits on the ash. Several ashes were washed three times using distilled water. Each cycle involved extended soak followed by a rinse during filtration. The ashes were dried, returned to powder form, and subdivided for various tests. The results were very similar for all ashes studied, and the data for one are presented in figure 6. These curves show the data for a given ash subjected to a variety of treatments and tested under one set of conditions with the exception that the water-washed specimen, of necessity, had to be tested using ascending temperature.

The curves suggest that water washing the ash eliminates any conducting surface films and/or leaches out the alkali metal ions in the immediate surface of the ash. By thermally annealing in dry air, the washed specimens seemingly are rejuvenated by either developing an activated surface with which the resistivity test environment can readily react and/or by the replacement of the leached alkali metal ions by diffusion from within the particles. This experiment suggests that a preexisting conducting film or deposit on the ash is not necessary for the operation of the suggested mechanism. However, in those cases in which a substantial amount of the surface conduction is related to adsorbed or condensed phases, one would not expect the resistivity to return to the value of an unwashed ash as a result of the thermal anneal.

It is concluded that the influence of chemical composition on the resistivity of fly ash is quite important, affecting all facets of the problems associated with resistivity and the dry collection of fly ash.

REFERENCES

1. S. Masuda, "Effects of Temperature and Humidity on the Apparent Conductivity of High Resistivity Dust," Electrotechn J. of Japan, 7 (108): 1963.

2. K. J. McLean, "Factors Affecting the Resistivity of a Particulate Layer in Electrostatic Precipitators," J. Air Poll Control Assoc., 26 (9): 866-870, 1976.

3. Ditl Pavel and Robert W. Coughlin, "Improving Efficiency of Electrostatic Precipitation by Physico-chemical Modification of the Electrostatic Resistivity of Flyash," AIChE Journal, 22 (4): 730-736, 1976.

4. Harry J. White, Industrial Electrostatic Precipitation, Reading, Massachusetts: Addison-Wesley Publishing Company, Inc., 1963, pp. 306-309.

5. O. J. Tassicker, Z. Herceg, and K. J. McLean, "Mechanism of Current Conduction Through Precipitated Fly Ash," Bulletin #10, Department of Electrical Engineering, Wallongong University College, The University of New South Wales, February 1966.

6. C. C. Shale, J. H. Holden, and G. E. Fasching, "Electrical Resistivity of Fly Ash at Temperatures to 1500¼F," Report 7041, Bureau of Mines, U.S. Department of Interior, Washington, D.C., March 1968.

7. R. A. Durie, "Investigation of the Electrostatic Precipitation of Fly Ashes from Coals to be Supplied to the Liddell Power Station, Part 2, Fuel Research Investigation Report 72, June 1968.

8. W. E. Bucher, "A Study of the Bulk Electrical Resistivity of Fly Ash from Lignite & Other Western Coals," M. S. Thesis, University of North Dakota, Grand Forks, North Dakota, December 1970.

9. R. E. Bickelhaupt and G. B. Nichols, "Investigation of the Volume Electrical Resistivity of Fly Ash from the Sundance and Wabamun Power Stations," Final Report Project 2865 submitted by Southern Research Institute, Birmingham, Alabama, to Calgary Power, Ltd. Calgary, Alberta, Canada, June 30, 1972.

10. R. E. Bickelhaupt, "Electrical Volume Conduction in Fly Ash," APCA Journal 24 (3): 251-255 (1974).

11. D. E. Carlson, K. W. Hang, and G. F. Stockdale, "Electrode polarization in alkali-containing glasses," J. Am. Cer. S., 55 (7): 337, 1972.

12. S. J. Selle, P. H. Tufte, and G. H. Gronhovd, "A Study of the Electrical Resistivity of Fly Ashes from Low-Sulfur Western Coals Using Various Methods," Paper 72-107 presented at the 65th Meeting of the Air Pollution Control Association, Miami Beach, Florida, 1972.

13. S. J. Selle, L. L. Hess, and E. A. Sondreal, "Western Fly Ash Composition as an Indicator of Resistivity and Pilot ESP Removal Efficiency," Paper 75-02.5 presented at the 68th Meeting of the Air Pollution Control Association, Boston, Massachusetts, June 15-20, 1975.

14. R. E. Bickelhaupt, "Volume Resistivity - Fly Ash Composition Relationship," Environmental Sc. & Tech., 9 (4): 336-342, 1975.

15. J. Dalmon and E. Raask, "Resistivity of Particulate Coal Minerals," J. Inst. Fuel, 46 (4): 201-205, 1972.

16. A. B. Walker, "Operating Experience with Hot Precipitators on Western Low Sulfur Coals," A Paper Presented at the American Power Conference, April 18-20, 1977, Chicago, Illinois.

17. H. J. White, "Resistivity Problems in Electrostatic Precipitation," APCA Journal 24, (4): April 1974.

18. R. A. Robinson and R. H. Stokes, Electrolyte Solutions. London: Butterworths Scientific Publications, 1955, pp. 116-117.

19. R. H. Holyoak, "Burning Western Coals in Northern Illinois," Paper, 73-WA/Fu-4, presented at the Winter Annual Meeting, ASME, Detroit, Michigan, November 11-15, 1973.

20. S. J. Selle, "Factors Affecting ESP Performance on Western Coals and Experience with North Dakota Lignites," Symposium on Particulate Control in Energy Processes, EPA - 600/7-76-010, September, 1976, pp. 105-125.

21. R. E. Bickelhaupt, "Surface Resistivity and the Chemical Composition of Fly Ash," APCA Journal, 25 (2): 148-152, 1975.

22. Robert H. Doremus, Glass Science, John Wiley & Sons, New York, 1973, chapters 12 and 13.

U.S. ENVIRONMENTAL PROTECTION AGENCY
Office of Research and Development
Technical Information Staff
Cincinnati, Ohio 45268

OFFICIAL BUSINESS
PENALTY FOR PRIVATE USE, $300
AN EQUAL OPPORTUNITY EMPLOYER

POSTAGE AND FEES PAID
U S ENVIRONMENTAL PROTECTION AGENCY
EPA-335

Special Fourth-Class Rate
Book

If your address is incorrect, please change on the above label; tear off; and return to the above address.
If you do not desire to continue receiving this technical report series, CHECK HERE ☐, tear off label, and return it to the above address.

PUBLICATION NO. EPA-600/7-78-037